



저작자표시-비영리-변경금지 2.0 대한민국

이용자는 아래의 조건을 따르는 경우에 한하여 자유롭게

- 이 저작물을 복제, 배포, 전송, 전시, 공연 및 방송할 수 있습니다.

다음과 같은 조건을 따라야 합니다:



저작자표시. 귀하는 원저작자를 표시하여야 합니다.



비영리. 귀하는 이 저작물을 영리 목적으로 이용할 수 없습니다.



변경금지. 귀하는 이 저작물을 개작, 변형 또는 가공할 수 없습니다.

- 귀하는, 이 저작물의 재이용이나 배포의 경우, 이 저작물에 적용된 이용허락조건을 명확하게 나타내어야 합니다.
- 저작권자로부터 별도의 허가를 받으면 이러한 조건들은 적용되지 않습니다.

저작권법에 따른 이용자의 권리는 위의 내용에 의하여 영향을 받지 않습니다.

이것은 [이용허락규약\(Legal Code\)](#)을 이해하기 쉽게 요약한 것입니다.

[Disclaimer](#)

이학박사학위논문

**Total Synthesis and Biological Evaluation
of the Indoleamine 2,3-Dioxygenase Inhibitors
Exiguamine A and *Iso*-Exiguamine A**

인돌아민 2,3-디옥시게나제 억제제
엑시구아민 에이와 *아이소*-엑시구아민 에이의
전합성 및 생물학적 평가

2018년 8월

서울대학교 대학원

화학부 유기화학 전공

노 승 주

Abstract

Described in this dissertation are total synthesis and biological evaluation of exiguamine A, an unprecedented alkaloid consisting of a hexacyclic skeleton. This marine natural product possesses potent inhibitory activity against the indoleamine 2,3-dioxygenase (IDO), which catalyzes the first and rate-limiting step of metabolic degradation of the essential amino acid tryptophan (Chapter 1). The immune-regulating enzyme IDO has emerged as a promising target for cancer immunotherapy as it is overexpressed in many human tumors and known to provide cancer cells with a mechanism to evade the immune system. Many endeavors have been made by our group and others to achieve biogenesis and chemical synthesis of exiguamine A (Chapter 2), and several synthetic pathways have been proposed. Our approach was based on the assembly of three domains – tryptamine quinone, dopamine, and hydantoin. Taking advantage of the redox equilibrium between quinone and hydroquinone, all subunits of exiguamine A were tethered in a convergent manner with concomitant construction of the core pyran framework through Mukaiyama-Michael and Claisen rearrangement reactions. After a series of cascade redox processes using hydrogen and oxygen, the efficient synthesis of exiguamine A was accomplished. Our synthetic route also allowed for the synthesis of an isomer of exiguamine A, named *iso-exiguamine A* (Chapter 3). The synthetic exiguamines were evaluated for IDO inhibitory activity in cell line (Chapter 4).

Keywords: Indoleamine 2,3-dioxygenase (IDO), IDO inhibitors, Natural products,

Total synthesis, Exiguamine A, *Iso-exiguamine A*, Biological evaluation

Student Number: 2008-22723

Table of Contents

Title Page	
Signature Page	
Abstract	i
Table of Contents	iii
List of Schemes	vi
List of Tables	ix
List of Figures	x
List of Abbreviations	xi
Abstract in Korean	131
Appendix A	S1
Appendix B	S41

Chapter 1: Indoleamine 2,3-Dioxygenase (IDO)

1.1 Introduction	1
1.2 IDO Inhibitors in Clinical Trials.....	4
1.3 Conclusion	9
1.4 References	9

Chapter 2: The Exiguamines

2.1 Introduction	13
2.2 Proposed Biogenesis by the Andersen Group	14
2.3 Total Synthesis of Exiguamines A and B by the Trauner Group	15

2.4 References	20
----------------------	----

Chapter 3: Total Synthesis of Exiguamine A and *Iso*-Exiguamine A

3.1 Retrosynthetic Analysis and Synthetic Plan	21
3.2 Preliminary Synthetic Studies by Dr. Venkataramanan Krishnamurthy in the Lee Group	22
3.3 Syntheses of Fragments	25
3.3.1 Tryptamine Quinone	26
3.3.2 <i>N,N'</i> -Dimethyl-5-Chlorohydantoin	28
3.3.3 Dopamine-Hydantoin	29
3.4 Union of Michael Donor and Acceptor	31
3.4.1 Lewis Acid Catalyzed Mukaiyama-Michael Reaction	31
3.4.2 Other Attempts: The Assembly of Quinone, Hydantoin and Dopamine Fragments	34
3.4.3 Lewis Base Mediated Mukaiyama-Michael Reaction	37
3.4.3.1 Coupling between Silyl Enol Ether and Tryptamine Quinone	37
3.4.3.2 Coupling between Silyl Enol Ether and Bromotryptamine Quinone: Discovery of <i>Iso</i> -Exiguamine A Precursor	41
3.5 Formation of the Pyran Ring	49
3.5.1 Oxidative Coupling Approach	49
3.5.2 Correction of the Preliminary Studies	51
3.5.3 The Claisen Rearrangement Approach	54
3.6 Completion of Total Synthesis of Exiguamine A	62
3.7 Total Synthesis of <i>Iso</i> -Exiguamine A.....	66
3.8 Conclusion	68

3.9 References	69
3.10 Experimental Section	71
3.10.1 General Information	71
3.10.2 Selected Experiments and Characterization	72

Chapter 4: Biological Evaluation of IDO Inhibitor Candidates

4.1 Introduction	112
4.2 Biological Evaluation of Exiguamine A and Its Derivatives.....	113
4.2.1 Exiguamine A	113
4.2.2 <i>Iso</i> -Exiguamine A	118
4.2.2.1 Enzymatic Assay	118
4.2.2.2 Cellular Assay	122
4.2.3 Precursor of Exiguamine A	125
4.2.3.1 Enzymatic Assay	125
4.2.3.2 Cellular Assay	127
4.3 Conclusion	129
4.4 Reference	130

List of Schemes

Scheme 1.1 The Kynurenine Pathway

Scheme 1.2 Dioxygenase Mechanism of Tryptophan

Scheme 2.1 Proposed Biogenesis by the Andersen Group

Scheme 2.2 Studies Toward Exiguamine A

Scheme 2.3 Revised Biosynthetic Approach

Scheme 2.4 Synthesis of Biaryl **2.28**

Scheme 2.5 Preparation of Indoloquinone **2.29**

Scheme 2.6 Synthesis of Exiguamine A and Discovery of Exiguamine B

Scheme 3.1 Retrosynthetic Analysis

Scheme 3.2 Example of Lewis Acid Catalyzed Mukaiyama-Michael Reaction

Scheme 3.3 Model Studies for Key Steps

Scheme 3.4 Strategies for the Syntheses of Fragments

Scheme 3.5 Synthesis of Tryptamine Quinone: Homologation Approach

Scheme 3.6 Synthesis of Tryptamine Quinone: Oxidation Approach

Scheme 3.7 Synthesis of 5-Chlorohydantoin **3.10**

Scheme 3.8 Synthesis of Dopamine-Hydantoin: Homologation Approach

Scheme 3.9 Synthesis of Dopamine-Hydantoin: Privileged Approach

Scheme 3.10 Preparation of Silyl Enol Ether **3.42**

Scheme 3.11 Lewis Acid Catalyzed Mukaiyama-Michael Type Reaction

Scheme 3.12 Exploring the Reactivity of Michael Acceptor

Scheme 3.13 The Mukaiyama-Michael Reaction

Scheme 3.14 Model Studies for the Mukaiyama-Michael Reaction

Scheme 3.15 Revised Approach for Key Precursor

Scheme 3.16 Example of the Michael Reaction with Stabilized Enol

Scheme 3.17 Michael Reaction with Hydantoin Fragments

Scheme 3.18 Synthetic Approaches for Modified Key Precursor

Scheme 3.19 Decarboxylation Problem in the Hydrolysis of Ester

Scheme 3.20 Lewis Base Catalyzed Mukaiyama-Michael Type Reaction

Scheme 3.21 Mukaiyama-Michael Type Reaction Using TASF

Scheme 3.22 Various Intermediates in the Mukaiyama-Michael Reaction Mixture

Scheme 3.23 Coupling Strategy Using Functionalized Quinone

Scheme 3.24 Bromination with *N*-Protected Indoloquinone

Scheme 3.25 Failure for Deprotection of *N*-Boc Group

Scheme 3.26 Synthesis of 5-Bromotryptamine Quinone

Scheme 3.27 Straightforward Approach for 5-Bromotryptamine Quinone **3.92**

Scheme 3.28 *N*-Boc Deprotection of Indoloquinone Moiety

Scheme 3.29 Coupling Reaction with 5-Bromoquinone: Discovery of Regioisomer

Scheme 3.30 Proposed Mechanism

Scheme 3.31 Michael Reaction with Bromoquinones

Scheme 3.32 Plan for Pyran Formation through Oxidative Coupling

Scheme 3.33 Difficulty in Hydroquinone Formation of **3.76**

Scheme 3.34 Failure of Oxidative Coupling through Friedel-Crafts Type Reaction

Scheme 3.35 Plan for Model Study of Pyran Formation

Scheme 3.36 Re-evaluation of Preliminary Studies by Dr. Venkataramanan
Krishnamurthy

Scheme 3.37 Proposed Mechanism for Synthesis of **3.129** and **3.131**

Scheme 3.38 Plan for Pyran Formation through Claisen Rearrangement

Scheme 3.39 Asymmetric O-alkylation followed by Claisen Rearrangement

Scheme 3.40 Formation of Pyran **3.137**

Scheme 3.41 Hypothesis for Decomposition of Michael Adducts

Scheme 3.42 Hydrogenation and Hydrogenolysis of **3.137**

Scheme 3.43 Proposed Mechanism for Competitive Formation of **3.141** and **3.143**

Scheme 3.44 Completion of Total Synthesis of Exiguamine A (**3.1**)

Scheme 3.45 Comparison of Key Intermediates **3.142** with **3.150**

Scheme 3.46 Synthesis of Michael Adduct **3.97**

Scheme 3.47 Claisen Rearrangement – Oxidation Reaction of Regioisomer

Scheme 3.48 Completion of Total Synthesis of *Iso*-Exiguamine A (**3.154**)

Scheme 3.49 Summary: Total Synthesis of Exiguamine A

List of Tables

Table 1.1 Clinical Trials for IDO Inhibitors

Table 3.1 Enolate Generation Reaction with Substrate **3.11**

Table 3.2 Investigation into Mukaiyama-Michael Type Reaction Using TASF

Table 3.3 Synthesis of 5- and 6-Bromoquinones Using Brominating Reagents

Table 3.4 Correction of Model Studies

Table 3.5 Investigation into Claisen Rearrangement Conditions

Table 3.6 Claisen Rearrangement – Oxidation Reactions

Table 4.1 Raw Data for the Effect of Exiguamine A (**3.1**) on IDO1 Activity

Table 4.2 Raw Data for the Effect of INCB24360 on IDO1 Activity

Table 4.3 IC₅₀ Values of Compounds Against IDO1 Activity in HeLa Cells

Table 4.4 Raw Data for the Effect of *Iso*-Exiguamine A (**3.154**) on IDO1 Activity

Table 4.5 Raw Data for the Effect of INCB24360 on IDO1 Activity

Table 4.6 IC₅₀ Values of Compounds Against Recombinant hIDO1 Activity

Table 4.7 Raw Data for the Effect of *Iso*-Exiguamine A (**3.154**) on IDO1 Activity

Table 4.8 Raw Data for the Effect of INCB24360 on IDO1 Activity

Table 4.9 IC₅₀ Values of Compounds Against IDO1 Activity in HeLa Cells

Table 4.10 Raw Data for the Effect of Exiguamine A Precursor on IDO1 Activity

Table 4.11 IC₅₀ Values of Compounds Against Recombinant hIDO1 Activity

Table 4.12 Raw Data for the Effect of Exiguamine A Precursor on IDO1 Activity

Table 4.13 IC₅₀ Values of Compounds Against IDO1 Activity in HeLa Cells

List of Figures

Figure 1.1 Effects of IDO Expression

Figure 1.2 Development of the Epacadostat

Figure 2.1 The Exiguamines

Figure 3.1 The ^1H NMR Comparison Between **3.76** and **3.97**

Figure 3.2 Byproducts Originated from Claisen Rearrangement

Figure 3.3 Stability of Phenols **3.135** and **3.136**

Figure 4.1 Effect of the Exiguamine A (**3.1**) on IDO1 Activity in HeLa Cells

Figure 4.2 Effect of the INCB24360 on IDO1 Activity in HeLa Cells

Figure 4.3 Effect of the *Iso*-Exiguamine A on Recombinant hIDO1 Activity

Figure 4.4 Effect of the INCB24360 on Recombinant hIDO1 Activity

Figure 4.5 Effect of the Compounds on IDO1 Activity in HeLa Cells

Figure 4.6 Precursor of Exiguamine A **3.141**

Figure 4.7 Effect of the Compounds on Recombinant hIDO1 Activity

Figure 4.8 Effect of the Compounds on IDO1 Activity

Figure 4.9 Summary: Biological Evaluation of Exiguamine A and Its Derivatives

List of Abbreviations

Ac	acyl
Ar	aryl
aq.	aqueous
atm	atmosphere
Boc	<i>tert</i> -butyloxycarbonyl
Bn	benzyl
Bu	butyl
cat.	catalytic
CAN	ceric ammonium nitrate
cod	cyclooctadiene
COSY	correlation spectroscopy
DABCO	1,4-diazabicyclo[2.2.2]octane
DCM	dichloromethane
DMAP	4-dimethylamino pyridine
DMF	<i>N,N</i> -dimethylformamide
<i>dr</i>	diastereomeric ratio
dtbbpy	4,4'-di- <i>tert</i> -butyl-2,2-bipyridyl
EC₅₀	half maximal effective concentration
El	electrophile
ESI	electrospray ionization
Et	ethyl

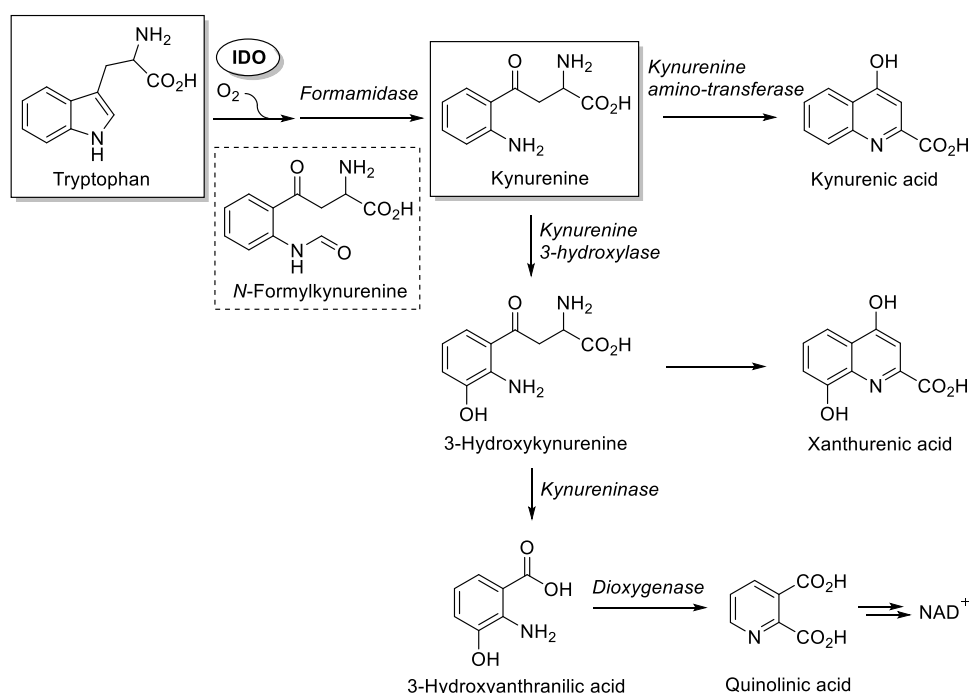
equiv	equivalent
EtOAc	ethyl acetate
Frémy's salt	potassium nitrosodisulfonate
g	gram
h	hour
HFIP	1,1,1,3,3,3-hexafluoro-2-propanol
HMBC	heteronuclear multiple bond correlation
HMPA	hexamethylphosphoramide
HRMS	high-resolution mass spectrometry
HSQC	heteronuclear single quantum correlation
<i>i</i>	iso
IC₅₀	half maximal inhibitory concentration
L	liter
LDA	lithium diisopropylamide
LDMP	lithium 2,6-dimethylpiperidide
LDEA	lithium diethylamide
LiHMDS	lithium bis(trimethylsilyl)amide
M	molar
μ	micro
Me	methyl
MeCN	acetonitrile
MeOH	methanol
min	minute

mol	mole
m/z	mass to charge ratio
<i>n</i>	normal
<i>N</i>	normal concentration
NBS	<i>N</i> -bromosuccinimide
NMR	nuclear magnetic resonance
Nuc	nucleophile
PIDA	phenyliodine(III) diacetate
Ph	phenyl
Pr	propyl
pyr	pyridine
<i>t</i>	tert
TASF	tris(dimethylamino)sulfonium difluorotrimethylsilicate
TBAF	tetrabutylammonium fluoride
TBS	<i>tert</i> -butyldimethylsilyl
TBSOTf	<i>tert</i> -butyldimethylsilyl trifluoromethanesulfonate
Tf	trifluoromethylsulfonate
TFE	trifluoroethanol
THF	tetrahydrofuran
TLC	thin layer chromatography
TMS	trimethylsilyl
Tr	triphenylmethyl
Ts	<i>para</i> -toluenesulfonyl

Chapter 1: Indoleamine 2,3-Dioxygenase (IDO)

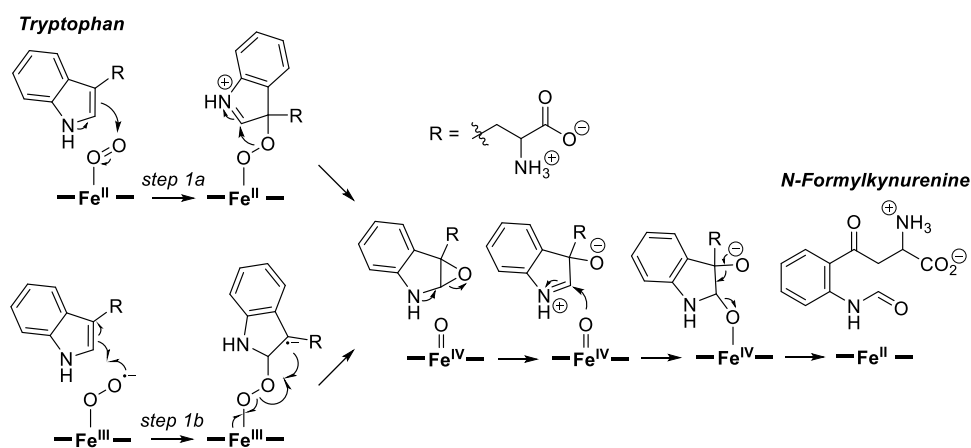
1.1 Introduction

Indoleamine 2,3-dioxygenase (IDO; EC 1.13.11.17) is a heme containing enzyme catalyzes the first and rate-limiting step in the metabolic degradation of the essential amino acid tryptophan. This extrahepatic enzyme responsible for catabolizing nondietary tryptophan is concerned in the cleavage of the indole C2-C3 double bond, and the cleavage product, *N*-formylkynurenine, is hydrolyzed to form kynurenine. From this, a series of metabolic processes called kynurenine pathway produces biologically active metabolites affecting immune and nervous systems (Scheme 1.1).¹



Scheme 1.1 The Kynurenine Pathway

The dioxygenation of tryptophan is initiated by binding molecular oxygen to the ferrous heme of IDO (Scheme 1.2).² It is assumed that the electrophilic (*step 1a*) or radical addition (*step 1b*) of oxygen to tryptophan induces the formation of an epoxide with one oxygen added through an alkylperoxo intermediate. And then, the ferryl species attacks the epoxide to form *N*-formylkynurenine with second oxygen inserted while regenerating ferrous species.



Scheme 1.2 Dioxygenase Mechanism of Tryptophan^{2c}

Depletion of tryptophan inhibits the growth of viruses and other bacteria since tryptophan is the least available and thus most important essential amino acid for their growth. Based on this phenomenon, when the induction of IDO was observed in cancer patients in the 1950s, it was hypothesized cancer growth could be suppressed due to starvation of an essential amino acid.³ But in 1998, the biological significance of IDO induction has been examined by the Munn and Mellor group.⁴ They reported that IDO prevents fetus from maternal T-cell attack during the pregnancy by degrading tryptophan present in cells. It is identified that the

concentration of T lymphocytes is highly sensitive to tryptophan deprivation, and therefore IDO induces immune tolerance. As a result of the continuous studies on the correlation between IDO and immune response,⁵ it is found that IDO contributes to immune regulation through two mechanisms. The one is based on tryptophan depletion which triggers downstream stress-response pathways including general control non-depressible 2 (GCN2) and mammalian target of rapamycin (mTOR). GCN2 is activated when uncharged tRNA levels are increased by lack of tryptophan and causes G1 T cell cycle arrest and apoptosis.⁶ Depletion of tryptophan can also stop T-cell proliferation through suppression of an immunoregulatory kinase mTOR.⁷ The other one is based on kynurenine production. The kynurenine acts as an endogenous ligand for the aryl hydrocarbon receptor (AhR).⁸ The AhR is a ligand-activated transcription factor, activated by xenotoxins such as dioxin and involved in tumorigenesis. Kynurenine binding to AhR promotes the differentiation of regulatory T cells (T_{reg}), which leads to suppression of antitumor immune responses. In addition, other accumulated tryptophan catabolites such as 3-hydroxyanthranilic and quinolinic acids can cause T-cell apoptosis.⁹ Overall, expression of IDO induces immunosuppression (Figure 1.1).

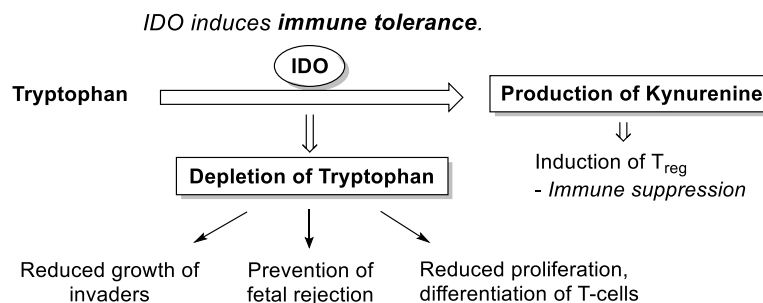


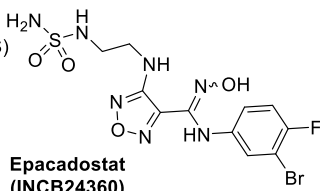
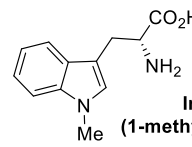
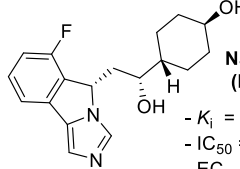
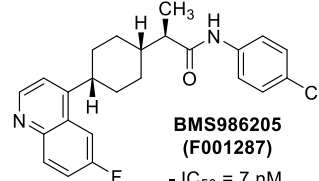
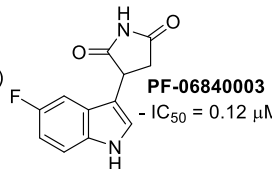
Figure 1.1 Effects of IDO Expression

The discovery of IDO role has led to redefinition of the meaning of increased IDO activity observed in cancer patients. It has been hypothesized that solid tumors evade the effective immune response by IDO expression. Indeed, IDO is found to be overexpressed in many cancers, and increased expression of IDO is correlated with a poor prognosis for patients with cancers.¹⁰ Thus, IDO has emerged as a promising and powerful therapeutic target in cancer treatment. Efforts have been made to find small-molecule IDO inhibitors based on the assumption that blockade of IDO activity would restore immunity and anticancer effects.¹¹ In 2005, Prendergast and coworkers reported the synergistic effect of IDO inhibitors and the cytotoxic agent to tumor.¹² In their observations, tumor growth was suppressed when 1-methyltryptophan (1MT), a well known IDO inhibitor, was treated alone toward tumor bearing breast cancer mice, but, regression of tumors was not confirmed. On the other hand, treatment with a combination of the famous anti-cancer drug paclitaxel (Taxol[®]) and 1MT resulted in tumor regression. Starting from these studies, there have been continued attempts to obtain the anticancer effect through the inhibition of IDO, and some IDO inhibitors are currently undergoing clinical trials either independently or in combination with chemotherapy, vaccines and immune checkpoint inhibitors.

1.2 IDO Inhibitors in Clinical Trials

According to a recent report,¹³ companies that have developed small-molecule IDO inhibitors have made large contracts with big pharmaceutical companies, and preclinical studies and clinical trials are under way to evaluate the anticancer effects

of these molecules. The current clinical status of representative IDO inhibitors is summarized in the following table (Table 1.1).^{11,13} In this section, the five small-molecule inhibitors are described briefly.

Developer	Molecule	Partner(s)	Deal terms	Clinical status
Incyte (Delaware, US)	 <p>Epacadostat (INCB24360) - IC₅₀ = 73 nM - IC₅₀ = 7.1 nM (HeLa)</p>	Advaxis (Princeton, NJ) AstraZeneca (London) Bristol-Myers Squibb (BMS) Genentech (Roche, Basel) & Merck (Kenilworth, NJ)	Undisclosed	Phase III
NewLink Genetics (Iowa, US)	 <p>Indoximod (1-methyl-D-tryptophan) - K_i = 35-62 μM - IC₅₀ = 2.5 μM (HeLa)</p>	Unpartnered	Not applicable	Phase I/II
NewLink Genetics (Iowa, US)	 <p>Navoximod (NLG-919) - K_i = 7 nM - IC₅₀ = 13 nM - EC₅₀ = 75 nM</p>	Genentech <i>handing back rights (June, 6, 2017)</i>	License agreement, \$150 million upfront plus \$1 billion milestones	Phase IB
Flexus Bioscience (California, US)	 <p>BMS986205 (F001287) - IC₅₀ = 7 nM</p>	BMS	Acquisition, \$800 million upfront plus \$450 million development milestones	Phase II
iTeos Therapeutics (Gosselies, Belgium)	 <p>PF-06840003 - IC₅₀ = 0.12 μM</p>	Pfizer (New York) <i>handing back rights (January, 4, 2017)</i>	\$35 million upfront plus undisclosed milestones, equity investment and research funding	Phase I
IOmet Pharma (Edinburgh, UK)	Undisclosed IDO, TDO inhibitors & dual IDO/TDO inhibitors IOM 2983	Unpartnered	Not applicable	Preclinical

Nature Biotechnology 2015, 33, 321.
2018 updated

Table 1.1 Clinical Trials for IDO Inhibitors

a. Epacadostat (INCB24360)

Epacadostat is a reversible, tryptophan-competitive inhibitor with high potency. Incyte corporation discovered a hydroxyamidine hit as a micromolar level IDO inhibitor through high throughput screening (HTS) of their internal collection of approximately 300,000 compounds (Figure 1.2).¹⁴ Various carboximidamides were synthesized and tested for inhibitory activity of IDO, resulting in INCB14943 as a proof-of-concept compound. INCB14943 proved good efficacy in IDO enzymatic and cellular assays but low oral bioavailability in rodent pharmacokinetics. The metabolism studies revealed that hydroxyamidine compounds are susceptible to glucuronidation. As a result of structure-activity relationship (SAR) studies, the IDO inhibitor Epacadostat, which has a low glucuronidation rate while maintaining cellular efficacy, was developed through introduction of bulky and polar side chain at the C3 position of furazan. The X-ray crystal structure of Epacadostat revealed that the compound formed a broad intramolecular hydrogen bonding network. It is believed that this structural feature not only increases the cell permeability by reducing the effective polarity of the compound but also contributes to stabilizing the high energy *cis*-form of amidine.^{14b}

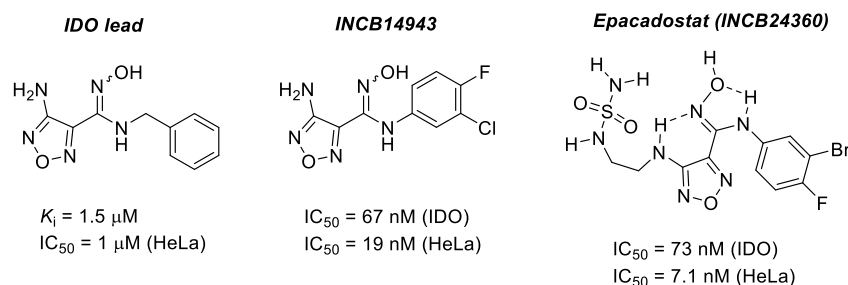


Figure 1.2 Development of the Epacadostat

Epacadostat is currently being evaluated in a phase III clinical trial as a monotherapy and in combination with various antibodies in patients with advanced and metastatic tumors. But recently, Incyte and Merck& Co. reported a disappointing result that the Phase III trial combining Epacadostat with Merck's checkpoint inhibitor Keytruda (pembrolizumab) failed to treat metastatic melanoma patients.¹⁵

b. Indoximod (1-methyl-D-tryptophan)

1-Methyltryptophan (1MT) is the most widely used IDO inhibitor in preclinical studies. The two isomers of 1MT – L and D forms, exhibit different biological activities.¹⁶

The L isomer is found to be a more potent inhibitor of IDO activity in purified enzyme assays. On the other hand, the D isomer does not bind to or inhibit a purified IDO enzyme and is more effective as an anticancer agent in chemotherapy *in vivo*. The Prendergast and coworkers reported¹⁷ an explanatory mechanism of action of Indoximod. Interestingly, Indoximod is interpreted by mTORC1 (mammalian target of rapamycin complex 1) in cells as a mimicking L-tryptophan. The protein kinase complex mTORC1 regulates cell growth including T cells, and its activity is inhibited by deprivation of essential amino acids such as tryptophan. Indoximod acts as a mimetic of tryptophan and restore mTORC1 activity, which can lead to anticancer efficacy. Indoximod is in phase I/II clinical studies in combination with chemotherapeutic agents and immune checkpoint inhibitors for a variety of cancer treatments.

c. Navoximod (NLG-919)

The 4-phenylimidazole(4-PI) is known as a weak noncompetitive IDO1 inhibitor that binds to heme.¹⁸ As a co-crystal structure between 4-PI and IDO was reported in 2006,¹⁹ various 4-PI derivatives were designed by structure-based approach and Navoximod was developed based on fused phenylimidazole scaffold. The *in vivo* study revealed that the treatment of Navoximod resulted in significant reduction of tumor size.²⁰ But disappointingly, Navoximod showed only a 10% overall response rate in several tumor types in combination with checkpoint inhibitor Tecentriq (Atezolizumab). Therefore, Genentech has handed back rights of Navoximod to NewLink Genetics.

d. BMS-986205 (F001287)

BMS-986205 identified as an irreversible IDO inhibitor with differentiated mechanism.²¹ This compound inhibits IDO by competing heme binding to apo-IDO, the heme dissociated form. It is found that heme binding to IDO is reversible process and heme lability is dependent on the oxidation state of iron in the heme. Especially in the inactive ferric form, the dissociation between enzyme and heme occurs relatively high rate than ferrous form. Heme is replaced by the inhibitor in the enzyme, which causes IDO inhibition. BMS-986205 is being studied in phase I/II clinical trials as a monotherapy and in combination with Opdivo (nivolumab) to treat advanced cancers.

e. PF-06840003

PF-06840003 is a noncompetitive, non-heme binding inhibitor.²² The co-crystal structure of PF-06840003 and hIDO1 shows no direct interaction between the compound and iron atom. The inhibitor entered phase I study in malignant glioma patients as monotherapy, but interim data fell short of Pfizer's expectation. Therefore, Pfizer has handed back rights of PF-06840003 to iTeos Therapeutics.

1.3 Conclusion

In recent years, exciting progresses in the development of immunotherapeutics for oncology have been achieved, rendering IDO as the key target in cancer immunotherapy. Thus, the discovery of IDO inhibitors has been the subject of intensely ongoing research in academia and in pharmaceutical companies. Several IDO inhibitors have undergone clinical evaluation. Due to the recent negative clinical results, there is much attention towards the result of ongoing clinical programs. Therefore, further understanding of the IDO is required for the development its inhibitor.

1.4 References

- [1] (a) Grohmann, U.; Fallarino, F.; Puccetti, P. *Trends Immunol.* **2003**, *24*, 242. For reviews on kynurenines, see: (b) Cervenka, I; Agudelo, L. Z.; Ruas, J. L. *Science* **2017**, *357*, 369. (c) Vécsei, L.; Szalárdy, L.; Fülöp, F.; Toldi, J. *Nat. Rev. Drug Discov.* **2013**, *12*, 64.
- [2] (a) Lewis-Ballester, A.; Batabyal, D.; Egawa, T.; Lu, C.; Lin, Y.; Marti, M. A.; Capece, L.; Estrin, D. A.; Yeh, S. R. *Proc. Natl. Acad. Sci. U. S. A.* **2009**, *106*, 17371.

(b) Capece, L.; Lewis-Ballester, A.; Batabyal, D.; Di Russo, N.; Yeh, S. R.; Estrin, D. A.; Marti, M. A. *JBIC, J. Biol. Inorg. Chem.* **2010**, *15*, 811. (c) Basran, J.; Efimov, I.; Chauhan, N.; Thackray, S. J.; Krupa, J. L.; Eaton, G.; Griffith, G. A.; Mowat, C. G.; Handa, S.; Raven, E. L. *J. Am. Chem. Soc.* **2011**, *133*, 16251. (d) Capece, L.; Lewis-Ballester, A.; Yeh, S. R.; Estrin, D. A.; Marti, M. A. *J. Phys. Chem. B* **2012**, *116*, 1401.

[3] (a) Ozaki, Y.; Edelstein, M. P.; Duch, D. S. *Proc. Natl. Acad. Sci. U. S. A.* **1988**, *85*, 1242. (b) Yasui, H.; Takai, K.; Yoshida, R.; Hayaishi, O. *Proc. Natl. Acad. Sci. U. S. A.* **1986**, *83*, 6622.

[4] Munn, D. H.; Zhou, M.; Attwood, J. T.; Bondarev, I.; Conway, S. J.; Marshall, B.; Brown, C.; Mellor, A. L. *Science* **1998**, *281*, 1191.

[5] For selected reviews on IDO, see: (a) Munn, D. H.; Mellor, A. L. *Trends Immunol.* **2016**, *37*, 193. (b) Munn, D. H.; Mellor, A. L. *Trends Immunol.* **2013**, *34*, 137. (c) Mellor, A. L.; Lemos, H.; Huang, L. *Front. Immunol.* **2017**, *8*, 1360. (d) Van Baren, N.; Van den Eynde, B. J. *Front. Immunol.* **2015**, *6*, 34.

[6] (a) Munn, D. H.; Sharma, M. D.; Baban, B.; Harding, H. P.; Zhang, Y.; Ron, D.; Mellor, A. L. *Immunity* **2005**, *22*, 633. (b) Munn, D. H.; Shafizadeh, E.; Attwood, J. T.; Bondarev, I.; Pashine, A.; Mellor, A. L. *J. Exp. Med.* **1999**, *189*, 1363.

[7] Metz, R.; Rust, S.; Duhadaway, J. B.; Mautino, M. R.; Munn, D. H.; Vahanian, N. N.; Link, C. J.; Prendergast, G. C. *Oncoimmunology* **2012**, *1*, 1460.

[8] (a) Opitz, C. A.; Litzenburger, U. M.; Sahm, F.; Ott, M.; Tritschler, I.; Trump, S.; Schumacher, T.; Jestaedt, L.; Schrenk, D.; Weller, M.; Jugold, M.; Guillemin, G. J.; Miller, C. L.; Lutz, C. Radlwimmer, B.; Lehmann, I.; von Deimling, A.; Wick, W.; Platten, M. *Nature* **2011**, *478*, 197. (b) Mezrich, J. D.; Fechner, J. H.; Zhang, X.; Johnson, B. P.; Burlingham, W. J.; Bradfield, C. A. *J. Immunol.* **2010**, *185*, 3190.

[9] (a) Fallarino, F.; Grohmann, U.; Vacca, C.; Bianchi, R.; Orabona, C.; Spreca, A.; Fioretti, M. C.; Puccetti, P. *Cell Death Differ.* **2002**, *9*, 1069. (b) Terness, P.; Bauer, T.M.; Röse, L.; Dufter, C. Watzlik, A.; Simon, H. Opelz, G. *J. Exp. Med.* **2002**, *196*, 447.

[10] Uyttenhove, C.; Pilotte, L.; Théate, I.; Stroobant, V.; Colau, D.; Parmentier, N.; Boon, T.; Van den Eynde, B. *J. Nat. Med.* **2003**, *9*, 1269.

[11] For selected recent reviews on IDO inhibitors, see: (a) Prendergast, G. C.; Malachowski, W. P.; DuHadaway, J. B.; Muller, A. J. *Cancer. Res.* **2017**, *77*, 6795. (b) Röhrig, U. F.; Majjigapu, S. R.; Vogel, P.; Zoete, V.; Michielin, O. *J. Med. Chem.* **2015**, *58*, 9421. (c) Weng, T.; Qiu, X.; Wang, J.; Li, Z.; Bian, J. *Eur. J. Med. Chem.* **2018**, *143*, 656. (d) Coletti, A.; Greco, F. A.; Dolciami, D.; Camaioni, E.; Sardella, R.; Pallotta, M. T.; Volpi, C.; Orabona, C. Grohmann, U.; Macchiarulo, A. *Med. Chem. Commun.* **2017**, *8*, 1378. (e) Qian, S.; Zhang, M.; Chen, Q.; He, Y.; Wang, W.; Wang, Z. *RSC Adv.* **2016**, *6*, 7575. (f) Dolušić, E.; Frédérick, R. *Expert Opin. Ther. Patents* **2013**, *23*, 1367.

[12] Muller, A. J.; DuHadaway, J. B.; Donover, P. S.; Sutanto-Ward, E.; Prendergast, G. C. *Nat. Med.* **2005**, *11*, 312.

[13] Sheridan, C. *Nat. Biotechnol.* **2015**, *33*, 321.

[14] (a) Yue, E. W.; Douty, B.; Wayland, B.; Bower, M.; Liu, X.; Leffet, L.; Wang, Q.; Bowman, K. J.; Hansbury, M. J.; Liu, C.; Wei, M.; Li, Y.; Wynn, R.; Burn, T. C.; Koblish, H. K.; Fridman, J. S.; Metcalf, B.; Scherle, P. A.; Combs, A. P. *J. Med. Chem.* **2009**, *52*, 7364. (b) Yue, E. W.; Sparks, R.; Polam, P.; Modi, D.; Douty, B.; Wayland, B.; Glass, B.; Takvorian, A.; Glenn, J.; Zhu, W.; Bower, M.; Liu, X.; Leffet, L.; Wang, Q.; Bowman, K. J.; Hansbury, M. J.; Wei, M.; Li, Y.; Wynn, R.; Burn, T. C.; Koblish, H. K.; Fridman, J. S.; Emm, T.; Scherle, P. A.; Metcalf, B.;

- Combs, A. P. *ACS Med. Chem. Lett.* **2017**, *8*, 486.
- [15] Long, G. V. Proceeding of the American Society of Clinical Oncology (ASCO) annual meeting, Chicago, Jun 1-5, 2018; Abst 108.
- [16] Hou, D. Y.; Muller, A. J.; Sharma, M. D.; DuHadaway, J.; Banerjee, T.; Johnson, M.; Mellor, A. L.; Prendergast, G. C.; Munn, D. H. *Cancer Res.* **2007**, *67*, 792.
- [17] Metz, R.; Rust, S.; Duhadaway, J. B.; Mautino, M. R.; Munn, D. H.; Vahanian, N. N.; Link, C. J.; Prendergast, G. C. *Oncoimmunology* **2012**, *1*, 1460.
- [18] Sono, M.; Cady, S. G. *Biochemistry* **1989**, *28*, 5392.
- [19] Sugimoto, H.; Oda, S.; Otsuki, T.; Hino, T.; Yoshida T, Shiro Y. *Proc. Natl. Acad. Sci. U. S. A.* **2006**, *103*, 2611.
- [20] Mautino, M. R.; Jaipuri, F. A.; Waldo, J.; Kumar, S.; Adams, J.; Van Allen, C.; Marcinowicz-Flick, A; Munn, D. H.; Vahanian, N. N.; Link, C. J. *Cancer Res.* **2013**, *73*, 491.
- [21] Nelp, M. T.; Kates, P. A.; Hunt, J. T.; Newitt, J. A.; Balog, A.; Maley, D.; Zhu, X.; Abell, L.; Allentoff, A.; Borzilleri, R.; Lewis, H. A.; Lin, Z.; Seitz, S. P.; Yan, C.; Groves, J. T. *Proc. Natl. Acad. Sci. U. S. A.* **2018**, *115*, 3249.
- [22] Crosignani, S.; Bingham, P.; Bottemanne, P.; Cannelle, H.; Cauwenberghs, S.; Cordonnier, M.; Dalvie, D.; Deroose, F.; Feng, J. L.; Gomes, B.; Greasley, S.; Kaiser, S. E.; Kraus, M.; Négrerie, M.; Maegley, K.; Miller, N.; Murray, B. W.; Schneider, M.; Soloweij, J.; Stewart, A. E.; Tumang, J.; Torti, V. R.; Van Den Eynde, B.; Wythes, M. *J. Med. Chem.* **2017**, *14*, 9617.

Chapter 2: The Exiguamines

2.1 Introduction

Exiguamine A (Figure 2.1, **2.1**) was isolated from the marine sponge *Neopetrosia exigua* in 2006 by Raymond Andersen and co-workers.¹ Exiguamine A, discovered in library screening for small molecule IDO inhibitors, is found to be a very potent compound in *in vitro* assay against a purified recombinant human IDO at submicromolar levels ($K_i = 41 \pm 3$ nM).

The first total synthesis of this compound was achieved by the Trauner group in 2008. They also synthesized exiguamine B (Figure 2.1, **2.2**), a hydroxylated derivative of exiguamine A. Later, it was also extracted from the same *Neopetrosia exigua* by the Andersen group and confirmed to be a natural product.²

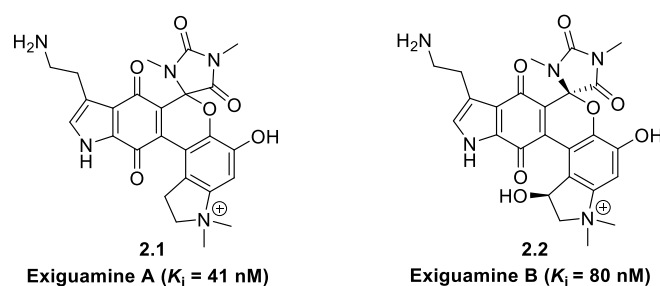


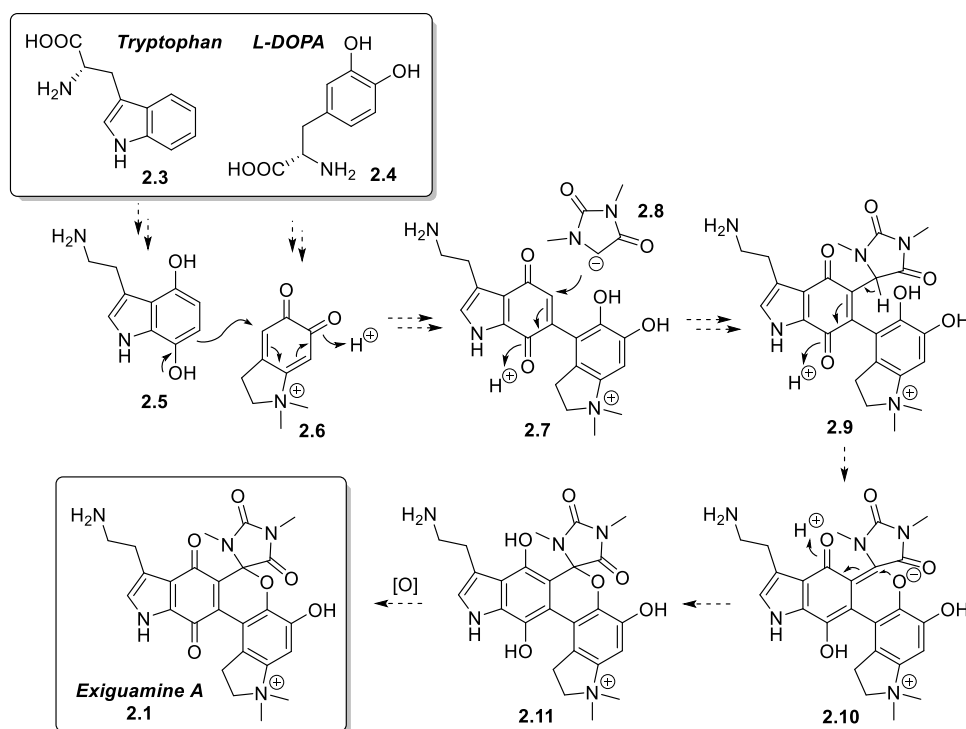
Figure 2.1 The Exiguamines

Exiguamine A, occurring as a racemate, is an unprecedented alkaloid molecule in which the hexacyclic skeleton is made of six continuously connected ring systems. The five rings on the plane are bent at the pyran with which tryptamine quinone and dihydroindolinium moieties are fused and a hydantoin is spiro-connected. It has a

highly conjugated quinone system, with a quaternary ammonium ion and many polar nitrogen and oxygen functional groups. Its potent bioactivity and characteristic structural features render exiguamine A an attractive candidate for total synthesis studies.

2.2 Proposed Biogenesis by the Andersen Group

The Andersen group suggests a biosynthetic pathway of exiguamine A as shown in Scheme 2.1.



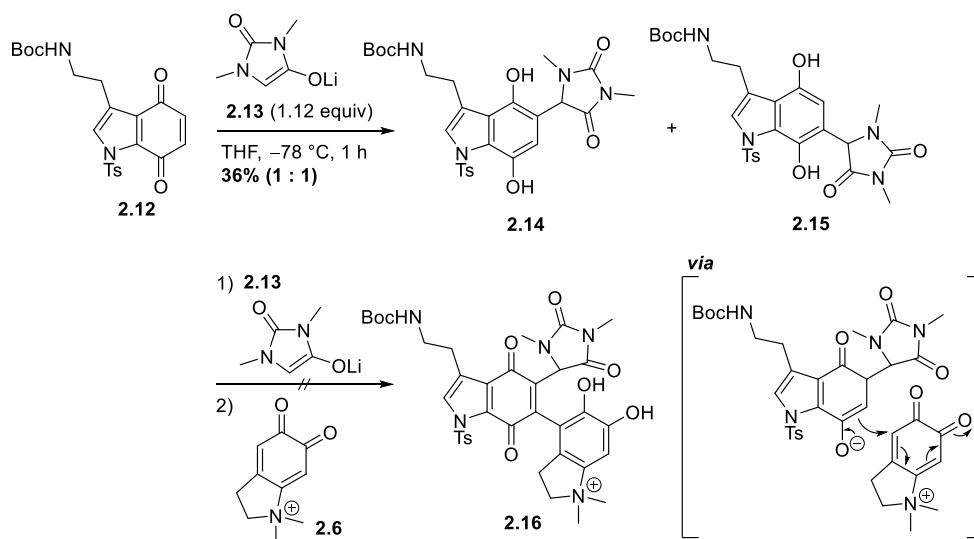
Scheme 2.1 Proposed Biogenesis by the Andersen Group

First, it was proposed that the coupling reaction would proceed between hydroquinone **2.5** derived from tryptophan and *ortho*-quinone **2.6** derived from

DOPA. The *N,N'*-dimethylhydantoin unit is then added to the resulting tetracyclic biaryl compound **2.7** to afford the central skeleton. After the three-component coupling stage, it is assumed that a series of tautomerization, Michael addition, and oxidation processes would have produced exiguamine A.

2.3 Total Synthesis of Exiguamines A and B by the Trauner Group

The first strategy for the synthesis of exiguamine A in the Trauner group was to follow the biosynthetic pathway proposed by the Andersen group. Three fragments, indoloquinone, indolinium-quinone and hydantoin, were synthesized, and three component coupling reactions were attempted (Scheme 2.2).³

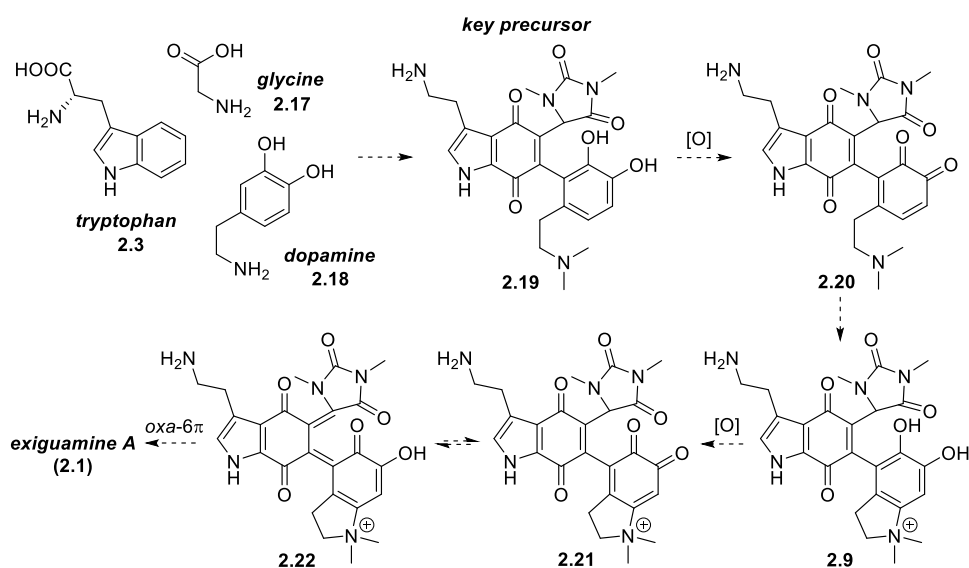


Scheme 2.2 Studies Toward Exiguamine A

They investigated the reactivity between the *N*-protected tryptamine quinone **2.12** and an enolate derived from the hydantoin. It was observed enolate **2.13** addition to quinone **2.12** gave a low yield with poor regioselectivity.

Based on this, further attempts were made to reach for the exiguamine A precursor

in one step through three component coupling, in which indoloquinone **2.12** would act sequentially as an electrophile and a nucleophile. However, this ambitious plan failed as the reaction did not generate desired three-component coupled product **2.16**. Therefore, they proposed a revised synthetic plan (Scheme 2.3).

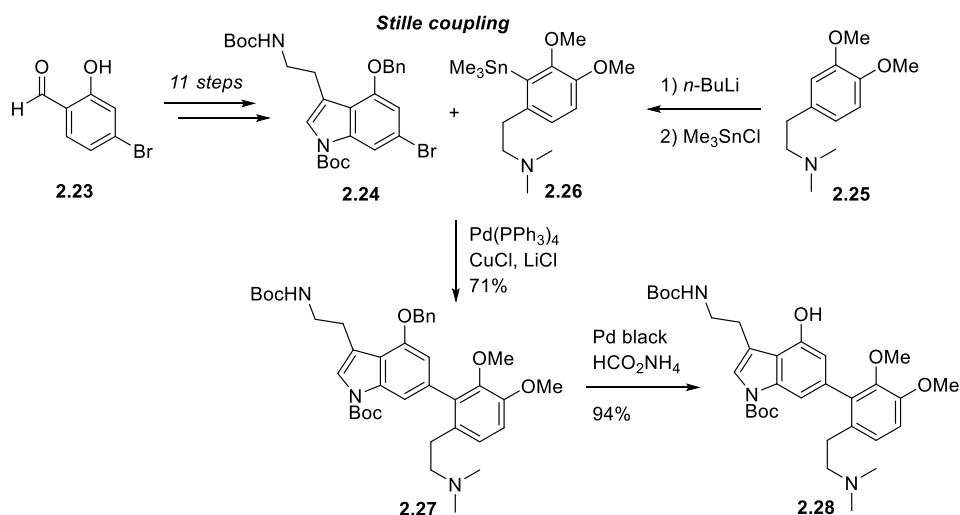


Scheme 2.3 Revised Biosynthetic Approach

The proposed pathway was to form a quaternary ammonium ion at the end of the synthesis by applying an oxidative catecholamine chemistry. It was assumed that when oxidation of key precursor **2.19**, having indoloquinone, hydantoin and dopamine moieties in place, to bisquinone **2.20** would induce an intramolecular nucleophilic attack by the tertiary amine. After tautomerization, indolinium intermediate **2.9** would proceed further oxidation and tautomerization to form exiguamine A *via* oxa-6 π electrocyclization.

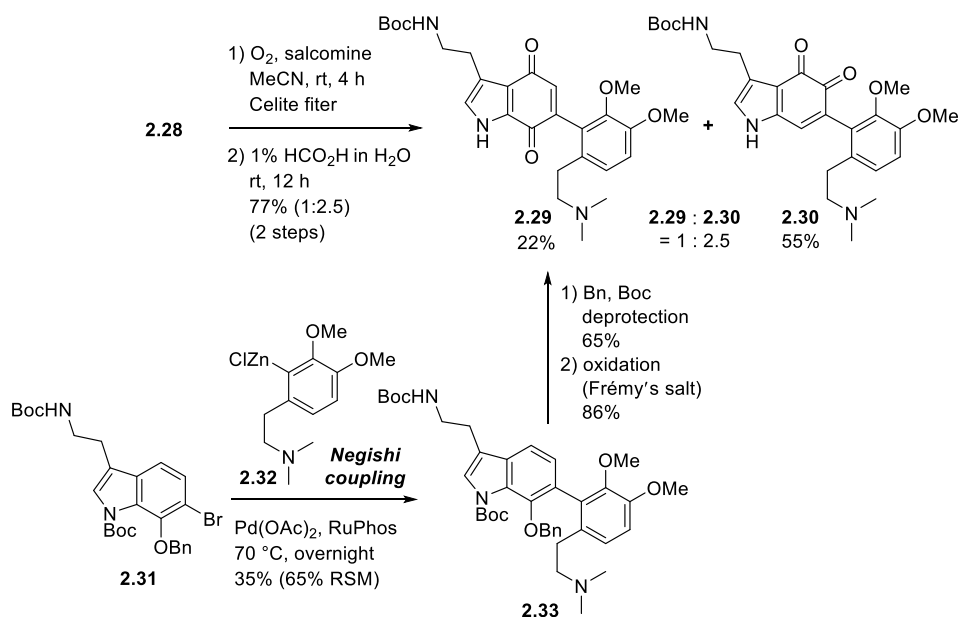
To obtain key intermediate **2.19**, tryptamine and dopamine derivatives were combined *via* formation of biaryl **2.28** (Scheme 2.4). The biaryl linkage was formed

by the Stille coupling between bromotryptamine and phenethylamine derivatives. It was notable that the requisite aryl stannane could be prepared *via* regioselective lithiation of dopamine derivative **2.25**.



Scheme 2.4 Synthesis of Biaryl **2.28**

The phenol **2.28** obtained by debenzylation of **2.27** was oxidized to afford indoloquinone **2.29** (Scheme 2.5). The salcomine-mediated oxidation of phenol **2.28**, however, produced more of the undesired *ortho*-quinone **2.30** than the desired *para*-quinone **2.29**. The regioselectivity issue associated with oxidation of a 4-hydroxyindole derivative was solved by employing a 7-hydroxyindole compound as the substrate for oxidation. While oxidation of 7-hydroxyindole **2.33** using Frémy's salt gave only *para*-quinone **2.29**, the Negishi coupling for the preparation of biaryl **2.33** took place in a low yield.

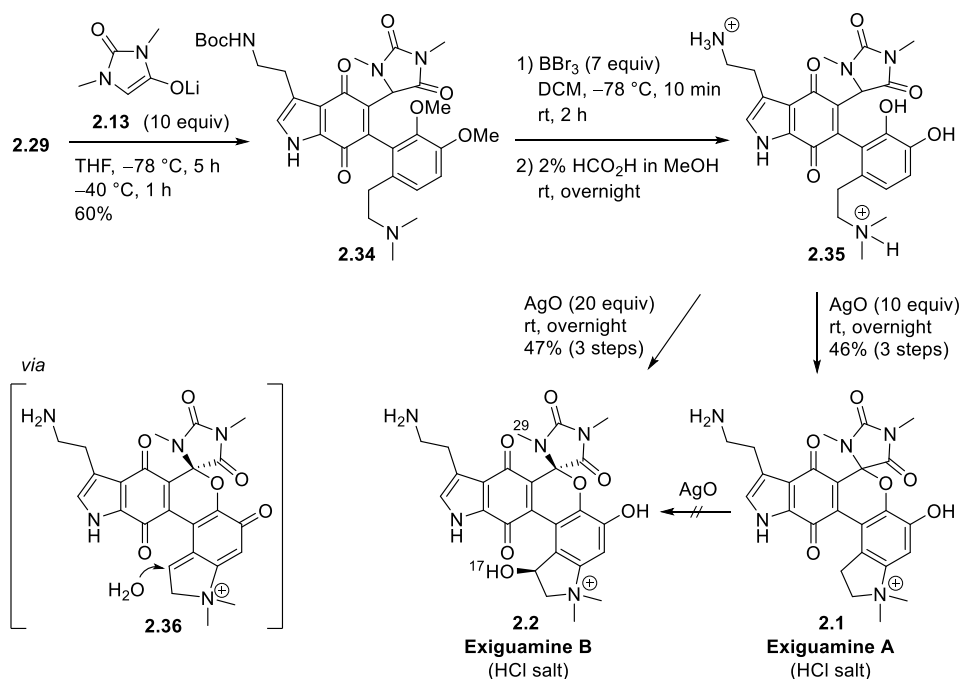


Scheme 2.5 Preparation of Indoloquinone **2.29**

The skeleton of exiguamine A was constructed by adding enolate **2.13** derived from *N,N'*-dimethylhydantoin to *para*-quinone **2.29**, and key precursor **2.35**, containing all the carbon atoms of exiguamine A, was obtained by removing all the protecting groups using boron tribromide (Scheme 2.6).

Oxidative catecholamine chemistry of the fully deprotected precursor **2.35** was investigated with various oxidants. It was found that exiguamine A could be synthesized from the oxidation of catechol **2.35** only when 10 equivalents of AgO was used. Interestingly, a new compound was discovered from the reaction with 20 equivalents of AgO, which were used to improve the low yield. The new compound was an oxidized form of exiguamine A and named exiguamine B. In order to determine whether exiguamine B was derived from exiguamine A, exiguamine A was treated with excess AgO, but exiguamine B could not be obtained. Therefore, the possibility that exiguamine A was converted to exiguamine B through oxidation to quinone methide **2.36** and hydration was excluded. The relative stereochemistry

of the two stereocenters of exiguamine B was determined by observing the correlation between hydroxygroup (OH-17) and hydantoin methyl (CH₃-29) resonance signals in the ROESY spectra.



Scheme 2.6 Synthesis of Exiguamine A and Discovery of Exiguamine B

The Trauner group proved their biosynthetic hypothesis of exiguamine A by synthesizing the key biomimetic precursor and completing the total synthesis. Despite many appreciable features, there are some disadvantages and limitations in the Trauner synthesis. To avoid regioselectivity issues encountered in the introduction of the hydantoin into the indoloquinone, biaryl **2.28** had first to be prepared by coupling the dopamine moiety and the indoloquinone precursor. In this approach, the Stille cross-coupling required pre-functionalization of both coupling partners. In the oxidation process, another regiochemistry issue arose from the formation of the undesired *ortho*-quinone **2.30** as the major product. We proposed

new synthetic strategies that could overcome these regioselectivity and pre-functionalization issues, and completed total synthesis of exiguamine A as described in Chapter 3.

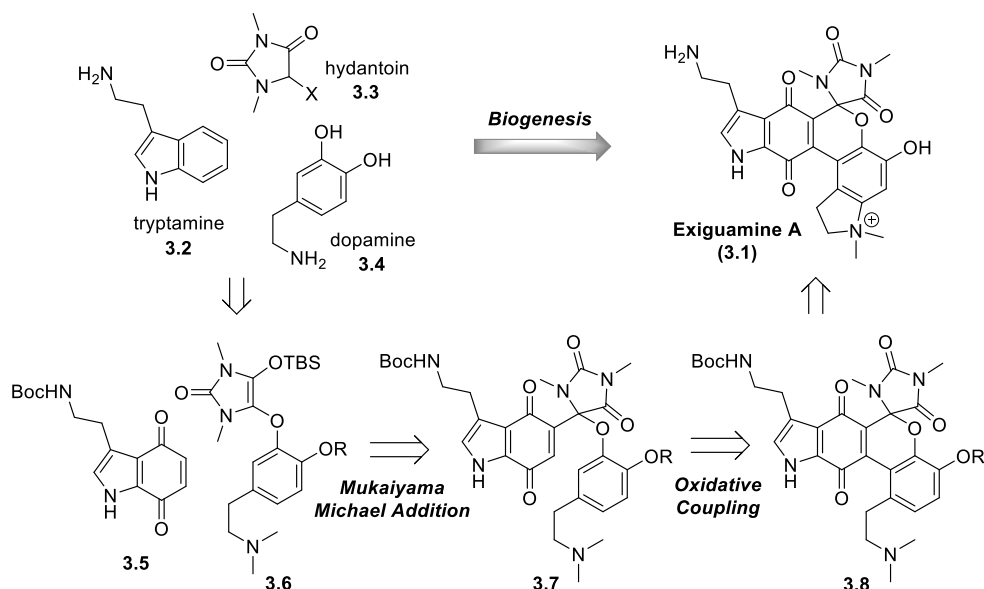
2.4 References

- [1] Brastianos, H. C.; Vottero, E.; Patrick, B. O.; Soest, R. V.; Matainaho, T.; Mauk, A. G.; Andersen, R. J. *J. Am. Chem. Soc.* **2006**, *128*, 16046.
- [2] Volgraf, M.; Lumb, J.-P.; Brastianos, H. C.; Carr, G.; Chung, M. K. W.; Munzel, M.; Mauk, A. G.; Andersen, R. J.; Trauner, D. *Nat. Chem. Biol.* **2008**, *4*, 535.
- [3] Sofiyev, V.; Lumb, J.-P.; Volgraf, M.; Trauner, D. *Chem. Eur. J.* **2012**, *18*, 4999.

Chapter 3: Total Synthesis of Exiguamine A and *Iso-Exiguamine A*

3.1 Retrosynthetic Analysis and Synthetic Plan

Our retrosynthetic analysis and synthetic plan of exiguamine A were based on the notion that exiguamine A consists of three building blocks: tryptamine quinone, dopamine, and hydantoin. In designing a synthetic plan with the three building blocks whose counterparts might exist in the biosynthetic pathway, formulated a convergent route that would assemble these three fragments efficiently (Scheme 3.1).



Scheme 3.1 Retrosynthetic Analysis

We envisioned that the hydantoin fragment might serve as a lynchpin to bring together the tryptamine quinone and dopamine moieties, constructing the pyran framework. The synthetic strategy of the pyran was designed by considering the oxidation - reduction equilibrium process between quinone and hydroquinone. An

addition reaction to quinone induces aromatization to hydroquinone which can become quinone again after re-oxidation. The tryptamine quinone and dopamine fragments are combined with the hydantoin as a linchpin that would tether the two aromatic fragments. Once put together, electron-deficient quinone and electron-rich aryl rings would spontaneously form the key C-C bond of the pyran. As a way to bundle up three fragments based on this plan, we first decided the construction of the C-O bond between dopamine and hydantoin via a S_N2 reaction of the phenoxide with the hydantoin having a suitable leaving group. Subsequently, addition of silyl enol ether **3.6** generated at the hydantoin fragment to tryptamine fragment **3.5** would form the key C-C bond *via* a Mukaiyama-Michael addition. This addition inducing a series of quinone-hydroquinone oxidation-reduction processes would give key precursor **3.7**. In this plan, the synthesis converges on securing two subunits for the Mukaiyama-Michael type addition. It was envisioned that they could be obtained from tryptamine, dopamine and hydantoin as suggested in biogenesis.

3.2 Preliminary Synthetic Studies by Dr. Venkataramanan Krishnamurthy in the Lee Group

Preliminary synthetic studies were conducted in the Lee group at Princeton University to verify that the proposed retrosynthesis might indeed be conceptually possible.

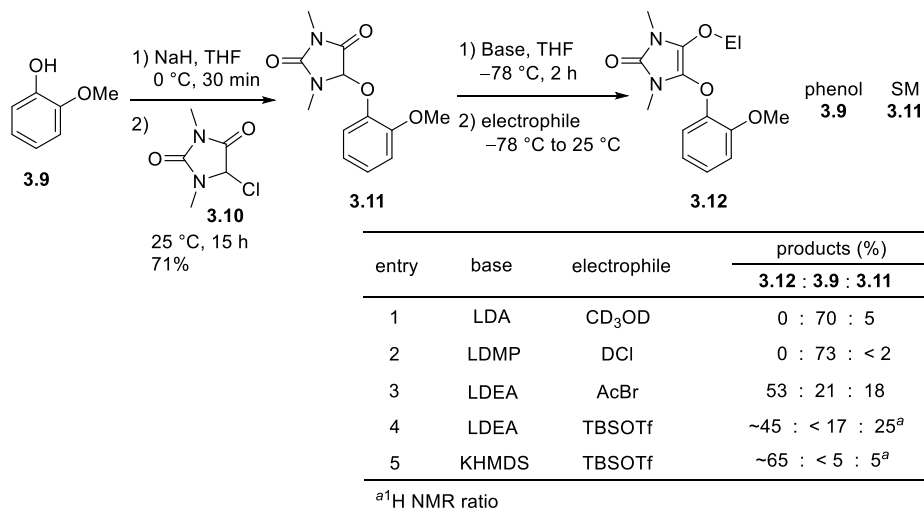
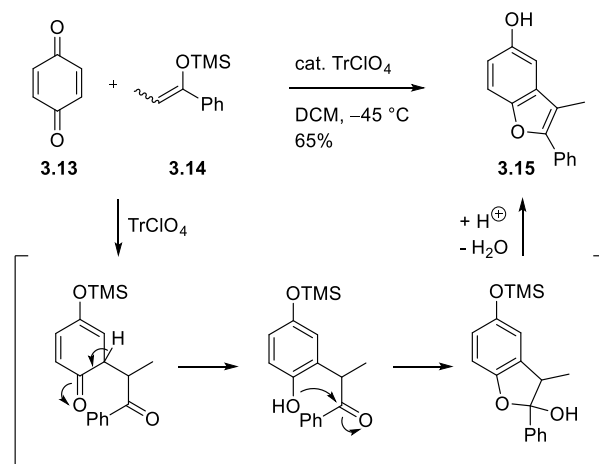


Table 3.1 Enolate Generation Reaction with Substrate **3.11**

In order to investigate the formation of the silyl enol ether, a simple model substrate was prepared by coupling hydantoin **3.10** with guaiacol, a commercially available phenol. The results for the enolate generation with a variety of bases and conditions are summarized (Table 3.1). Lithium diisopropyl amide (LDA, entry 1) and lithium 2,6-dimethylpiperidide (LDMP, entry 2) could not generate the enolate. It was observed that the C-O bond was susceptible to cleavage, forming phenol **3.9**. When lithium diethylamide (LDEA) and KHMDS were used as bases (entries 4, 5), the desired silyl enol ether was produced in a moderate yield.

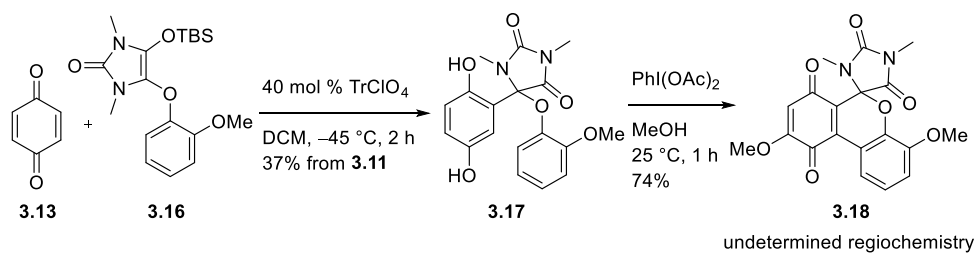
The obtained silyl enol ether was used to perform the Mukaiyama-Michael reaction, the key reaction of the approach. The Mukaiyama group reported that the reaction of 1,4-benzoquinone with a silyl enol ether in the presence of a catalytic amount of trityl perchlorate generated the benzofuran derivative in 65% yield (Scheme 3.2).¹ This product seemed to be produced by 1,4-addition of the silyl enol ether to benzoquinone, followed by aromatization and cyclocondensation as shown in this scheme. It was anticipated that our silyl enol ether and tryptamine quinone

would follow an addition pathway similar to this reaction.



Scheme 3.2 Example of Lewis Acid Catalyzed Mukaiyama-Michael Reaction

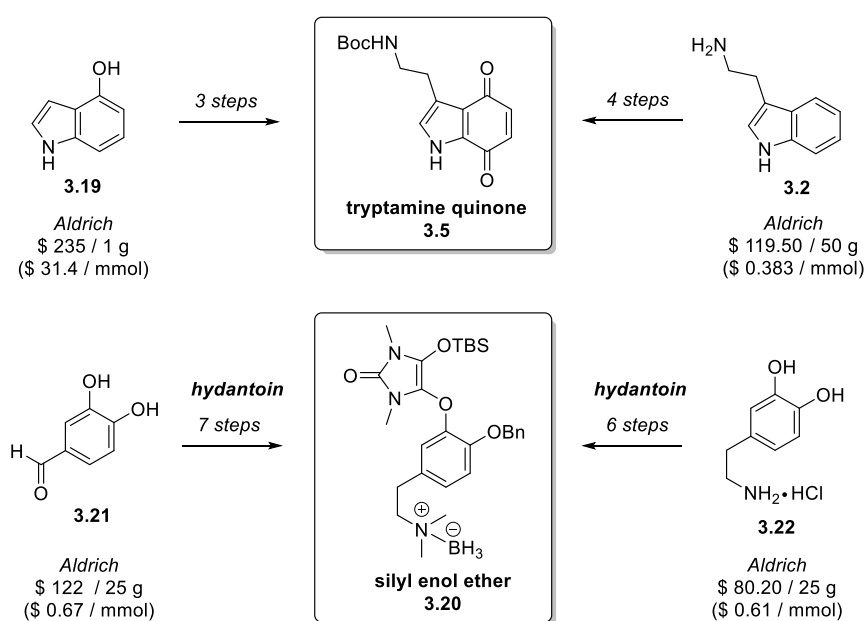
With silyl enol ether and 1,4-benzoquinone model substrates, the key Mukaiyama-Michael reaction was investigated (Scheme 3.3). Treatment of silyl enol ether **3.16** with benzoquinone **3.13** in the presence of a catalyst gave the desired bisphenol adduct **3.17** in moderate yields. Oxidation of bisphenol **3.17** using PIDA provided the required pyran **3.18** through cyclization, oxidation, and addition of MeOH. Thus, a series of quinone-hydroquinone oxidation chemistry has proven that it is possible to form a pyran moiety while forming C-C bonds.



Scheme 3.3 Model Studies for Key Steps

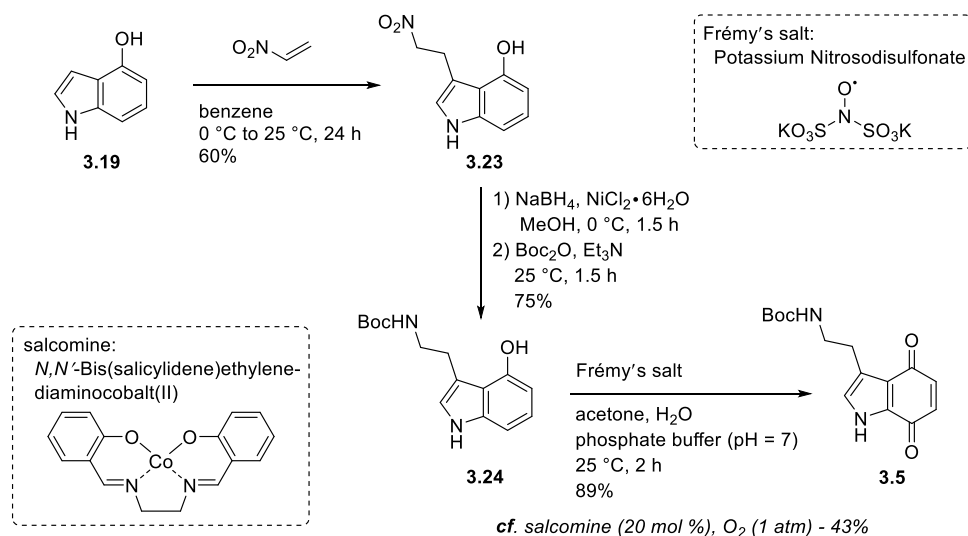
3.3 Syntheses of Fragments

The synthesis of two fragments that constitute the key precursors was achieved each with two methods (Scheme 3.4). One is a route that started from the compound with all carbon skeleton of the molecule, the other is a route that begins with a simple molecule and attaches the additional skeleton.



Scheme 3.4 Strategies for the Syntheses of Fragments

3.3.1 Tryptamine Quinone

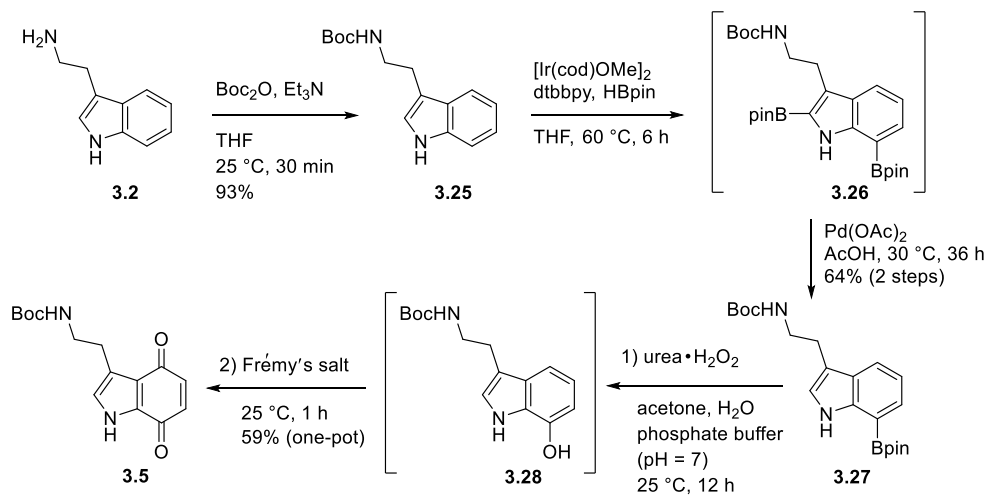


Scheme 3.5 Synthesis of Tryptamine Quinone: Homologation Approach

The tryptamine fragment was synthesized by converting 4-hydroxyindole to nitroethyl substituted indole **3.23** via a Michael reaction (Scheme 3.5).² Reduction of the nitro group by NaBH₄, followed by protection of the resulting amine with Boc₂O gave the Boc-protected tryptamine derivative **3.24**. Oxidation of hydroxyindole **3.24** using Frémy's salt gave tryptamine quinone **3.5** in 89% yield.³

Another synthetic route of the tryptamine quinone started from tryptamine, possessing all of carbon skeletons using C7 selective indole functionalization (Scheme 3.6). Recently, selective C7 borylation of indole using transition metal catalysts has been reported by several groups,⁴ and furthermore, the synthesis of indolequinone through continuous oxidation of the borylated product has been reported.^{4c,4d} According to a report by the Movassaghi group,^{4b} borylation was carried out using an Ir catalyst to produce C2 and C7 diborylated tryptamine **3.26**, which upon C2-selective protodeborylation using Pd(OAc)₂ gave the C7 boylated

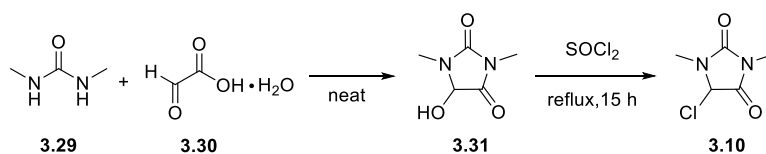
tryptamine **3.27** in 64% yield. Oxidation was achieved using hydrogen peroxide to afford a 7-hydroxytryptamine **3.28**. Further oxidation using Frémy's salt provided tryptamine quinone **3.5** in 59% yield.



Scheme 3.6 Synthesis of Tryptamine Quinone: Oxidation Approach

3.3.2 *N,N'*-Dimethyl-5-Chlorohydantoin

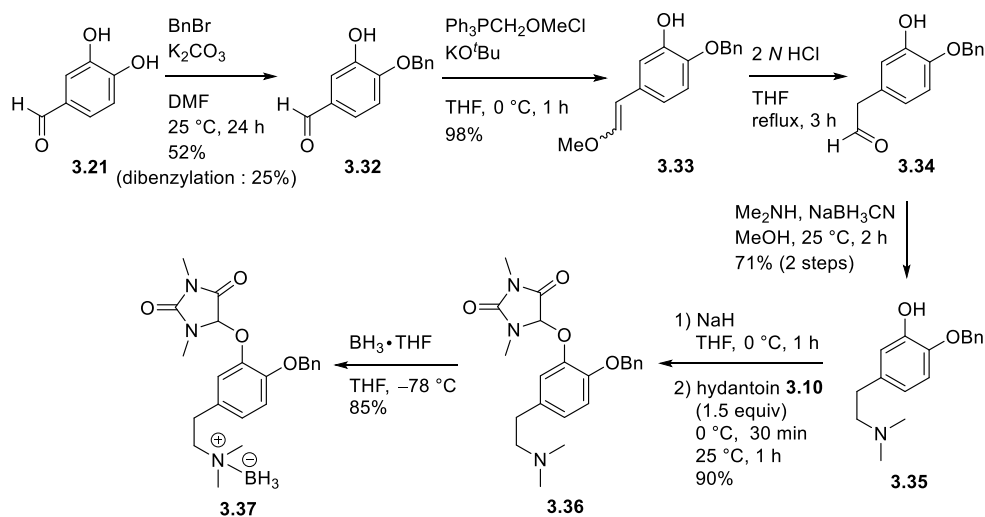
The synthesis of *N,N'*-dimethyl-5-chlorohydantoin **3.10** could be easily carried out starting from 5-hydroxyhydantoin (Scheme 3.7). *N,N'*-dimethylurea and glyoxylic acid monohydrate were condensed by reacting them neat to obtain 5-hydroxyhydantoin **3.31**.⁵ Heating a mixture of hydantoin **3.31** and thionyl chloride, followed by removal of excess thionyl chloride afforded 5-chlorohydantoin **3.10** in quantitative yield. It was found that 5-chlorohydantoin **3.10** is moisture sensitive and easily hydrolyzed to 5-hydroxyhydantoin **3.31**. Thus, the crude product was directly used for the next step without further purification.



Scheme 3.7 Synthesis of 5-Chlorohydantoin **3.10**

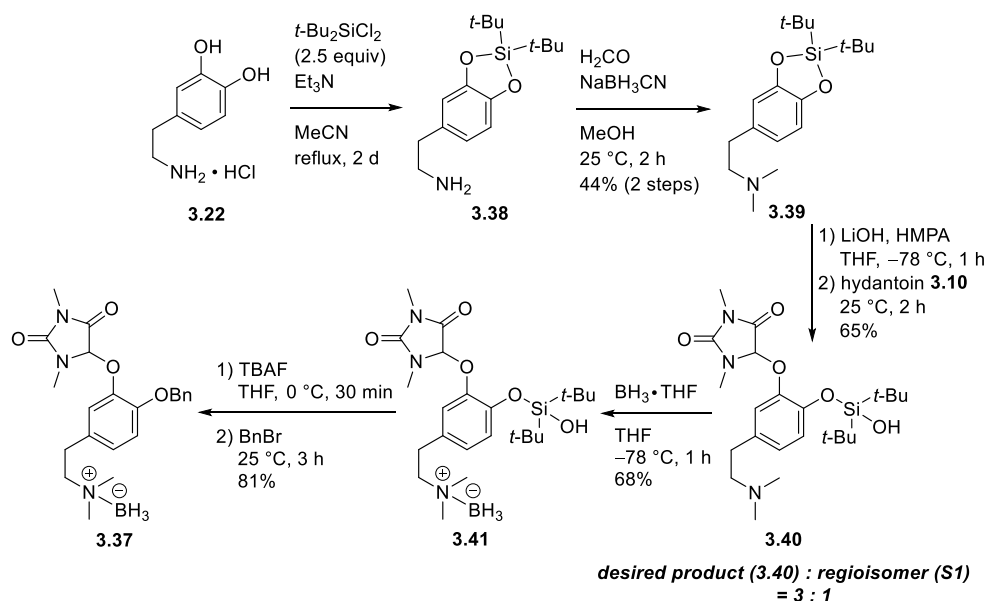
3.3.3 Dopamine-Hydantoin

For the synthesis of the dopamine-hydantoin fragment, our synthesis started with selective protection of protocatechuic aldehyde **3.21** (Scheme 3.8). Selective benzyl protection at the *para*-hydroxyl group of aldehyde,⁶ followed by a Wittig reaction gave desired enol ether **3.21**. Hydrolysis of the enol ether under acidic conditions generated homologous aldehyde **3.33**. Reductive amination of the aldehyde with dimethylamine yielded phenol **3.35** containing tertiary amine moiety. The coupling of phenol **3.35** with 5-chlorohydantoin **3.10** was achieved in 90% yield using sodium hydride as a base. Protection of the tertiary amine with borane-THF complex gave the targeted dopamine-hydantoin **3.37**. The crucial feature of the synthetic route starting from protocatechuic aldehyde was the differentiation of the two phenolic oxygen atoms, whereby the hydantoin moiety was installed in a site-selective manner.



Scheme 3.8 Synthesis of Dopamine-Hydantoin: Homologation Approach

Another synthetic route for the dopamine-hydantoin fragment was also developed by directly introducing the hydantoin into one of the two hydroxyl groups in dopamine (Scheme 3.9). The key step of this approach is to take advantage of a cyclic pentavalent silicon species by treating the silylene ether with a nucleophile, and then adding the 5-chlorohydantoin as an electrophile to form the desired mono alkylated product.⁷

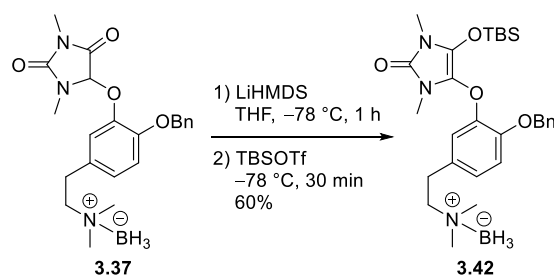


Scheme 3.9 Synthesis of Dopamine-Hydantoin: Privileged Approach

Treatment of dopamine with di-*tert*-butyldichlorosilane gave silylene **3.38**, which was subjected to reductive amination conditions to provide tertiary amine **3.39**. The coupling reaction between silylene **3.39** and chlorohydantoin **3.10** was achieved using LiOH and HMPA. Fortunately, this silicate approach produced the desired product **3.40** as the major isomer in a 3:1 regioisomeric ratio. Protection of the tertiary amine as a borane-THF complex and deprotection of the silicon group, followed by benzyl protection of the phenol, afforded the desired product **3.37**. The alternative route demonstrated that differential functionalization at the two hydroxyl

groups of dopamine could be possible using a selective silylene ring-opening strategy.

With dopamine-hydantoin **3.37** at hand, silyl enol ether **3.42** could be generated in 60% yield by using LiHMDS as base (Scheme 3.10). The silyl enol ether was found to be viable during workup and purification by flash column chromatography, but partial hydrolysis took place on a silica gel column. It was also found to be relatively unstable and could not be stored for a long time.

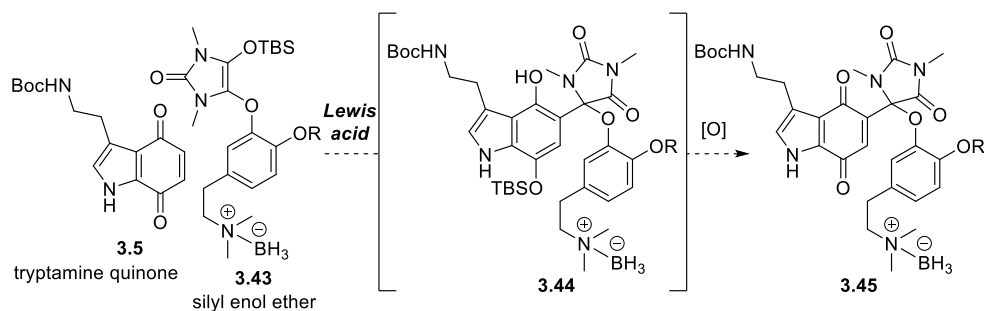


Scheme 3.10 Preparation of Silyl Enol Ether **3.42**

3.4 Union of Michael Donor and Acceptor

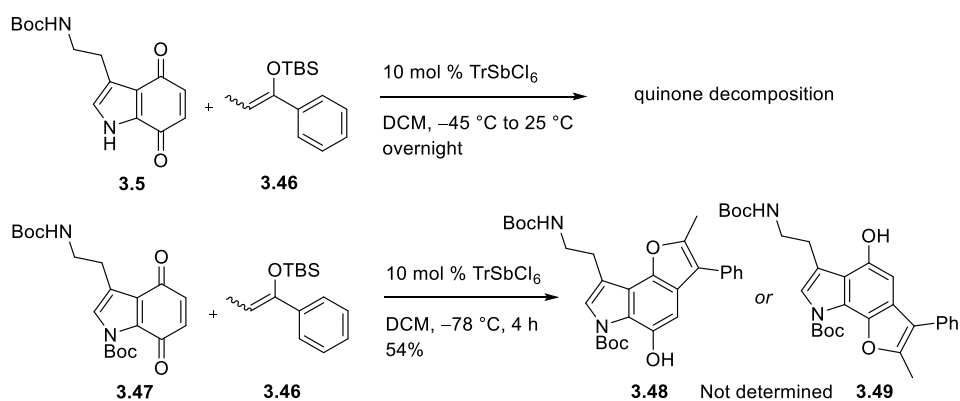
3.4.1 Lewis Acid Catalyzed Mukaiyama-Michael Reaction

Having the silyl enol ether and tryptamine quinone prepared, the key Mukaiyama-Michael reaction was investigated (Scheme 3.11).



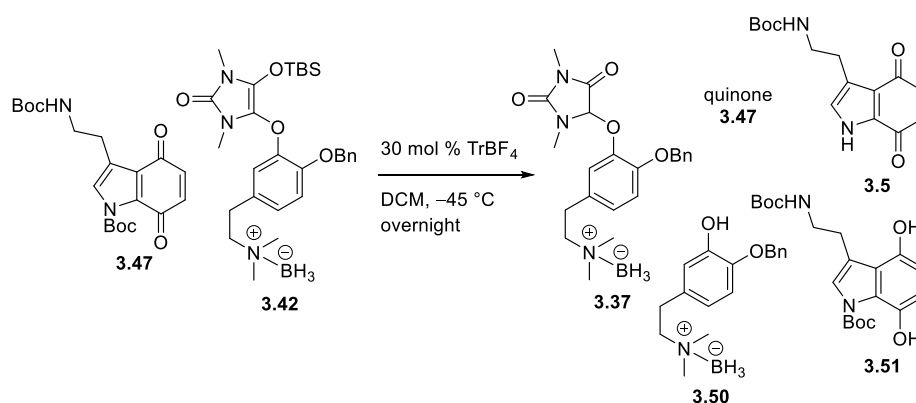
Scheme 3.11 Lewis Acid Catalyzed Mukaiyama-Michael Type Reaction

The scope of the Mukaiyama-Michael reaction was first investigated using Michael acceptors in free *N*-H and *N*-Boc forms with silyl enol ether **3.46** derived from propiophenone (Scheme 3.12). If the indole moiety was not protected, we could only observe consumption of tryptamine quinone **3.5**, which indicated that the protection of the indole nitrogen was important. We thought that the amine moiety could interrupt the action of the catalyst as a Lewis base. After protection of the indole nitrogen, the coupling of tryptamine quinone **3.47s** with silyl enol ether **3.46** was carried out using 10 mol % catalyst to obtain the product. While predicting the regiochemical outcome was difficult, only a single compound was obtained.



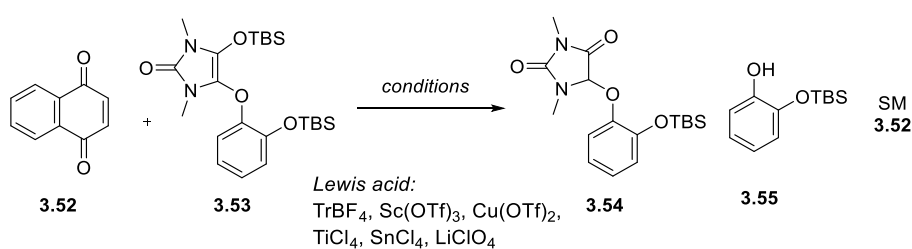
Scheme 3.12 Exploring the Reactivity of Michael Acceptor

Based on these observations, the Mukaiyama-Michael reaction was conducted with tryptamine quinone **3.47** and silyl enol ether **3.42** derived from the dopamine-hydantoin product (Scheme 3.13). However, unfortunately, the Mukaiyama-Michael addition of these elaborated reaction partners was disappointing. The major product was phenol **3.50**, which arose from the cleavage of between the hydantoin and dopamine. In addition, carbonyl compound **3.37** from hydrolysis of the silyl enol ether, starting quinone **3.47**, and quinone **3.5** could also be recovered.



Scheme 3.13 The Mukaiyama-Michael Reaction

Further model studies were conducted to identify the appropriate Mukaiyama-Michael reaction conditions (Scheme 3.14). Various Lewis acids were screened in the reaction of naphthoquinone and simple silyl enol ether **3.53**. However, formation of the desired C-C bond was not detected, while the reaction gave a mixture of hydrolysis product **3.54** and phenol **3.55**, along with unreacted quinone **3.52**. It was surmised that Lewis acids might activate the carbonyl oxygen but might also get close to the ether oxygen of the dopamine-hydantoin, weakening the C-O bond.

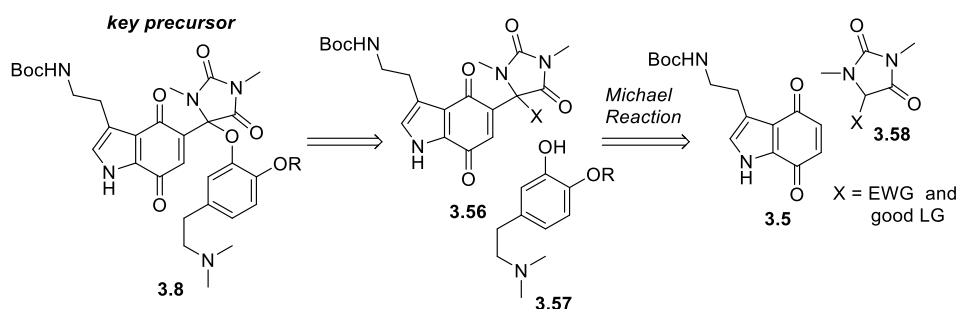


Scheme 3.14 Model Studies for the Mukaiyama-Michael Reaction

3.4.2 Other Attempts: The Assembly of Quinone, Hydantoin and

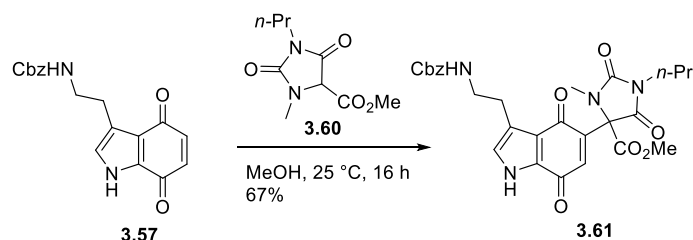
Dopamine Fragments

With these disappointing results, we had to consider other methods. Thus, a revised plan was made, which involved changing the coupling order of fragments (Scheme 3.15). After construction of the C-C bond between tryptamine quinone **3.5** and hydantoin **3.58**, phenol fragment **3.57** could be added to the hydantoin adduct *via* nucleophilic substitution. To practice this plan, the hydantoin required a suitable electron-withdrawing functional group which could also be easily cleaved.



Scheme 3.15 Revised Approach for Key Precursor

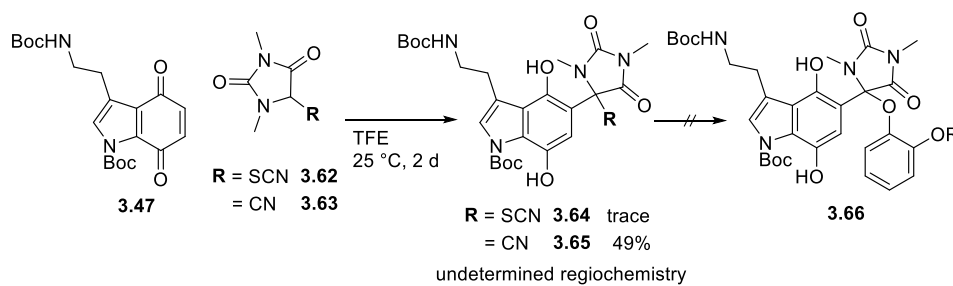
The feasibility of this idea was demonstrated in 2008 by the Andersen group who reported an example of a Michael reaction between the tryptamine quinone and hydantoin derivatives with a 1,3-dicarbonyl moiety under protic solvents (Scheme 3.16).^{3a}



Andersen, R. J. et al. *J. Med. Chem.* **2008**, *51*, 2634.

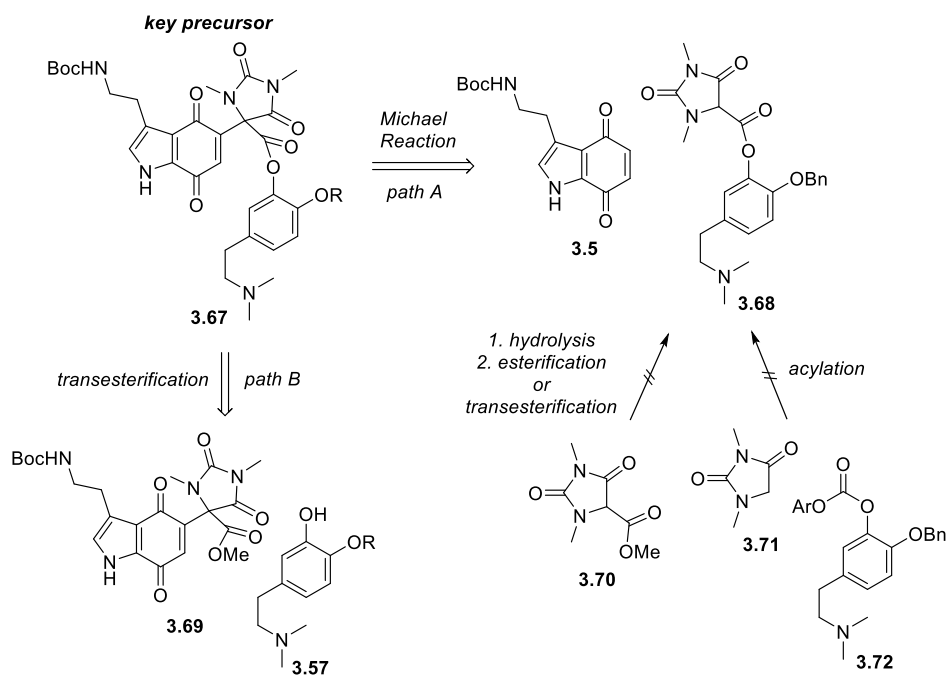
Scheme 3.16 Example of the Michael Reaction with Stabilized Enol

We set out to investigate various conditions for the coupling of hydantoin derivatives and a tryptamine quinone. Our studies began with examining the reaction of tryptamine quinone **3.47** with hydantoin containing thiocyanato (SCN) and cyano (CN) groups (Scheme 3.17). In the case of thiocyanatohydantoin **3.62**, the yield of coupling product **3.64** was very low. The reaction of cyanohydantoin **3.63** with tryptamine quinone **3.47** provided desired hydantoin adduct **3.65** in moderate yield. However, displacement of the cyano group with a phenol nucleophile proved difficult.

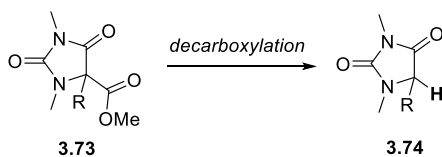


Scheme 3.17 Michael Reaction with Hydantoin Fragments

Due to difficulties encountered in the sequential attachment approach, we modified the strategy in which the hydantoin-dopamine fragment was employed with ether-to-ester linkage change (Scheme 3.18). Two approaches were considered for the preparation of the modified key precursor **3.67**. One was to make dicarbonyl compound **3.68** with a dopamine fragment and then proceed with the Michael reaction with quinone **3.5** (*path A*). The second involved transesterification of methyl ester **3.69** with phenol **3.5** from dopamine after the Michael reaction (*path B*).



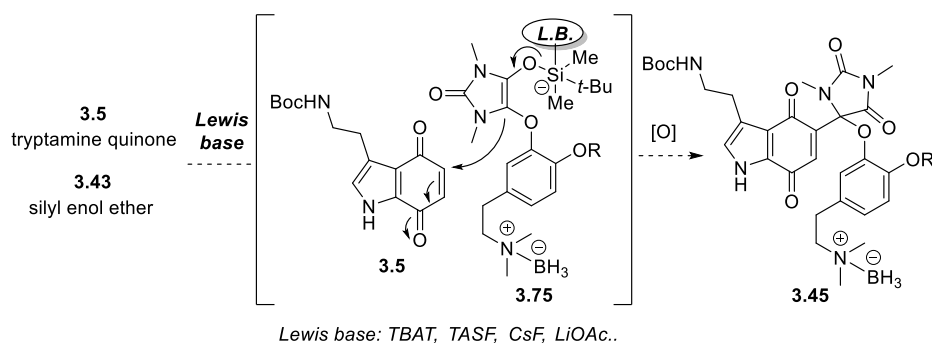
Despite considerable experimentation, the strategy based on the 1,3-dicarbonyl nucleophile was not successful. Neither phenol ester **3.68** formation nor the transesterification could be implemented. In particular, the use of a hydantoin carboxylic acid as an intermediate was not feasible due to facile decarboxylation (Scheme 3.19).



3.4.3 Lewis Base Mediated Mukaiyama-Michael Reaction

3.4.3.1 Coupling Between Silyl Enol Ether and Tryptamine Quinone

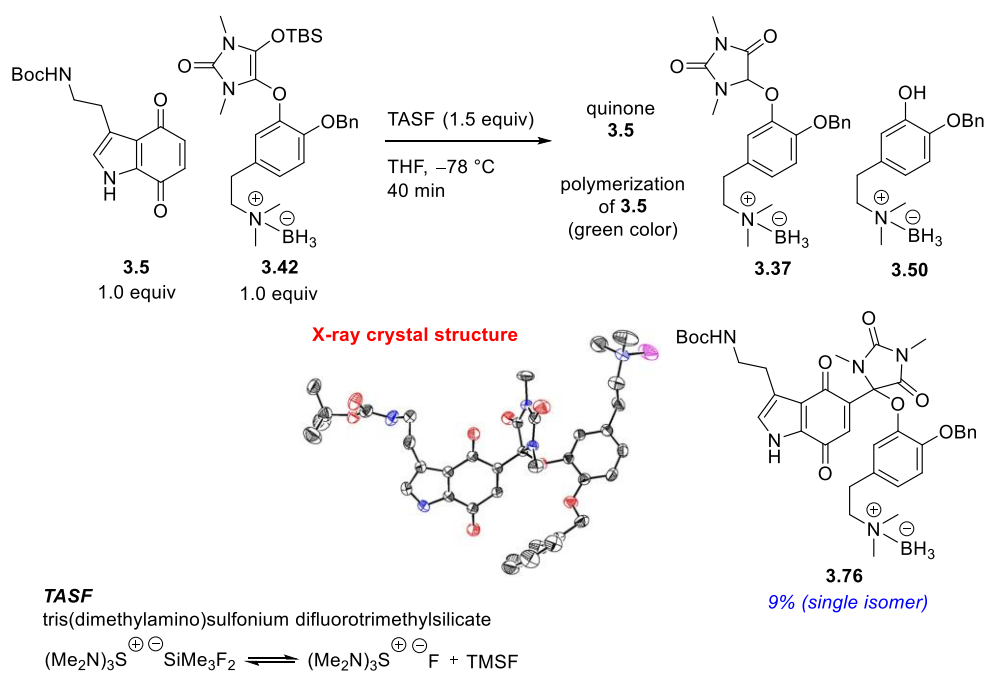
Due to the failure in the exploration of alternative strategies, we considered again the Mukaiyama-Michael reaction between the quinone and the silyl enol ether. Instead of using a Lewis acid catalyst, which has a high affinity for various sensitive oxygen functionality in the substrate, a Michael reaction using as a Lewis base was attempted to generate the desired C-C bond (Scheme 3.20). When a Lewis base reacts with the silyl enol ether to form hypervalent silicate **3.75**, the oxygen-silicon bond is weakened to generate a nucleophile.



Scheme 3.20 Lewis Base Catalyzed Mukaiyama-Michael Type Reaction

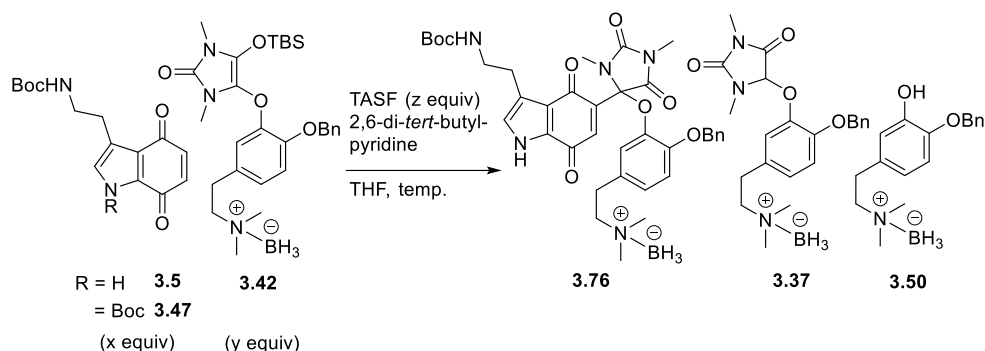
Based on this idea, several Lewis bases were examined for the Michael reaction between quinone **3.5** and silyl enol ether **3.42**. While most of the Lewis bases were found ineffective, formation of the desired product was observed, for the first time, when tris (dimethylamino)sulfonium difluorotrimethylsilicate (TASF) was used as the Lewis base (Scheme 3.21).⁸ In this case, treatment of a 1:1 mixture of quinone **3.5** and silyl enol ether **3.42** with 1.5 equiv of TASF at $-78\text{ }^{\circ}\text{C}$ induced a rapid reaction from which desired Michael adduct **3.76** was isolated as a single isomer in 9% yield along with hydrolysis and cleavage products. Of the two reactants, small

loss was observed during the recovery of quinone **3.5**, probably due to polymerization. The regiochemistry of the product was unequivocally assigned based on X-ray crystal structure analysis and fortunately proved to be of the desired isomer.



Scheme 3.21 Mukaiyama-Michael Type Reaction Using TASF

Having obtained for the first time the key precursor containing all the carbon atoms of exiguamine A, we turned our attention to improving the Mukaiyama-Michael reaction (Table 3.2).



entry	electrophile x	nucleophile y	TASF z	additive	temp.	time	results		
							3.76^a	3.37	3.50^b
1	3.5 (1.0)	1.6	0.5	-	-45 °C	1 h	17%	5 : 1	
2	3.5 (1.0)	1.7	1.7	-	-78 °C	1 h	35%	3 : 1	
3	3.5 (2.0)	1.0	1.5	-	-78 °C to 0 °C	1 h, 20 min	10%	1 : 1.2	
4	3.5 (1.0)	2.0	3.0	-	-78 °C	40 min	-	1 : 1	
5	3.5 (1.0)	1.7	1.7	TMSF (5-10 equiv)	-78 °C	40 min	42% (BRSM 70%)	3 : 1	
6	3.47 (1.0)	1.1	1.4	-	-78 °C	40 min	-	1 : 1	
7	3.47 (2.0)	1.0	1.4	-	-78 °C	1 h	trace	1 : 1.3	

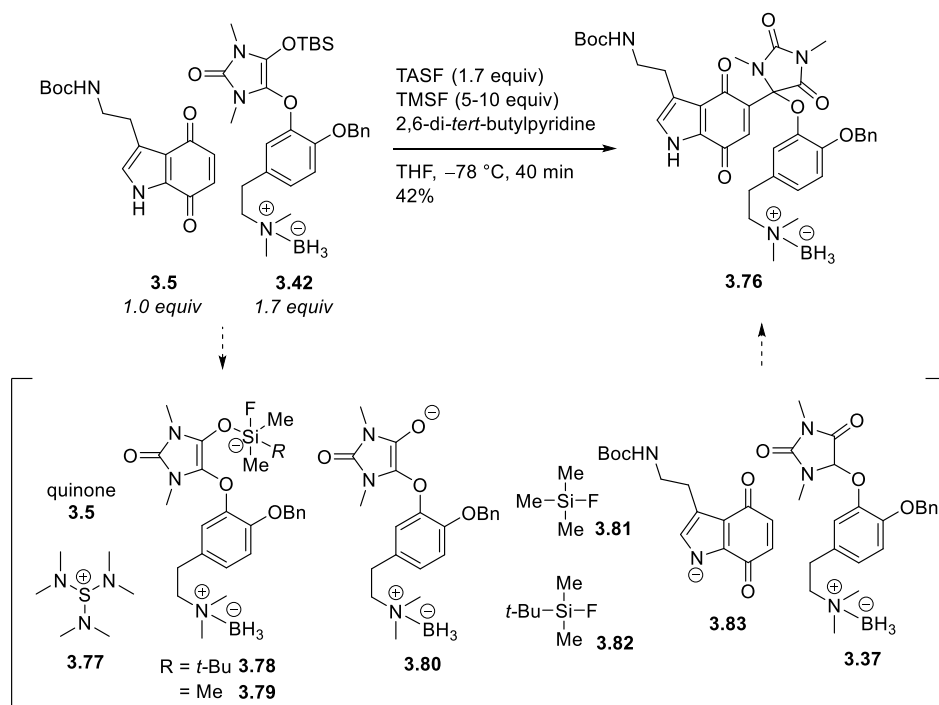
^aIsolated yield. ^bThe ratio was determined by ¹H NMR.

Table 3.2 Investigation into Mukaiyama-Michael Type Reaction Using TASF

The effect of the reactant ratio on the yield was investigated. A yield of 17% was obtained when catalytic TASF was added at -45 °C (entry 1). When 1.7 equiv of both nucleophile and TASF were added, the yield was doubled (entry 1 vs. entry 2). Interestingly, when the amount of the electrophile was higher than the nucleophile, the yield decreased (entry 3). Increasing the equivalent of the nucleophile and TASF did not generate the desired product at all (entry 4). Next screened was an additive effect. The Noyori group reported that the yield of the TASF-catalyzed Mukaiyama-aldol reaction was increased by adding trimethylsilyl fluoride (TMSF).^{8a} Therefore, according to the procedure described by Della,⁹ TMSF was prepared and tested for its effect on our Michael reaction (entry 5). When a 1:1.7 mixture of quinone **3.5** and silyl enol ether **3.42** reacted in the presence of 1.7 equiv of TASF and 5 equiv TMSF,

the yield of the product was increased to 42%, and, some of quinone **3.5** and hydrolyzed silyl enol ether **3.37** could be recovered (BRSM 70%). The TASF-mediated reaction was also examined with *N*-Boc protected tryptamine quinone **3.47**. No Michael adduct was obtained (entry 6) or only a trace amount of the product was produced (entry 7).

The Lewis base mediated Mukaiyama-Michael reaction is believed to proceed through a mechanism which is triggered by the activation of silyl enol ether **3.42** with TASF (Scheme 3.22). In this reaction, silicate **3.78**, enolate **3.80** or both can be served as nucleophile, though we could not exclude the possibility of additional interactions of silicon compounds **3.81** and **3.82** with compound **3.80**, as well as the acid-base equilibrium between **3.5**, **3.80** and **3.83**, **3.37**. Sulfonium **3.77** may also have acted as a Lewis acid in this reaction.



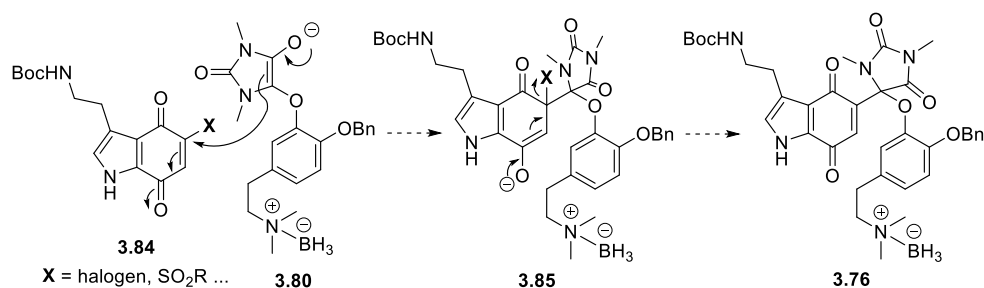
Scheme 3.22 Various Intermediates in the Mukaiyama-Michael Reaction Mixture

3.4.3.2 Coupling Between Silyl Enol Ether and Bromotryptamine Quinone:

Discovery of *Iso-Exiguamine A* Precursor

For the union of quinone and hydantoin-dopamine fragments, only the unsubstituted quinone substrate was examined in the Mukaiyama-Michael reaction. Although a yield of 42% was obtained from the reaction, it was less than desirable for the key convergent step, considering the 1:1.7 ratio of the reactants. Thus, a strategy was devised in the hope of improving the yield, in which the reaction between the functionalized quinone and the silyl enol ether was planned.

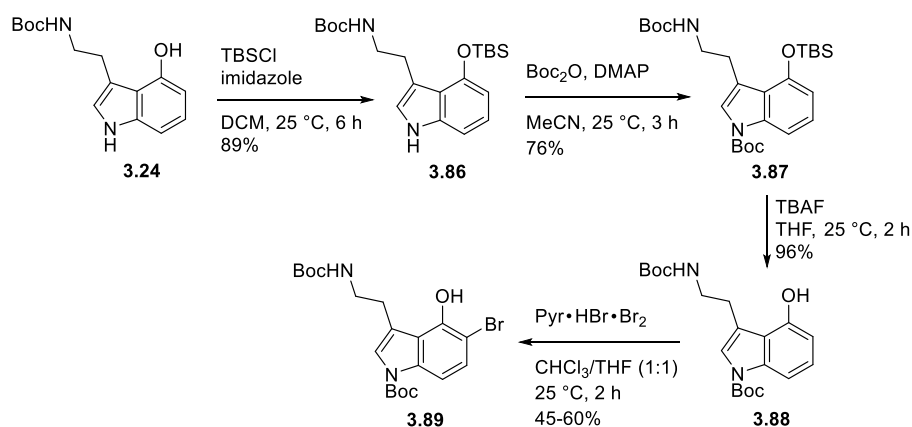
It was anticipated that introduction of a leaving group to the quinone would enhance the reactivity of the *ipso* position to facilitate an addition-elimination process (Scheme. 3.23).



Scheme 3.23 Coupling Strategy Using Functionalized Quinone

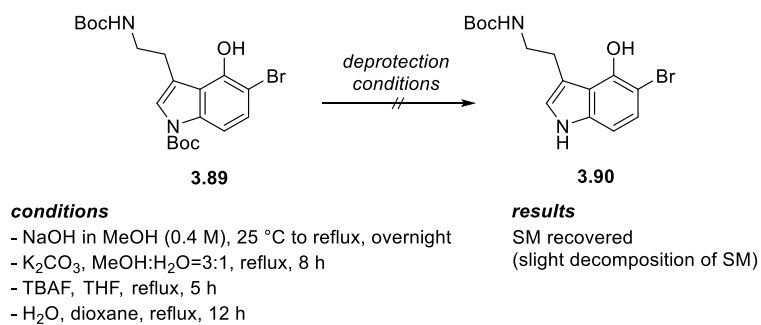
Although we hoped to introduce a variety of functional groups into quinone, little was known in the literature about the synthesis of indoloquinones incorporating these functional groups. In addition, late-stage functionalization that would directly introduce functional groups into indoloquinones was not known at all. So, it would seem not easy to synthesize functionalized quinones. As bromination at the 5-position of the *N*-Boc protected hydroxyindole derivative had been reported,¹⁰ it was expected that 5-bromoquinone could be easily produced.

Selective *N*-Boc protection was not possible due to the hydroxyl group acts as a more reactive nucleophile in indole **3.24**, so the *N*-Boc group was synthesized after phenol protection (Scheme 3.24). The bromide group was introduced to the hydroxyindole derivative after silicon group deprotection. Bromophenol **3.89** was unstable, isolated as a white solid, which became slightly blended with blue, and underwent decomposition upon storage. Due to the sensitivity, it was difficult to obtain bromide **3.89** with consistent yield, and the product was used in the next step immediately.



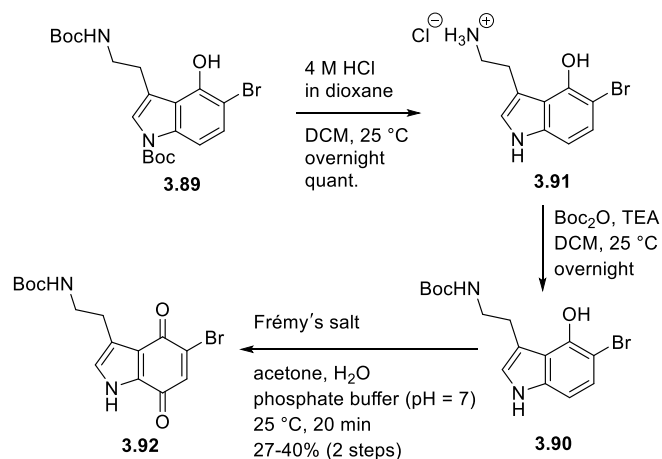
Scheme 3.24 Bromination with *N*-Protected Indoloquinone

We attempted to remove the Boc group of the indole nitrogen to obtain indoloquinone. When exposed to acidic conditions, the Boc group present in the primary amine could be removed as well. Thus, the deprotection was attempted under various basic or neutral conditions (Scheme 3.25). However, the Boc group was not removed with NaOH / MeOH conditions reported in the literature. Several other conditions were also investigated, to no avail. In general, starting material **3.89** remained, and slight decomposition occurred under these conditions.



Scheme 3.25 Failure for Deprotection of *N*-Boc Group

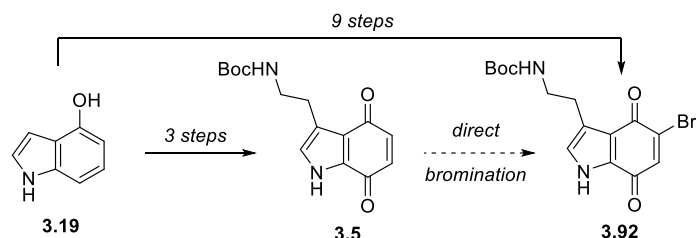
It was also found that oxidation of substrate **3.89** to a quinone did not occur under various conditions. Therefore, both of the Boc groups in the molecule were removed under acidic conditions, and the primary amine was protected again as a Boc group (Scheme 3.26). Treatment of bromoindole **3.90** with Frémy's salt induced rapid oxidation to provide 5-bromoquinone **3.92**. The low to moderate yield was believed to be due to the instability of starting material **3.90**.



Scheme 3.26 Synthesis of 5-Bromotryptamine Quinone

Although an authentic sample of 5-bromoquinone **3.92** could be obtained, the synthetic route was long and inefficient. Introduction of a bromo group directly at

the desired carbon position of tryptamine quinone **3.5** would be a more efficient synthetic route (Scheme 3.27).



Scheme 3.27 Straightforward Approach for 5-Bromotryptamine Quinone **3.92**

Therefore, direct introduction of a Br group into the quinone moiety of tryptamine quinone **3.5** was investigated. The results of using various brominating reagents are summarized in the following table (Table 3.3).

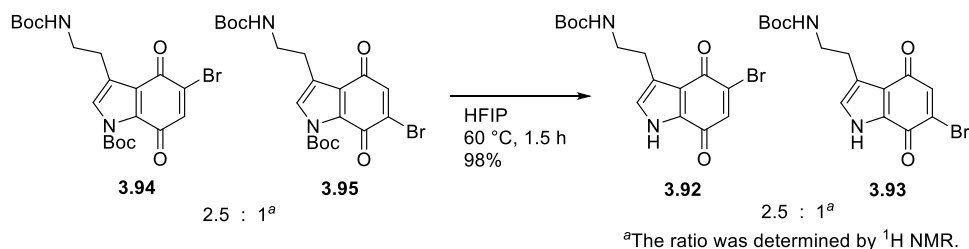
entry	substrate	reagents (equiv)	solvent	time	products	isolated yield ^a (ratio ^b)
1	3.5	Br ₂ (1.2)	MeCN	overnight	3.5, 3.96	-
2	3.5	NBS (1.2)	THF	2 h	3.96	-
3	3.5	NH ₄ Br (1.1), Oxone [®] (1.1)	MeOH	1 h	3.96	-
4	3.5	Pry•HBr•Br ₂ (1.2)	CHCl ₃ :THF = 1:1	40 min	3.92, 3.93	81% (1 : 3)
5	3.47	Pry•HBr•Br ₂ (1.2)	CHCl ₃ :THF = 1:1	1.5 h	3.94, 3.95	93% (2.5 : 1)

^aIsolated as regioisomeric mixture. ^bThe ratio was determined by ¹H NMR.

Table 3.3 Synthesis of 5- and 6-Bromoquinones Using Brominating Reagents

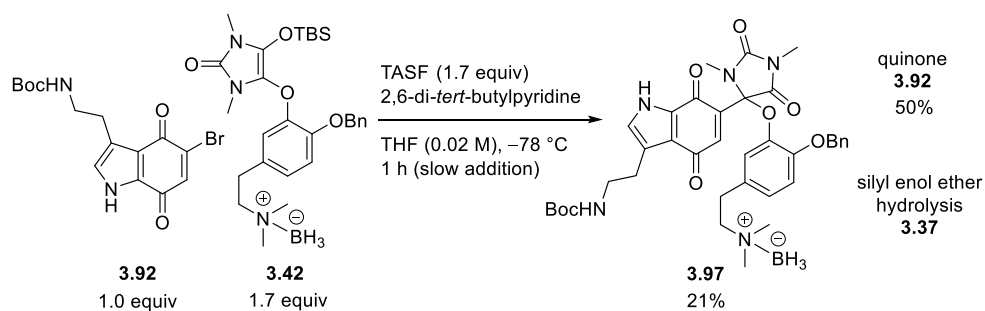
In most cases, 2-bromoquinone **3.96** was obtained as the major product (entries 1, 2, and 3). But, treatment of tryptamine quinone **3.5** with 1.2 equiv of pyridinium tribromide led to monobromination at the quinone moiety in 81% yield. Regioisomers were produced in a 3:1 ratio by comparing with the authentic sample. It was found that 5-bromoquinone **3.92** was a minor product and 6-bromoquinone **3.93** was a major product (entry 4). *N*-Boc-protected indoloquinone **3.47** was reacted with 1.2 equiv of pyridinium tribromide to give monobrominated compounds in 93% yield (entry 5). In this case, the regioselectivity was switched to favor the formation of 5-bromoquinone **3.94** as the major product.

In contrast to the bromoindole, deprotection of the Boc group of indoloquinones **3.94** and **3.95** took place smoothly in HFIP to give **3.92** and **3.93** in 98% yield (Scheme 3.28).



Scheme 3.28 *N*-Boc Deprotection of Indoloquinone Moiety

With 5-bromoquinone **3.92** in hand, we attempted the Mukaiyama-Michael type reaction with silyl enol ether **3.42** (Scheme 3.29). When the reaction was carried out by applying the optimized conditions found for unsubstituted quinone **3.5**, the Michael adduct was obtained only 21% yield along with 50% recovery of unreacted quinone **3.92**.



Scheme 3.29 Coupling Reaction with 5-Bromoquinone: Discovery of Regioisomer

Surprisingly, the NMR spectrum of the Michael adduct was not identical to the previously obtained Michael adduct **3.76** (Figure 3.1). Further analysis revealed the product was a regioisomer. Regioisomeric adduct **3.97** was found to be relatively unstable on a silica gel. Thus, column chromatography must be performed by rapid elution in order to avoid product decomposition.

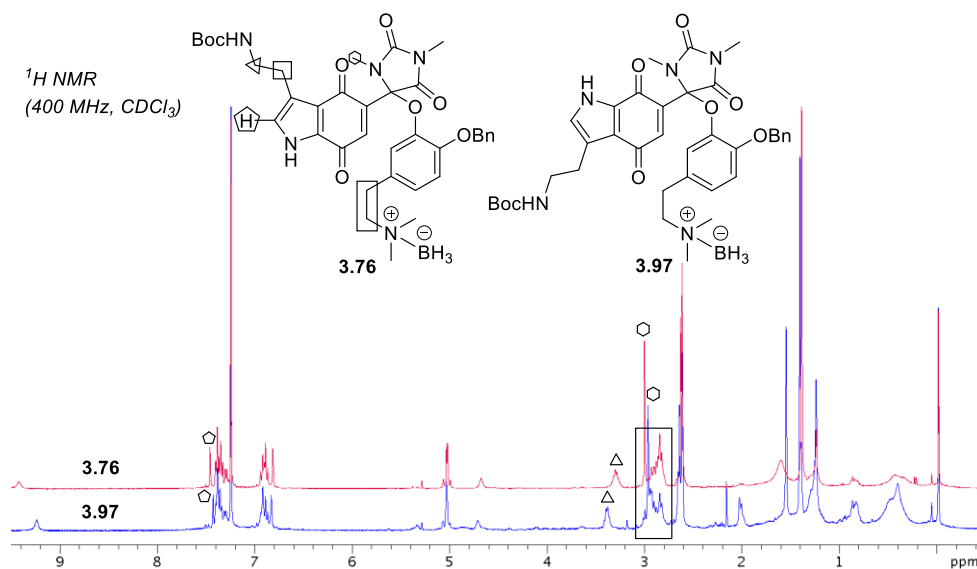
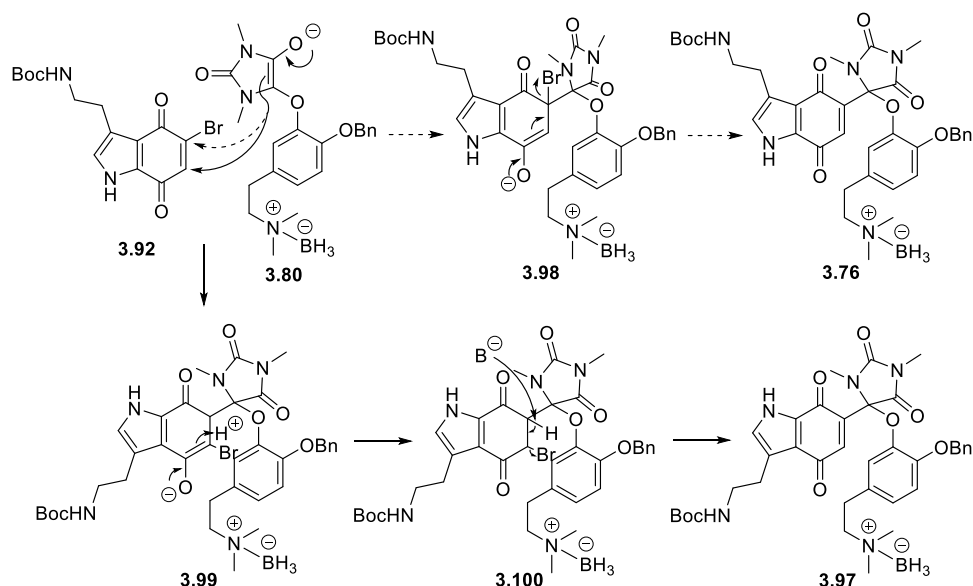


Figure 3.1 The ¹H NMR Comparison Between **3.76** and **3.97**

This result indicated that the reaction between 5-bromoquinone **3.92** and silyl enol

ether **3.42** occurred through a mechanism other than the proposed addition-elimination pathway (Scheme 3.30).¹¹ The observed regiochemical outcome suggests that enolate **3.80** generated from silyl enol ether **3.42** attack C6 of quinone **3.92**, presumably avoiding steric hindrance from the Br group. The resulting enolate **3.99** is expected to be a relatively more stable intermediate compared to **3.98** due to the electron-withdrawing effect of the Br group. After a series of protonation-deprotonation, hydrogen bromide is removed to generate the regioisomeric quinone **3.97**.

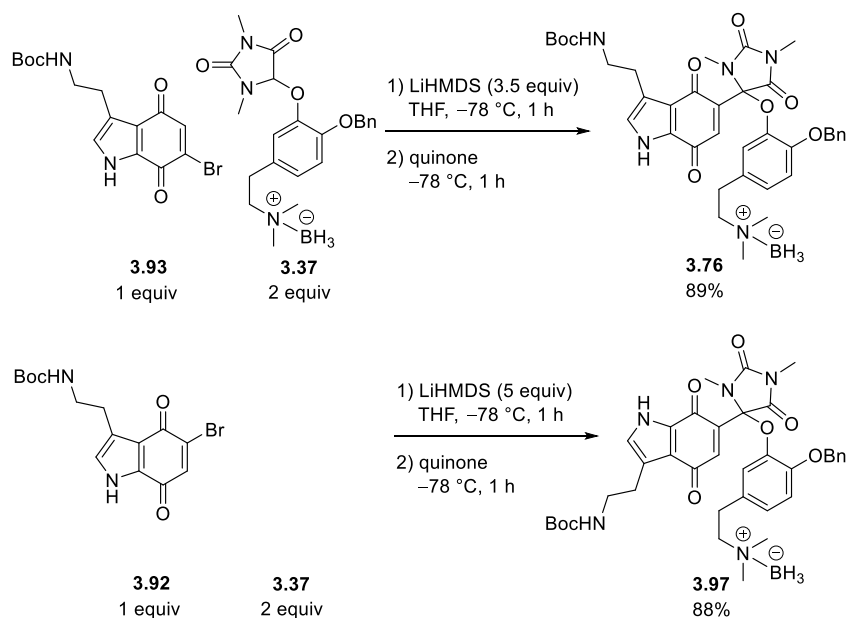


Scheme 3.30 Proposed Mechanism

Although the Mukaiyama-Michael reaction employing the bromoquinone substrate did not lead to improvement in yield, the obtained regioisomeric Michael adduct **3.97** offered the possibility of synthesizing *iso*-exiguamine A.

In the face of the unexpected regioselectivity with 5-bromoquinone **3.92**, we then turned our attention to the reaction of 6-bromoquinone **3.93**, which was expected to

produce the desired regioisomer. Because the use of silyl enol ether **3.42** in the conjugate addition resulted in a poor yield, we set out to examine the reaction with an enolate of **3.37** (Scheme 3.31). When a lithium enolate of **3.37** was added to 6-bromoquinone **3.93** at $-78\text{ }^{\circ}\text{C}$, a clean reaction took place to provide the desired product **3.76**. Surprisingly, the yield was increased to 89%. Similarly, 5-bromoquinone **3.92** underwent the Michael reaction with **3.37** to give the adduct **3.97** in 88% yield.



Scheme 3.31 Michael Reaction with Bromoquinones

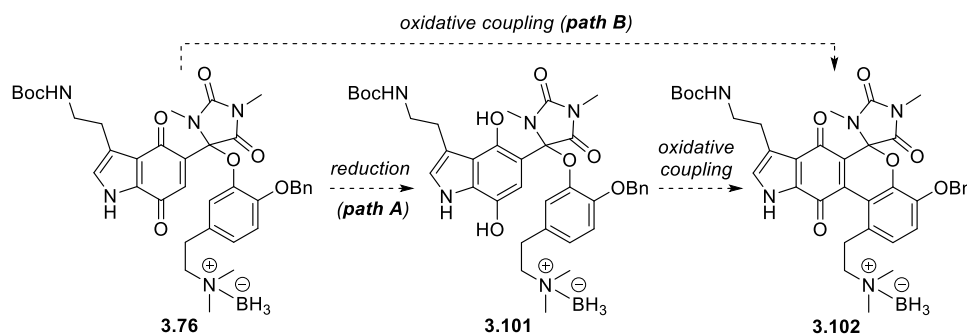
In summary, we found that the Michael reaction with an enolate derived from dopamine-hydantoin and bromoquinones gives a much better yield of each coupling product. Thus, it was possible to synthesize large amounts of precursors capable of sustaining total synthesis campaigns toward exiguamine A and *iso*-exiguamine A. It was also hoped that the new route would be amenable for large scale synthesis of exiguamines and their analogs for relevant biological evaluations.

3.5 Formation of the Pyran Ring

Compound **3.76**, in which all fragments constituting exiguamine A were introduced, was subjected to a reaction to form the central pyran ring structure. It was found through the above-mentioned experiments that the C-O bond between hydantoin and dopamine moieties is rather weak susceptible to cleavage. Thus, the formation of the C-C bond directly conjoining the two six-membered rings was first attempted en route to the pyran ring synthesis.

3.5.1 Oxidative Coupling Approach

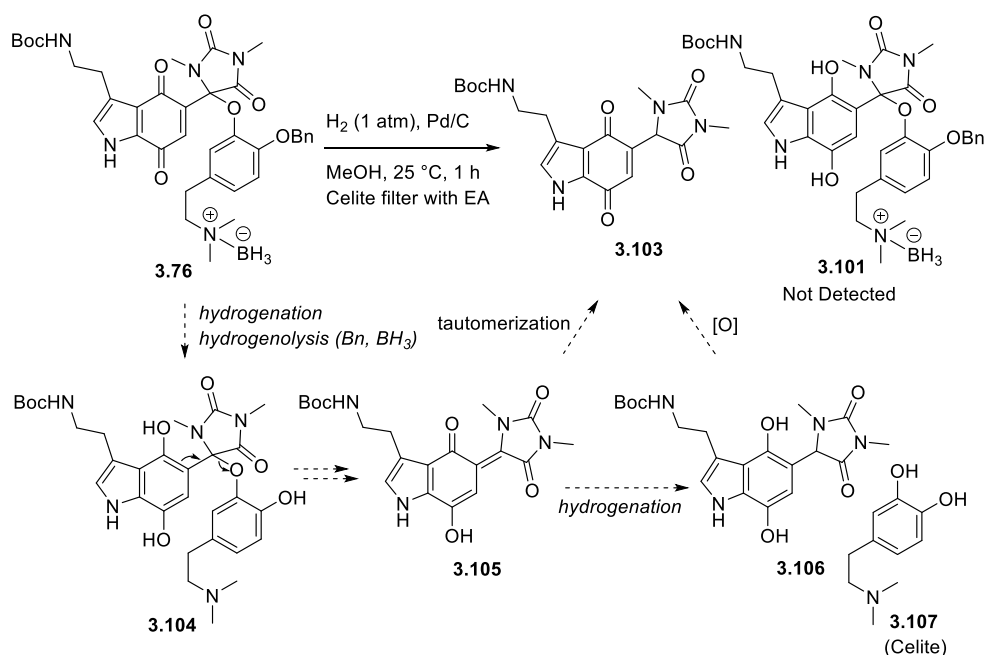
We attempted oxidative coupling through two approaches. One was to apply the reaction conditions that were successful in making the pyran structure in the model study (Scheme 3.32, *path A*). The other is to induce the intramolecular conjugate addition of the arene to the quinone (Scheme 3.32, *path B*).



Scheme 3.32 Plan for Pyran Formation through Oxidative Coupling

In order to verify the feasibility of *path A*, quinone **3.76** was exposed to hydrogen gas in the presence of Pd/C catalyst to form hydroquinone (Scheme 3.33). The hydrogenation produced only **3.103**, instead of the desired product, **3.101** via cleavage of the phenoxy group. This result is presumably due to the instability of the

hydroquinone. The phenol group present at the benzylic position of hydroquinone **3.104** might act as a leaving group to form a quinone methide. The resulting quinone methide **3.105** might be hydrogenated again under the reaction conditions to give hydroquinone **3.106** which could be oxidized to quinone **3.103**. The debenzylated dopamine **3.107** was presumed to be lost during filtration for Pd removal.

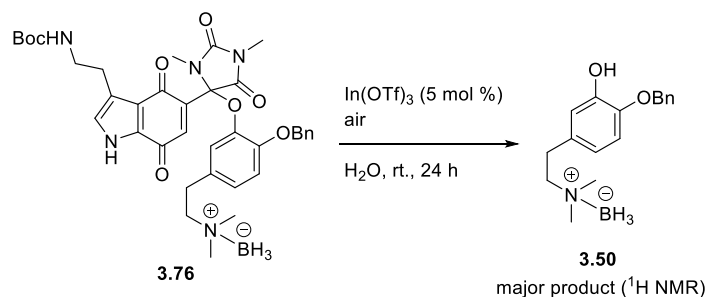


Scheme 3.33 Difficulty in Hydroquinone Formation of **3.76**

Based on these results, we concluded that biaryl compounds could not be made through a hydroquinone intermediate because of the inherent reactivity associated with the molecular skeleton.

Thus, a Friedel-Crafts type reaction in which the arene is directly added to the quinone moiety was attempted (Scheme 3.34, *path B*). The procedure reported by the Li group, the conjugate addition of the arene,¹² was carried out using Lewis acid catalysts. However, similarly to the results of the previous reactions using Lewis

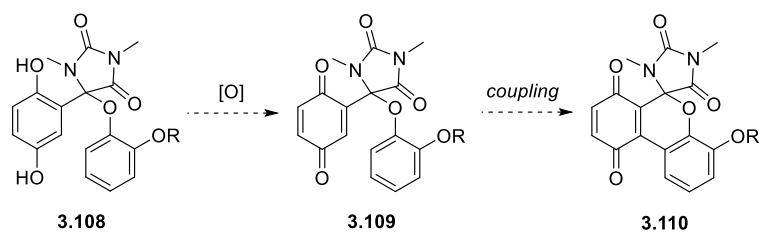
acids, only phenol **3.50** could be obtained as the major product (Scheme 3.34).



Scheme 3.34 Failure of Oxidative Coupling through Friedel-Crafts Type Reaction

3.5.2 Correction of the Preliminary Studies

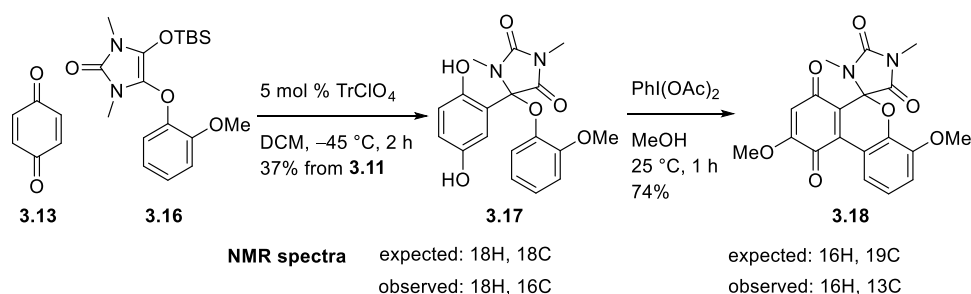
Due to the continuous failure to obtain pyran compounds from the key precursors *via* oxidative coupling, we sought to find suitable conditions through model studies. Based on the well-known redox equilibrium between hydroquinone and quinone, the oxidation of the biaryl compound **3.108** obtained from the model study was expected to undergo oxidative coupling *via* quinone **3.109** to lead to the pyran formation (Scheme 3.35).



Scheme 3.35 Plan for Model Study of Pyran Formation

In the model study performed by Dr. Venkataramanan Krishnamurthy at Princeton University, it was reported that hydroquinone **3.17** obtained by the Mukaiyama-Michael reaction was converted to pyran **3.18** through a sequence of oxidative

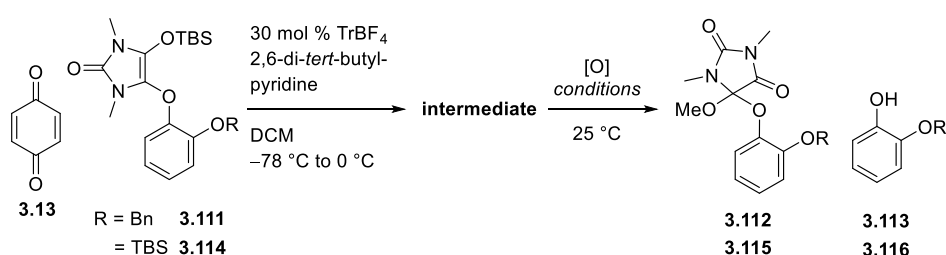
process effecting cyclization and MeOH addition (Scheme 3.36). However, detailed analysis of the NMR data revealed that while the number of hydrogen resonance signals was correct, there was discrepancy between the ^{13}C NMR peaks in the spectra and those expected for the proposed structures of **3.17** and **3.18**. Therefore, a series of experiments were carried out to reproduce the results of the model study with suspicion that the structures were mistakenly assigned.



Scheme 3.36 Re-evaluation of Preliminary Studies by Dr. Venkataramanan
Krishnamurthy

Benzoquinone and the model silyl enol ether were reacted in the presence of a trityl ion catalyst, and the resulting product was exposed to various oxidation conditions (Table 3.4). Under a variety of conditions, neither quinone **3.117** nor pyran **3.118** could be obtained. Unexpectedly, the reaction using CAN led to formation of complex mixtures and phenol **3.113** (entry 1), while starting material remained under oxidation with MnO_2 or O_2 -salcomine (entries 2, 3). Interestingly, in the case of oxidation with PIDA (entries 4, 5), when the reaction was allowed to proceed for a long time, only phenol **3.116**, rather than quinone **3.121** or pyran **3.122**, was obtained. When the reaction time was shortened to 10 min, formation of mixed ketal **3.115** was observed. The structure of **3.115** was assigned based on the

correlation between the quaternary carbon at the hydantoin and the proton of the methoxy group in HMBC spectra, which indicated direct connection between the hydantoin and the methoxy group. Also, the compound considered as the Mukaiyama-Michael adduct (**3.17**, cf. **3.119** and **3.123**) was found to be phenol **3.124**, formed through C-O bond rather than C-C bond formation between benzoquinone and the silyl enol ether.



entry	substrate	reagents	solvent	time	products ^a
1	3.111	CAN	MeCN:H ₂ O = 1:1	overnight	complex mixture + 3.113
2	3.111	MnO ₂ , Na ₂ SO ₄	DCM	3 h	No reaction
3	3.111	O ₂ , salcomine	MeCN	overnight	No reaction
4	3.114	PhI(OAc) ₂	MeOH	overnight	complex mixture + 3.116
5	3.114	PhI(OAc) ₂	MeOH	10 min	3.115 (64%)

^abased on ¹H NMR. Value in parenthesis is isolated yield.

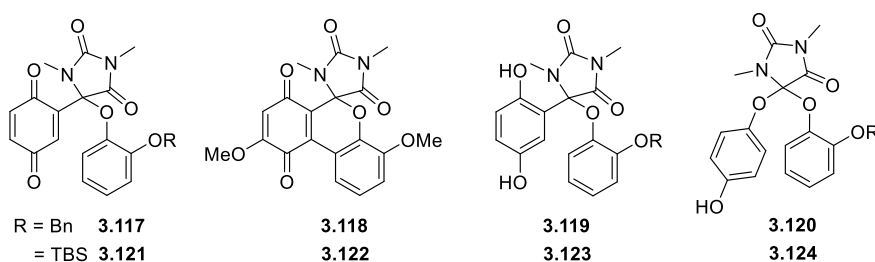
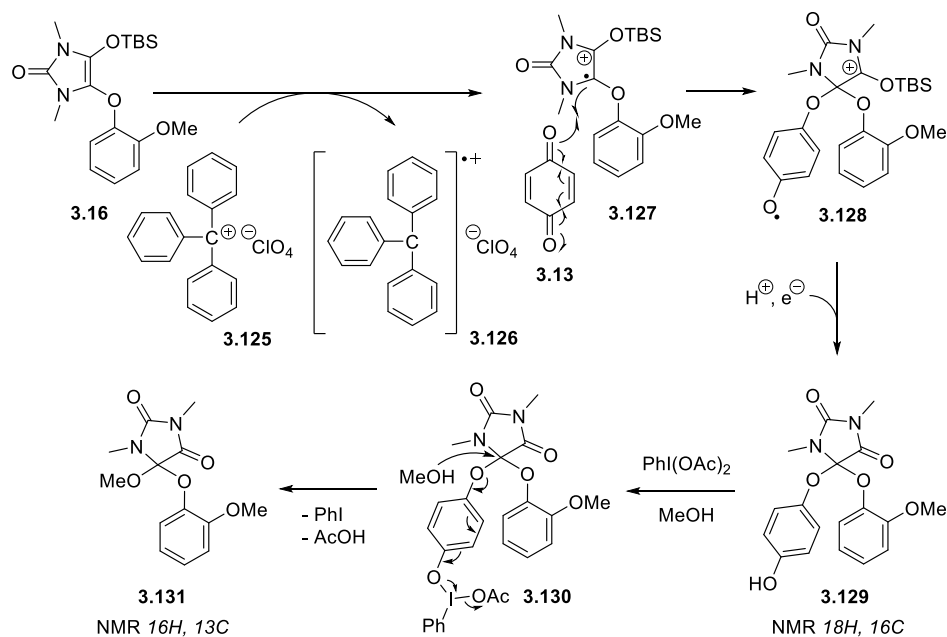


Table 3.4 Correction of Model Studies

Based on these observations, a mechanism was proposed for the re-interpretation of the model study results (Scheme 3.37).¹³ It is expected that a trityl cation can induce a radical pathway by oxidizing electron rich silyl enol ether **3.16** through electron transfer. The resulting radical **3.127** may form a C-O bond with quinone

3.13 and undergo a series of electron and proton transfer and desilylation to produce phenol **3.129**. Treatment of **3.129** with PIDA activates the phenol moiety to serve as a leaving group, which is displaced by solvent MeOH to a produce mixed ketal **3.131**.

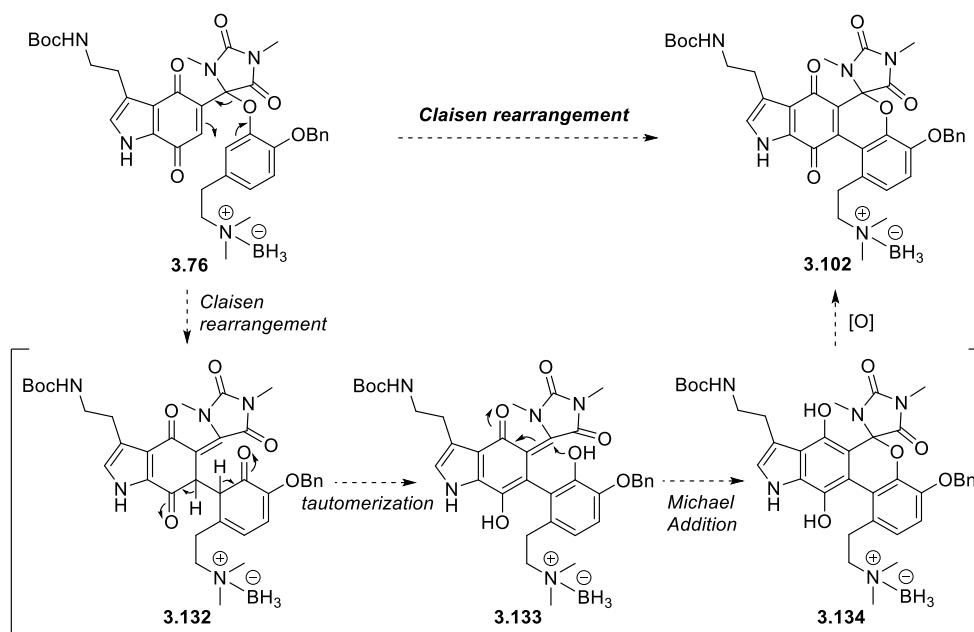


Scheme 3.37 Proposed Mechanism for Synthesis of **3.129** and **3.131**

3.5.3 Claisen Rearrangement Approach

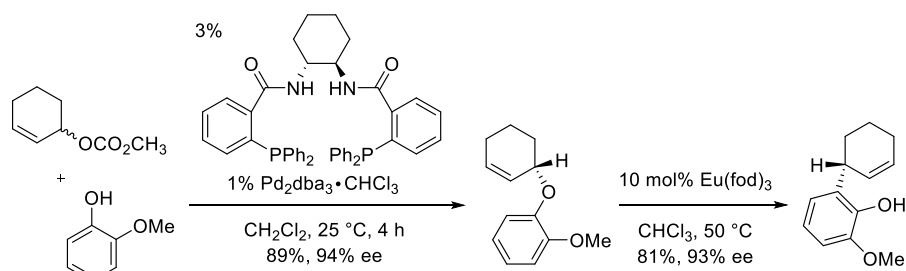
With the disappointing results from a Friedel-Crafts approach, we set out to explore a new strategy for the formation of the core pyran structure *via* a Claisen rearrangement. The Claisen rearrangement is a well-known classical reaction in which allyl vinyl ethers or allyl aryl ethers are converted to γ,δ -unsaturated carbonyls through a [3,3]-sigmatropic rearrangement.¹⁴ Therefore, it was expected that the allyl aryl ether moiety present in **3.76** would participate in the Claisen rearrangement to form a C-C bond between the two six-membered rings. The Claisen rearrangement was also envisioned to set the stage for the formation of pyran **3.102** according to

the following mechanism (Scheme 3.38). After the pericyclic process, a series of tautomerization, cyclization and oxidation reactions might occur readily, giving rise to the desired pyran **3.102**.



Scheme 3.38 Plan for Pyran Formation through Claisen Rearrangement

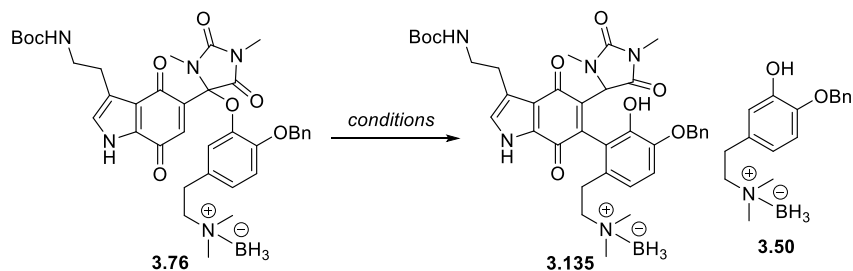
Most of the literature examples of the Claisen rearrangement of aryl allyl ethers were performed under Lewis acid catalyzed or thermal conditions. An exceptionally mild protocol was reported in 1998 by the Trost group, by which chiral aryl allyl ethers prepared by Pd-catalyzed enantioselective O-alkylation were efficiently rearranged to C-allylated products with high chirality transfer under europium catalysis (Scheme 3.39).¹⁵



Trost, B. M.; Toste, D. *J. Am. Chem. Soc.* **1998**, *120*, 815.

Scheme 3.39 Asymmetric O-alkylation followed by Claisen Rearrangement

Although the propensity of phenol elimination observed in various Lewis acid-catalyzed reactions was of great concern, the mildness of the Trost-Toste protocol was encouraging. Thus, we examined the possibility of performing the Claisen rearrangement of **3.76** by screening lanthanide catalysts (Table 3.5).



entry	catalyst	solvent	conc.(M)	temp.	time	products ^a
						3.135 : 3.50
1	Eu(fod) ₃ (15 mol %)	CDCl ₃	0.02	75 °C	9 h	1 (20%) : 2.5
2	Eu(hfc) ₃ (25 mol %)	DCE	0.02	85 °C	5 h	1 : 4
3	Eu(fod) ₃ (15 mol %)	CHCl ₃	0.005	75 °C	24 h	1 (37%) : 1.4, SM
4	Ho(fod) ₃ (15 mol %)	CHCl ₃	0.005	75 °C	24 h	1 : 5
5	Pr(fod) ₃ (15 mol %)	CHCl ₃	0.005	75 °C	24 h	1 : 1.6, SM
6	-	toluene	0.005	110 °C	3.5 h	1 : 1.3

^a based on ¹H NMR ratio. Values in parentheses are isolated yields.

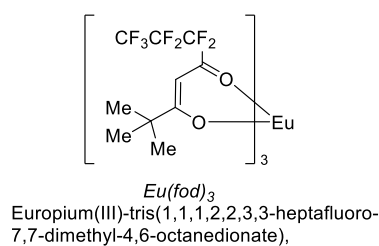
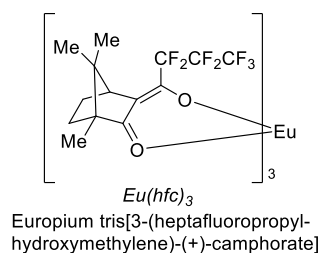


Table 3.5 Investigation into Claisen Rearrangement Conditions

When the reaction was carried out in a sealed system at 75 °C using 15 mol % Eu(fod)₃ catalyst and CHCl₃, the phenol cleavage product **3.50** was obtained as a major product. However, careful examination of the product mixture revealed that the reaction did produce the rearrangement product in 20% yield. It appeared that after a Claisen rearrangement, the resulting product **3.132** underwent simple tautomerization processes without cyclization to form a pyran. With these promising and yet unsatisfactory initial results, further efforts were made to increase the yield of the Claisen rearrangement product. When the ligand of the Eu catalyst was changed to hfc, more cleavage product **3.50** was produced (entry 2). In a lower concentration, the reaction rate was the slower, but the yield was increased to 37% (entry 3). In the cases of Ho catalysis, the formation of phenol cleavage product **3.50** was significantly increased (entry 4). The reaction with a Pr catalyst (entry 5) gave a result similar to those obtained with the Eu catalyst. When the reaction was carried out at a low concentration in toluene without a lanthanide catalyst, the reaction was completed within a few hours and formation of the phenol cleavage product **3.50** was diminished (entry 6).

Despite considerable attempts employing various reaction conditions, there was no significant improvement in yield. Therefore, we performed thorough analysis on all the byproducts generated from the Claisen rearrangement reaction (Figure 3.2). Detailed analysis of the outcome of the Claisen rearrangement revealed that in addition to **3.135** and **3.50**, the reaction produced pyran **3.102** and **3.137**, decomplexed phenol **3.136**, and fragmented product **3.103** and **3.35**. It appeared that heating **3.76** at 110 °C induced not only the desired Claisen rearrangement but also phenol cleavage, oxidation cyclization and borane-decomplexation. Consequently, the low yield of **3.135** was mainly due to the fact that the Claisen rearrangement

products were differentiated into four compounds.

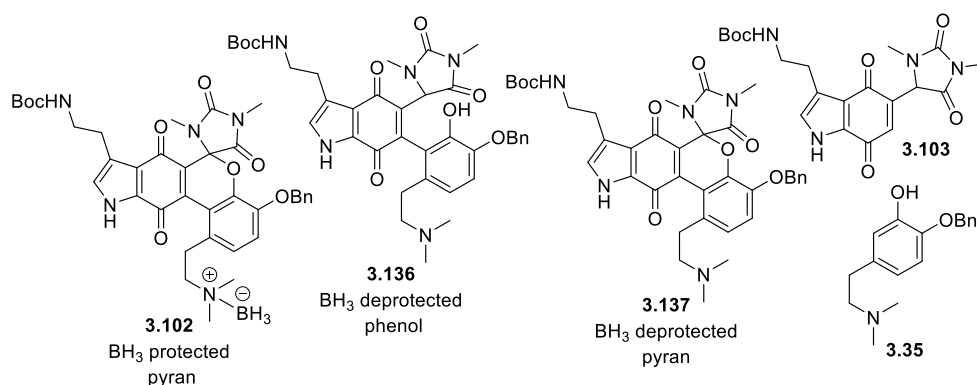
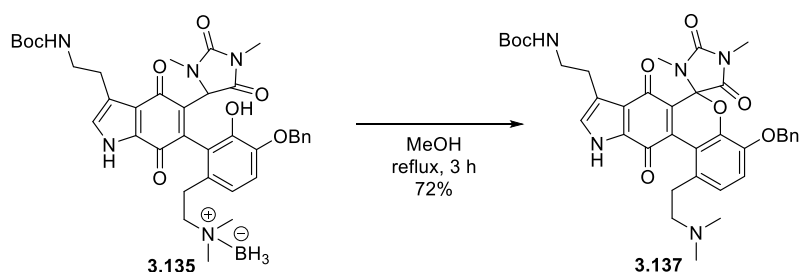


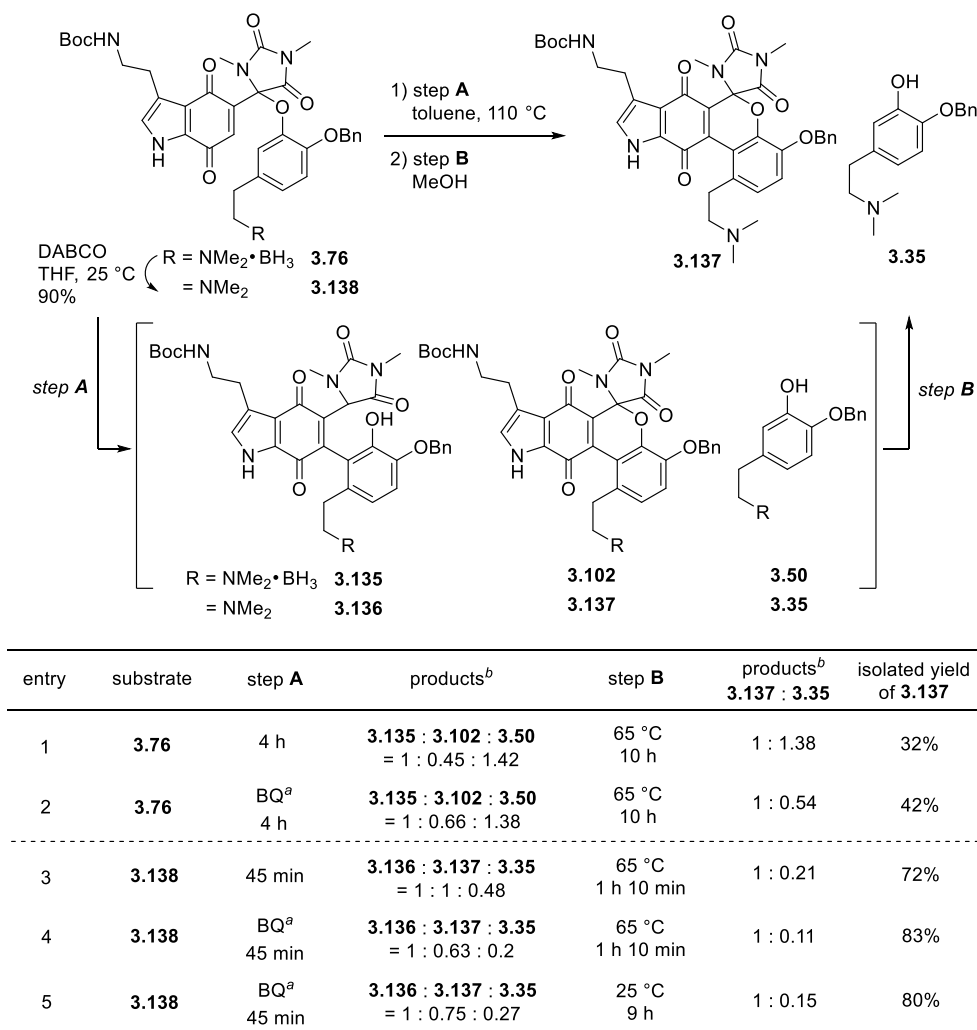
Figure 3.2 Byproducts Originated from Claisen Rearrangement

Therefore, it was envisioned that if these products could be converged into a single compound, the yield would be increased. Along this line of thought, we examined first the borane decomplexation of phenol **3.135** (Scheme 3.40). The decomplexation reaction of the amine-borane complex **3.135** was attempted by refluxing a methanolic solution of **3.135**. Surprisingly, pyran **3.137** was provided in 72% yield presumably through the borane removal followed by an oxidation process in which C-O bond formation between the hydantoin and the phenol occurred. The unexpected formation of a pyran *via* oxidative cyclization was believed to arise from facile tautomerization of **3.135** in methanol to a quinone methide such as **3.132** or **3.133**. But, the radical pathway could not be ruled out.



Scheme 3.40 Formation of Pyran **3.137**

Taking advantage of this reactivity, the mixture of products generated from the Claisen rearrangement could be converge to **3.137** through a procedure involving immediate solvent change and reflux (Table 3.6).



^a 20 mol %. ^b ¹H NMR ratio.

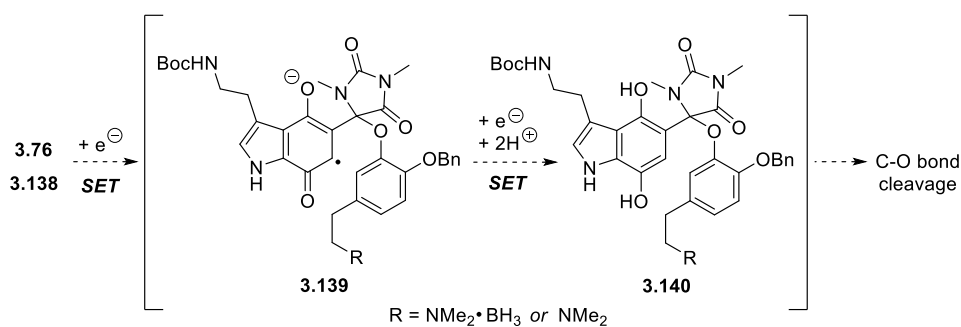
Table 3.6 Claisen Rearrangement – Oxidation Reactions

With the allyl aryl ether prepared from a Mukaiyama or Michael reaction, the sequence of the Claisen rearrangement and pyran formation was examined. Heating a toluene solution of **3.76** at 110 °C followed by change of solvents and reflux in

methanol indeed produced **3.137** as the major product. However, the yield of **3.137** from this procedure was still low. Interestingly, when the two-step sequence was carried out in the presence of 20 mol % 1,4-benzoquinone, a meaningful increase in yield by 10% was observed.

More significant improvement came from the use of the borane-free **3.138** as the substrate for the Claisen rearrangement. When the Claisen rearrangement was performed with **3.138**, prepared from **3.76** via removal of borane using DABCO, pyran **3.137** was formed in 72% yield, which could be further increased to 83% yield with the addition of benzoquinone. The reaction time was significantly shorter than that of the reaction of **3.76**. It was also found to be possible to conduct *step B* at room temperature albeit for a longer reaction time.

The remarkable increase in the yield of pyran **3.137** can be ascribed to suppression of the phenol cleavage process. Thus, it is reasonable to speculate that addition of benzoquinone and removal of borane reduce the C-O cleavage. Michael adduct **3.76** has an electron rich aryl moiety as well as an electron deficient quinone moiety in one molecule. Therefore, prolonged exposure of the molecule to high temperature could lead to intra- or intermolecular electron transfer. This redox process may bring about reduction of **3.76** to a radical anion, which can be further reduce to hydroquinone **3.140** (Scheme 3.41). Once the quinone is reduced, the C-O bond between the hydantoin and dopamine moieties become vulnerable to dissociation. It is presumed that benzoquinone could modulate the delicate redox equilibrium by interfering with electron transfer processes or serve as a radical scavenger.



Scheme 3.41 Hypothesis for Decomposition of Michael Adducts

Another discovery during the course of experiments was that phenols produced in the Claisen rearrangement exhibit different stability depending on the electronic environment of the tertiary amine (Figure 3.3). Phenol **3.135** found to quite stable upon long-term storage at $-20\text{ }^{\circ}\text{C}$. On the other hand, phenol **3.136** was unstable, frequently generating a small amount of pyran **3.137** after column chromatography. Storage of phenol **3.136** at $-20\text{ }^{\circ}\text{C}$ for a few days led to spontaneous conversion to **3.137** with slight decomposition. These observations suggested that the oxidation state of the tertiary amine has an important influence on the oxidation process of the whole molecule.

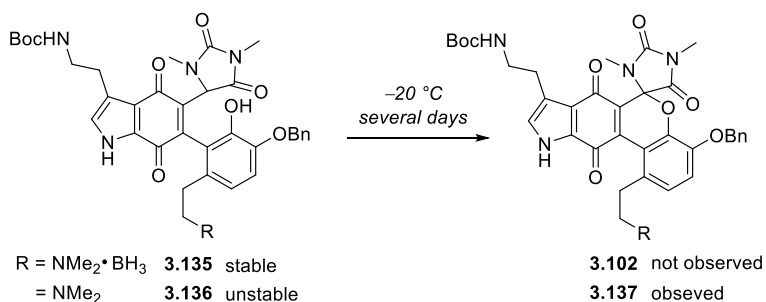
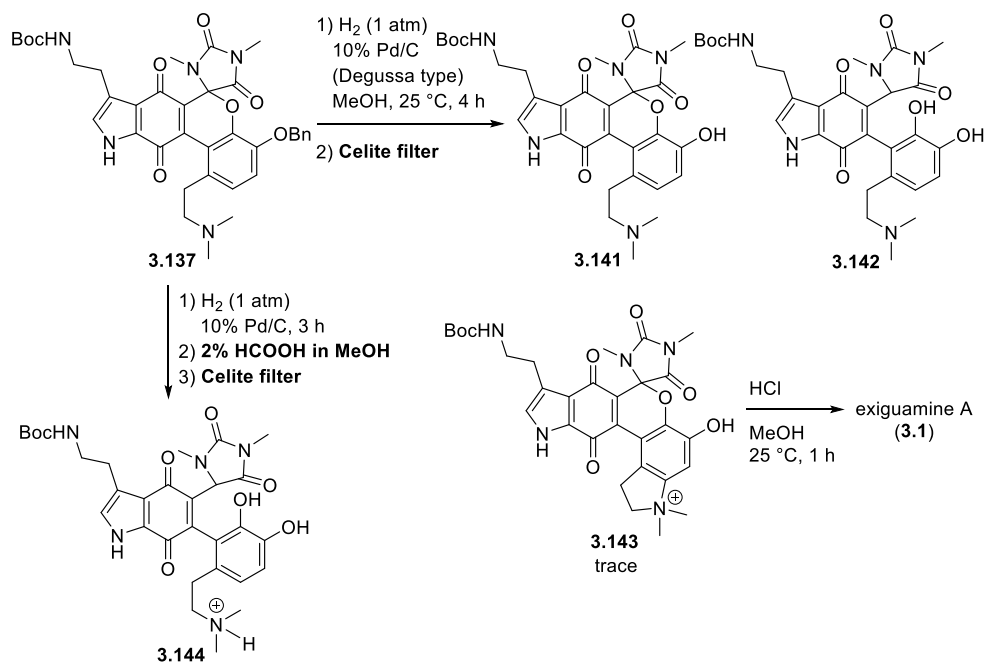


Figure 3.3 Stability of Phenols **3.135** and **3.136**

3.6 Completion of Total Synthesis of Exiguamine A

Having installed five out of six rings in exiguamine A, we set out to complete the total synthesis through deprotection and oxidative cyclization to form the indolinium.

Benzyl ether **3.137** was hydrogenated using 10% Pd/C (Degussa type) to obtain phenol **3.141**. In this hydrogenolysis, two additional products, bisphenol **3.142** and indolinium **3.143**, were also produced in varying amounts. It was found that the distribution of these products was dependent on the exposure time of the crude hydrogenolysis product mixture to air during the Celite filtration. Indolinium **3.143**, which was formed in the least amount, was treated with methanolic HCl to afford exiguamine A (**3.1**) (Scheme 3.42).

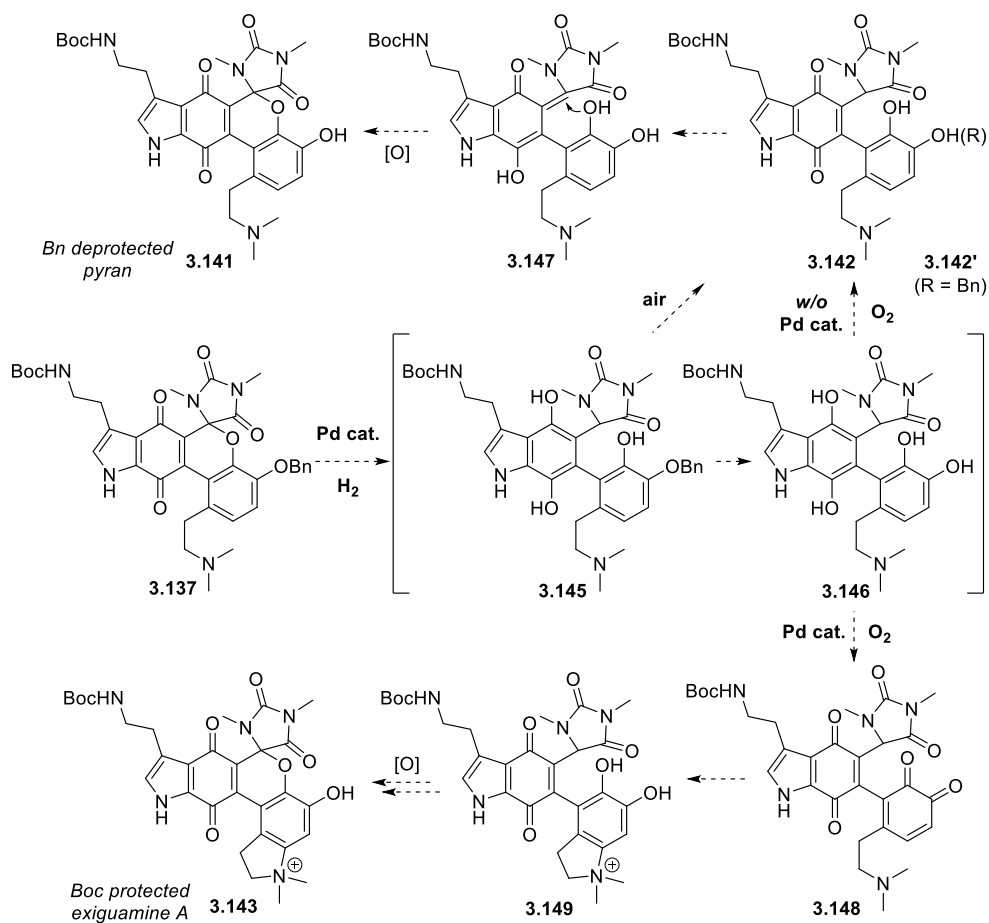


Scheme 3.42 Hydrogenation and Hydrogenolysis of **3.137**

To investigate the mechanism of unexpected formation of indolinium **3.143**, we examined possible processes occurring during and after the hydrogenolytic

debenzylation event. An attempt was made to obtain an intermediate by treating the hydrogenation product with an acid in anticipation of the following two effects. The first was that the tertiary amine would be converted to an ammonium form, protected against intramolecular nucleophilic addition. Second, based on the results of previous experiments, we predicted that if the amine was made electronically deficient, formation of the pyran ring would be suppressed. On the basis of these assumptions, a solution of degassed methanolic formic acid was added immediately after the hydrogenation reaction. After Celite filtration, the major product obtained was found to be the bisphenolic ammonium **3.144** in which the amine did not participate in the cyclization and the phenol did not form the pyran moiety.

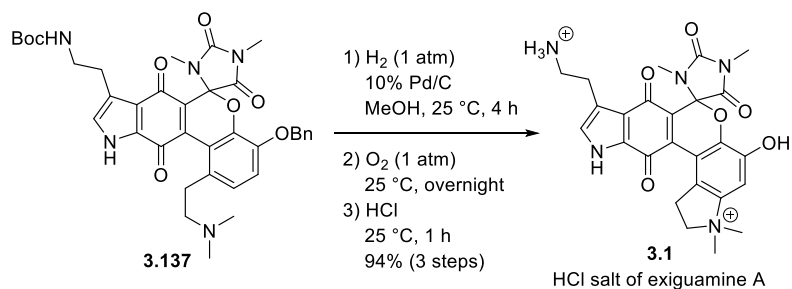
Based on this result, the mechanism for the formation of various products is proposed (Scheme 3.43). In the presence of hydrogen and 10% Pd/C catalyst, the hydrogenation reaction would form a hydroquinone, rendering the C-O bond benzylic and susceptible to hydrogenolysis. Further hydrogenolysis of the benzyl protecting group occurs to yield tetraphenol **3.146**, which is readily converted to bisphenol **3.142**. The sequence of three reductive events – hydroquinone formation, C-O bond cleavage and debenzylation – has been confirmed by the hydrogenation reaction using 5% Pd/C catalyst, from which a quinone form of **3.145** (a benzyl ether of **3.141**) was isolated. When the catechol is oxidized *in situ* to form *ortho*-quinone **3.148**, a series of oxidative cascade reactions, starting with intramolecular nucleophilic addition of the tertiary amine, gives **3.143** via **3.149**. On the other hand, when the catechol oxidation is delayed, **3.142** undergoes cycloisomerization-oxidation to form pyran **3.141**.



Scheme 3.43 Proposed Mechanism for Competitive Formation of **3.141** and **3.143**

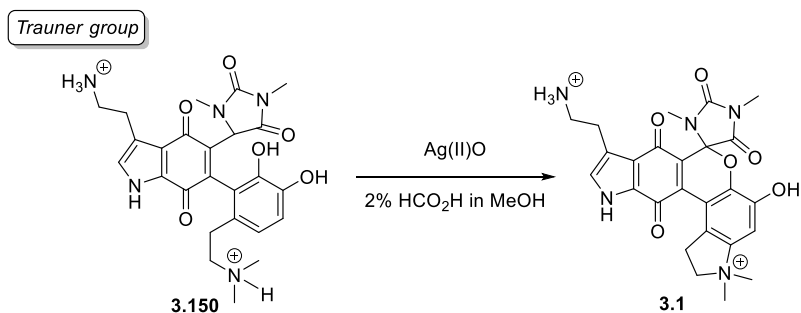
Based on the mechanistic picture, it was assumed that the Boc-protected exiguamine A **3.143** could be produced more efficiently by *in situ* oxidation of the catechol **3.146** generated in the hydrogenation reaction. Indeed, subsequent to hydrogenation, immediate oxidation using an oxygen balloon produced the Boc-protected exiguamine A **3.143** almost exclusively.

Thus, using a series of reaction conditions identified above, the total synthesis was completed by proceeding three steps from **3.137** in one-pot to obtain a HCl salt form of exiguamine A (**3.1**) in 94% yield (Scheme 3.44).

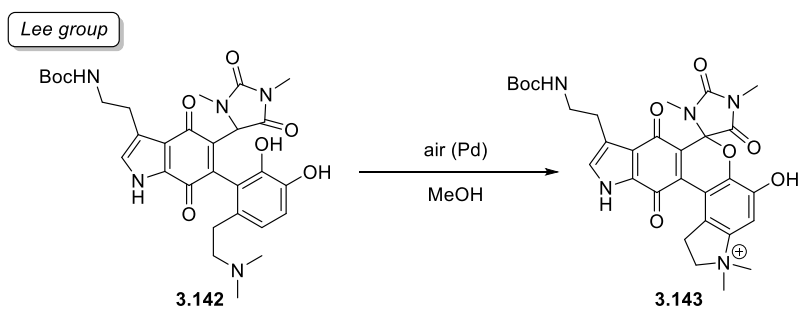


Scheme 3.44 Completion of Total Synthesis of Exiguamine A (**3.1**)

The key precursor **3.142** has a reactivity different from that of the Trauner group. (Scheme 3.45).¹⁶ The Trauner group reported that it was difficult to oxidize their key precursor catechol which was isolated as a bisammonium form. Many oxidants proved ineffective for oxidation of **3.150**, including ambient atmosphere conditions, and only AgO gave exiguamine A (**3.1**). In contrast, catechol **3.142** obtained in our route as a neutral form was converted to the Boc-protected exiguamine A **3.143** in 50% yield under ambient atmospheric conditions and in quantitative yield under oxygen atmosphere. Similar to the results of the post-Claisen rearrangement reactions, the electronic environment of the tertiary amine, and possibly the primary amine as well, had, once again, a significant effect on the oxidation process of the whole molecule.



The use of Ag(II)O proved essential to promote this reaction cascade, as subjecting of crude **3.150** to **an ambient oxygen atmosphere** along with other oxidation conditions failed to oxidize the catechol moiety and **resulted in the recovery of pure 3.150**. – *Chem. Eur. J.* **2012**, *18*, 4999.

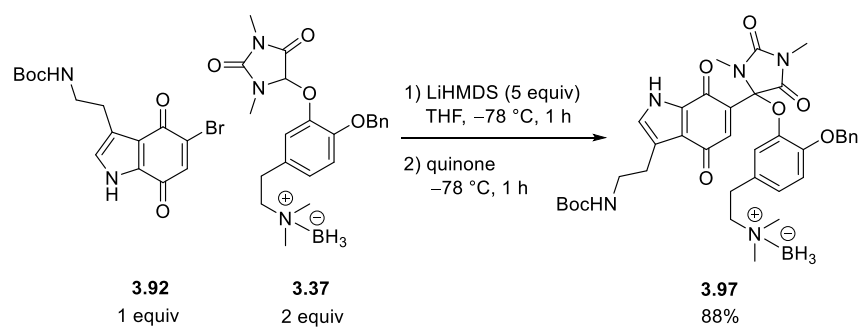


An ambient oxygen atmosphere promote the reaction cascade (ca. 50%).

Scheme 3.45 Comparison of Key Intermediates **3.142** with **3.150**

3.7 Total Synthesis of *Iso*-Exiguamine A

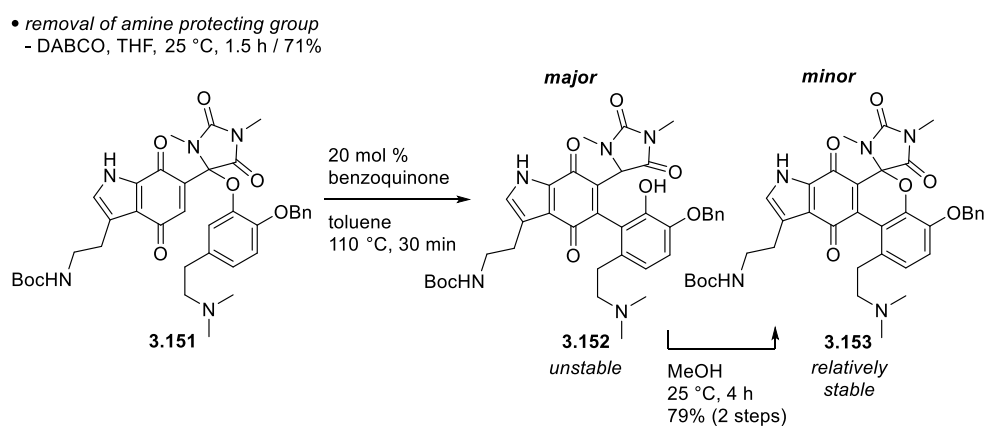
Having completed the total synthesis of exiguamine A, we turned our attention to the synthesis of exiguamine analogues that could be used for biological evaluation studies. Among possible candidates, particularly interesting was an analogue that would be synthesized from the intermediate resulted from the coupling of 5-bromoquinone **3.92** with dopamine-hydantoin **3.37** (Scheme 3.46).



Scheme 3.46 Synthesis of Michael Adduct **3.97**

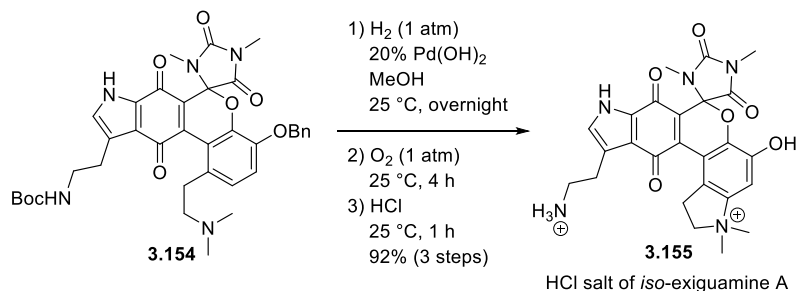
Advancing this intermediate through the late-stage operations employed in the total synthesis of exiguamine A would produce an isomeric exiguamine, namely *iso*-exiguamine A.

Using the reaction conditions found during the synthesis of exiguamine A, the Claisen rearrangement of the debrominated **3.151** was attempted (Scheme 3.47). After performing the Claisen rearrangement of **3.151** in the presence of 20 mol % benzoquinone, the resulting mixture was dissolved in methanol and exposed to air to afford pyran **3.153** in 79% yield. The reaction rates of each step were relatively faster than those of the compound used in the exiguamine series.



Scheme 3.47 Claisen Rearrangement – Oxidation Reaction of Regioisomer

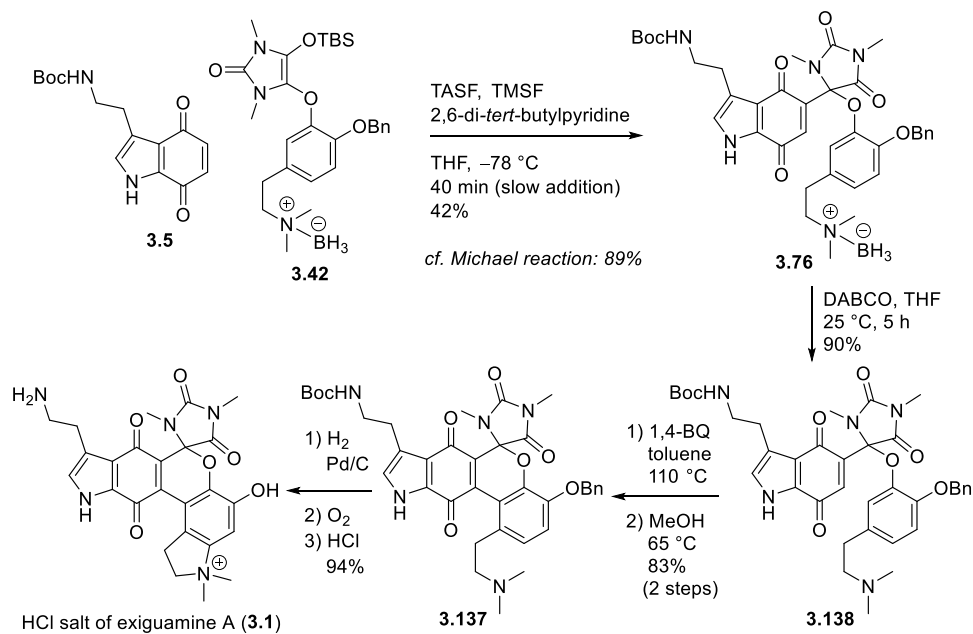
Pyran **3.153** was subsequently subjected to a series of one-pot reactions involving hydrogen, oxygen and acid treatments to furnish an HCl salt form of *iso*-exiguamine A (**3.154**) in good yield (Scheme 3.48).



Scheme 3.48 Completion of Total Synthesis of *Iso*-Exiguamine A (**3.154**)

3.8 Conclusion

A concise total synthesis of exiguamine A, a compound with a high molecular complexity and significant inhibitory activity against IDO, was completed. The key reactions are summarized in Scheme 3.49.



Scheme 3.49 Summary: Total Synthesis of Exiguamine A

Each fragment has been synthesized by two routes, one starting from commercially available compounds with privileged carbon skeletons and the other attaching the necessary carbon units to simple feedstock compounds. Particularly noteworthy is the development of a new method for differential functionalization of dihydroxyl groups present in dopamine. All components of exiguamine A were assembled into one molecule by the Mukaiyama-Michael reaction or the Michael reaction, and the subsequent Claisen rearrangement constructed the central six-membered pyran framework. Finally, through a series of cascade oxidation-reduction processes using hydrogen and oxygen, it was possible to complete the total synthesis of the novel alkaloid natural product exiguamine A. In addition, convergent synthesis strategies provided an opportunity to prepare a regioisomer of exiguamine A, named *iso*-exiguamine A. The efficient synthesis of exiguamine A allowed for cell-based evaluation of its IDO inhibitory activity, which had been reported based only on an enzymatic assay (Chapter 4). By synthesizing *iso*-exiguamine A, an opportunity to identify novel IDO inhibitor candidates was also provided. The convergent synthesis accomplished in our studies is expected to contribute to the discovery of novel IDO inhibitors and further development of immune-modulating therapeutics.

3.9 References

- [1] Mukaiyama, T.; Sagawa, Y.; Kobayashi, S. *Chem. Lett.* **1987**, 2169.
- [2] (a) Ranganathan, D.; Rao, C. B.; Ranganathan, S.; Mehrotra, A. K.; Iyengar, R. *J. Org. Chem.* **1980**, *45*, 1185. (b) Lancianesi, S.; Palmieri, A.; Petrini, M. *Chem. Rev.* **2014**, *114*, 7108.
- [3] (a) Carr, G.; Chung, M. K. W.; Mauk, A. G.; Andersen, R. J. *J. Med. Chem.* **2008**,

- 51, 2634. For a review on Frémy's salt, see: (b) Zimmer, H.; Lankin, D. C.; Horgan, S. W. *Chem. Rev.* **1971**, *71*, 229.
- [4] (a) Robbins, D. W.; Boebel, T. A.; Hartwig, J. F. *J. Am. Chem. Soc.* **2010**, *132*, 4068. (b) Loach, R. P.; Fenton, O. S.; Amaike, K.; Siegel, D. S.; Ozkal, E.; Movassaghi, M. *J. Org. Chem.* **2014**, *79*, 11254. (c) Wang, C.; Sperry, J. *J. Org. Chem.* **2012**, *77*, 2584. (d) Eastabrook, A. S.; Wang, C.; Davison, E. K.; Sperry, J. *J. Org. Chem.* **2015**, *80*, 1006.
- [5] Ben-Ishai, D.; Altman J.; Bernstein Z. *Tetrahedron* **1977**, *33*, 1191.
- [6] Nakazato, A.; Ohta, K.; Sekiguchi, Y.; Okuyama, S.; Chaki, S.; Kawashima, Y.; Hatayama, K. *J. Med. Chem.* **1999**, *42*, 1076.
- [7] For regioselective cleavage of a cyclic silyl ether, see: (a) Tanino, K.; Shimizu, T.; Kuwahara, M. Kuwajima, I. *J. Org. Chem.* **1998**, *63*, 2422. (b) Chando, K. M.; Bailey, P. A.; Abramite, J. A.; Sammakia, T. *Org. Lett.* **2015**, *17*, 5196–5199
- [8] (a) Noyori, R.; Nishida, I.; Sakata, J. *J. Am. Chem. Soc.* **1983**, *105*, 1598. (b) RajanBabu, T. V. *J. Org. Chem.* **1984**, *49*, 2084.
- [9] Della, E. W.; Tsanaktsidis, J. *Synthesis* **1988**, *5*, 407.
- [10] Yamada, F.; Tamura, M.; Hasegawa, A.; Somei, M. *Chem. Pharm. Bull.* **2002**, *50*, 92.
- [11] Comer, E.; Murphy, W. S. *ARKIVOC* **2003**, 286.
- [12] Zhang, H.-B.; Liu, L.; Chen, Y.-J.; Wang, D.; Li, C.-J. *Adv. Synth. Catal.* **2006**, *348*, 229.
- [13] Bhattacharya, A.; DiMichele, L. M.; Dolling, U.-H.; Grabowski, E. J. J.; Grenda, V. *J. Org. Chem.* **1989**, *54*, 6118.
- [14] For reviews, see: (a) Martín Castro, A. M. *Chem. Rev.* **2004**, *104*, 2939. (b) Majumdar, K. C.; Alam, S.; Chattopadhyay, B. *Tetrahedron* **2008**, *64*, 597.

[15] Trost, B. M.; Toste, D. *J. Am. Chem. Soc.* **1998**, *120*, 815.

[16] (a) Volgraf, M.; Lumb, J.-P.; Brastianos, H. C.; Carr, G.; Chung, M. K. W.; Munzel, M.; Mauk, A. G.; Andersen, R. J.; Trauner, D. *Nat. Chem. Biol.* **2008**, *4*, 535. (b) Sofiyev, V.; Lumb, J.-P.; Volgraf, M.; Trauner, D. *Chem. Eur. J.* **2012**, *18*, 4999.

3.10 Experimental Section

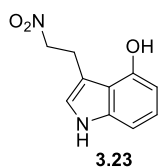
3.10.1. General Information

NMR spectra were obtained on an Agilent 400-MR DD2 Magnetic Resonance System (400 MHz) or a Varian/Oxford As-500 (500 MHz) spectrometer. ¹H NMR spectrum of exiguamine A was recorded on a Bruker Avance III 600 (600 MHz) spectrometer from National Center for Inter-University Research Facilities (Seoul National University, Seoul). Chemical shift values were recorded as parts per million (δ) relative to tetramethylsilane as an internal standard unless otherwise indicated, and coupling constants in Hertz (Hz). The following abbreviations (or combinations thereof) were used to explain the multiplicities: s = singlet, d = doublet, t = triplet, q = quartet, m = multiplet, br = broad. IR spectra were measured on a Thermo Scientific Nicolet 6700 spectrometer. Optical rotations were measured in a 50.00 mm cell with a Jasco P-1030 polarimeter equipped with a sodium lamp (589 nm). High resolution mass spectra (HRMS) were recorded from the Organic Chemistry Research Center (Sogang University, Seoul) or National Center for Inter-University Research Facilities (Seoul National University, Seoul) using either electrospray ionization (ESI) or fast atom bombardment (FAB) method.

All reactions were carried out in flame-dried glassware under a nitrogen atmosphere unless otherwise specified. The progress of the reaction was checked on

thin layer chromatography (TLC) plates (Merck 5554 Kiesel gel 60 F₂₅₄), and the spots were visualized under 254 nm UV light and/or charring after dipping the TLC plate into a vanillin solution (15.0 g of vanillin and 2.5 mL of concentrated sulfuric acid in 250 mL of ethanol), a KMnO₄ solution (3.0 g of KMnO₄, 20.0 g of K₂CO₃, and 5.0 mL of 5% NaOH solution in 300 mL of water), a ceric ammonium molybdate solution (0.5 g of ceric ammonium sulfate, 12 g of ammonium molybdate and 15 mL of concentrated H₂SO₄ in 235 mL of H₂O) or a phosphomolybdic acid solution (250 mg phosphomolybdic acid in 50 mL ethanol). Chromatographic purification of products was performed using flash column chromatography on silica gel (Merck 9385 Kiesel gel 60), preparative layer plates (PLC) on silica gel (Merck 3895 Kiesel gel 60 F₂₅₄, 1 mm) or C18 cartridges (Discovery® DSC-18 SPE Tube). All solvents were obtained by passing through activated alumina columns of solvent purification systems from Glass Contour. Commercially available reagents were obtained from Sigma-Aldrich, Tokyo Chemical Industry (TCI), Acros Organics, Strem or Alfa Aesar and used without further purification.

3.10.2. Selected Experiments and Characterization

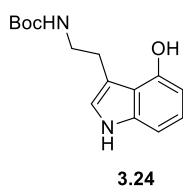


Nitroethylindole **3.23**

To a solution of 4-hydroxyindole (3.35 g, 25 mmol) in benzene (50 mL) was added nitroethylene¹ (12.15 M in toluene, 4.1 mL, 50 mmol) dropwise at 0 °C and the

¹ Chi, Y.; Guo, L.; Kopf, N. A.; Gellman, S. H. *J. Am. Chem. Soc.* **2008**, *130*, 17, 5608.

resulting suspension was stirred at room temperature for 24 h.² The reaction mixture was concentrated *in vacuo* and the residue was purified by flash column chromatography to give nitroethylindole **3.23** (3.08 g, 60%) as a yellow oil. R_f 0.19 (hexanes-EtOAc, 3:1); ¹H NMR (400 MHz, CDCl₃) δ 7.98 (br s, 1H), 6.99 (t, J = 7.8 Hz, 1H), 6.91 (d, J = 8.2 Hz, 1H), 6.89 (d, J = 1.5 Hz, 1H), 6.37 (d, J = 7.5 Hz, 1H), 5.21 (s, 1H), 4.77 (t, J = 7.1 Hz, 2H), 3.54 (t, J = 7.1 Hz, 2H); ¹³C NMR (100 MHz, CDCl₃) δ 149.9, 138.8, 123.3, 122.2, 116.0, 110.1, 104.7, 104.3, 77.2, 25.5; IR (neat) ν_{\max} 3518, 3403, 2360, 2342, 1592, 1549, 1506, 1451, 1383, 1306, 1262, 1038, 836, 726 cm⁻¹; HRMS (ESI) m/z calcd. for C₁₀H₁₀N₂NaO₃ [M+Na]⁺ 229.0584, found 229.0586.

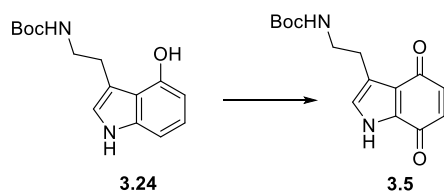


Carbamate **3.24**

To a solution of nitroethylindole **3.23** (45.4 mg, 0.22 mmol) in MeOH (3 mL) were added NiCl₂•6H₂O (104.6 mg, 0.44 mmol) and sodium borohydride (42 mg, 1.1 mmol) at 0 °C. After stirring at 0 °C for 1.5 h, Boc₂O (0.06 mL, 0.24 mmol) and triethylamine (0.04 mg, 0.29 mmol) were added and the resulting mixture was slowly warmed to room temperature while stirring for 1.5 h. The reaction was quenched with saturated aq. NH₄Cl solution and filtered through a pad of Celite. After concentration of the filtrate, the residue was diluted with CH₂Cl₂, washed with brine,

² Ranganathan, D.; Rao, C. B.; Ranganathan, S.; Mehrotra, A. K.; Iyengar, R. *J. Org. Chem.* **1980**, *45*, 1185.

dried over Na₂SO₄, filtered and concentrated under reduced pressure. Purification by flash column chromatography afforded carbamate **3.24** (45.6 mg, 75%) as a white solid. *R_f* 0.17 (hexanes-EtOAc, 2:1); ¹H NMR (400 MHz, CDCl₃) δ 7.95 (br s, 1H), 7.01 (t, *J* = 7.8 Hz, 1H), 6.93 (d, *J* = 8.1 Hz, 1H), 6.89 (s, 1H), 6.48 (d, *J* = 6.7 Hz, 1H), 6.30 (br. s, 1H), 4.86 (br s, 1H), 3.43 (dd, *J* = 13.4, 6.8 Hz, 2H), 3.07 (t, *J* = 7.1 Hz, 2H), 1.43 (s, 9H); ¹³C NMR (100 MHz, CDCl₃) δ 156.9, 151.0, 139.0, 123.1, 121.3, 116.7, 113.0, 104.6, 103.9, 79.7, 42.4, 28.6, 27.0; IR (neat) *v*_{max} 3405, 2977, 2932, 2360, 1683, 1506, 1456, 1260, 1167, 1040, 909, 853, 734 cm⁻¹; HRMS (ESI) *m/z* calcd. for C₁₅H₂₀N₂NaO₃ [M+Na]⁺ 299.1366, found 299.1368.

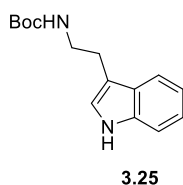


Indoloquinone **3.5** from **3.24**

Method A: Salcomine (65 mg, 0.2 mmol) was added to a solution of hydroxyindole **3.24** (276 mg, 1.0 mmol) in acetonitrile (5 mL). The flask was purged with 3 cycles of O₂/vacuum. After 4 h, the reaction mixture was filtered through a pad of Celite and washed with EtOAc. The filtrate was concentrated *in vacuo* and purified by flash column chromatography to provide indoloquinone **3.5** (125 mg, 43%) as an orange solid.

Method B: To a solution of hydroxyindole **3.24** (268 mg, 0.97 mmol) in acetone/H₂O (2:3, 40 mL) and phosphate buffer (0.1 M, pH = 7.4, 8 mL) was added potassium nitrosodisulfonate (Acros, 50-75% remainder water and methanol, 1.08 g, 2.7 mmol)

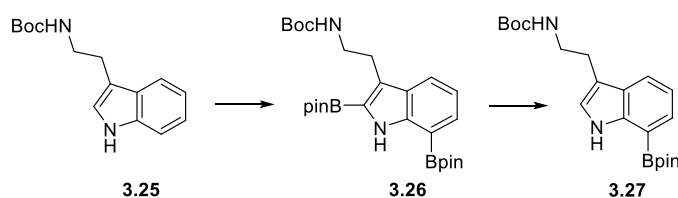
at room temperature. After stirring for 2 h, the reaction mixture was diluted with H₂O and extracted with CH₂Cl₂ until the aqueous layer showed purple color. The combined organic layer was washed with brine, dried over Na₂SO₄, filtered and concentrated under reduced pressure. The crude mixture was purified by flash column chromatography to give indoloquinone **3.5** (251 mg, 89%) as an orange solid. *R*_f 0.40 (hexanes-EtOAc, 1:1); ¹H NMR (400 MHz, DMSO-*d*₆) δ 12.55 (br s, 1H), 7.05 (s, 1H), 6.81 (br s, 1H), 6.59 (q, *J* = 10.2 Hz, 2H), 3.16 (dd, *J* = 12.9, 6.7 Hz, 2H), 2.77 (t, *J* = 6.9 Hz, 2H), 1.35 (s, 9H); ¹³C NMR (100 MHz, DMSO-*d*₆) δ 184.1, 176.8, 155.5, 137.9, 136.2, 130.6, 124.9, 123.0, 122.2, 77.4, 39.7, 28.2, 25.6; IR (neat) ν_{max} 3353, 3198, 2360, 2342, 1680, 1662, 1640, 1531, 1390, 1252, 1170, 1099, 841 cm⁻¹; HRMS (ESI) *m/z* calcd. for C₁₅H₁₈N₂NaO₄ [M+Na]⁺ 313.1159, found 313.1158.



N-Boc tryptamine **3.25**

To a solution of tryptamine (3.20 g, 20 mmol) in MeOH (100 mL) was added triethylamine (3.6 mL, 26 mmol). The mixture was cooled to 0 °C and Boc₂O (5.5 mL, 24 mmol) was added dropwise. After stirring at 0 °C for 3 h, the reaction mixture was concentrated and diluted with CH₂Cl₂. The organic layer was washed with water and brine, dried over MgSO₄, filtered and concentrated *in vacuo*. The residue was purified by flash column chromatography to give *N*-Boc tryptamine **3.25** (4.84 g, 93%) as a white powder. *R*_f 0.33 (hexanes-EtOAc, 2:1); ¹H NMR (400 MHz, CDCl₃) δ 8.10 (br s, 1H), 7.61 (d, *J* = 7.8 Hz, 1H), 7.36 (d, *J* = 8.1 Hz, 1H), 7.20 (t, *J* = 7.5

Hz, 1H), 7.12 (t, $J = 7.5$ Hz, 1H), 7.02 (s, 1H), 4.61 (br s, 1H), 3.52 – 3.40 (m, 2H), 2.95 (t, $J = 6.6$ Hz, 2H), 1.44 (s, 9H); ^{13}C NMR (100 MHz, CDCl_3) δ 156.2, 136.5, 127.4, 122.2, 122.1, 119.4, 118.9, 113.0, 111.3, 79.3, 41.0, 28.6, 25.9.

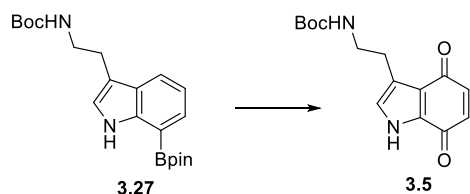


Boronic ester **3.27**

According to the procedure described by Movassaghi,³ to a flame-dried round-bottom flask were added *N*-Boc tryptamine **3.25** (78 mg, 0.3 mmol), (1,5-cyclooctadiene)(methoxy)iridium(I) dimer (5 mg, 0.0075 mmol), and 4,4'-di-*tert*-butyl-2,2'-bipyridine (4 mg, 0.015 mmol). The flask was placed under argon atmosphere and THF (3 mL) was added. To the mixture was added pinacolborane (0.21 mL, 1.5 mmol) and stirred at 65 °C for 20 h. After cooling to room temperature, the reaction mixture was concentrated and the resulting residue (diborotryptamine **3.26**) was dissolved in acetic acid (0.9 mL), palladium (II) acetate (3.4 mg, 0.015 mmol) was added and stirred under argon at 30 °C. After 36 h, the mixture was cooled to room temperature and was filtered through a pad of Celite with EtOAc as an eluent. The filtrate was washed with saturated aq. NaHCO_3 solution, the organic layer was dried over Na_2SO_4 , filtered and concentrated under reduced pressure. Purification by flash column chromatography provided the boronic ester **3.27** (74 mg, 64%) as a white foamy solid. R_f 0.31 (hexanes-EtOAc, 4:1); ^1H NMR (400 MHz, CDCl_3) δ 9.07 (br s, 1H), 7.73 (d, $J = 7.9$ Hz, 1H), 7.66 (d, $J = 7.0$ Hz, 1H), 7.13 (t,

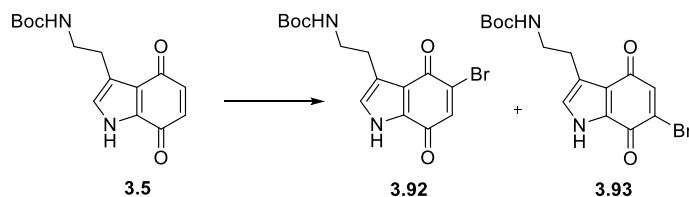
³ Loach, R. P.; Fenton, O. S.; Amaike, K.; Siegel, D. S.; Ozkal, E.; Movassaghi, M. *J. Org. Chem.* **2014**, *79*, 11254-11263.

$J = 7.5$ Hz, 1H), 7.09 (s, 1H), 4.58 (br s, 1H), 3.50 – 3.36 (d, 2H), 2.97 (t, $J = 6.6$ Hz, 2H), 1.43 (s, 9H), 1.39 (s, 12H); ^{13}C NMR (100 MHz, CDCl_3) δ 156.1, 141.6, 129.5, 126.4, 122.5, 122.1, 119.0, 112.7, 83.9, 79.1, 41.1, 28.5, 25.8, 25.1; IR (neat) ν_{max} 3452, 2974, 2926, 1702, 1509, 1435, 1367, 1327, 1166, 1134, 965, 753, 683 cm^{-1} ; HRMS (ESI) m/z calcd. for $\text{C}_{21}\text{H}_{31}\text{BN}_2\text{NaO}_4$ $[\text{M}+\text{Na}]^+$ 409.2273, found 409.2275.



Indoloquinone **3.5** from **3.27**

Urea-hydrogenperoxide (11.3 mg, 0.12 mmol) was added to a solution of boronic ester **3.27** (38.7 mg, 0.10 mmol) in acetone/ H_2O (2:3, 4.0 mL) and sodium phosphate buffer (0.1 M, $\text{pH} = 7.4$, 0.8 mL) at room temperature. After complete consumption of the boronic ester judged by TLC analysis (ca. 1 h), Frémy's salt (80.5 mg, 0.30 mmol) was added to the reaction mixture. After stirring for 12 h, the mixture was diluted with water and extracted with CH_2Cl_2 until the aqueous layer showed purple color. The combined organic layer was washed with brine, dried over Na_2SO_4 , filtered and concentrated *in vacuo*. The resulting mixture was purified by flash column chromatography to give indoloquinone **3.5** (17.1 mg, 59%) as an orange solid.



Bromoquinons **3.92** and **3.93**

Pyridinium tribromide (technical grade, 90%, 64.0 mg, 0.18 mmol) was added to a solution of quinone **3.5** (43.5 mg, 0.15 mmol) in CH₃Cl/THF (1:1, 3.0 mL). After stirring at room temperature for 40 min, the reaction mixture was quenched with brine and extracted with CH₂Cl₂. The combined organic extracts were dried over Na₂SO₄, filtered and concentrated under reduced pressure. The residue was purified by flash column chromatography to provide mixture of isomers **3.92** and **3.93** (44.9 mg, 81%) as an orange solid (Ratio of isomers was determined to be 1:3 (**3.92**:**3.93**) using ¹H NMR analysis of the purified product.).

Separation of **3.92** and **3.93**

Pyridinium tribromide (technical grade, 90%, 60.8 mg, 0.17) was added to a solution of quinone **3.5** (45.0 mg, 0.16 mmol) in CH₃Cl/THF (1:1, 3.1 mL). After stirring at room temperature for 40 min, the reaction mixture was quenched with brine and extracted with CH₂Cl₂. The combined organic extracts were dried over Na₂SO₄, filtered and concentrated under reduced pressure. The residue was purified by flash column chromatography (silica gel 60, 0.015-0.040 mm) to provide bromoquinone **3.92** (38.0 mg, 66%) as an orange solid and a mixture of **3.92** and **3.93** (15.4 mg, 27%) also obtained as an orange solid.

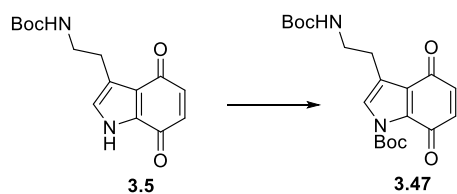
5-bromoquinone **3.92**

An orange solid. *R*_f 0.39 (hexanes-EtOAc, 1:1); ¹H NMR (400 MHz, CDCl₃) δ 9.46 (br s, 1H), 7.12 (s, 1H), 6.90 (s, 1H), 4.71 (br s, 1H), 3.40 (q, *J* = 6.6 Hz, 2H), 2.96 (t, *J* = 6.5 Hz, 2H), 1.42 (s, 9H); ¹³C NMR (100 MHz, CDCl₃) δ 175.9, 174.9, 156.3, 140.2, 137.3, 131.2, 125.6, 124.7, 121.9, 79.5, 40.8, 28.5, 26.3; IR (neat) *v*_{max} 3345,

2975, 2930, 2868, 1653, 1576, 1505, 1400, 1365, 1271, 1167, 1106, 1036, 878, 809 cm^{-1} ; HRMS (ESI) m/z calcd. for $\text{C}_{15}\text{H}_{17}\text{BrN}_2\text{NaO}_4$ $[\text{M}+\text{Na}]^+$ 391.0264, found 391.0266.

6-bromoquinone **3.93**

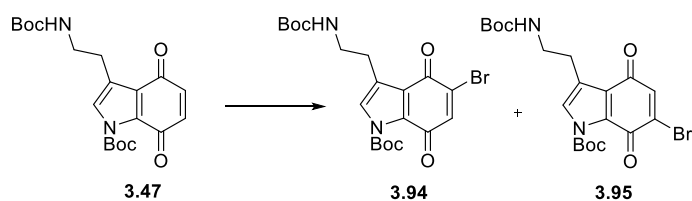
An orange solid. R_f 0.44 (hexanes-EtOAc, 1:1); ^1H NMR (400 MHz, $\text{DMSO-}d_6$) δ 12.83 (br s, 1H), 7.19 (s, 1H), 7.11 (s, 1H), 6.82 (br s, 1H), 3.15 (dd, $J = 12.7, 6.4$ Hz, 2H), 2.76 (t, $J = 6.9$ Hz, 2H), 1.34 (s, 9H); ^{13}C NMR (100 MHz, $\text{DMSO-}d_6$) δ 181.3, 168.9, 155.5, 138.7, 136.8, 129.0, 126.4, 123.8, 122.9, 77.4, 39.3, 28.3, 25.7; IR (neat) ν_{max} 3378, 3173, 2976, 2932, 1684, 1670, 1643, 1522, 1507, 1475, 1386, 1367, 1250, 1163, 1069, 988, 889 cm^{-1} ; HRMS (ESI) m/z calcd. for $\text{C}_{15}\text{H}_{17}\text{BrN}_2\text{NaO}_4$ $[\text{M}+\text{Na}]^+$ 391.0264, found 391.0265.



N-Boc indoloquinone **3.47**

To a suspension of sodium hydride (50.4 mg, 1.26 mmol) in THF (12 mL) was added indoloquinone **3.5** (335 mg, 1.15 mmol) dissolved in THF (0.5 mL) at 0 °C. After stirring for 40 min, Boc_2O (0.015 mL, 0.06 mmol) was added to the purple color solution and the reaction mixture was stirred at 0 °C for additional 1.5 h. The resulting yellow mixture was quenched with water and extracted with CH_2Cl_2 . The combined organic extracts were dried over Na_2SO_4 , concentrated and purified by flash column chromatography to afford *N*-Boc indoloquinone **3.47** (384 mg, 85%)

as a yellow solid. R_f 0.30 (hexanes-EtOAc, 3:1); ^1H NMR (400 MHz, CDCl_3) δ 7.31 (s, 1H), 6.59 (q, $J = 10.2$ Hz, 2H), 4.70 (br s, 1H), 3.38 (dd, $J = 12.9, 6.5$ Hz, 2H), 2.93 (t, $J = 6.6$ Hz, 2H), 1.64 (s, 9H), 1.42 (s, 9H); ^{13}C NMR (100 MHz, CDCl_3) δ 184.9, 175.4, 156.0, 147.6, 138.0, 135.8, 130.8, 127.7, 122.8, 86.6, 79.3, 40.3, 28.5, 27.7, 26.0; IR (neat) ν_{max} 3371, 2977, 2933, 1755, 1707, 1659, 1519, 1411, 1367, 1338, 1275, 1152, 1003, 842, 767 cm^{-1} ; HRMS (ESI) m/z calcd. for $\text{C}_{20}\text{H}_{26}\text{N}_2\text{NaO}_6$ $[\text{M}+\text{Na}]^+$ 413.1683, found 413.1687.



Bromoquinones **3.94** and **3.95**

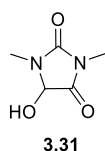
Pyridinium tribromide (technical grade, 90%, 110 mg, 0.31 mmol) was added to a solution of quinone **3.47** (101 mg, 0.26 mmol) in $\text{CH}_2\text{Cl}_2/\text{THF}$ (1:1, 5.2 mL). After stirring at room temperature for 1.5 h, the reaction mixture was quenched with brine and extracted with CH_2Cl_2 . The combined organic extracts were dried over Na_2SO_4 , filtered and concentrated under reduced pressure. The residue was purified by flash column chromatography to provide a mixture of bromoquinones **3.94** and **3.95** (113 mg, 93%) as a yellow solid (Ratio of isomers was determined to be 2.5:1 (**3.94**:**3.95**) using ^1H NMR analysis of the purified product. The isomers could not be separated due to similar polarity. For characterization, isomers were separated after deprotection of *N*-Boc group of indoloquinone moiety and *N*-Boc group was introduced again to each isomer.)

N-Boc-5-bromoquinone **3.94**

A yellow solid. R_f 0.38 (hexanes-EtOAc, 3:1); ^1H NMR (400 MHz, CDCl_3) δ 7.31 (s, 1H), 7.14 (s, 1H), 4.65 (br s, 1H), 3.37 (dd, $J = 13.1, 6.6$ Hz, 2H), 2.94 (t, $J = 6.7$ Hz, 2H), 1.63 (s, 9H), 1.42 (s, 9H); ^{13}C NMR (100 MHz, CDCl_3) δ 176.8, 172.8, 156.0, 147.3, 139.0, 136.5, 130.8, 128.1, 126.6, 124.0, 87.0, 79.4, 40.2, 28.5, 27.7, 26.2; IR (neat) ν_{max} 3410, 2976, 2930, 1758, 1670, 1659, 1507, 1484, 1395, 1368, 1338, 1256, 1150, 1067, 844, 771 cm^{-1} ; HRMS (ESI) m/z calcd. for $\text{C}_{20}\text{H}_{25}\text{BrN}_2\text{NaO}_6$ $[\text{M}+\text{Na}]^+$ 491.0788, found 491.0791.

N-Boc-6-bromoquinone **3.95**

A yellow solid. R_f 0.38 (hexanes-EtOAc, 3:1); ^1H NMR (400 MHz, CDCl_3) δ 7.33 (s, 1H), 7.11 (s, 1H), 4.68 (br s, 1H), 3.37 (d, $J = 6.2$ Hz, 2H), 2.92 (t, $J = 6.2$ Hz, 2H), 1.64 (s, 9H), 1.42 (s, 9H); ^{13}C NMR (100 MHz, CDCl_3) δ 182.0, 168.0, 156.0, 147.4, 139.1, 137.3, 129.2, 128.8, 128.1, 123.1, 87.1, 79.4, 40.2, 28.5, 27.6, 26.0; IR (neat) ν_{max} 3407, 2976, 2932, 1757, 1677, 1657, 1510, 1489, 1395, 1367, 1340, 1254, 1150, 1072, 1022, 843, 768 cm^{-1} ; HRMS (ESI) m/z calcd. for $\text{C}_{20}\text{H}_{25}\text{BrN}_2\text{NaO}_6$ $[\text{M}+\text{Na}]^+$ 491.0788, found 491.0792.

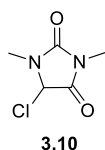


N,N'-dimethyl-5-hydroxyhydantoin **3.31**

Hydantoin **3.31** was prepared using a modified procedure of previously described

method.⁴

N,N-dimethyl urea (2.20 g, 25.0 mmol) and glyoxylic acid monohydrate (2.30 g, 25.0 mmol) were added to a round-bottom flask. After 3-5 min stirring, the mixture turned into a homogeneous solution (*Caution*: Exothermic reaction). Additional acetone (0.50 mL) was added to rinse undissolved reagent on the wall of the round-bottom flask. After stirring at room temperature for 5 h, the reaction mixture was diluted with CH₂Cl₂, dried over MgSO₄, filtered and concentrated *in vacuo* to give hydroxyhydantoin **3.31** (quantitative yield, 3.6 g) as a colorless oil. The product slowly solidified to a white solid upon standing and used without further purification. *R*_f 0.29 (hexanes-EtOAc, 1:3); ¹H NMR (400 MHz, CDCl₃) δ 5.33 (br s, 1H), 5.15 (s, 1H), 3.01 (s, 6H). ¹³C NMR (100 MHz, CDCl₃) δ 172.2, 155.7, 79.7, 26.8, 24.9.

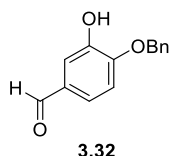


N,N'-dimethyl-5-chlorohydantoin **3.10**

Hydroxyhydantoin **3.31** (51.9 mg, 0.36 mmol) was dissolved in thionyl chloride (3.0 mL) and the mixture was heated to reflux for 12 h. After cooling to room temperature, thionyl chloride was removed under reduced pressure. Volatiles were distilled off azeotropically 5 times using toluene to provide chlorohydantoin **3.10** as a bright yellow oil. The crude product was used without further purification in the next step (*Note*: Chlorohydantoin **3.10** is moisture sensitive and easily hydrolyzed to hydroxyhydantoin **3.31**. But it could be stored over 1 month under argon atmosphere at -20 °C.). ¹H NMR (400 MHz, CDCl₃) δ 5.63 (s, 1H), 3.09 (s, 3H), 3.05 (s, 3H);

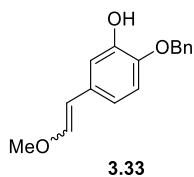
⁴ Ben-Ishai, D.; Altman, J.; Bernstein, Z. *Tetrahedron* **1977**, *33*, 1191-1196.

^{13}C NMR (100 MHz, CDCl_3) δ 167.5, 155.2, 68.7, 27.5, 25.5; IR (neat) ν_{max} 2953, 2360, 2342, 1791, 1727, 1459, 1425, 1395, 1013, 784, 752, 573 cm^{-1} ; HRMS (FAB) m/z calcd. for $\text{C}_5\text{H}_8\text{ClN}_2\text{O}_2$ $[\text{M}+\text{H}]^+$ 163.0269, found 163.0271.



Aldehyde **3.32**

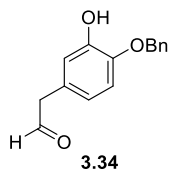
To a solution of 3,4-dihydroxybenzaldehyde (414 mg, 3.0 mmol) in DMF (12 mL) were added benzyl bromide (0.39 mL, 3.3 mmol) and potassium carbonate (622 mg, 4.5 mmol). After stirring at room temperature for 24 h, the reaction mixture was concentrated *in vacuo*, diluted with saturated aq. NH_4Cl solution and EtOAc. The aqueous phase was extracted with EtOAc. The combined organic extracts were dried over MgSO_4 and concentrated under reduced pressure to give a brown solid. Purification by flash column chromatography provided aldehyde **3.32** (360 mg, 52%) as a white crystal. R_f 0.23 (hexanes-EtOAc, 3:1); ^1H NMR (400 MHz, CDCl_3) δ 9.84 (s, 1H), 7.47 (d, $J = 1.7$ Hz, 1H), 7.45 – 7.37 (m, 6H), 7.04 (d, $J = 8.3$ Hz, 1H), 5.79 (s, 1H), 5.21 (s, 2H); ^{13}C NMR (125 MHz, CDCl_3) δ 191.2, 151.0, 146.4, 135.3, 130.9, 129.0, 128.9, 128.0, 124.5, 114.5, 111.6, 71.4; IR (neat) ν_{max} 3226, 2871, 1674, 1605, 1582, 1514, 1454, 1258, 1166, 1117, 1017, 963, 813, 740 cm^{-1} ; HRMS (ESI) m/z calcd. for $\text{C}_{14}\text{H}_{12}\text{NaO}_3$ $[\text{M}+\text{Na}]^+$ 251.0679, found 251.0678.



Enol ether **3.33**

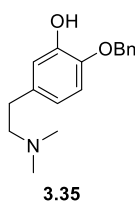
Potassium *tert*-butoxide (3.77 g, 33.6 mmol) was added to a solution of (methoxymethyl)triphenylphosphonium chloride (11.5 g, 33.6 mmol) in THF (70 mL) at 0 °C. The resulting red solution was stirred for 10 min at the same temperature and followed by dropwise addition of aldehyde **3.32** (3.83 g, 16.8 mmol) in THF (14 mL) was added dropwise *via* cannula. The reaction mixture was stirred at 0 °C for 30 min and allowed to warm to room temperature then stirred for additional 30 min. The reaction mixture was quenched with saturated aq. NaHCO₃ solution and extracted with Et₂O. The combined organic layer was dried over MgSO₄, concentrated and purified by flash column chromatography to afford enol ether **3.33** (4.24 g, 98% *E:Z*=1:1 mixture) as a colorless sticky oil. *R*_f 0.4 (hexanes-EtOAc, 3:1); ¹H NMR (500 MHz, CDCl₃) δ 7.44 – 7.33 (m, 10H), 7.30 (d, *J* = 1.7 Hz, 1H), 6.99 (dd, *J* = 8.3, 1.8 Hz, 1H), 6.93 (d, *J* = 13.0 Hz, 1H), 6.87 – 6.80 (m, 3H), 6.67 (dd, *J* = 8.3, 1.8 Hz, 1H), 6.05 (d, *J* = 7.0 Hz, 1H), 5.72 (d, *J* = 12.9 Hz, 1H), 5.60 (dd, *J* = 12.4, 1.1 Hz, 2H), 5.13 (d, *J* = 6.9 Hz, 1H), 5.08 (s, 2H), 5.07 (s, 2H), 3.74 (s, 3H), 3.65 (s, 3H); ¹³C NMR (125 MHz, CDCl₃) δ 148.1, 147.0, 146.1, 145.5, 144.2, 144.0, 136.6, 136.5, 130.5, 130.2, 128.8, 128.8, 128.5, 128.4, 127.9, 127.9, 120.3, 117.3, 114.7, 112.6, 112.1, 111.2, 105.3, 104.7, 71.4, 71.2, 60.7, 56.6; IR (neat) *v*_{max} 3525, 3034, 2935, 1651, 1582, 1511, 1454, 1399, 1271, 1204, 1148, 1126, 1092, 1010, 936, 810, 746 cm⁻¹; HRMS (ESI) *m/z* calcd. for C₁₆H₁₆NaO₃ [M+Na]⁺ 279.0992, found

279.0993.



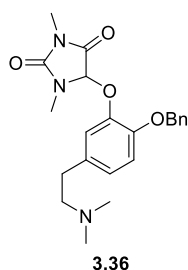
Aldehyde **3.34**

To a solution of enol ether **3.33** (1.32 g, 5.14 mmol) in THF (51 mL) was added 2 *N* HCl (5.14 mL, 10.3 mmol) at room temperature and the reaction mixture was heated under 65 °C for 3 h. After cooling to room temperature, the reaction mixture was quenched with saturated aq. NaHCO₃ solution and extracted with CH₂Cl₂. The combined organic extracts were dried over Na₂SO₄ and concentrated *in vacuo* to give crude aldehyde **3.34** as a yellow oil that was immediately used without further purification in the next step (Although aldehyde **3.34** can be purified by column chromatography, it decomposes upon extended exposure to silica gel.). *R*_f 0.26 (hexanes-EtOAc, 3:1); ¹H NMR (500 MHz, CDCl₃) δ 9.69 (d, *J* = 2.3 Hz, 1H), 7.45 – 7.33 (m, 6H), 6.90 (d, *J* = 8.2 Hz, 1H), 6.81 (s, 1H), 6.66 (d, *J* = 8.0 Hz, 1H), 5.74 (d, *J* = 5.5 Hz, 1H), 5.10 (s, 2H), 3.57 (s, *J* = 1.8 Hz, 2H); ¹³C NMR (125 MHz, CDCl₃) δ 199.8, 146.3, 145.3, 136.2, 128.9, 128.6, 127.9, 125.3, 121.3, 116.1, 112.6, 71.3, 50.0; HRMS (ESI) *m/z* calcd. for C₁₅H₁₄NaO₃ [M+Na]⁺ 265.0835, found 265.0836.



Amine **3.35**

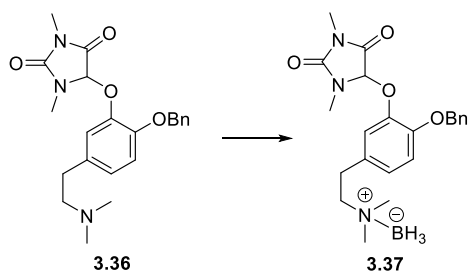
To a solution of crude aldehyde **3.34** (5.14 mmol approximately) in MeOH (51 mL) were added dimethylamine (2.0 M in THF, 7.7 mL, 15.4 mmol) and sodium cyanoborohydride (958 mg, 15.4 mmol) at 0 °C. After stirring at room temperature for 2 h, the reaction mixture was quenched with water and extracted with CH₂Cl₂. The combined organic layer was dried over Na₂SO₄ and concentrated under reduced pressure to give a brown solid. Purification of the residue by flash column chromatography afforded amine **3.35** (990 mg, 71%) as a yellow oil. *R*_f 0.15 (CHCl₃-MeOH, 6:1); ¹H NMR (400 MHz, CDCl₃) δ 7.45 – 7.32 (m, 5H), 6.84 (d, *J* = 8.2 Hz, 1H), 6.80 (d, *J* = 2.0 Hz, 1H), 6.66 (dd, *J* = 8.2, 2.0 Hz, 1H), 5.08 (s, 2H), 2.71 (dd, *J* = 9.7, 6.3 Hz, 2H), 2.54 (dd, *J* = 9.6, 6.4 Hz, 2H), 2.31 (s, 6H); ¹³C NMR (100 MHz, CDCl₃) δ 146.0, 144.4, 136.7, 134.1, 128.8, 128.4, 127.9, 120.0, 115.3, 112.5, 71.4, 61.7, 45.5, 33.8; IR (neat) *v*_{max} 3034, 2945, 2868, 2822, 2360, 2342, 1585, 1511, 1454, 1279, 1259, 1214, 1128, 1021, 860, 737 cm⁻¹; HRMS (ESI) *m/z* calcd. for C₁₇H₂₂NO₂ [M+H]⁺ 272.1645, found 272.1646.



Dopamine-hydantoin adduct **3.36**

Sodium hydride (11.6 mg, 0.29 mmol) was added to a solution of amine **3.35** (66.4

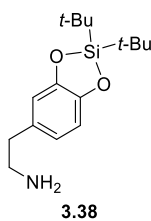
mg, 0.24 mmol) in THF (0.50 mL) at 0 °C. After stirring for 1 h, chlorohydantoin **3.31** (58.5 mg, 0.36 mmol) dissolved in THF (0.25 mL) was added dropwise at 0 °C and the resulting mixture was stirred for 2 h while the temperature gradually warming to room temperature. The reaction mixture was quenched with saturated aq. NaHCO₃ solution and extracted with CH₂Cl₂. The combined organic extracts were washed with brine, dried over Na₂SO₄ and concentrated *in vacuo*. The residue was purified by flash column chromatography to provide dopamine-hydantoin adduct **3.36** (85.3 mg, 90%) as a yellow oil. *R*_f 0.28 (CHCl₃-MeOH, 6:1); ¹H NMR (400 MHz, CDCl₃) δ 7.43 – 7.32 (m, 5H), 7.15 (d, *J* = 1.4 Hz, 1H), 6.95 – 6.90 (m, 2H), 5.42 (s, 1H), 5.07 (s, 2H), 3.02 (s, 3H), 2.84 (s, 3H), 2.76 – 2.69 (m, 2H), 2.55 – 2.48 (m, 2H), 2.29 (s, 6H); ¹³C NMR (100 MHz, CDCl₃) δ 169.2, 156.0, 148.5, 145.3, 136.5, 134.0, 128.8, 128.5, 128.1, 125.4, 122.8, 114.0, 86.1, 71.2, 61.5, 45.6, 33.6, 27.3, 24.8; IR (neat) *v*_{max} 2943, 2770, 1787, 1726, 1508, 1467, 1394, 1268, 1128, 1037, 912, 737 cm⁻¹; HRMS (FAB) *m/z* calcd. for C₂₂H₂₈N₃O₄ [M+H]⁺ 398.2080, found 398.2074.



Amine-borane complex **3.37**

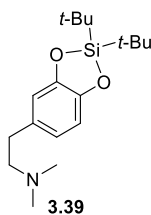
BH₃•THF (1.0 M in THF, 1.13 mL, 1.13 mmol) was added dropwise to a solution of **3.36** (150 mg, 0.38 mmol) in THF (3.8 mL) at -78 °C. After stirring for 2 h, the reaction mixture was concentrated *in vacuo* and purified by flash column

chromatography to give amine-borane complex **3.37** (132 mg, 85%) as a white foamy solid. R_f 0.28 (hexanes-EtOAc, 1:1); $^1\text{H NMR}$ (400 MHz, CDCl_3) δ 7.44 – 7.31 (m, 5H), 7.14 (s, 1H), 6.95 (s, 2H), 5.40 (s, 1H), 5.07 (s, 2H), 3.02 – 2.96 (m, 5H), 2.95 – 2.90 (m, 2H), 2.83 (s, 3H), 2.63 (s, 6H); $^{13}\text{C NMR}$ (100 MHz, CDCl_3) δ 169.0, 155.7, 148.8, 145.2, 136.2, 131.3, 128.6, 128.4, 128.0, 125.4, 122.9, 114.0, 85.8, 71.0, 65.9, 51.7, 29.9, 27.1, 24.6; IR (neat) ν_{max} 2940, 2367, 2321, 2273, 1787, 1727, 1510, 1463, 1270, 1169, 1129, 1030, 994, 751 cm^{-1} ; HRMS (ESI) m/z calcd. for $\text{C}_{22}\text{H}_{30}\text{BN}_3\text{NaO}_4$ $[\text{M}+\text{Na}]^+$ 434.2226, found 434.2224.



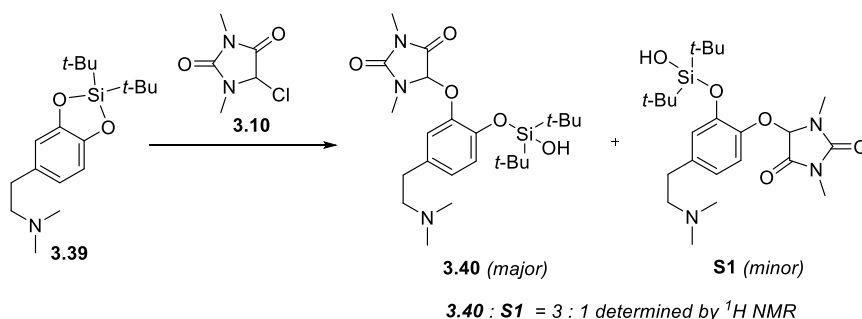
Silylene **3.38**

To a solution of dopamine hydrochloride (1.74 g, 9.2 mmol) in MeCN (46 mL) were sequentially added trimethylamine (7.1 mL, 51 mmol) and di-*tert*-butyldichlorosilane (4.9 mL, 23 mmol) at room temperature. The reaction mixture was heated to reflux for 2 days until the mixture turned into dark orange color. After cooling to room temperature, the mixture was quenched with saturated aq. NaHCO_3 solution and extracted with CH_2Cl_2 . The organic extracts were dried over Na_2SO_4 , filtered and concentrated. The crude silylene **3.38** was used without further purification in the next step.



Amine **3.39**

To a solution of of silylene **3.38** in MeOH (46 mL) were sequentially added 37% aq. formaldehyde (2.1 mL, 27.6 mmol) and NaBH₃CN (1.74 g, 27.6 mmol). After stirring at room temperature for 2 h, the reaction mixture was quenched with saturated aq. NaHCO₃ solution and extracted with CH₂Cl₂. The combined organic extracts were washed with brine, dried over Na₂SO₄, filtered and concentrated under reduced pressure. Purification by flash column chromatography afforded amine **3.39** (1.3 g, 44%, 2 steps) as a yellow oil. *R_f* 0.09 (CHCl₃-MeOH, 6:1); ¹H NMR (500 MHz, CDCl₃) δ 6.80 (d, *J* = 7.9 Hz, 1H), 6.76 (s, 1H), 6.61 (d, *J* = 7.9 Hz, 1H), 2.74 – 2.64 (m, 2H), 2.57 – 2.48 (m, 2H), 2.30 (s, 6H), 1.09 (s, 18H); ¹³C NMR (125 MHz, CDCl₃) δ 149.8, 148.1, 132.8, 120.6, 113.4, 112.6, 61.9, 45.5, 34.0, 26.2, 21.7; IR (neat) *v*_{max} 2934, 2890, 2859, 1512, 1471, 1364, 1290, 1119, 984, 877, 828 cm⁻¹; HRMS (ESI) *m/z* calcd. for C₁₈H₃₂NO₂Si [M+H]⁺ 322.2197, found 322.2199.



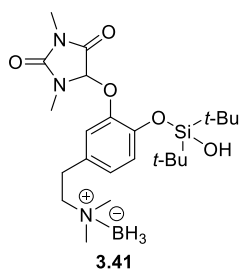
Dopamine-hydantoin adduct **3.40**

Lithium hydroxide (8.6 mg, 0.36 mmol) and HMPA (0.06 mL, 0.36 mmol) were

sequentially added to a stirred solution of amine **3.39** (38.6 mg, 0.12 mmol) in THF (1.20 mL) at $-78\text{ }^{\circ}\text{C}$. After stirring for 1 h, a solution of chlorohydantoin **3.10** (39.0 mg, 0.24 mmol) in THF (0.80 mL) was added dropwise at $-78\text{ }^{\circ}\text{C}$ and the resulting mixture was warmed to room temperature. After stirring for 2 h, the mixture was quenched with saturated aq. NaHCO_3 solution and extracted with CH_2Cl_2 . The combined organic layer was washed with brine, dried over Na_2SO_4 , filtered and concentrated. The residue was purified by flash column chromatography to provide dopamine-hydantoin adduct **3.40** (36 mg, 65%) as a sticky yellow oil (Ratio of isomers was determined to be 3:1 (**3.40**:**S1**) using ^1H NMR analysis of crude reaction mixture.). R_f 0.11 (CHCl_3 -MeOH, 6:1); ^1H NMR (500 MHz, CDCl_3) δ 7.06 – 7.00 (m, 2H), 6.84 (d, $J = 8.2$ Hz, 1H), 5.58 (s, 1H), 4.45 (br s, 1H), 3.07 (s, 3H), 2.96 (s, 3H), 2.73 – 2.68 (m, 2H), 2.52 – 2.47 (m, 2H), 2.29 (s, 6H), 1.09 (s, 9H), 1.00 (s, 9H); ^{13}C NMR (125 MHz, CDCl_3) δ 169.1, 155.8, 146.7, 145.1, 134.2, 125.2, 122.2, 120.8, 86.0, 61.5, 45.5, 33.4, 28.8, 27.6, 27.5, 25.1, 21.0, 20.7; IR (neat) ν_{max} 3500, 2935, 2858, 2783, 2254, 1788, 1724, 1512, 1471, 1289, 1125, 1037, 910, 827, 732 cm^{-1} ; HRMS (ESI) m/z calcd. for $\text{C}_{23}\text{H}_{40}\text{N}_3\text{O}_5\text{Si}$ $[\text{M}+\text{H}]^+$ 466.2732, found 466.2733.

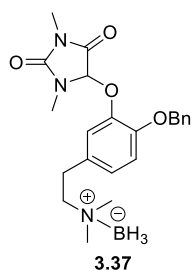
Minor adduct **S1**

A yellow oil. R_f 0.16 (CHCl_3 -MeOH, 6:1); ^1H NMR (500 MHz, CDCl_3) δ 7.08 (d, $J = 8.2$ Hz, 1H), 6.98 (s, 1H), 6.74 (d, $J = 8.2$ Hz, 1H), 5.54 (s, 1H), 3.07 (s, 3H), 2.96 (s, 3H), 2.75 – 2.69 (m, 2H), 2.56 – 2.50 (m, 2H), 2.30 (s, 6H), 1.10 (s, 9H), 1.01 (s, 9H).



Amine-borane complex **3.41**

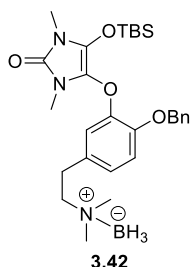
BH₃•THF (1.0 M in THF, 0.6 mL, 0.6 mmol) was added dropwise to a solution of the dopamine-hydantoin adduct **3.40** (93 mg, 0.2 mmol) in THF (2 mL) at -78 °C. After stirring for 2 h, the reaction mixture was concentrated *in vacuo* and purified by flash column chromatography to give amine-borane complex **3.41** (71 mg, 68%) as a white foamy solid. *R*_f 0.36 (hexanes-EtOAc, 1:1); ¹H NMR (400 MHz, CDCl₃) δ 7.04 (d, *J* = 8.3 Hz, 2H), 6.87 (d, *J* = 8.2 Hz, 1H), 5.58 (s, 1H), 3.80 (s, 1H), 3.08 (s, 3H), 3.03 – 2.89 (m, 7H), 2.65 (s, 6H), 1.09 (s, 9H), 1.00 (s, 9H); ¹³C NMR (100 MHz, CDCl₃) δ 168.9, 155.8, 146.9, 145.5, 131.9, 125.2, 122.5, 120.7, 85.9, 66.1, 51.9, 30.2, 28.7, 27.5, 27.4, 26.1, 25.1, 20.9, 20.7; IR (neat) ν_{max} 3494, 2936, 2893, 2859, 2372, 2321, 2274, 1787, 1725, 1515, 1475, 1292, 1168, 1039, 910, 829, 651 cm⁻¹; HRMS (ESI) *m/z* calcd. for C₂₃H₄₂BN₃NaO₅Si [M+Na]⁺ 502.2884, found 502.2885.



Benzyl ether **3.37**

TBAF (1.0 M in THF, 0.02 mL, 0.02 mmol) was added dropwise to a solution of silanol **3.41** (8.0 mg, 0.017 mmol) in THF (0.9 mL) at 0 °C. After complete

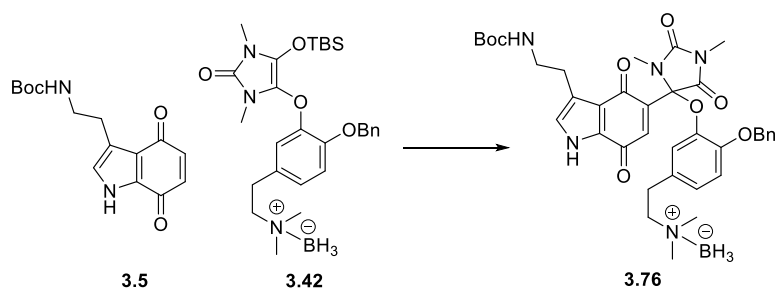
consumption of the silanol **3.41** judged by TLC analysis (ca. 30 min), benzyl bromide (0.1 M in THF, 0.33 mL, 0.033 mmol) was added and the resulting solution was warmed to room temperature. After stirring for 3 h, the mixture was quenched with water and extracted with CH₂Cl₂. The combined organic extracts were washed with brine, dried over Na₂SO₄, filtered and concentrated under reduced pressure. Purification by flash column chromatography provided benzyl ether **3.37** (5.6 mg, 81%) as a white foamy solid. *R*_f 0.28 (hexanes-EtOAc, 1:1); ¹H NMR (400 MHz, CDCl₃) δ 7.44 – 7.31 (m, 5H), 7.14 (s, 1H), 6.95 (s, 2H), 5.40 (s, 1H), 5.07 (s, 2H), 3.02 – 2.96 (m, 5H), 2.95 – 2.90 (m, 2H), 2.83 (s, 3H), 2.63 (s, 6H); ¹³C NMR (100 MHz, CDCl₃) δ 169.0, 155.7, 148.8, 145.2, 136.2, 131.3, 128.6, 128.4, 128.0, 125.4, 122.9, 114.0, 85.8, 71.0, 65.9, 51.7, 29.9, 27.1, 24.6; IR (neat) *v*_{max} 2940, 2367, 2321, 2273, 1787, 1727, 1510, 1463, 1270, 1169, 1129, 1030, 994, 751 cm⁻¹; HRMS (ESI) *m/z* calcd. for C₂₂H₃₀BN₃NaO₄ [M+Na]⁺ 434.2226, found 434.2224.



Silyl enol ether **3.42**

To a solution of LiHMDS (1.0 M in hexanes, 0.18 mL, 0.18 mmol) in THF (0.7 mL) was added dopamine-hydantoin adduct **3.37** (56 mg, 0.14 mmol) dissolved in THF (0.70 mL) dropwise over 40 min *via* syringe pump at –78 °C. After stirring for an additional 20 min, the mixture was treated with TBSOTf (0.05 mL, 0.20 mmol) and stirred at –78 °C for 1 h. The reaction mixture was quenched with saturated aq. NaHCO₃ solution at –78 °C and allowed to warm to room temperature. The crude

mixture was extracted with CH₂Cl₂, the combined organic layer was dried over Na₂SO₄, filtered and concentrated *in vacuo*. The resulting mixture was purified by flash column chromatography to furnish silyl enol ether **3.42** (43 mg, 60%) as a sticky white foamy solid (*Note*: Silyl enol ether **3.42** tends to be hydrolyzed, it was made just before use in the next step. Even if the silyl enol ether was prepared in advance, it was stored at -20 °C under argon atmosphere and used in a few days.). *R*_f 0.11 (hexanes-EtOAc, 1:4); ¹H NMR (400 MHz, CDCl₃) δ 7.47 – 7.30 (m, 5H), 6.92 (d, *J* = 8.2 Hz, 1H), 6.82 (d, *J* = 8.2 Hz, 1H), 6.65 (s, 1H), 5.15 (s, 2H), 3.18 (s, 3H), 3.02 (s, 3H), 2.96 – 2.90 (m, 2H), 2.90 – 2.84 (m, 2H), 2.64 (s, 6H), 0.93 (s, 9H), 0.13 (s, 6H); ¹³C NMR (100 MHz, CDCl₃) δ 147.5, 147.2, 146.4, 136.9, 131.3, 128.7, 128.1, 127.4, 123.6, 121.9, 115.2, 114.7, 114.3, 71.2, 66.0, 51.8, 30.3, 26.3, 25.9, 25.6, 18.1, -4.7; IR (neat) ν_{max} 2933, 2859, 2383, 2318, 2273, 1732, 1669, 1512, 1392, 1258, 1169, 1137, 984, 834, 735 cm⁻¹; HRMS (FAB) *m/z* calcd. for C₂₈H₄₄BN₃O₄Si [M]⁺ 525.3194, found 525.3189.

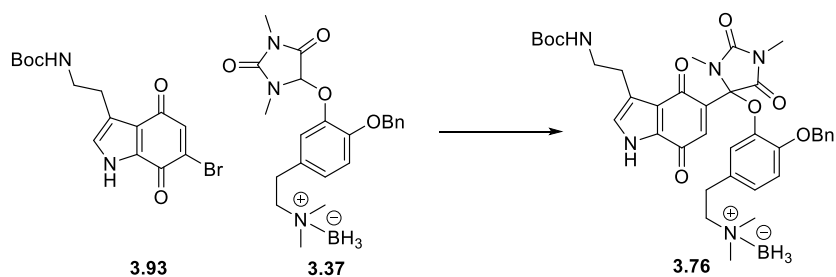


Michael adduct **3.76**

To a flame-dried 5 mL vial equipped with a magnetic stir bar was placed TASF (5.5 mg, 0.012 mmol). The vial was flushed with a stream of argon, THF (0.1 mL) and 2,6-di-*tert*-butylpyridine (5 μ L, 0.023 mmol) were sequentially added. After the

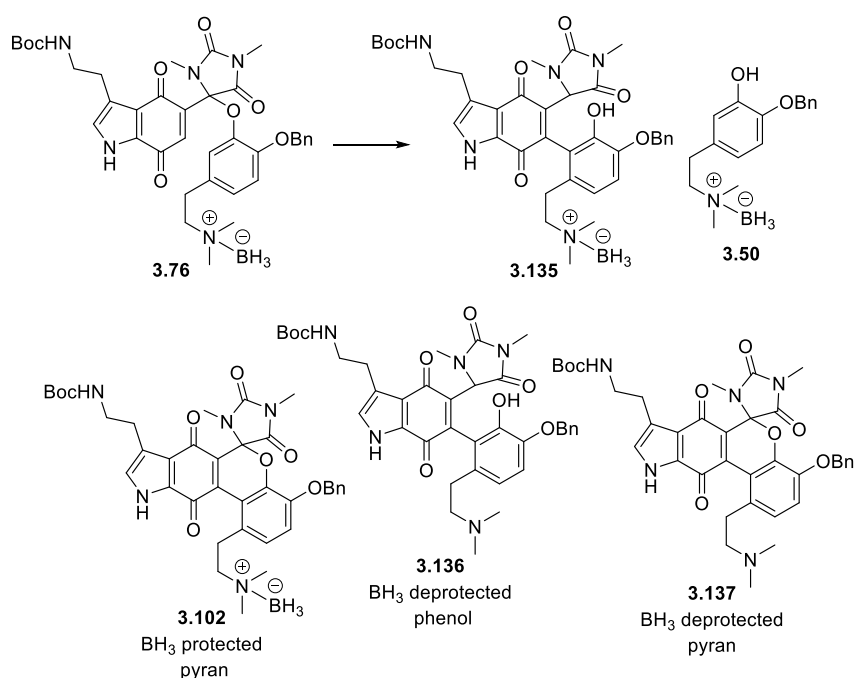
mixture was cooled to $-78\text{ }^{\circ}\text{C}$, TMSF⁵ (0.02 mL, 0.186 mmol) was added *via* cannula and then a solution of quinone **3.5** (3.4 mg, 0.012 mmol) and silyl enol ether **3.42** (10.4 mg, 0.020 mmol) in THF (0.3 mL) was added dropwise over 40 min *via* syringe pump. The reaction mixture was quenched with saturated aq. NaHCO₃ solution and warmed to room temperature. The resulting mixture was diluted with water, extracted with CH₂Cl₂. The combined organic extracts were washed with brine, dried over Na₂SO₄, filtered and concentrated under reduced pressure. Purification of the residue by flash column chromatography afforded Michael adduct **3.76** (3.4 mg, 42%) as a deep orange foamy solid. (*Note*: As the reaction was highly moisture sensitive, yields were not consistent. The average yield was about 30%. TMSF was usually used about 10 equivalents with respect to quinone.). Regiochemical assignment was based on X-ray crystal structure (See, page S41). *R*_f 0.14 (hexanes-EtOAc, 1:1); ¹H NMR (400 MHz, CDCl₃) δ 10.30 (s, 1H), 7.41 (d, *J* = 7.0 Hz, 3H), 7.35 (t, *J* = 7.4 Hz, 2H), 7.29 (d, *J* = 7.2 Hz, 1H), 6.95 (d, *J* = 8.3 Hz, 1H), 6.90 (d, *J* = 8.6 Hz, 2H), 6.84 (s, 1H), 5.08 – 5.00 (m, 2H), 4.85 (s, 1H), 3.37 – 3.25 (m, 2H), 3.02 (s, 3H), 2.97 – 2.79 (m, 6H), 2.65 (s, 3H), 2.63 (s, 6H), 1.40 (s, 9H); ¹³C NMR (100 MHz, CDCl₃) δ 181.6, 175.8, 169.9, 156.4, 151.3, 141.5, 141.3, 138.1, 136.4, 131.3, 131.1, 128.8, 128.2, 127.6, 126.9, 125.2, 124.7, 124.4, 122.9, 114.6, 90.3, 79.4, 71.2, 66.3, 52.1, 51.8, 40.5, 30.1, 28.5, 26.6, 26.0, 25.3; IR (neat) ν_{max} 2980, 2935, 2870, 2383, 2322, 2274, 1786, 1728, 1650, 1509, 1367, 1267, 1169, 1041, 739 cm⁻¹; HRMS (ESI) *m/z* calcd. for C₃₇H₄₆BN₅NaO₈ [M+Na]⁺ 722.3338, found 722.3337.

⁵Della, E. W.; Tsanaktsidis, J. *Synthesis* **1988**, 5, 407.



Michael adduct **3.76**

To a solution of LiHMDS (1.0 M in hexanes, 0.22 mL, 0.22 mmol) in THF (0.5 mL) was added dopamine-hydantoin adduct **3.37** (50.6 mg, 0.12 mmol) dissolved in THF (0.9 mL) dropwise over 1 h *via* syringe pump at -78 °C. Quinone **3.93** (22.8 mg, 0.06 mmol) dissolved in THF (0.55 mL) was added dropwise and the resulting mixture was stirred at -78 °C for 1 h. The reaction mixture was quenched with saturated aq. NaHCO₃ solution and extracted with CH₂Cl₂. The combined organic extracts were washed with brine, dried over Na₂SO₄, filtered and concentrated *in vacuo*. Purification of the residue by flash column chromatography provided Michael adduct **3.76** (38.5 mg, 89%) as a deep orange foamy solid.



Scheme S1. Products obtained by Claisen rearrangement of **3.76**

Phenol **3.135**

To a glass vial were added adduct **3.76** (10.0 mg, 0.014 mmol), Eu(fod)₃ (2.2 mg, 0.002 mmol) and CHCl₃ (2.8 mL). The vial was flushed with argon and sealed with a Teflon screw cap. The reaction vessel was placed into a pre-heated oil bath (75 °C) and stirred for 24 h. After cooling to room temperature, the solvent was evaporated under reduced pressure. The crude mixture was purified by flash column chromatography to give phenol **3.135** (3.6 mg, 37%) as an orange solid. *R_f* 0.44 (hexanes-EtOAc, 1:2); ¹H NMR (400 MHz, THF-*d*₈) δ 11.89 (br s, 1H), 8.18 (br s, 1H), 7.44 (d, *J* = 6.5 Hz, 2H), 7.38 – 7.23 (m, 3H), 7.02 (d, *J* = 8.3 Hz, 2H), 6.75 (d, *J* = 8.0 Hz, 1H), 6.15 (br s, 1H), 5.14 (s, 2H), 4.35 (s, 1H), 3.24 (d, *J* = 4.9 Hz, 2H), 3.20 – 3.10 (m, 1H), 3.03 – 2.98 (m, 1H), 2.94 (s, 3H), 2.90 – 2.82 (m, 2H), 2.75 (s, 3H), 2.71 – 2.65 (m, 2H), 2.49 (s, 3H), 2.38 (s, 3H), 1.38 (s, 9H); ¹³C NMR (100 MHz, THF-*d*₈) δ 182.3, 175.4, 172.1, 157.3, 156.4, 148.2, 146.1, 145.0, 139.6, 137.9,

132.4, 131.1, 129.0, 128.6, 128.5, 125.8, 124.7, 123.2, 120.10, 120.7, 114.0, 77.9, 71.6, 64.7, 62.0, 50.7, 50.3, 41.0, 28.5, 28.2, 27.9, 27.0, 24.9; IR (neat) ν_{\max} 3355, 2932, 2872, 2372, 2319, 2272, 1769, 1709, 1652, 1487, 1393, 1282, 1170, 1025, 934, 793 cm^{-1} ; HRMS (ESI) m/z calcd. for $\text{C}_{37}\text{H}_{46}\text{BN}_5\text{NaO}_8$ $[\text{M}+\text{Na}]^+$ 722.3338, found 722.3334.

As shown in Scheme S1, byproducts were partially isolated and characterized.

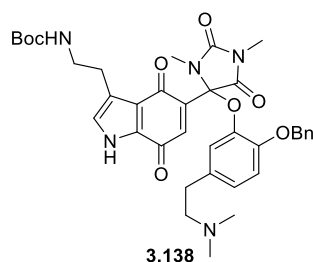
BH₃ protected pyran 3.102

An orange solid. R_f 0.46 (hexanes-EtOAc, 1:2); ^1H NMR (400 MHz, CDCl_3) δ 10.17 (s, 1H), 7.41 – 7.28 (m, 5H), 7.01 (d, $J = 8.5$ Hz, 1H), 6.89 (d, $J = 8.5$ Hz, 1H), 6.76 (s, 1H), 5.16 (dd, $J = 23.8, 12.6$ Hz, 2H), 4.70 (s, 1H), 3.27 (s, 3H), 3.24 – 3.16 (m, 3H), 3.14 – 3.05 (m, 1H), 2.89 – 2.75 (m, 2H), 2.73 – 2.63 (m, 2H), 2.60 (s, 3H), 2.55 (s, 3H), 2.44 (s, 3H), 1.42 (s, 9H); ^{13}C NMR (100 MHz, CDCl_3) δ 179.3, 173.6, 170.3, 156.1, 155.0, 146.0, 144.5, 140.2, 136.6, 131.9, 131.0, 130.2, 128.8, 128.3, 127.5, 125.6, 125.3, 124.5, 122.3, 118.6, 117.9, 85.6, 79.3, 71.6, 65.5, 53.3, 50.8, 40.4, 30.0, 28.5, 26.8, 26.0, 25.9; IR (neat) ν_{\max} 3371, 2936, 2362, 2342, 2272, 1791, 1728, 1652, 1507, 1475, 1366, 1277, 1169, 1056, 911, 733 cm^{-1} ; HRMS (ESI) m/z calcd. for $\text{C}_{37}\text{H}_{44}\text{BN}_5\text{NaO}_8$ $[\text{M}+\text{Na}]^+$ 720.3182, found 720.3186.

Phenol 3.50

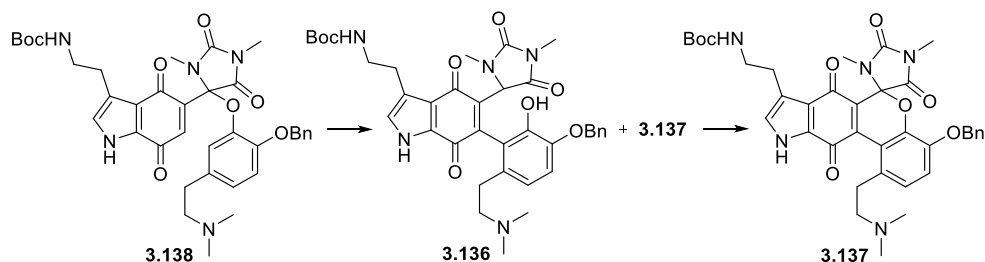
A White solid. R_f 0.19 (hexanes-EtOAc, 3:1); ^1H NMR (400 MHz, CDCl_3) δ 7.45 – 7.33 (m, 5H), 6.86 (d, $J = 8.2$ Hz, 1H), 6.79 (d, $J = 1.6$ Hz, 1H), 6.67 (dd, $J = 8.2, 1.7$ Hz, 1H), 5.63 (s, 1H), 5.09 (s, 2H), 3.00 – 2.89 (m, 4H), 2.64 (s, 6H); ^{13}C NMR (100 MHz, CDCl_3) δ 146.0, 144.5, 136.3, 131.6, 128.7, 128.4, 127.8, 120.2, 115.1,

112.5, 71.2, 66.1, 51.7, 30.2; IR (neat) ν_{\max} 3521, 2999, 2941, 2363, 2272, 1592, 1512, 1456, 1384, 1168, 1018, 878, 805, 740 cm^{-1} ; HRMS (ESI) m/z calcd. for $\text{C}_{17}\text{H}_{24}\text{BNNaO}_2$ $[\text{M}+\text{Na}]^+$ 308.1795, found 308.1792.



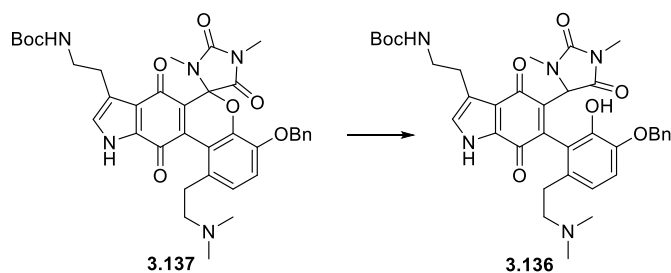
Amine **3.138**

DABCO (49 mg, 0.44 mmol) was added to a solution of Michael adduct **3.76** (51.1 mg, 0.051 mmol) in THF (2.4 mL) and the reaction mixture was stirred at room temperature for 2 h. Removal of the solvent *in vacuo*, followed by flash chromatography afforded amine **3.138** (45.3 mg, 90%) as a deep orange foamy solid. R_f 0.36 (CHCl_3 -MeOH, 6:1); ^1H NMR (400 MHz, CDCl_3) δ 10.26 (br s, 1H), 7.45 (s, 1H), 7.40 (d, $J = 7.1$ Hz, 2H), 7.35 (t, $J = 7.3$ Hz, 2H), 7.29 (d, $J = 7.2$ Hz, 1H), 6.93 (d, $J = 8.4$ Hz, 1H), 6.86 (d, $J = 8.3$ Hz, 2H), 5.06 – 4.97 (m, 2H), 4.76 (br s, 1H), 3.30 (dt, $J = 12.8, 6.2$ Hz, 2H), 2.99 (s, 3H), 2.87 (dt, $J = 13.6, 6.9$ Hz, 2H), 2.69 – 2.61 (m, 5H), 2.47 (m, 2H), 2.30 (s, 3H), 1.40 (s, 9H); ^{13}C NMR (100 MHz, CDCl_3) δ 181.7, 175.8, 169.9, 156.4, 156.1, 150.8, 141.4, 141.0, 138.1, 136.6, 133.0, 131.5, 128.6, 128.0, 127.5, 126.6, 125.5, 124.4, 124.2, 122.8, 114.3, 90.1, 79.2, 71.0, 61.3, 45.1, 40.5, 33.0, 28.4, 26.5, 25.9, 25.1; IR (neat) ν_{\max} 3384, 2934, 2865, 2781, 1786, 1723, 1646, 1506, 1456, 1391, 1364, 1266, 1166, 1096, 1036, 733, 697 cm^{-1} ; HRMS (ESI) m/z calcd. for $\text{C}_{37}\text{H}_{44}\text{N}_5\text{O}_8$ $[\text{M}+\text{H}]^+$ 686.3184 found 686.3187.



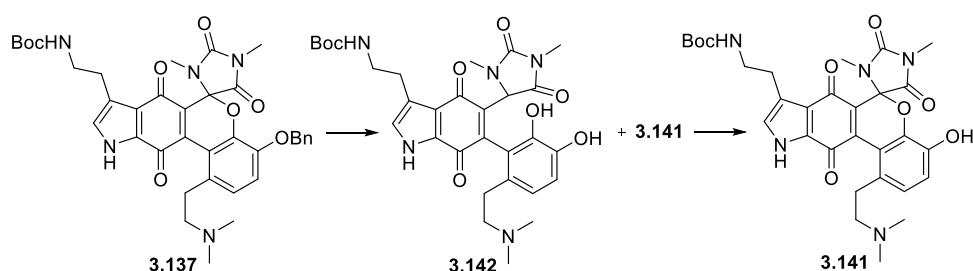
Pyran **3.137**

To a glass tube were added adduct **3.138** (37.1 mg, 0.054 mmol), 1,4-benzoquinone (1.2 mg, 0.011 mmol) and toluene (18 mL). The tube was flushed with argon and sealed with a Teflon screw cap. The reaction vessel was placed into a pre-heated oil bath (110 °C) and stirred for 45 min. After cooling to room temperature, the solvent was evaporated under reduced pressure. The resulting residue was dissolved in MeOH (18 mL) and heated to 65 °C for 1 h (*Note*: It can also be performed at room temperature for 10 h.). The reaction mixture was cooled to room temperature and concentrated *in vacuo*. The crude mixture was purified by preparative TLC (CHCl₃-MeOH, 8:1, The plate was immersed in the eluting solvent twice or 3 times) to provide pyran **3.137** (29.5 mg, 80%) as a deep orange foamy solid. *R_f* 0.28 (CHCl₃-MeOH, 6:1); ¹H NMR (400 MHz, CDCl₃) δ 7.41 – 7.29 (m, 5H), 6.95 (d, *J* = 8.5 Hz, 1H), 6.84 (d, *J* = 8.5 Hz, 1H), 6.73 (s, 1H), 5.15 (dd, *J* = 12.6 Hz, 2H), 4.85 (br. s, 1H), 3.26 (s, 3H), 3.23 – 3.12 (m, 2H), 3.03 – 2.91 (m, 1H), 2.84 – 2.66 (m, 3H), 2.65 – 2.55 (m, 1H), 2.47 (s, 3H), 2.43 – 2.37 (m, 1H), 2.19 (s, 6H), 1.42 (s, 9H); ¹³C NMR (100 MHz, CDCl₃) δ 179.6, 173.0, 170.1, 156.1, 155.2, 145.9, 144.6, 141.3, 136.8, 132.5, 131.8, 131.0, 128.7, 128.2, 127.4, 125.2, 125.1, 124.0, 122.0, 118.4, 117.8, 85.7, 79.2, 71.7, 60.8, 44.6, 40.6, 32.4, 28.5, 26.8, 26.0, 25.8; IR (neat) *v*_{max} 3378, 2977, 2934, 2360, 2342, 1791, 1728, 1647, 1474, 1365, 1253, 1172, 1054, 736 cm⁻¹; HRMS (ESI) *m/z* calcd. for C₃₇H₄₂N₅O₈ [M+H]⁺ 684.3028, found 684.3025.



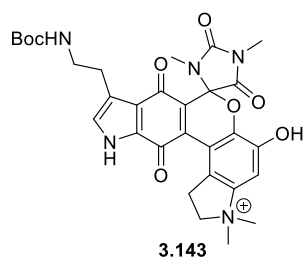
Phenol **3.136**

To a solution of pyran **3.137** (37.7 mg, 0.055 mmol) in MeOH (3.5 mL) was added palladium on activated carbon (extent of labeling: 5 wt. % loading (dry basis), matrix activated carbon support (Sigma-Aldrich 205680), 11.7 mg, 0.0055 mmol). The flask was purged with 3 cycles of H₂/vacuum. The resulting suspension was stirred under H₂ atmosphere at room temperature (The color of reaction mixture changed from orange to colorless within 1 h). After stirring for 6 h, the reaction mixture was filtered through a pad of Celite, washed with MeOH and concentrated. The residue was immediately purified by flash column chromatography afforded phenol **3.136** (27.3 mg, 73%) as a deep orange solid (Phenol **3.136** was unstable and a small amount of pyran **3.137** was generated after column chromatography.). *R*_f 0.19 (CHCl₃-MeOH, 6:1); ¹H NMR (400 MHz, CDCl₃) δ 7.45 – 7.31 (m, 5H), 7.04 (s, 1H), 6.94 (d, *J* = 8.4 Hz, 1H), 6.78 (d, *J* = 8.4 Hz, 1H), 5.08 (s, 2H), 4.86 (br s, 1H), 4.27 (s, 1H), 3.27 (m, 2H), 3.09 (s, 3H), 2.98 – 2.85 (m, 2H), 2.73 (s, 3H), 2.63 (m, 4H), 2.34 (s, 6H), 1.42 (s, 9H); ¹³C NMR (100 MHz, CDCl₃) δ 181.4, 174.2, 171.9, 157.2, 156.1, 147.3, 144.2, 143.0, 138.1, 136.0, 131.8, 131.4, 128.9, 128.7, 128.1, 126.5, 124.3, 122.7, 120.5, 119.1, 113.1, 79.0, 71.5, 61.4, 59.9, 44.6, 40.7, 30.6, 28.6, 28.1, 26.0, 25.4; IR (neat) *v*_{max} 3370, 2977, 2931, 2870, 2360, 2342, 1768, 1711, 1651, 1486, 1394, 1280, 1172, 1026, 736 cm⁻¹; HRMS (ESI) *m/z* calcd. for C₃₇H₄₄N₅O₈ [M+H]⁺ 686.3184, found 686.3181.



Phenol **3.141**

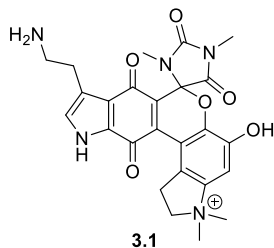
To a solution of pyran **3.137** (5.8 mg, 0.0085 mmol) in MeOH (3.4 mL) was added palladium on activated carbon (10 wt.% loading (dry basis), Degussa type E101 NE/W (Sigma-Aldrich 330108), 2.2 mg, 0.001 mmol). The flask was purged with 3 cycles of H₂/vacuum. The resulting suspension was stirred under H₂ atmosphere at room temperature (The color of reaction mixture changed from orange to colorless within 1 h). After stirring overnight, the reaction mixture was immediately filtered through a pad of silica gel with MeOH as an eluent (This process must be performed right after the removal of lid from a vessel.). The filtrate was stirred at room temperature for 3 h. The solvent was evaporated *in vacuo* and the residue was purified by flash column chromatography to give phenol **3.141** (1.8 mg, 36%) as a deep orange solid. *R_f* 0.06 (CH₃Cl-MeOH, 6:1); ¹H NMR (400 MHz, CDCl₃) δ 6.97 (d, *J* = 8.3 Hz, 1H), 6.89 (d, *J* = 8.3 Hz, 1H), 6.82 (s, 1H), 4.80 (br. s, 1H), 3.36 – 3.30 (m, 2H), 3.05 – 2.94 (m, 2H), 2.93 – 2.76 (m, 3H), 2.66 – 2.57 (m, 2H), 2.55 (s, 3H), 2.44 – 2.34 (m, 2H), 2.18 (s, 4H), 1.43 (s, 9H); IR (neat) *v*_{max} 2972, 2933, 1790, 1721, 1649, 1560, 1510, 1476, 1392, 1364, 1277, 1252, 1170, 1106, 1058 cm⁻¹; HRMS (ESI) *m/z* calcd. for C₃₀H₃₆N₅O₈ [M+H]⁺ 594.2558, found 594.2562.



N-Boc exiguamine A **3.143** (HCOOH salt form)

To a solution of pyran **3.137** (16.3 mg, 0.024 mmol) in MeOH (4.4 mL) was added palladium on activated carbon (10 wt.% loading (dry basis), Degussa type E101 NE/W (Sigma-Aldrich 330108), 7.7 mg, 0.0036 mmol). The flask was purged with 3 cycles of H₂/vacuum. The resulting suspension was stirred under H₂ atmosphere at room temperature (The color of reaction mixture changed from orange to colorless within 1 h). After stirring for 4 h, the atmosphere was exchanged from H₂ to O₂ by purging with 3 cycles of O₂/vacuum (As soon as oxygen gas was added, the mixture color turned orange.). Under O₂ atmosphere, the heterogeneous solution was stirred at room temperature overnight. The mixture was filtered through a pad of Celite, washed with MeOH and concentrated. The crude mixture was purified by passing through a C18 cartridge (Discovery[®] DSC-18 SPE Tube, 0.1% HCO₂H in H₂O as an eluent). The filtrate was concentrated to provide HCOOH salt of *N*-Boc exiguamine A **3.143** (14.2 mg, 94%) as a deep orange solid. ¹H NMR (400 MHz, CD₃OD) δ 7.42 (s, 1H), 7.07 (s, 1H), 6.59 (br s, 1H), 4.31 – 4.19 (m, 1H), 4.06 – 3.90 (m, 2H), 3.58 (s, 3H), 3.51 (s, 3H), 3.28 – 3.21 (m, 2H), 3.19 (s, 3H), 2.96 – 2.77 (m, 3H), 2.57 (s, 3H), 1.40 (s, 9H); ¹³C NMR (100 MHz, CD₃OD) δ 181.2, 174.6, 170.9, 158.5, 156.5, 149.7, 145.1, 144.2, 139.7, 132.9 (132.89), 132.9 (132.85), 127.3, 125.3, 123.4, 123.1, 116.5, 109.0, 87.5, 79.9, 69.4, 55.4, 54.3, 41.3, 30.0, 28.8, 27.0, 26.7, 25.7; IR (neat) ν_{max} 3395, 2979, 2932, 2816, 2732, 1788, 1725, 1649, 1592, 1469, 1392, 1352, 1255, 1170, 1065, 876 cm⁻¹; HRMS (ESI) *m/z* calcd. for C₃₀H₃₄N₅O₈ [M]⁺

592.2402, found 592.2403.



Exiguamine A **3.1** (HCl salt form)

To a solution of pyran **3.137** (3.6 mg, 0.0053 mmol) in MeOH (4 mL) was added palladium on activated carbon (10 wt.% loading (dry basis), Degussa type E101 NE/W (Sigma-Aldrich 330108), 1.7 mg, 0.0008 mmol). The flask was purged with 3 cycles of H₂/vacuum. The resulting suspension was stirred under H₂ atmosphere at room temperature (The color of reaction mixture changed from orange to colorless within 1 h). After stirring for 4 h, the atmosphere was exchanged from H₂ to O₂ by purging with 3 cycles of O₂/vacuum (As soon as oxygen gas was added, the mixture color turned orange.). Under O₂ atmosphere, the heterogeneous solution was stirred at room temperature overnight. To the reaction mixture was added conc. HCl (1/3 volume of remaining MeOH. Volume of MeOH changed during gas exchanges.) and stirred for an additional 1 h. The mixture was filtered through a pad of Celite, washed with MeOH and concentrated. The crude mixture was purified by passing through a C18 cartridge (Discovery® DSC-18 SPE Tube, 0.1% HCO₂H in H₂O as an eluent) and the filtrate was concentrated. The residue was dissolved in 3 N HCl and the solvent was evaporated to provide HCl salt of exiguamine A **3.1** (2.8 mg, 94%) as a deep orange solid. IR (neat) ν_{\max} 3403, 3025, 2928, 2853, 2814, 1787, 1720, 1649, 1472, 1369, 1258, 1067, 949, 875 cm⁻¹; HRMS (ESI) m/z calcd. for C₂₅H₂₆N₅O₆ [M]⁺ 492.1878, found 492.1880.

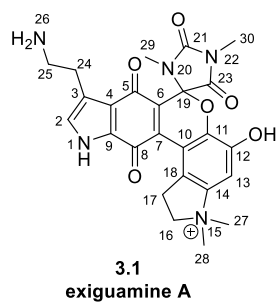


Table S1. Comparison of the NMR spectral data in DMSO- d_6^a

Atom number	Andersen group (isolation) ⁶		Trauner group (synthetic) ⁷		Lee group (synthetic)	
	¹ H NMR	¹³ CNMR	¹ H NMR	¹³ CNMR	¹ H NMR	¹³ CNMR
	600 MHz	150MHz	500 MHz	125MHz	600 MHz	100MHz ^b
1	13.10 (br s)		13.09 (s, 1H)		13.11 (s, 1H)	
2	7.30 (d, $J = 2.2$ Hz)	126.5	7.33 (d, 1H, $J = 2.5$ Hz)	126.5	7.34 (d, 1H, $J = 2.7$Hz)	126.5
3		120.7		120.9		120.9
4		121.3		121.3		121.3
5		179.7		179.7		179.7
6		130.5		130.5		130.5
7		138.8		138.8		138.8
8		173.4		173.4		173.3
9		131.6		131.6		131.5

⁶ Brastianos, H. C.; Vottero, E.; Patrick, B. O.; Soest, R. V.; Matainaho, T.; Mauk, A. G.; Andersen, R. J. *J. Am. Chem. Soc.* **2006**, *128*, 16046.

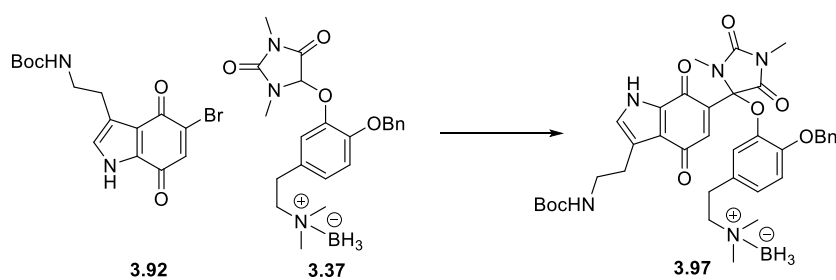
⁷ Volgraf, M.; Lumb, J.-P.; Brastianos, H. C.; Carr, G.; Chung, M. K. W.; Munzel, M.; Mauk, A. G.; Andersen, R. J.; Trauner, D. *Nat. Chem. Biol.* **2008**, *4*, 535.

10		114.7		114.8		114.8
11		146.5		146.5		146.6
12		142.7		142.7		142.7
13	7.52 (s)	108.7	7.54 (s, 1H)	108.7	7.56 (s, 1H)	108.6
14		142.8		142.8		142.8
16, 16'	3.84 (m) 4.17 (m)	67.4	3.85 (m, 1H) 4.19 (m, 1H)	67.4	3.86 (m, 1H) 4.19 (m, 1H)	67.4
17, 17'	3.22 (br dd, <i>J</i> =16.9, 7.5) 3.73 (m)	28.5	3.24 (br dd, 1H, <i>J</i> = 16.0, 7.5) 3.73 (m, 1H)	28.4	3.24 (br dd, 1H, <i>J</i> = 16.5, 7.6) 3.73 (m, 1H)	28.4
18		122.8		122.8		122.7
19		85.4		85.5		85.4
21		154.5		154.5		154.5
23		168.6		168.6		168.6
24	2.92 (m)	23.3	2.94 (m, 2H)	23.3	2.95 (m, 2H)	23.3
25	2.99 (m)	38.3	2.99 (m, 2H)	38.1	2.99 (m, 2H)	38.1

26	7.82 (br s)		7.95 (br s, 3H)		8.09 (br s, 3H)	
27	3.43 (s)	54.3	3.44 (s, 3H)	54.3	3.45 (s, 3H)	54.3
28	3.51 (s)	53.2	3.53 (s, 3H)	53.2	3.53 (s, 3H)	53.2
29	2.44 (s)	26.0	2.45 (s, 3H)	26.1	2.45 (s, 3H)	26.1
30	3.07 (s)	25.2	3.08 (s, 3H)	25.2	3.08 (s, 3H)	25.2
12-OH	10.42 (s)		10.40 (s, 1H)		10.46 (s)	

^a ¹H and ¹³C chemical shifts [ppm] are referenced to the DMSO-*d*₆ (δ_{H} 2.49 ppm and δ_{C} 39.5 ppm)

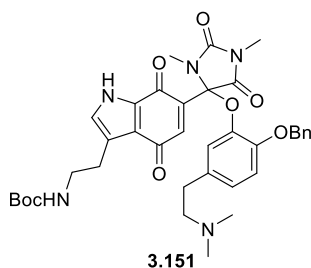
^b Data was obtained on 400 MHz NMR spectrometer.



Michael Adduct **3.97**

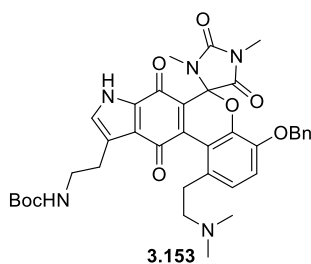
To a solution of LiHMDS (1.0 M in hexanes, 0.1 mL, 0.1 mmol) in THF (0.25 mL) was added dopamine-hydantoin adduct **3.37** (16.9 mg, 0.041 mmol) dissolved in

THF (0.45 mL) dropwise over 1 h *via* syringe pump at $-78\text{ }^{\circ}\text{C}$. Quinone **3.92** (7.6 mg, 0.021 mmol) dissolved in THF (0.55 mL) was added dropwise and the resulting mixture was stirred at $-78\text{ }^{\circ}\text{C}$ for 1 h. The reaction mixture was quenched with saturated aq. NaHCO_3 solution and extracted with CH_2Cl_2 . The combined organic extracts were washed with brine, dried over Na_2SO_4 , filtered and concentrated *in vacuo*. Purification of the residue by flash column chromatography provided Michael adduct **3.97** (13 mg, 88%) as a deep orange foamy solid. R_f 0.29 (hexanes-EtOAc, 1:2); ^1H NMR (400 MHz, CDCl_3) δ 9.89 (s, 1H), 7.45 – 7.39 (m, 3H), 7.36 (t, $J = 7.3$ Hz, 2H), 7.30 (d, $J = 7.0$ Hz, 1H), 6.95 (d, $J = 8.1$ Hz, 1H), 6.90 (d, $J = 8.3$ Hz, 2H), 6.84 (s, 1H), 5.05 (q, $J = 11.8$ Hz, 2H), 4.77 (s, 1H), 3.38 – 3.25 (m, 2H), 3.02 (s, 3H), 2.96 – 2.79 (m, 6H), 2.65 (s, 3H), 2.63 (s, 6H), 1.40 (s, 9H); ^{13}C NMR (100 MHz, CDCl_3) δ 181.6, 175.8, 169.9, 156.4, 156.2, 151.3, 141.5, 141.2, 138.1, 136.4, 131.2, 131.0, 128.8, 128.2, 127.6, 126.9, 125.3, 124.7, 124.4, 122.9, 114.6, 90.3, 79.4, 71.1, 66.2, 52.1, 51.8, 40.5, 30.0, 28.5, 26.6, 26.0, 25.3.; IR (neat) ν_{max} 2972, 2933, 2860, 2371, 2318, 2270, 1785, 1725, 1649, 1508, 1460, 1365, 1269, 1168, 1038, 813 cm^{-1} ; HRMS (ESI) m/z calcd. for $\text{C}_{37}\text{H}_{46}\text{BN}_5\text{NaO}_8$ $[\text{M}+\text{Na}]^+$ 722.3338, found 722.3335.



Amine **3.151**

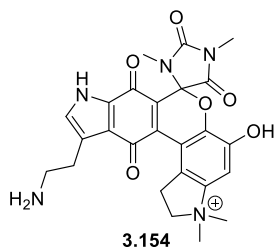
DABCO (16.2 mg, 0.144 mmol) was added to a solution of Michael adduct **3.97** (17.1 mg, 0.024 mmol) in THF (0.8 mL) and the reaction mixture was stirred at room temperature for 2 h. Removal of the solvent *in vacuo*, followed by flash chromatography afforded amine **3.151** (11.4 mg, 71%) as a deep orange foamy solid. R_f 0.31 (CH₂Cl₂-MeOH, 6:1); ¹H NMR (400 MHz, CDCl₃) δ 9.86 (br. s, 1H), 7.47 (s, 1H), 7.41 (d, $J = 7.4$ Hz, 2H), 7.35 (t, $J = 7.4$ Hz, 2H), 7.30 (d, $J = 7.3$ Hz, 1H), 6.93 (d, $J = 8.4$ Hz, 1H), 6.90 – 6.84 (m, 3H), 5.07 – 4.97 (m, 2H), 4.72 (br. s, 1H), 3.38 – 3.22 (m, 2H), 2.99 (s, 3H), 2.94 – 2.82 (m, 2H), 2.71 – 2.59 (m, 5H), 2.54 – 2.45 (m, 2H), 2.31 (s, 6H), 1.40 (s, 9H).



Pyran **3.153**

To a glass tube were added adduct **3.151** (5.7 mg, 0.0083 mmol), 1,4-benzoquinone (0.2 mg, 0.0017 mmol) and toluene (2 mL). The tube was flushed with argon and sealed with a Teflon screw cap. The reaction vessel was placed into a pre-heated oil bath (110 °C) and stirred for 30 min. After cooling to room temperature, the solvent was evaporated under reduced pressure. The resulting residue was dissolved in MeOH (2 mL) and stirred at room temperature for 4 h. The solvent was evaporated *in vacuo* and the residue was purified by flash column chromatography to give pyran **3.153** (4.5 mg, 79%) as a deep orange solid. R_f 0.42 (CH₂Cl₂-MeOH, 6:1); ¹H NMR (500 MHz, CDCl₃) δ 7.41 – 7.34 (m, 4H), 7.31 (d, $J = 6.2$ Hz, 1H), 6.96 (d, $J = 8.5$ Hz, 1H), 6.86 (d, $J = 8.5$ Hz, 1H), 6.81 (s, 1H), 5.16 (dd, $J = 27.5, 12.7$ Hz, 2H), 4.79

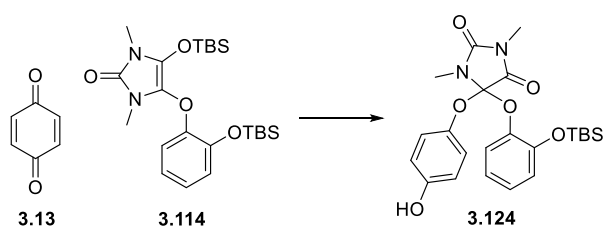
(s, 1H), 3.27 (s, 5H), 3.03 – 2.96 (m, 1H), 2.89 – 2.83 (m, 1H), 2.81 – 2.73 (m, 2H), 2.68 – 2.60 (m, 1H), 2.50 (s, 3H), 2.17 (s, 6H), 1.43 (s, 9H).



Iso-exiguamine A **3.154** (HCl salt form)

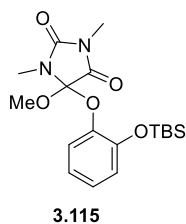
To a solution of pyran **3.153** (2.1 mg, 0.0031 mmol) in MeOH (3 mL) was added palladium hydroxide on carbon (20 wt.% loading (dry basis), matrix carbon, wet support, Degussa type E101 NE/W (Sigma-Aldrich 212911), ~50% water, 0.9 mg, 0.0006 mmol). The flask was purged with 3 cycles of H₂/vacuum. The resulting suspension was stirred under H₂ atmosphere at room temperature (The color of reaction mixture changed from orange to colorless within 1 h). After stirring overnight, the atmosphere was exchanged from H₂ to O₂ by purging with 3 cycles of O₂/vacuum (As soon as oxygen gas was added, the mixture color turned orange.). Under O₂ atmosphere, the heterogeneous solution was stirred at room temperature for 4 h. To the reaction mixture was added conc. HCl (1/3 volume of remaining MeOH. Volume of MeOH changed during gas exchanges.) and stirred for an additional 1 h. The mixture was filtered through a pad of Celite, washed with MeOH and concentrated. The crude mixture was purified by passing through a C18 cartridge (Discovery[®] DSC-18 SPE Tube, 0.1% HCO₂H in H₂O as an eluent) and the filtrate was concentrated. The residue was dissolved in 3 N HCl and the solvent was evaporated to provide HCl salt of *iso*-exiguamine A **3.154** (1.6 mg, 92%) as a deep orange solid. ¹H NMR (400 MHz, CD₃OD) δ 7.45 (s, 1H), 7.20 (s, 1H), 4.29 – 4.21

(m, 1H), 4.04 – 3.94 (m, 2H), 3.59 (s, 3H), 3.52 (s, 3H), 3.23 – 3.14 (m, 5H), 3.09 – 3.01 (m, 3H), 2.58 (s, 3H); IR (neat) ν_{max} 3383, 3239, 3017, 1785, 1719, 1649, 1512, 1472, 1366, 1254, 1066, 1018, 945, 875 cm^{-1} ; HRMS (ESI) m/z calcd. for $\text{C}_{25}\text{H}_{26}\text{N}_5\text{O}_6$ $[\text{M}]^+$ 492.1878, found 492.1885.



Phenol **3.124**

1,4-Benzoquinone (10.8 mg, 0.10 mmol) and trityl tetrafluoroborate (TrBF_4 , 9.9 mg, 0.03 mmol) were dissolved in CH_2Cl_2 (0.60 mL) and cooled to at -78°C . 2,6-di-*tert*-butylpyridine (0.06 mL, 0.30 mmol) and a solution (0.60 mL) of crude silyl enol ether **3.114** (0.12 mmol approximately) in CH_2Cl_2 were added sequentially to this solution and the resulting solution was warmed to 0°C . After warming up to 0°C the reaction mixture was stirred for 4 h. the solvent was evaporated *in vacuo* and the residue was purified by flash column chromatography to afford phenol **3.123** (38 mg, 83%) as a colorless oil. R_f 0.34 (hexanes-EtOAc, 2:1); ^1H NMR (400 MHz, CDCl_3) δ 7.38 (dd, $J = 8.1, 1.6$ Hz, 1H), 7.09 – 7.04 (m, 1H), 6.94 – 6.85 (m, 4H), 6.68 – 6.62 (m, 2H), 5.34 (s, 1H), 3.08 (s, 3H), 2.87 (s, 3H), 0.94 (s, 9H), 0.15 (s, 3H), 0.14 (s, 3H); ^{13}C NMR (100 MHz, CDCl_3) δ 165.8, 155.0, 153.4, 148.5, 145.2, 143.5, 126.2, 123.9, 123.3, 121.8, 121.5, 116.1, 104.7, 25.7, 25.0, 24.6, 18.4, -4.3, -4.4.



Mixed ketal **3.115**

To a solution of phenol **3.124** (10.1 mg, 0.021 mmol) in MeOH (0.20 mL) was added PIDA (8.1 mg, 0.025 mmol) at room temperature. After stirring for 10 min, the reaction mixture was concentrated under reduced pressure and purified by flash column chromatography to give mixed ketal **3.115** (5.3 mg, 64%) as a colorless oil. R_f 0.40 (hexanes-EtOAc, 5:1); ^1H NMR (400 MHz, CDCl_3) δ 7.08 (dd, $J = 8.7, 1.3$ Hz, 1H), 7.01 (ddd, $J = 8.0, 1.6, 0.8$ Hz, 1H), 6.89 – 6.82 (m, 2H), 3.58 (s, 3H), 3.01 (s, 3H), 2.87 (s, 3H), 0.97 (s, 9H), 0.17 (s, 3H), 0.14 (s, 3H); ^{13}C NMR (100 MHz, CDCl_3) δ 166.7, 154.8, 148.3, 143.4, 125.7, 122.6, 121.6, 121.5, 103.5, 52.6, 25.6, 24.3, 24.3, 18.2, -4.5, -4.6.

Chapter 4: Biological Evaluation of IDO Inhibitor Candidates

4.1 Introduction

Indoleamine 2,3-dioxygenase (IDO) catalyzes the degradation of tryptophan to produce kynurenine *via* *N*-formylkynurenine. Thus, the presence of a compound acting as an IDO inhibitor increases residual tryptophan and decreases the produced kynurenine. By measuring the concentration of these compounds, the effect of inhibitors on the activity of IDO could be determined. In collaboration with the laboratory of Prof. Eun Young Choi at the College of Medicine, Seoul National University, we have developed a strain of HEK293 cells transfected with hIDO. Candidates of IDO inhibitors based on tryptophan analogues were synthesized and their IDO inhibitory effects were measured. Some compounds found to be efficacious are pending patent application. There are two methods, HPLC and absorbance measurements, that have been used to measure the inhibitory concentration.¹

a. HPLC

After a series of cell cultures with the compound of interest and with a known IDO inhibitor (1-methyl-L-tryptophan, L-1MT) as a reference, the culture medium is centrifuged. The collected supernatant is analyzed by HPLC to determine the concentration of tryptophan and kynurenine, based on the retention time and the UV absorption (280 nm for tryptophan, 360 nm for kynurenine)

b. Absorbance Assay

This assay measures the concentration of kynurenine by making use of 4-(dimethylamino)benzaldehyde (Ehrlich reagent) which can react with kynurenine to act as an indicator. The collected supernatant of the cell culture is mixed with the Ehrlich reagent in acetic acid. After 10 min incubation, the yellow color derived from the action of Ehrlich reagent on kynurenine is recorded by measuring absorbance at 480 nm using a microplate reader.

4.2. Biological Evaluation of Exiguamine A and Its Derivatives

Herein, described are the details of biological evaluation of exiguamines. The inhibitory effect of exiguamine A and analogues were measured by absorbance assay. A collection of the synthesized compounds was sent to BPS Bioscience, Inc. with service request to determine their inhibitory effect of IDO activity in cell lines.

4.2.1 Exiguamine A

The IDO inhibitory effect of exiguamine A has been reported based only on purified IDO enzyme assay ($K_i = 41 \pm 3$ nM). In order for exiguamines to be developed into therapeutics, cellular assays must be conducted. We performed HeLa cell-based assay to evaluate the inhibitory activity of exiguamine A against IDO in the cells. In this assay, INCB24360, a known IDO1 inhibitor, was used as the reference compound.

a. Assay Conditions

To perform the HeLa cell-based IDO1 assay, HeLa cells were seeded at 25,000 cells

per well into 96-well microplate in 100 μ l of growth medium. Cells were incubated at 37 °C and 5% CO₂ overnight. The next day 100 μ l per well of diluted inhibitor in growth medium was added at a final concentration of 100 ng/mL human IFN γ . Cells were incubated at 37 °C in a CO₂ incubator for 28 hours. The next day 140 μ l of medium was removed into a new 96-well plate and 10 μ l of 6.1 *N* TCA (trichloroacetic acid) was added. The plate was incubated at 65 °C for 15 min to hydrolyze *N*-formylkynurenine produced by IDO to kynurenine. The plate was then centrifuged at 3000 rpm for 10 min to remove sediments. 100 μ l of supernatant per well was transferred to another 96-well plate and mixed with 100 μ l of 2% (w/v) 4-(dimethylamino)benzaldehyde in acetic acid. The plate was incubated at room temperature for 10 minutes, the yellow color derived from kynurenine was recorded by measuring absorbance at 480 nm using a microplate reader (TECAN Infinite M1000 Pro).

b. Data Analysis

Cell based assays were performed in triplicate at each concentration. The absorbance data were analyzed using the computer software, Graphpad Prism. In the absence of the compound and presence of 100 ng/mL IFN γ , the absorbance (A_t) in each data set was defined as 100%. The absorbance of medium blank (A_b) in each data set was defined as 0%. The percent absorbance in the presence of each compound was calculated according to the following equation: % Absorbance = $(A - A_b) / (A_t - A_b)$, where A = the absorbance in the presence of the compound and IFN γ , A_b = the absorbance of medium blank, and A_t = the absorbance in the absence of the compounds and presence of IFN γ .

The values of % absorbance versus a series of compound concentrations were then

plotted using non-linear regression analysis of Sigmoidal dose-response curve generated with the equation $Y=B+(T-B)/1+10^{((\text{LogEC}_{50}-X)\times\text{Hill Slope})}$, where Y = percent absorbance, B = minimum percent absorbance, T = maximum percent absorbance, X = logarithm of compound and Hill Slope = slope factor or Hill coefficient. The IC₅₀ value was determined by the concentration causing a half-maximal percent activity.

c. Effect of Individual Compounds

• Exiguamine A (3.1)

– The external molecular code for assay is CBL01.

Raw data for the effect of exiguamine A (3.1) on IDO1 activity are summarized in Table 4.1 and Figure 4.1.

3.1 (nM)	Absorbance OD 480 nm			% Activity		
	Repeat1	Repeat2	Repeat3	Repeat1	Repeat2	Repeat3
No Cpd	0.28	0.28	0.28	102	100	101
0.1	0.28	0.29	0.29	97	107	107
1	0.28	0.28	0.29	101	97	108
10	0.26	0.29	0.29	89	109	108
25	0.25	0.27	0.29	83	93	106
50	0.27	0.30	0.29	96	114	110
100	0.27	0.28	0.30	90	98	112
250	0.27	0.38*	0.30	94	169*	111
500	0.28	0.29	0.31	103	108	117
1000	0.30	0.27	0.30	111	94	112

5000	0.28	0.31	0.28	100	121	101
no IFN γ , no inhibitor	0.14	0.13	0.13			
Background	0.13	0.13	0.13			

*point excluded from analysis

Table 4.1 Raw Data for the Effect of Exiguamine A (3.1) on IDO1 Activity

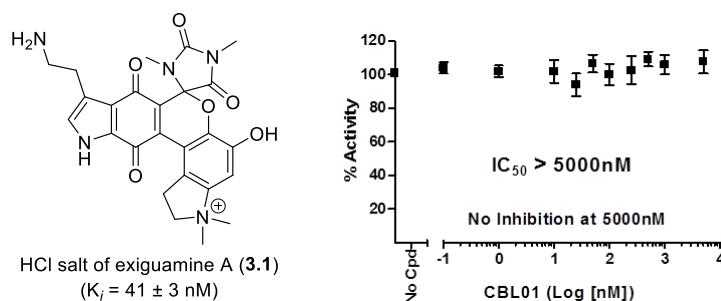


Figure 4.1 Effect of the Exiguamine A (3.1) on IDO1 Activity in HeLa Cells

• **INCB24360**

Raw data for the effect of INCB24360 on IDO1 activity are summarized in Table 4.2 and Figure 4.2.

INCB24360 (nM)	Absorbance OD 480 nm			% Activity		
	Repeat1	Repeat2	Repeat3	Repeat1	Repeat2	Repeat3
No Cpd	0.29	0.29	0.29	102	100	101
0.1	0.30	0.29	0.29	104	102	103
1	0.28	0.28	0.28	95	95	95
10	0.21	0.21	0.21	49	50	50
25	0.17	0.18	0.17	25	30	27

50	0.16	0.15	0.15	16	16	15
100	0.15	0.15	0.14	10	10	9
250	0.14	0.14	0.14	4	5	3
500	0.13	0.13	0.13	3	3	2
1000	0.13	0.13	0.13	1	2	1
5000	0.13	0.13	0.13	0	2	1
no IFN γ , no inhibitor	0.14	0.13	0.13			
Background	0.13	0.13	0.13			

Table 4.2 Raw Data for the Effect of INCB24360 on IDO1 Activity

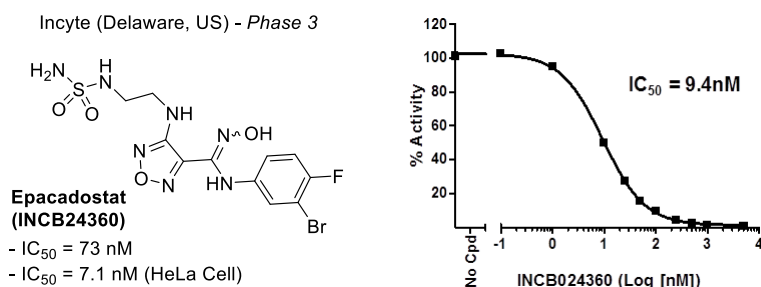


Figure 4.2 Effect of the INCB24360 on IDO1 Activity in HeLa Cells

d. Summary of the Inhibitory Effect of the Compounds on IDO1 Activity

The inhibition efficacy of compounds against IDO1 activity is summarized in Table 4.3. Exiguamine A (**3.1**) is found to have an IC₅₀ value more than 5000 nM on IDO activity in HeLa cells which was far more decreased activity in enzyme assay and much more inferior to IC₅₀ of a well known INCB24360.

compound	IC ₅₀ (nM)
Exiguamine A (3.1)	>5000 NI* at 5000 nM
INCB24360	9.4

* NI = No Significant Inhibition

Table 4.3 IC₅₀ Values of Compounds Against IDO1 Activity in HeLa Cells

4.2.2 *Iso*-Exiguamine A

4.2.2.1 Enzymatic Assay

a. Assay Conditions

The assay was performed by UV absorption using a recombinant human IDO1 and L-Tryptophan substrate. The UV absorption signal at 321 nm is correlated with the amount of *N*-formylkynurenine reaction product of IDO1. The compound was diluted in 10 % DMSO and 5 µl of the dilution was added to a 100 µl reaction so that the final concentration of DMSO is 0.5% in all of reactions.

All of the reactions were conducted at room temperature. The 100 µl reaction mixture in IDO Assay Buffer contains 40 nM IDO1, the indicated amount of the inhibitor, 900 µM tryptophan, and the coupled reaction components. The reaction mixture incubated for 180 min prior to reading the UV absorption signal. For the negative control (blank), 5 µl of the assay buffer was added instead of the IDO1. Absorption signals were measured using a Tecan Infinite M1000 plate reader.

b. Data Analysis

Binding experiments were performed in duplicate at each concentration. The data were analyzed using the computer software, Graphpad Prism. In the absence of the

compound, the absorption signal (A_t) in each data set was defined as 100% activity. In the absence of the IDO1, the absorption signal (A_b) in each data set was defined as 0% activity. The percent activity in the presence of each compound was calculated according to the following equation: % activity = $[(A - A_b)/(A_t - A_b)] \times 100$, where A = the absorption signal in the presence of the compound. The percent inhibition was calculated according to the following equation: % inhibition = 100 - % activity.

The values of % activity versus a series of compound concentrations were then plotted using non-linear regression analysis of Sigmoidal dose-response curve generated with the equation $Y = B + (T - B) / (1 + 10^{((\text{Log}IC_{50} - X) \times \text{Hill Slope}))}$, where Y = percent activity, B = minimum percent activity, T = maximum percent activity, X = logarithm of compound and Hill Slope = slope factor or Hill coefficient. The IC_{50} value was determined by the concentration causing a half-maximal percent activity.

c. Effect of Individual Compounds

- ***Iso-Exiguamine A (3.154)***

– The external molecular code for assay is 18-010.

Raw data for the effect of *iso-exiguamine A (3.154)* on IDO1 activity are summarized in Table 4.4 and Figure 4.3.

3.154 (nM)	UV absorption at 321 nm		% Activity	
	Repeat1	Repeat2	Repeat1	Repeat2
No Cpd	0.8614	0.8759		
0.1	0.8380	0.8300	96	95
1	0.8114	0.8102	93	93
10	0.5326	0.5259	59	58

25	0.3384	0.3306	35	34
50	0.2698	0.2706	26	26
100	0.2445	0.2535	23	24
250	0.2470	0.2513	24	24
500	0.2580	0.2633	25	26
1000	0.2767	0.2888	27	29
5000*	0.4170	0.4414	44	47
Background	0.0539	0.0568		

*Data removed from graph due to increase in signal. Reasons unknown

Table 4.4 Raw Data for the Effect of *Iso*-Exiguamine A (3.154) on IDO1 Activity

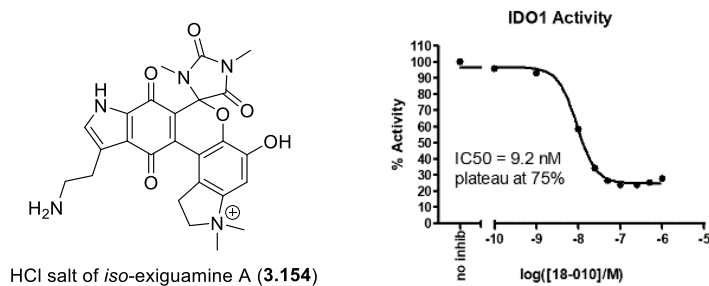


Figure 4.3 Effect of the *Iso*-Exiguamine A on Recombinant hIDO1 Activity

• **INCB24360**

Raw data for the effect of INCB24360 on IDO1 activity are summarized in Table 4.5 and Figure 4.4.

INCB24360 (nM)	UV absorption at 321 nm		% Activity	
	Repeat1	Repeat2	Repeat1	Repeat2
No Cpd	0.8614	0.8759		

0.1	0.8686	0.8539	100	98
1	0.8753	0.8387	101	96
10	0.7809	0.7558	89	86
25	0.6954	0.6491	79	73
50	0.5293	0.4780	58	52
100	0.4029	0.3746	43	39
250	0.1886	0.1797	16	15
500	0.1149	0.1037	7	6
1000	0.0784	0.0754	3	2
5000*	0.0584	0.0596	0	1
Background	0.0539	0.0568		

Table 4.5 Raw Data for the Effect of INCB24360 on IDO1 Activity

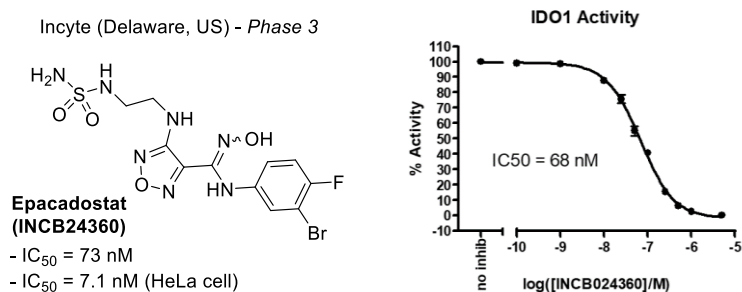


Figure 4.4 Effect of the INCB24360 on Recombinant hIDO1 Activity

d. Summary of the Inhibitory Effect of the Compounds on IDO1 Activity

The inhibition efficacy of compounds against IDO1 activity is summarized in Table 4.6. *Iso-exiguamine A* (**3.154**) exhibited significant inhibitory activity in the recombinant hIDO1 assay with an IC₅₀ value of 9.2 nM.

compound	IC ₅₀ (nM)
<i>Iso-exiguamine A</i>	9.2
3.154	Plateau at 75% inhibition
INCB24360	68

Table 4.6 IC₅₀ Values of Compounds Against Recombinant hIDO1 Activity

4.2.2.2 Cellular Assay

a. Assay Conditions

See. section 4.2.1 a. Assay Conditions

b. Data Analysis

See. section 4.2.1 b. Data Analysis

c. Effect of Individual Compounds

• *Iso-Exiguamine A* (3.154)

– The external molecular code for assay is 18-010.

Raw data for the effect of *iso-exiguamine A* (3.154) on IDO1 activity are summarized in Table 4.7.

3.154 (nM)	Absorbance OD 480 nm			% Activity		
	Repeat1	Repeat2	Repeat3	Repeat1	Repeat2	Repeat3
No Cpd	0.33	0.34	0.34	959	100	100
1	0.31	0.34	0.35	85	100	105
2	0.32	0.33	0.34	90	95	100
5	0.33	0.35	0.37	95	105	115

10	0.33	0.34	0.31	95	100	85
40	0.32	0.34	0.36	90	100	110
120	0.34	0.35	0.35	100	105	105
370	0.34	0.34	0.35	100	100	105
1110	0.33	0.34	0.35	95	100	105
3330	0.33	0.34	0.36	95	100	110
10000	0.34	0.34	0.36	100	100	110
Background	0.15	0.15	0.13			

Table 4.7 Raw Data for the Effect of *Iso-Exiguamine A (3.154)* on IDO1 Activity

● **INCB24360**

Raw data for the effect of INCB24360 on IDO1 activity are summarized in Table 4.8.

INCB24360 (nM)	Absorbance OD 480 nm			% Activity		
	Repeat1	Repeat2	Repeat3	Repeat1	Repeat2	Repeat3
No Cpd	0.34	0.34	0.35	100	100	105
1	0.31	0.32	0.33	85	90	95
2	0.29	0.30	0.31	75	80	85
5	0.25	0.25	0.26	55	55	60
10	0.19	0.20	0.21	25	30	35
40	0.24	0.17	0.17	50	15	15
120	0.15	0.16	0.16	5	10	10
370	0.14	0.15	0.15	0	5	5
1110	0.14	0.15	0.15	0	5	5
3330	0.14	0.15	0.15	0	5	5

10000	0.14	0.15	0.15	0	5	5
Background	0.14	0.15	0.14			

Table 4.8 Raw Data for the Effect of INCB24360 on IDO1 Activity

d. Summary of the Inhibitory Effect of the Compounds on IDO1 Activity

The inhibition efficacy of compounds against IDO1 activity is summarized in Figure 4.5 and Table 4.9. In contrast to the high inhibitory effect of *iso*-exiguamine A (**3.154**) observed from enzymatic assay ($IC_{50} = 9.2$ nM), results from HeLa cells showed no IDO inhibition at concentrations up to 10000 nM.

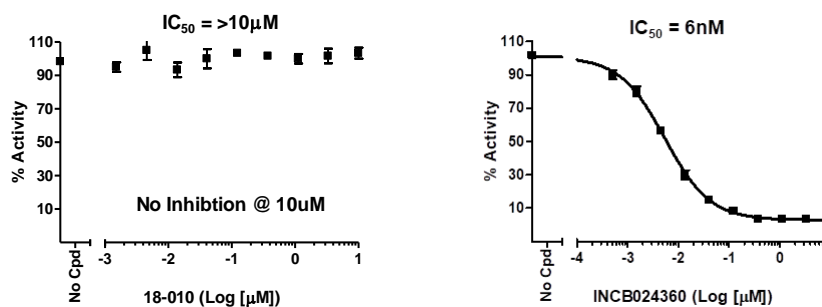


Figure 4.5 Effect of the Compounds on IDO1 Activity in HeLa Cells

compound	IC ₅₀ (nM)
<i>Iso</i> -exiguamine A 3.154	>10000 NI* at 10000 nM
INCB24360	6

* NI = No Significant Inhibition

Table 4.9 IC₅₀ Values of Compounds Against IDO1 Activity in HeLa Cells

4.2.3 Precursor of Exiguamine A

The IDO inhibitory activity of compound **3.141** that could be potential precursor for the biosynthesis of exiguamine A by further oxidation was evaluated (Figure 4.6).

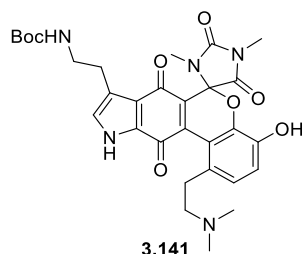


Figure 4.6 Precursor of Exiguamine A **3.141**

4.2.3.1 Enzymatic Assay

The enzymatic assay of compound **3.141** was performed concurrently with that of compound **3.154**.

a. Assay Conditions

See. section 4.2.2.1 a. Assay Conditions

b. Data Analysis

See. section 4.2.2.1 b. Data Analysis

c. Effect of Individual Compounds

• Precursor of Exiguamine A (**3.141**)

- The external molecular code for assay is 18-012.

Raw data for the effect of exiguamine A precursor (**3.141**) on IDO1 activity are summarized in Table 4.10

3.141 (nM)	UV absorption at 321 nm		% Activity	
	Repeat1	Repeat2	Repeat1	Repeat2
No Cpd	0.8614	0.8759		
0.1	0.8375	0.8537	96	98
1	0.8557	0.8526	98	98
10	0.7215	0.7230	82	82
25	0.4924	0.5000	54	55
50	0.3826	0.3815	40	40
100	0.3220	0.3172	33	32
250	0.2540	0.2565	24	25
500	0.2415	0.2448	23	23
1000	0.2455	0.2431	23	23
5000	0.2967	0.3080	30	31
Background	0.0539	0.0568		

Table 4.10 Raw Data for the Effect of Exiguamine A Precursor on IDO1 Activity

● **INCB24360**

Raw data for the effect of INCB24360 on IDO1 activity, see. Table 4.5

d. Summary of the Inhibitory Effect of the Compounds on IDO1 Activity

The inhibition efficacy of compounds against IDO1 activity is summarized in Figure 4.7 and Table 4.11. Compound **3.141** was determined as a potent IDO inhibitor with an enzymatic IC₅₀ value of 20 nM.

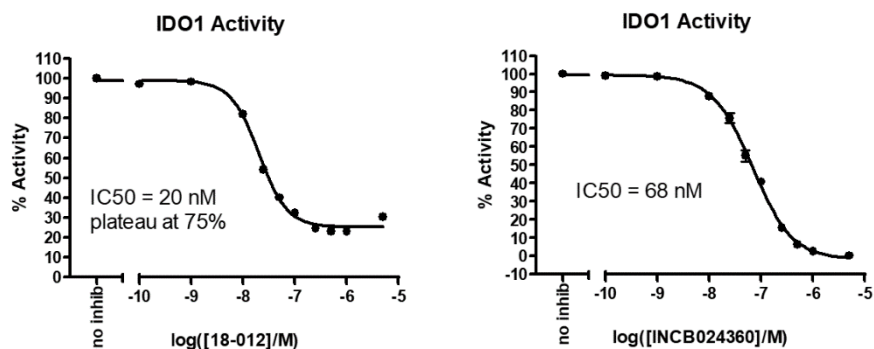


Figure 4.7 Effect of the Compounds on Recombinant hIDO1 Activity

compound	IC ₅₀ (nM)
3.141	20 Plateau at 75% inhibition
INCB24360	68

Table 4.11 IC₅₀ Values of Compounds Against Recombinant hIDO1 Activity

4.2.3.2 Cellular Assay

The cellular assay of **3.141** compound was performed concurrently with that of **3.154** compound.

a. Assay Conditions

See. section 4.2.1 a. Assay Conditions

b. Data Analysis

See. section 4.2.1 b. Data Analysis

c. Effect of Individual Compounds

● Precursor of Exiguamine A (3.141)

– The external molecular code for assay is 18-012.

Raw data for the effect of exiguamine A precursor (**3.141**) on IDO1 activity are summarized in Table 4.12.

3.141 (nM)	Absorbance OD 480 nm			% Activity		
	Repeat1	Repeat2	Repeat3	Repeat1	Repeat2	Repeat3
No Cpd	0.32	0.33	0.33	95	100	100
1	0.33	0.33	0.33	100	100	100
2	0.32	0.33	0.33	95	100	100
5	0.32	0.33	0.33	95	100	100
10	0.33	0.34	0.33	100	105	100
40	0.33	0.33	0.33	100	100	100
120	0.26	0.34	0.35	63	105	111
370	0.35	0.34	0.41	111	105	142
1110	0.34	0.34	0.28	105	105	74
3330	0.33	0.34	0.33	100	105	100
10000	0.31	0.31	0.32	89	89	95
Background	0.15	0.15	0.13			

Table 4.12 Raw Data for the Effect of Exiguamine A Precursor on IDO1 Activity

● INCB24360

Raw data for the effect of INCB24360 on IDO1 activity, see. Table 4.8

d. Summary of the Inhibitory Effect of the Compounds on IDO1 Activity

The inhibition efficacy of compounds against IDO1 activity is summarized in Figure 4.8 and Table 4.13. The inhibitory activity was tested with neutral compound due to the possibly decreased cell permeability of cationic exiguamines. However, compound **3.141** was found to have no inhibition activity at concentrations up to 10000 nM in cell-based assay.

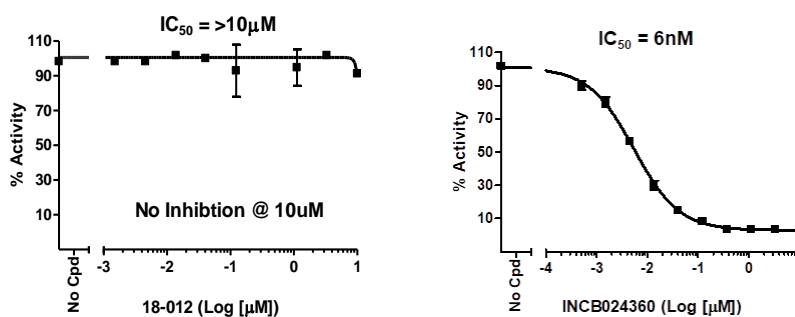


Figure 4.8 Effect of the Compounds on IDO1 Activity

compound	IC ₅₀ (nM)
3.141	>10000 NI* at 10000 nM
INCB24360	6

* NI = No Significant Inhibition

Table 4.13 IC₅₀ Values of Compounds Against IDO1 Activity in HeLa Cells

4.3 Conclusion

Biological evaluation of the synthesized exiguanine A and its derivatives as inhibitors of IDO activity is summarized in Figure 4.9.

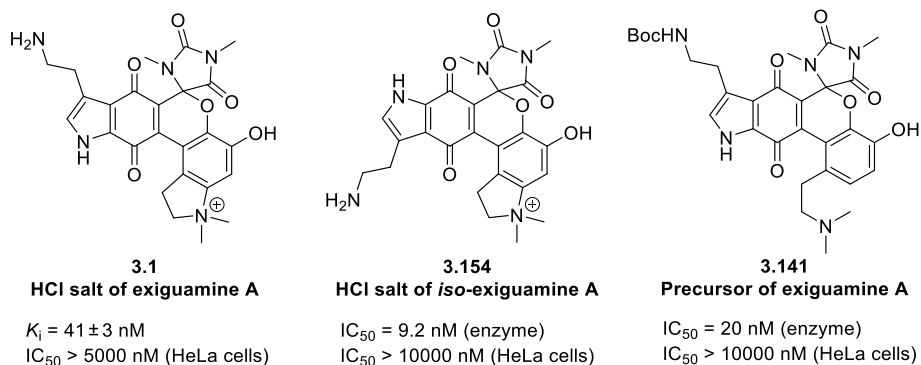


Figure 4.9 Summary: Biological Evaluation of Exiguamine A and Its Derivatives

All three compounds were observed to have little efficacy on IDO activity in HeLa cells in contrast to the promising results from enzymatic assay. Conflicting results observed in enzyme and cell line might be accounted by the unsuitable polarity of these compounds that interferes the penetration of compounds into a cell membrane. Therefore, it is necessary to verify this hypothesis by measuring the cell permeability of the compounds, and further efforts should be made to discover potent IDO inhibitor candidates in cells as well as enzymes through the synthesis of various exiguamine A derivatives possessing appropriate physicochemical properties.

4.4 Reference

[1] Röhrig, U. F.; Awad, L.; Grosdidier, A.; Larrieu, P.; Stroobant, V.; Colau, D.; Cerundolo, V.; Simpson, A. J. G.; Vogel, P.; Van den Eynde, B. J.; Zoete, V.; Michielin, O. *J. Med. Chem.* **2010**, *53*, 1172.

국문초록

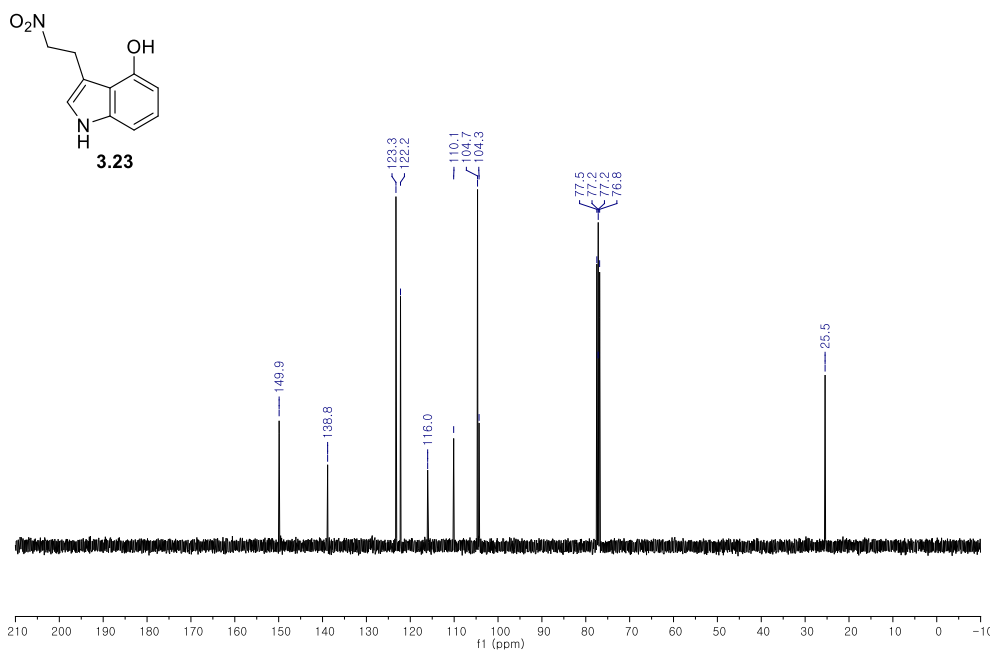
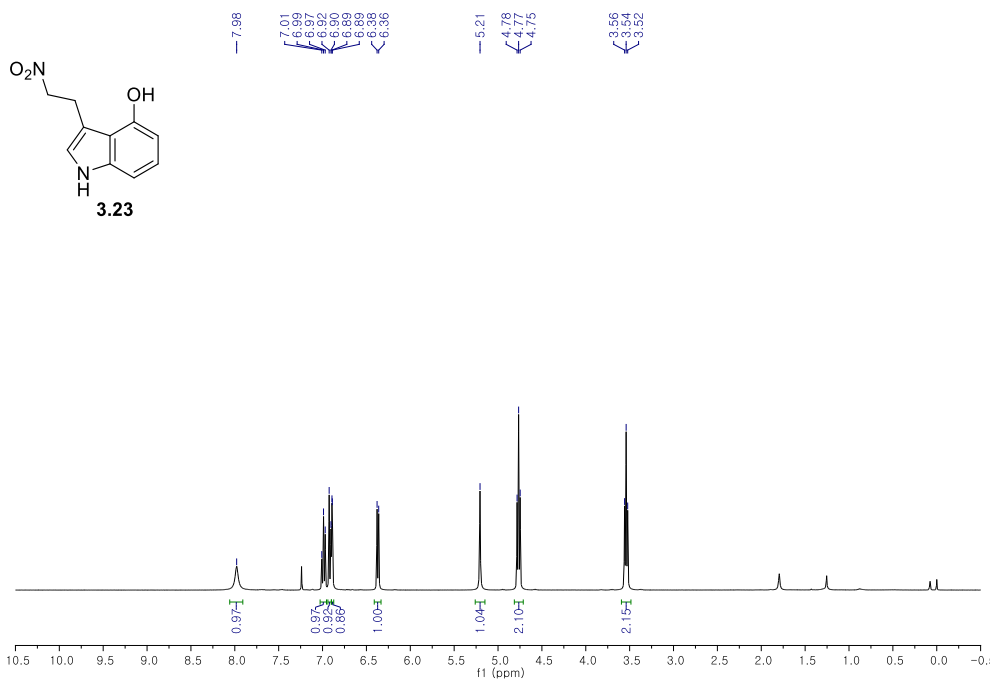
해양 천연물 엑시구아민 에이의 전합성과 생물학적 활성 연구를 수행하였다. 엑시구아민 에이는 6개의 고리가 연속적으로 연결된 전혀 없는 골격을 지닌 알칼로이드 분자로서 인돌아민 2,3-디옥시게나제 효소에 대해 강한 억제 효능을 지닌 것으로 알려져있다. 인돌아민 2,3-디옥시게나제는 필수아미노산인 트립토판의 분해대사의 첫 번째이자 속도결정단계에 관여하는 효소이다 (1장). 면역 조절에 관여하는 이 효소는 여러 암세포에서 과발현되고 있으며, 암이 면역체계를 회피하는데 기여한다는 사실이 밝혀지면서 면역항암치료의 주요 타겟으로 자리잡았다. 구조적으로, 그리고 생물학적으로 독특한 성질을 지닌 엑시구아민 에이의 합성을 위해 먼저 관련 문헌을 고찰하고 (2장), 이를 바탕으로 새로운 합성 전략을 고안하였다. 엑시구아민 에이가 트립타민 퀴논, 도파민, 히단토인 이 세 개의 구성요소로 이루어져 있다는 개념에 기초하여 이들을 효율적으로 조합하는 수렴적 합성을 구상하였다. 퀴논과 하이드로퀴논간의 산화-환원 평형을 이용하여 엑시구아민 에이의 모든 구성요소를 한 분자 내로 도입하였고, 뒤이어 중심의 6각 고리구조를 형성하였다. 이후 수소와 산소를 이용한 연속적인 산화-환원반응을 통하여 엑시구아민 에이의 간결한 전합성을 완결하였다. 이러한 수렴적 합성법으로 엑시구아민 에이의 이성질체인 *아/소*-엑시구아민 에이의 전합성도 완결하였다 (3장). 합성된 화합물들을 세포주 기반에서 생물학적 효능을 평가하여 인돌아민 2,3-디옥시게나제 억제제로서의 활용 가능성에 대하여 탐구하였다 (4장).

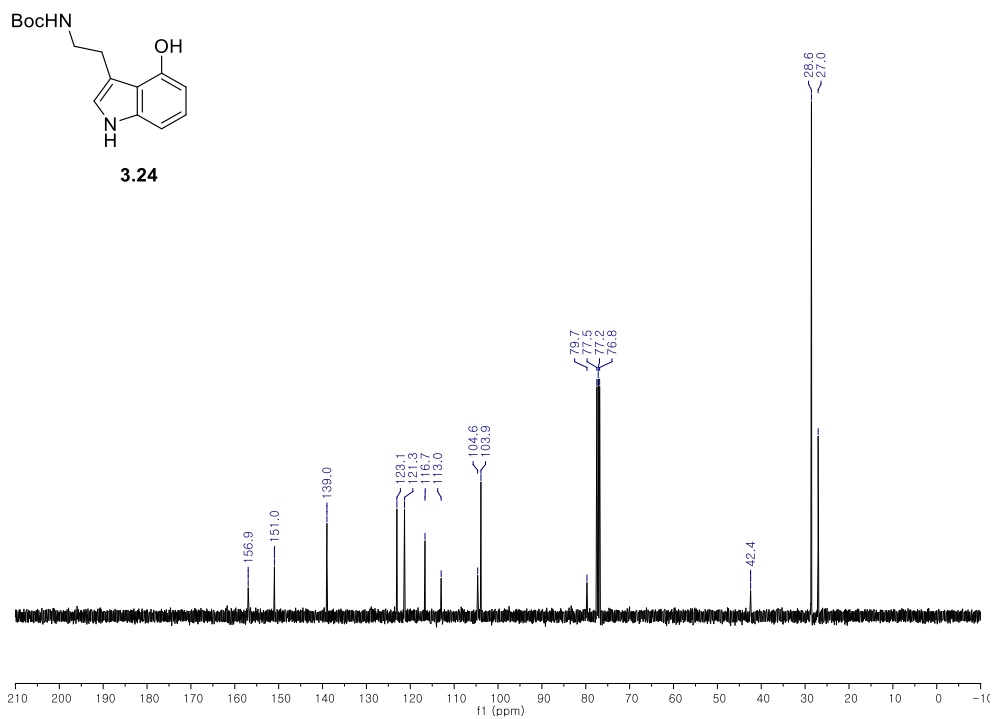
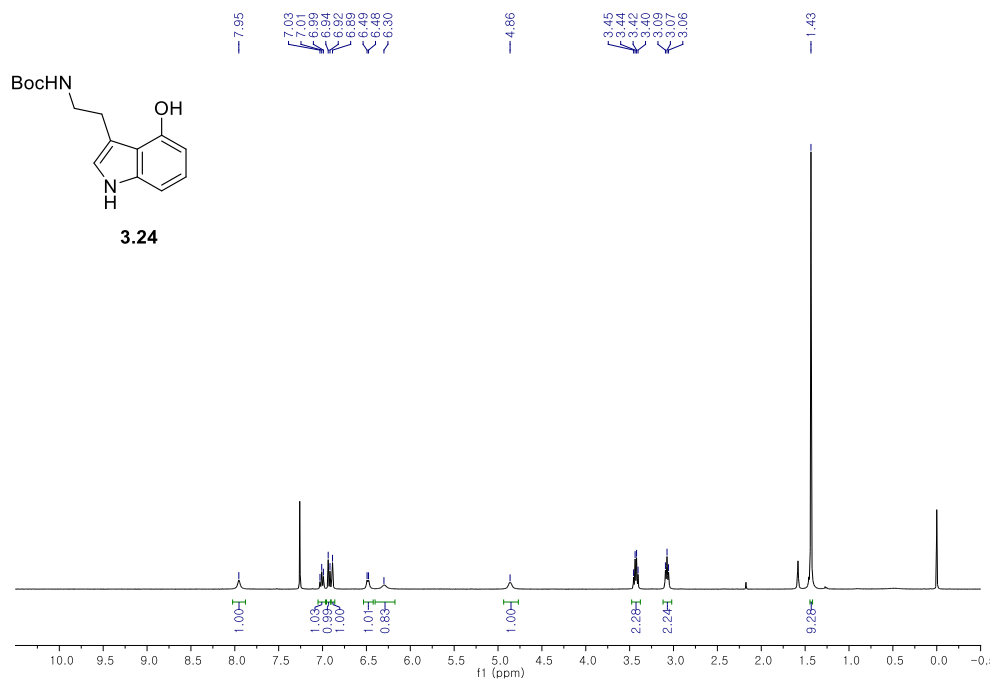
주제어: 인돌아민 2,3-디옥시게나제 억제제, 천연물, 전합성, 엑시구아민
에이, *아이*소-엑시구아민 에이, 생물학적 평가

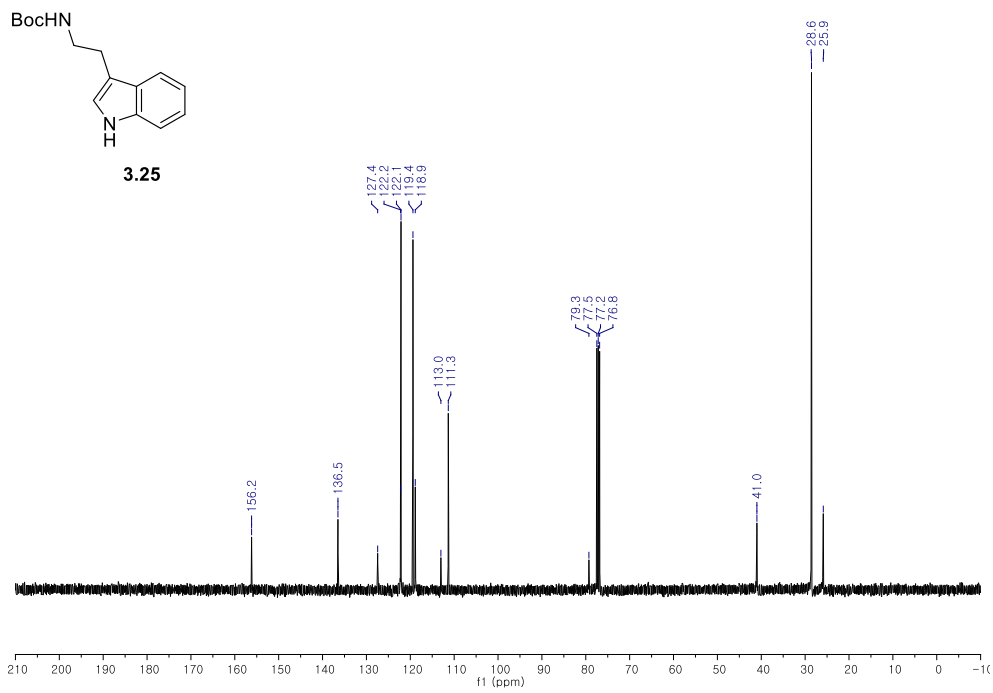
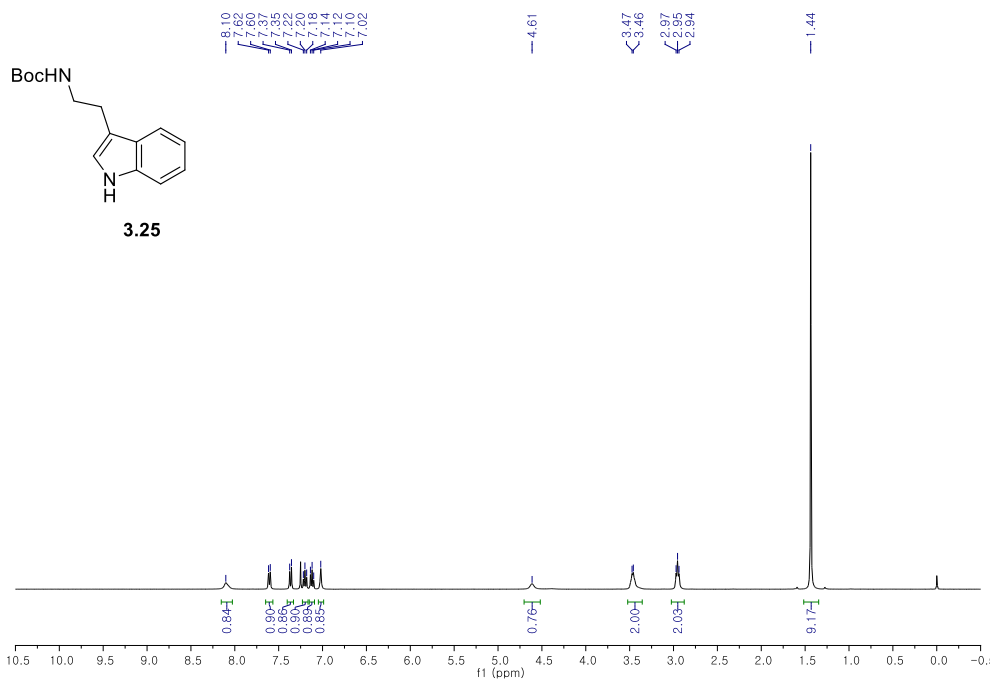
학번: 2008-22723

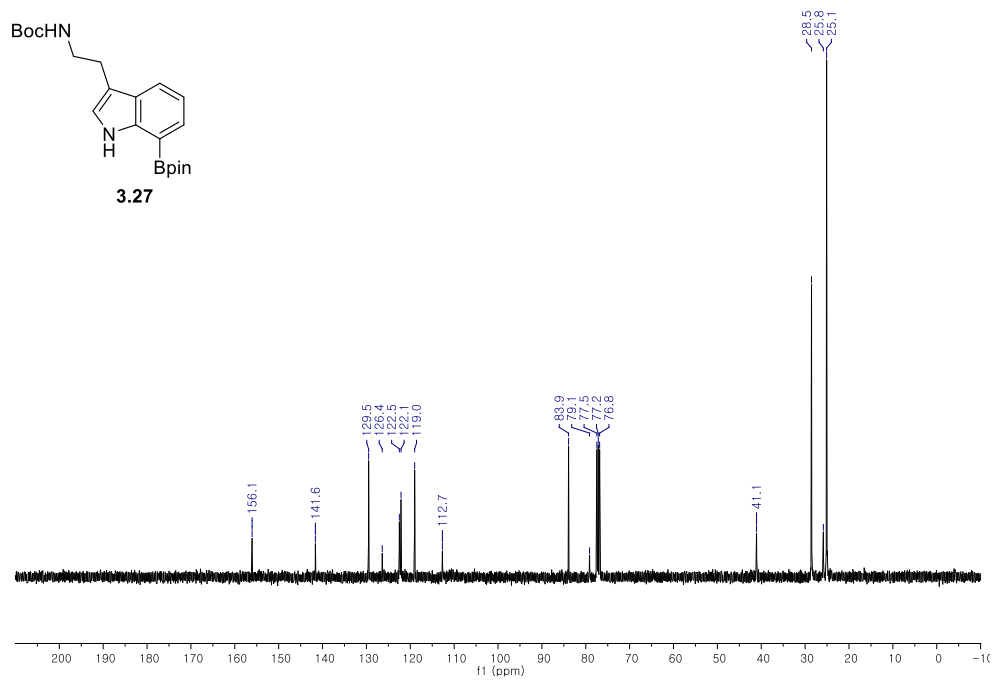
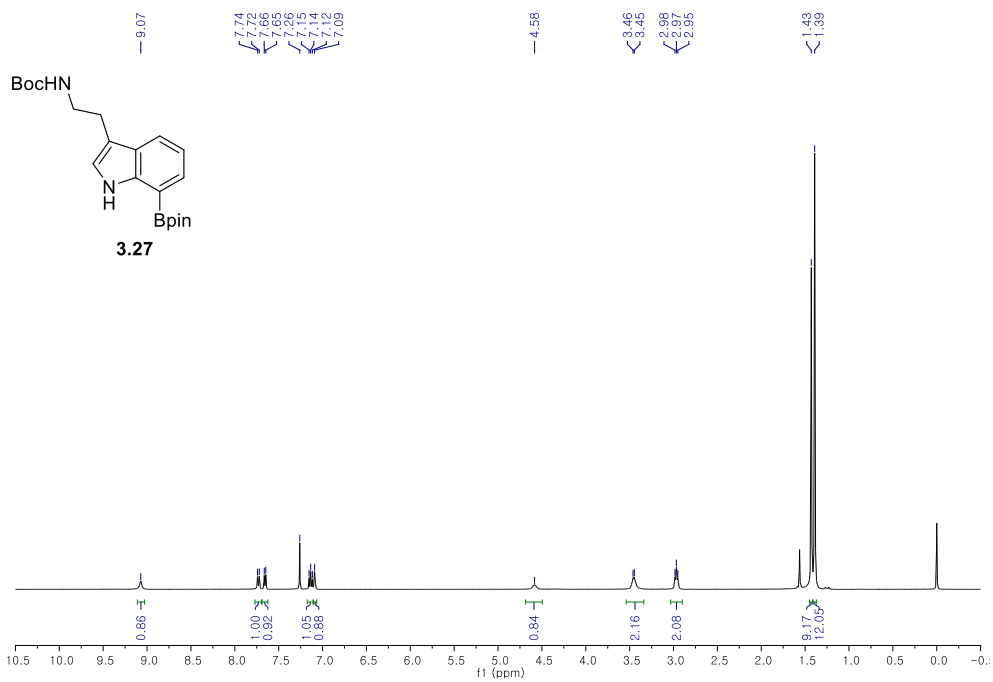
Appendix A

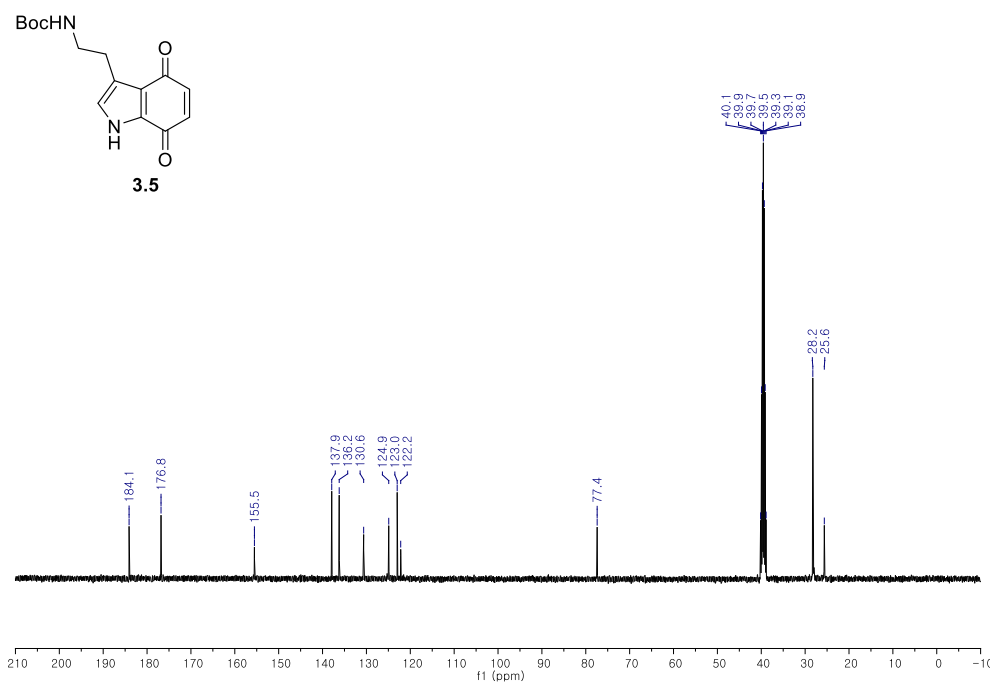
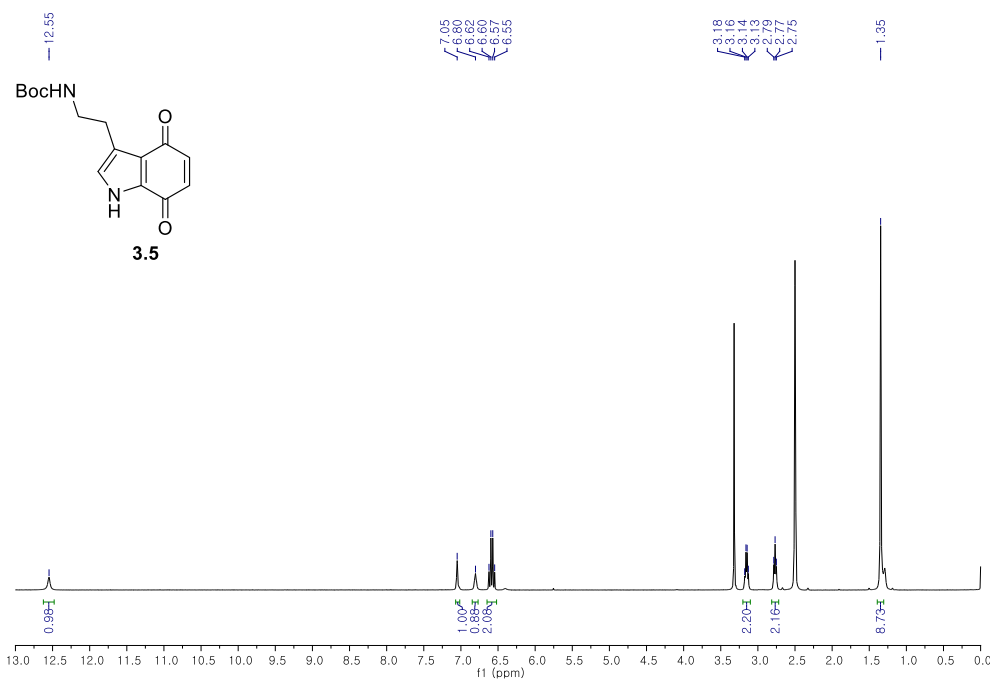
Selected NMR Spectra

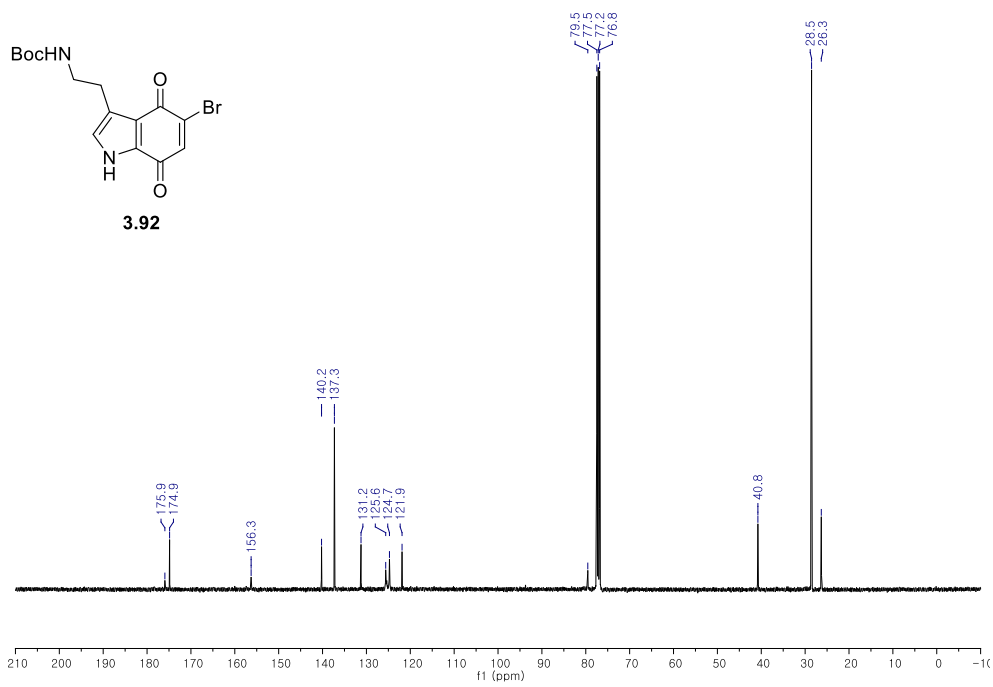
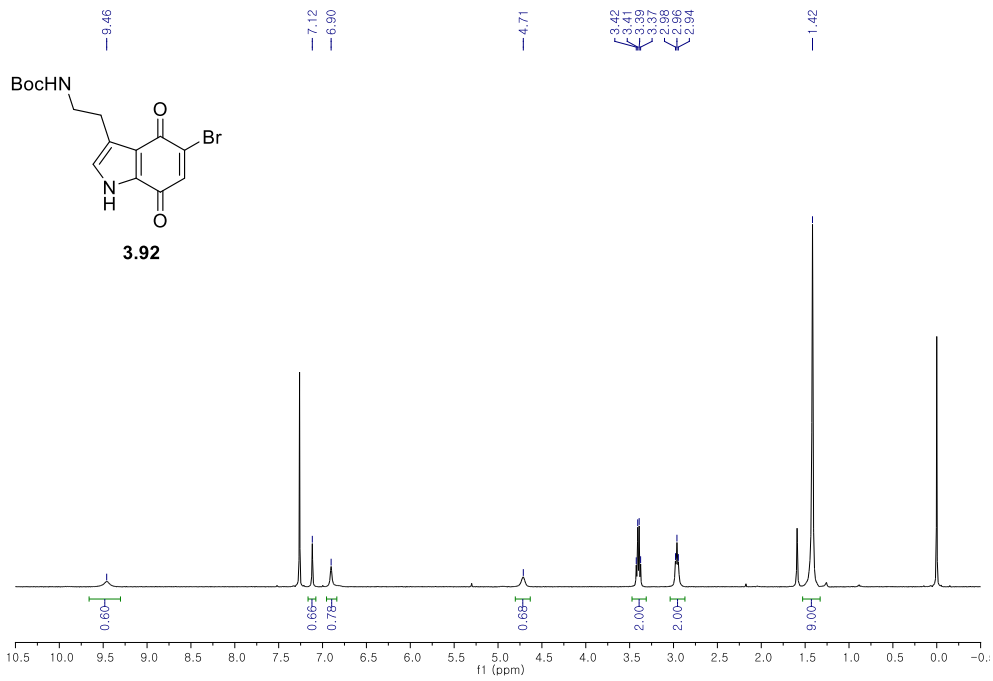


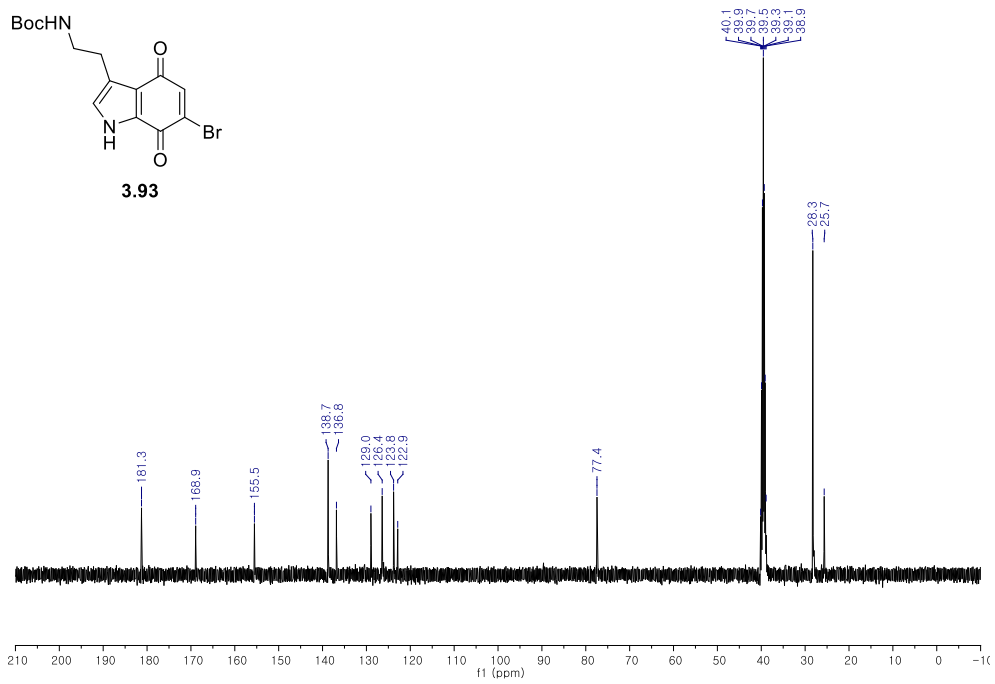
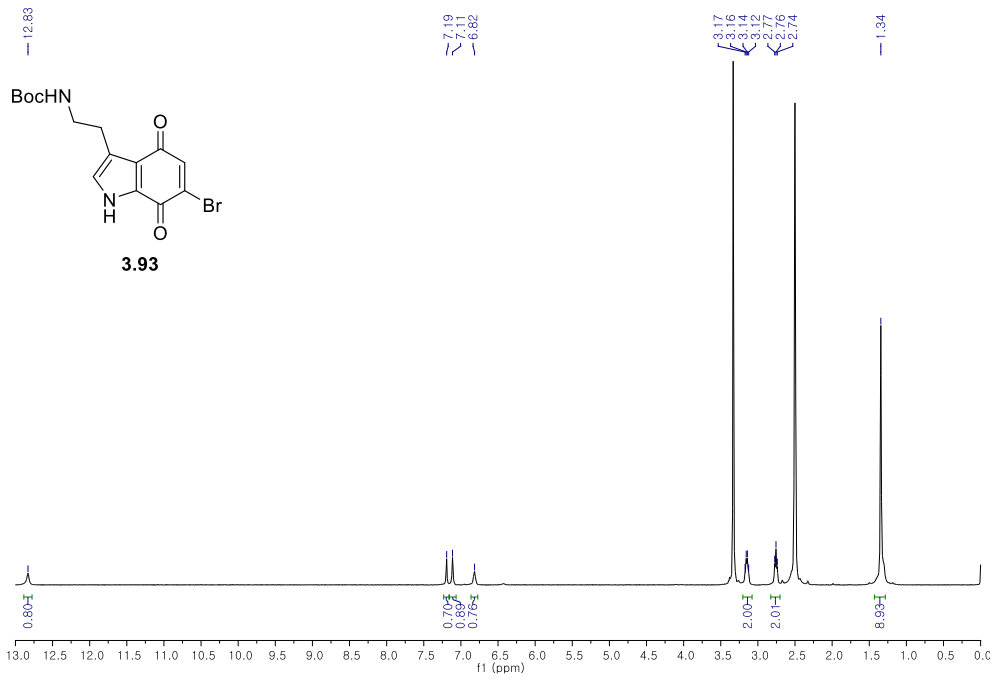


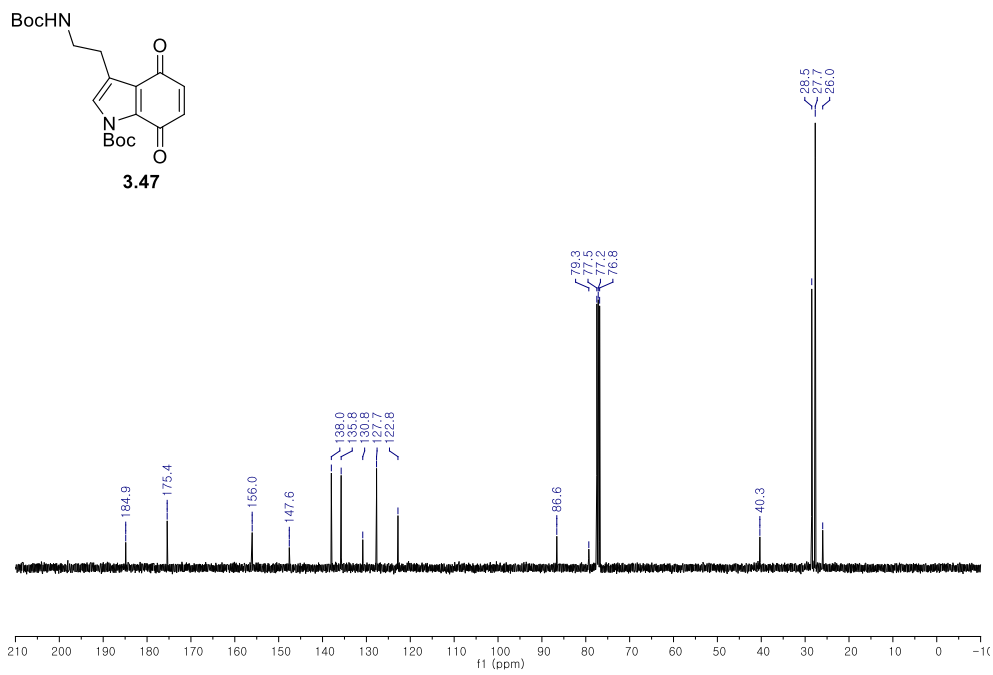
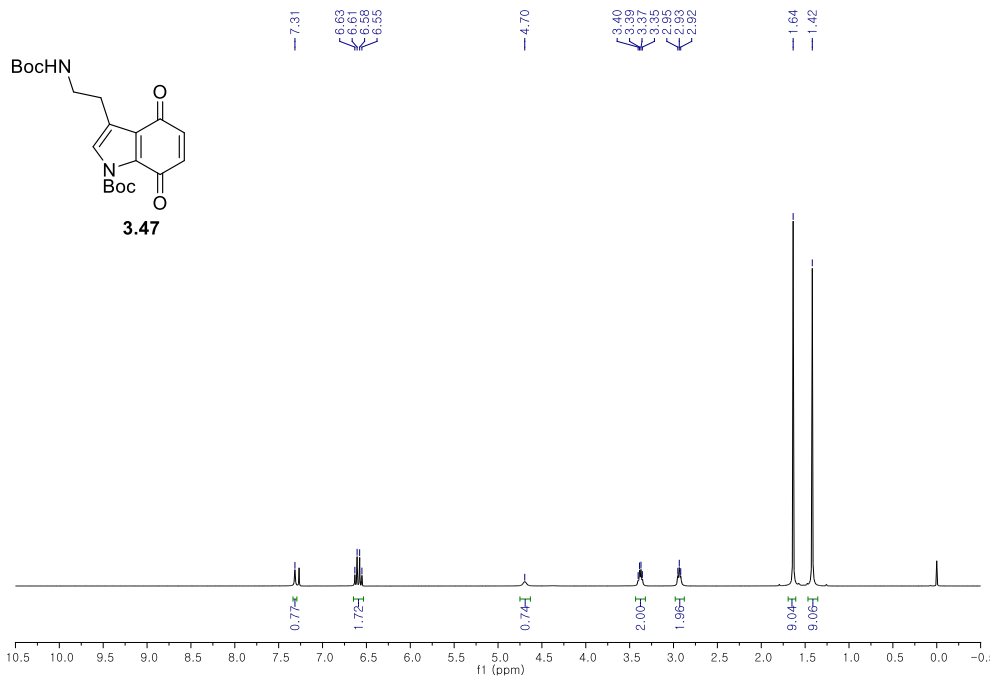


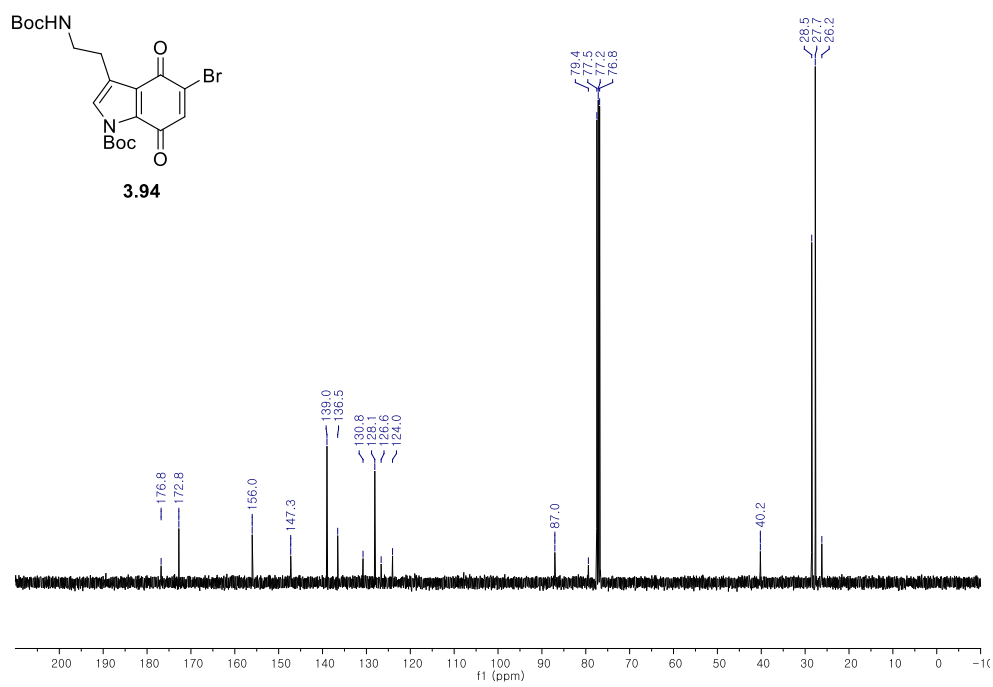
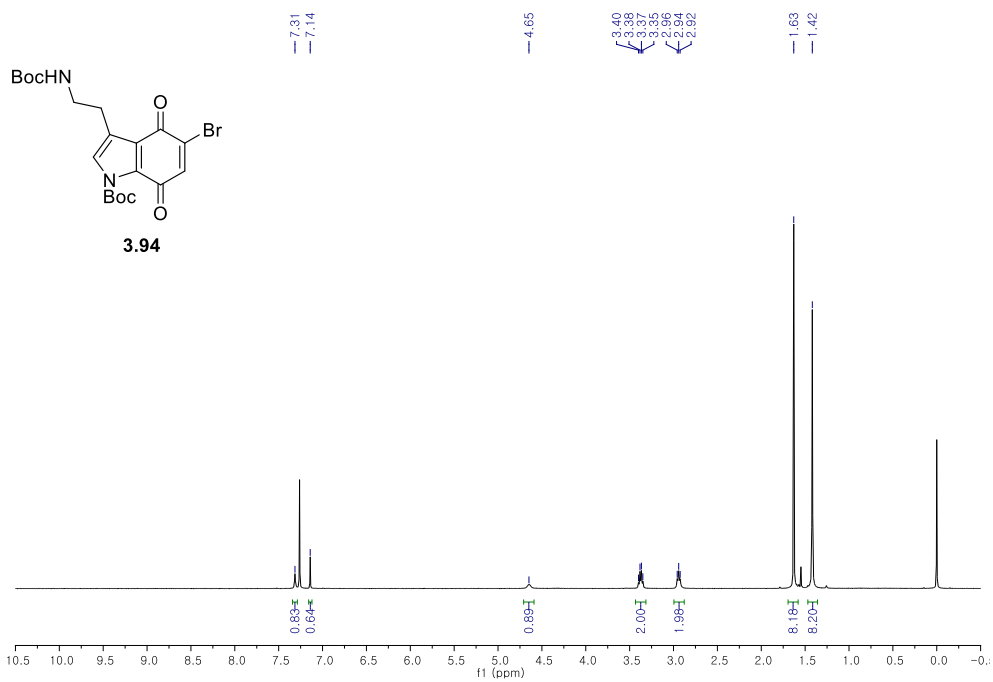


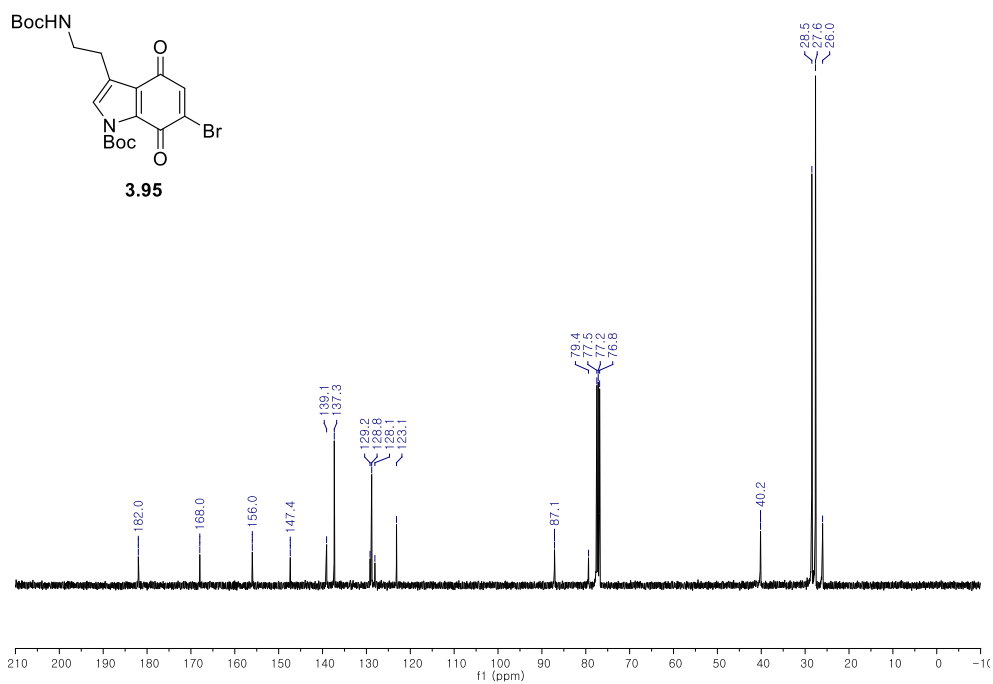
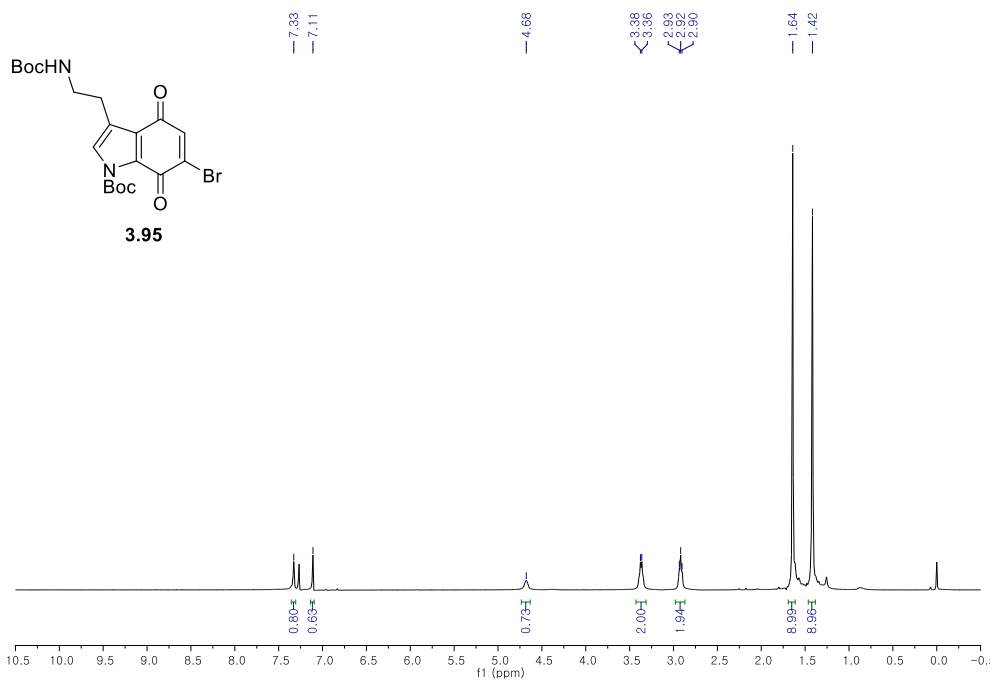


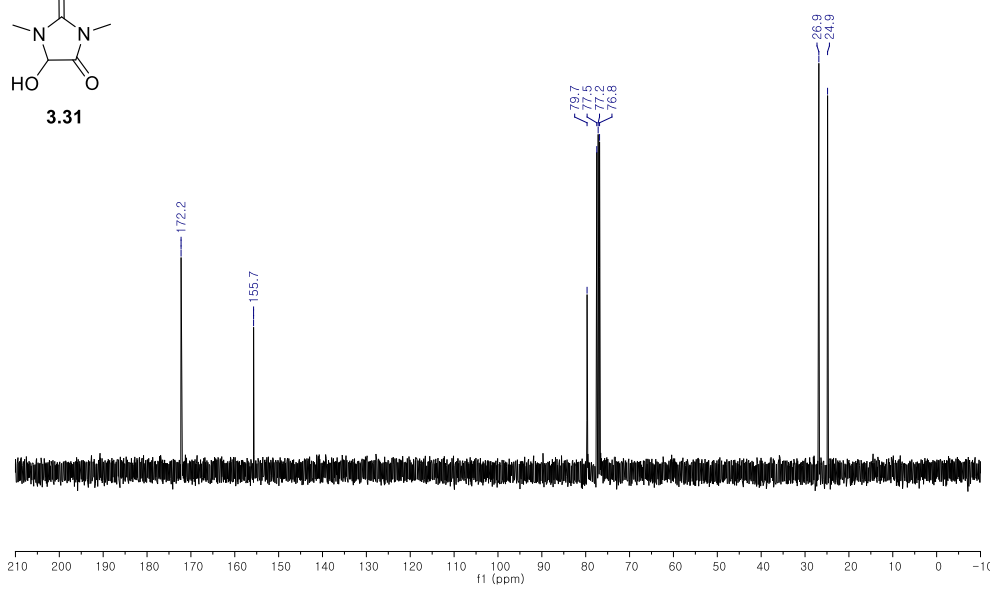
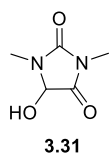
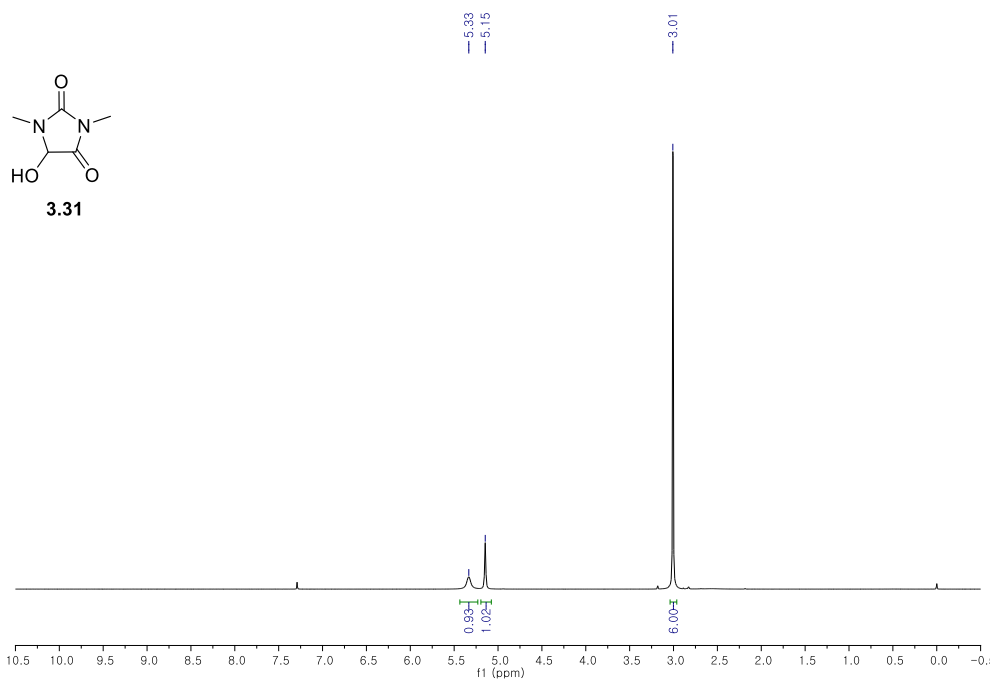
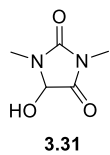


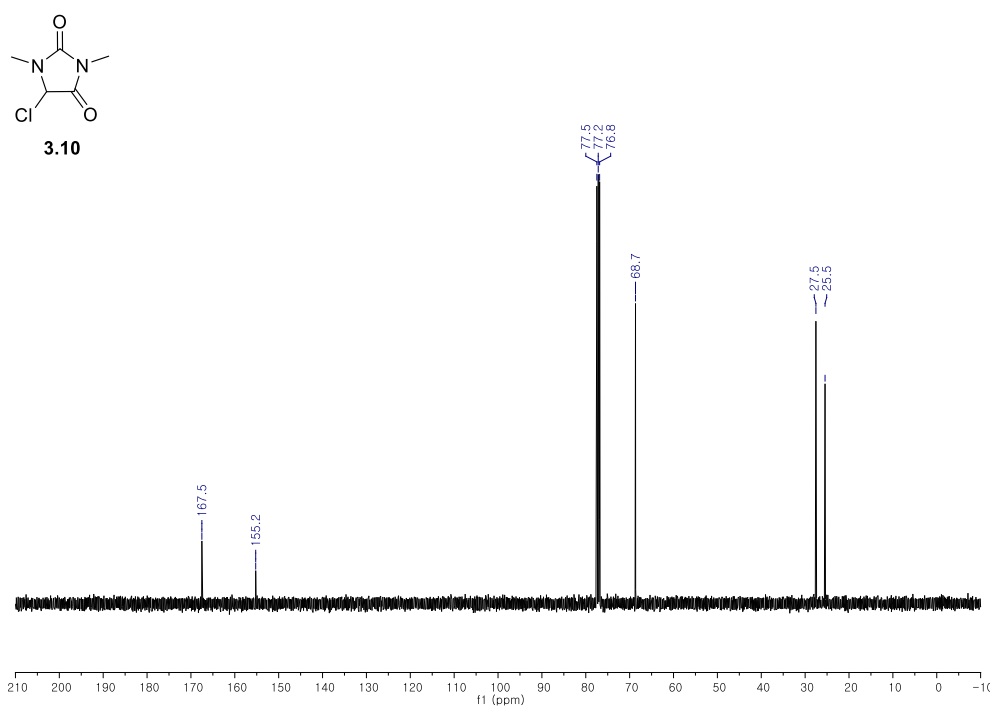
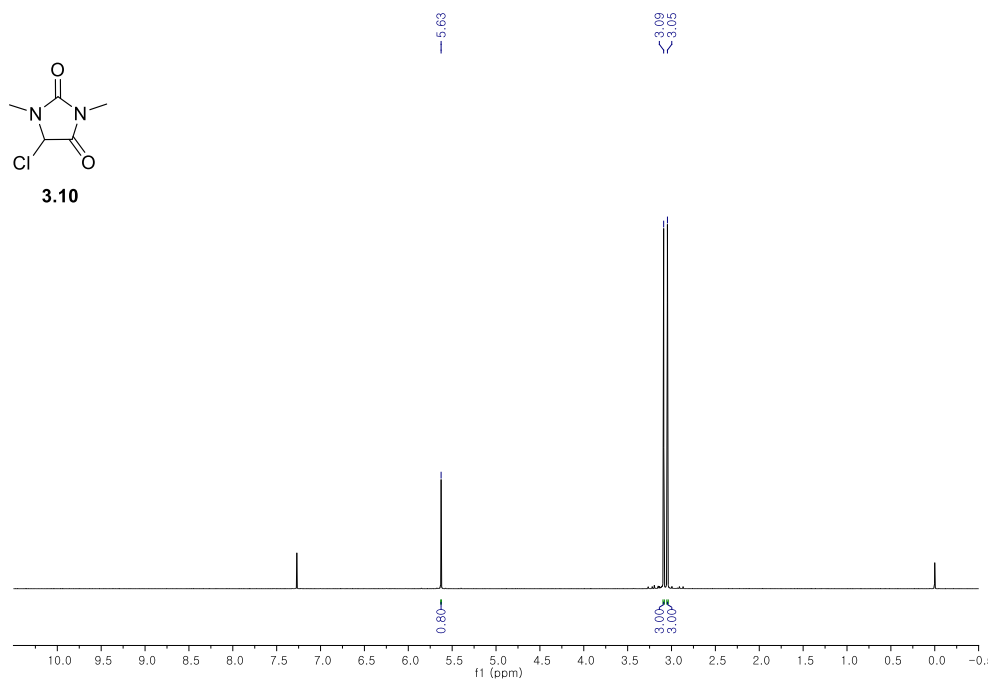


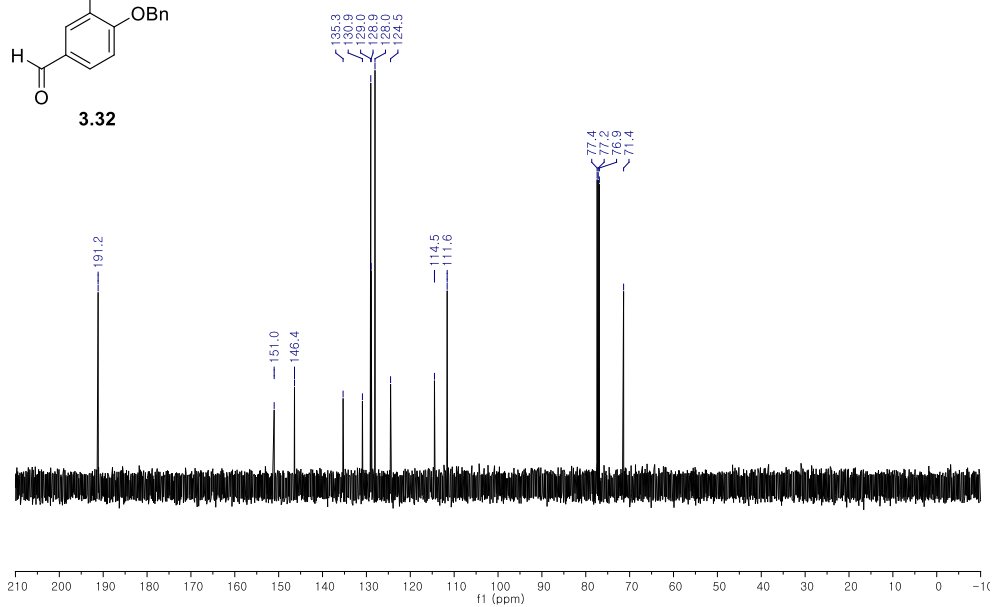
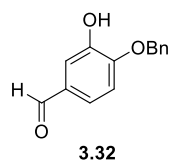
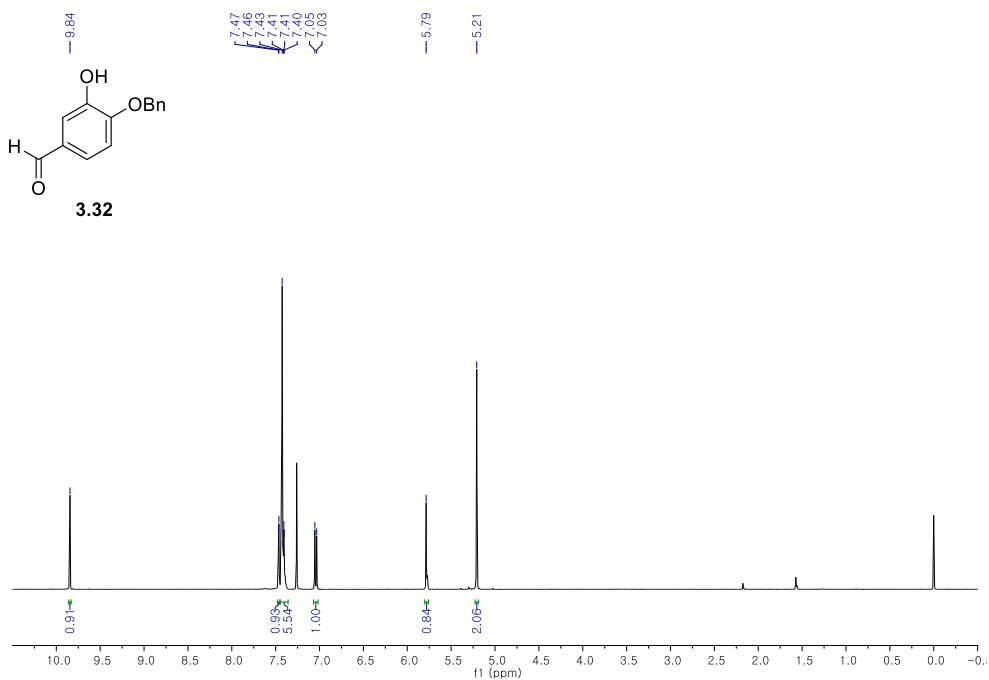
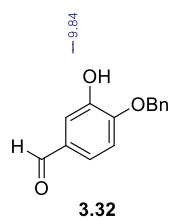


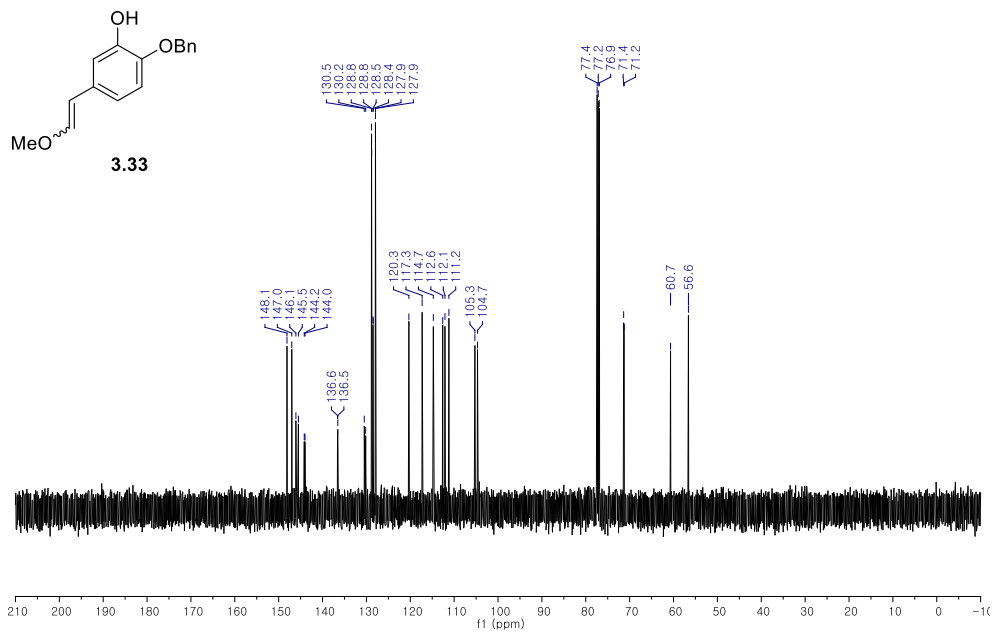
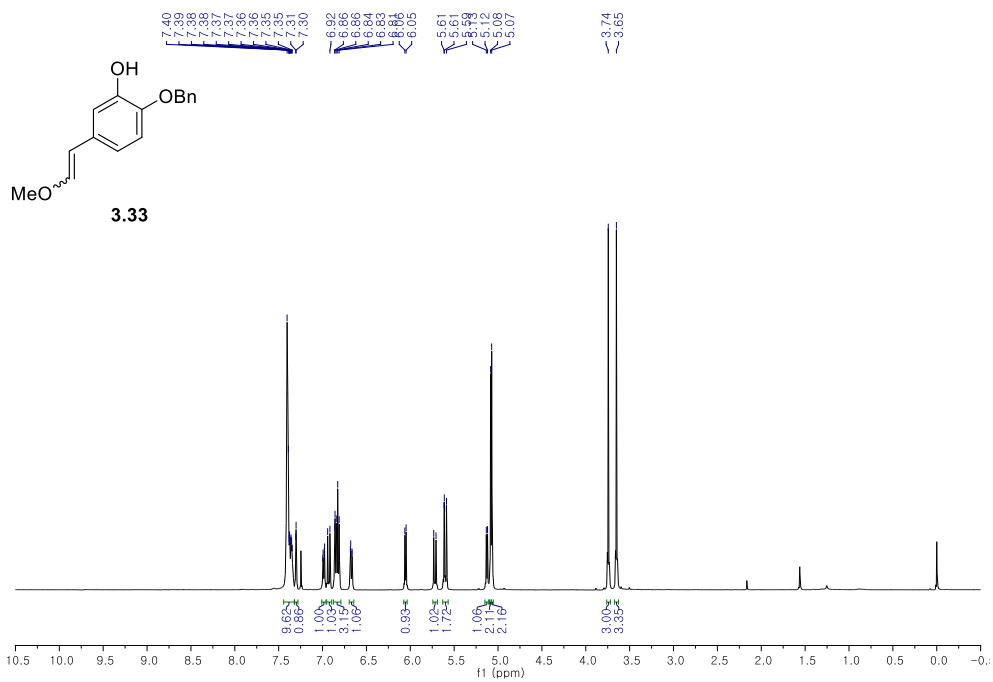


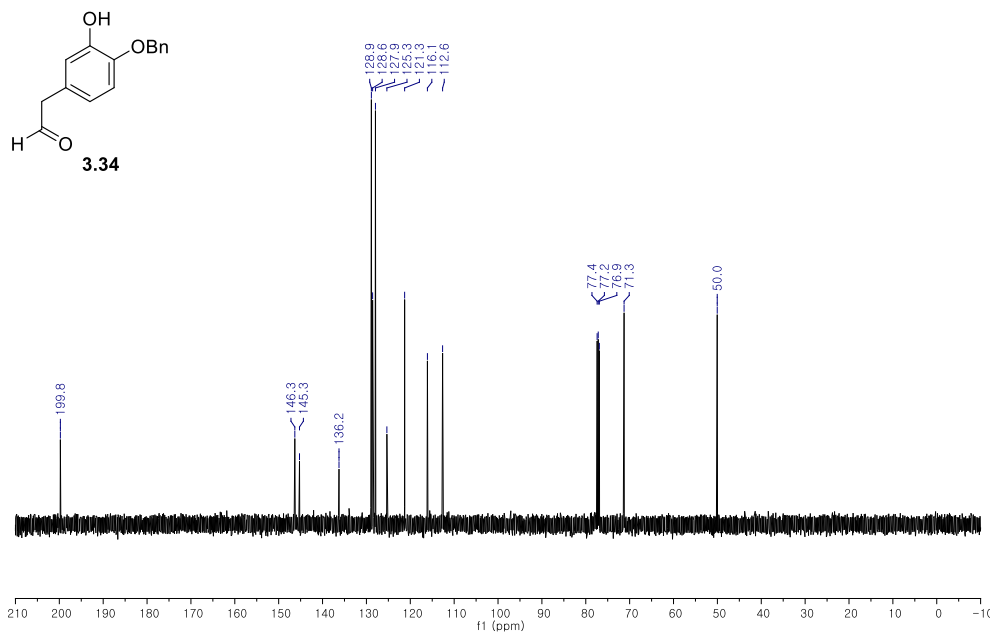
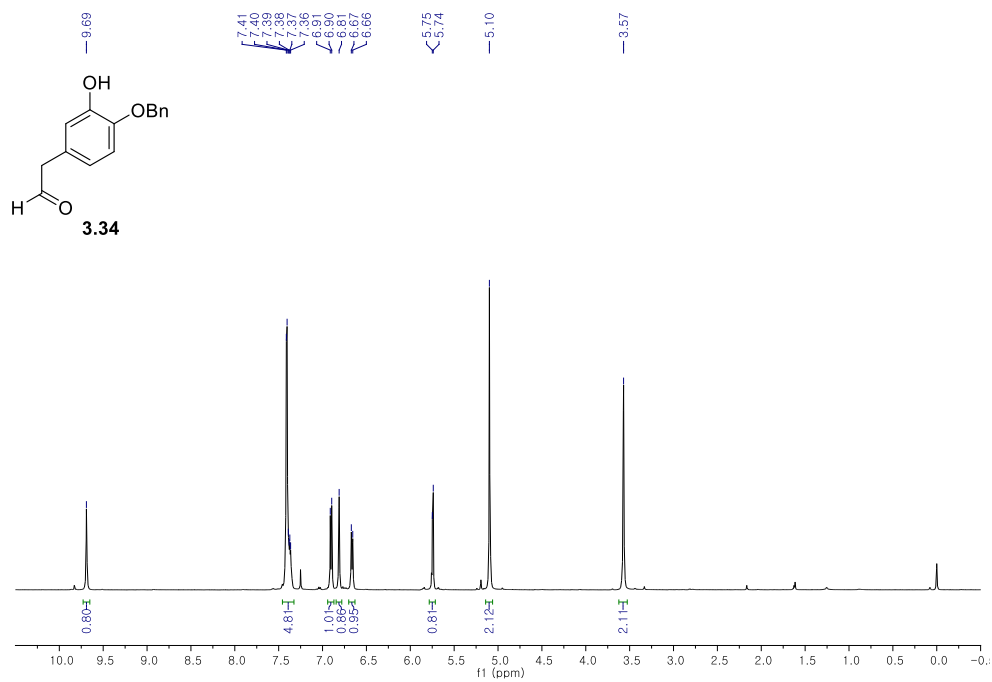


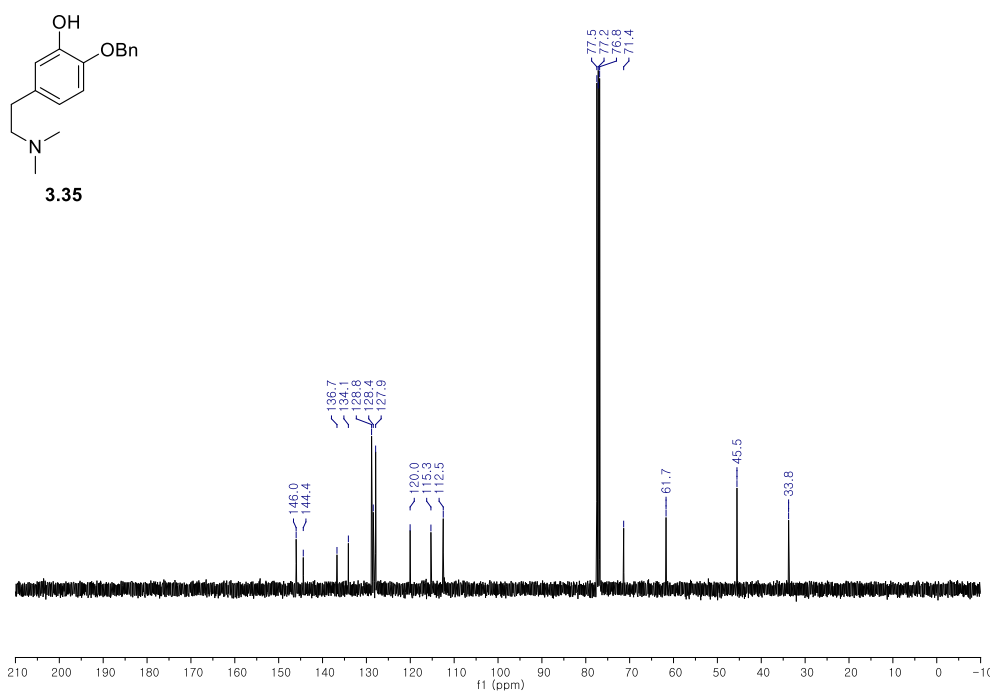
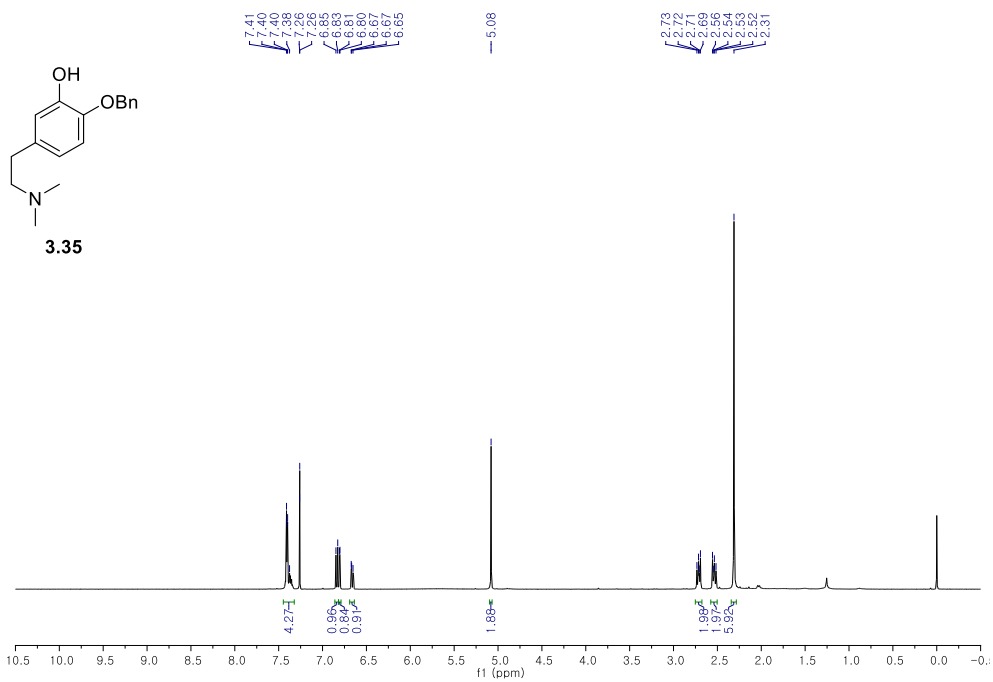


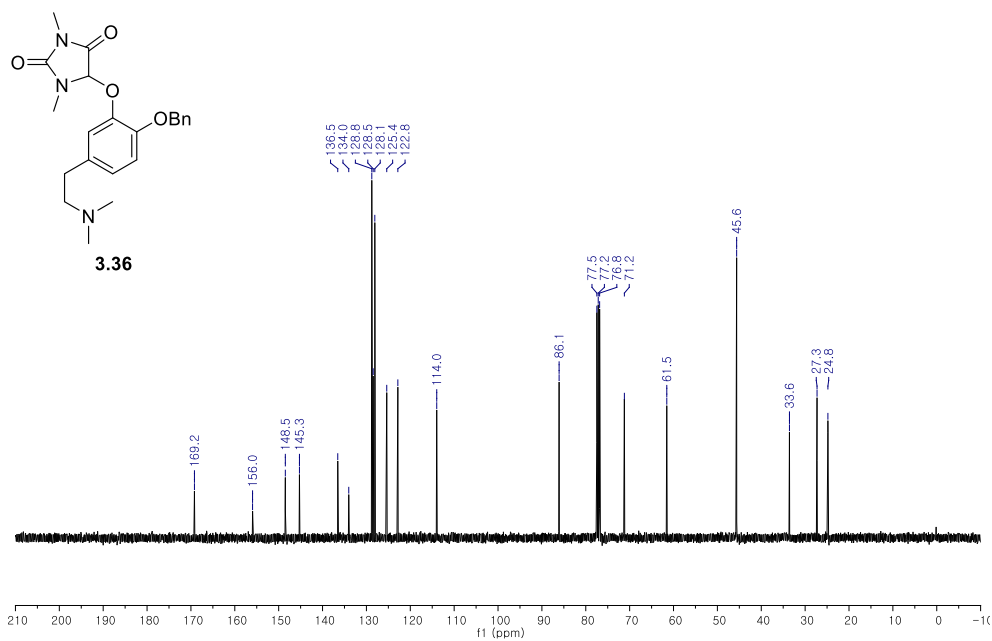
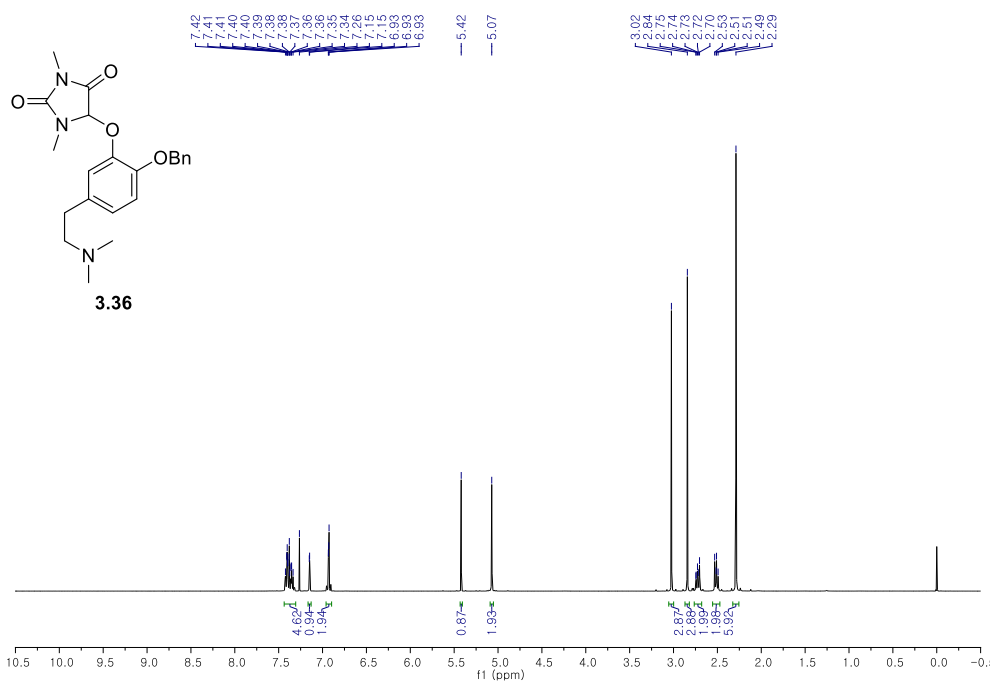


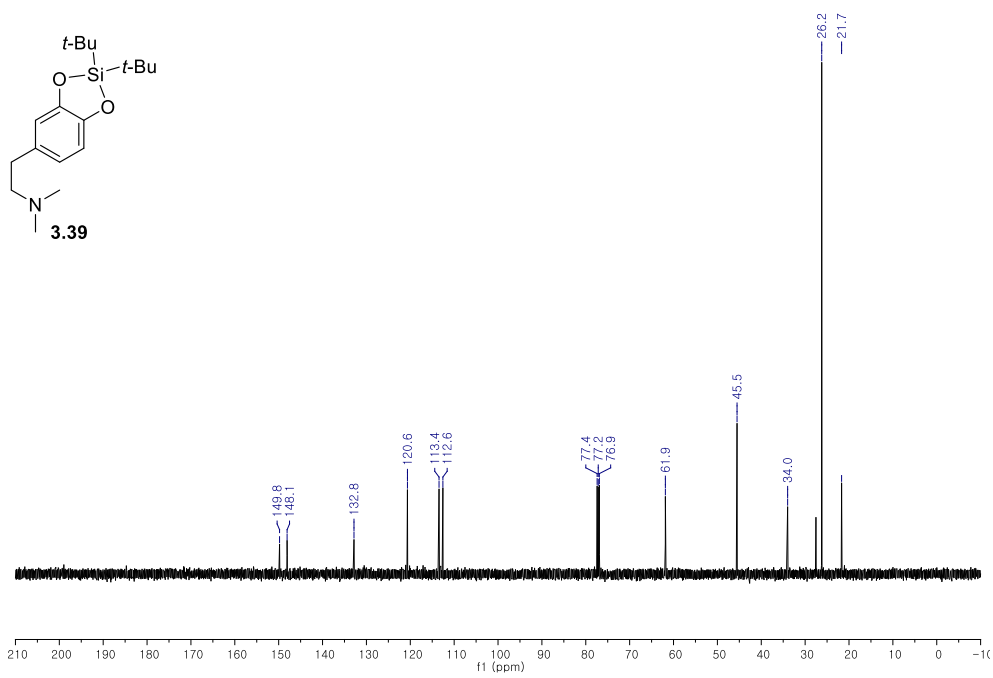
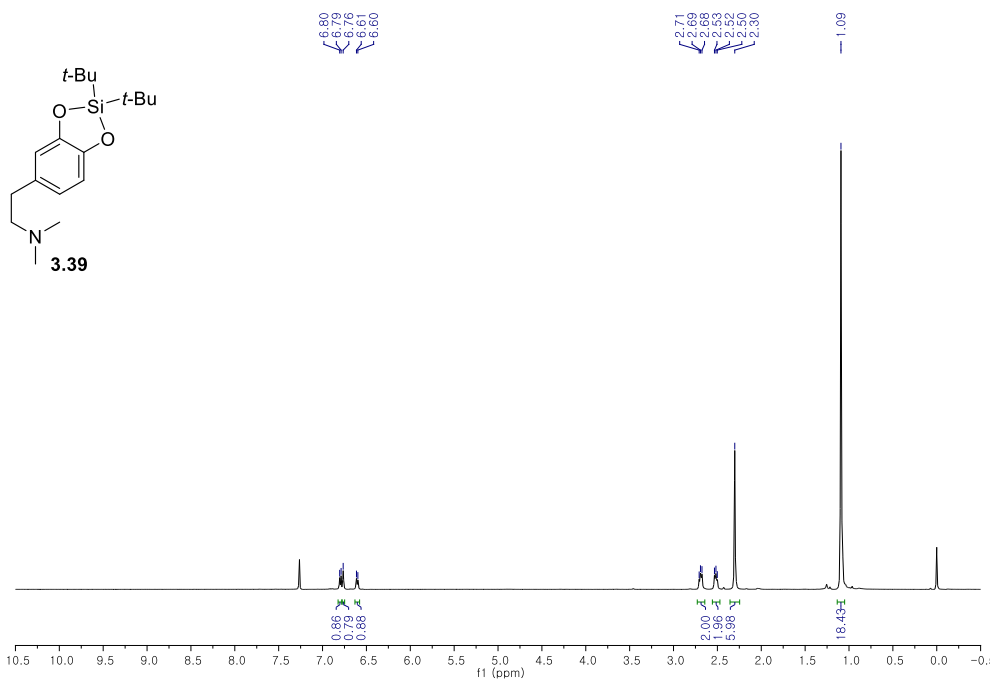


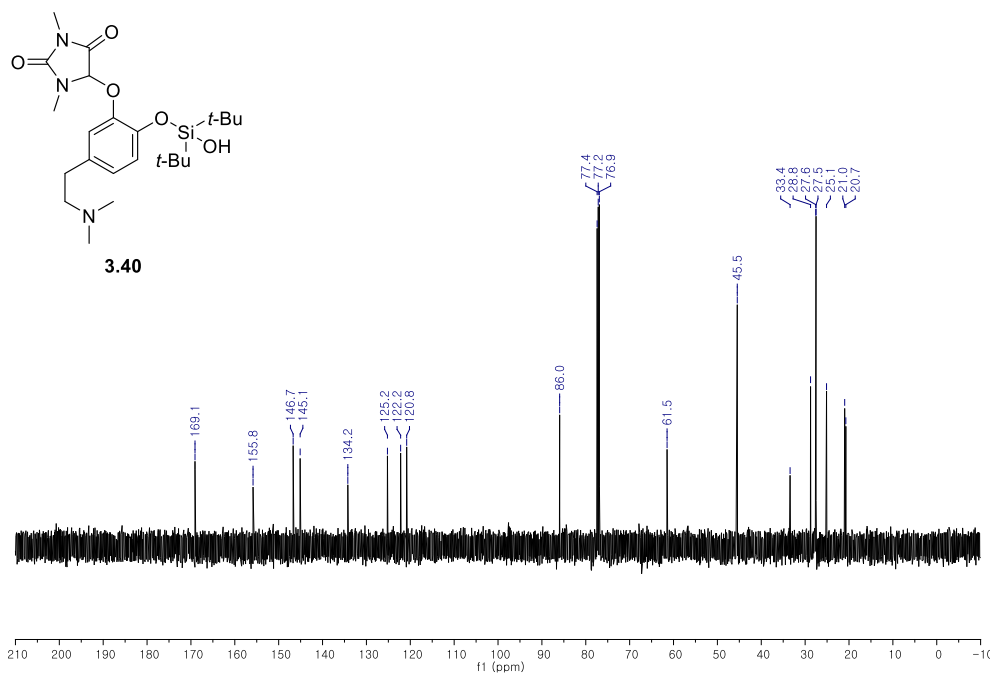
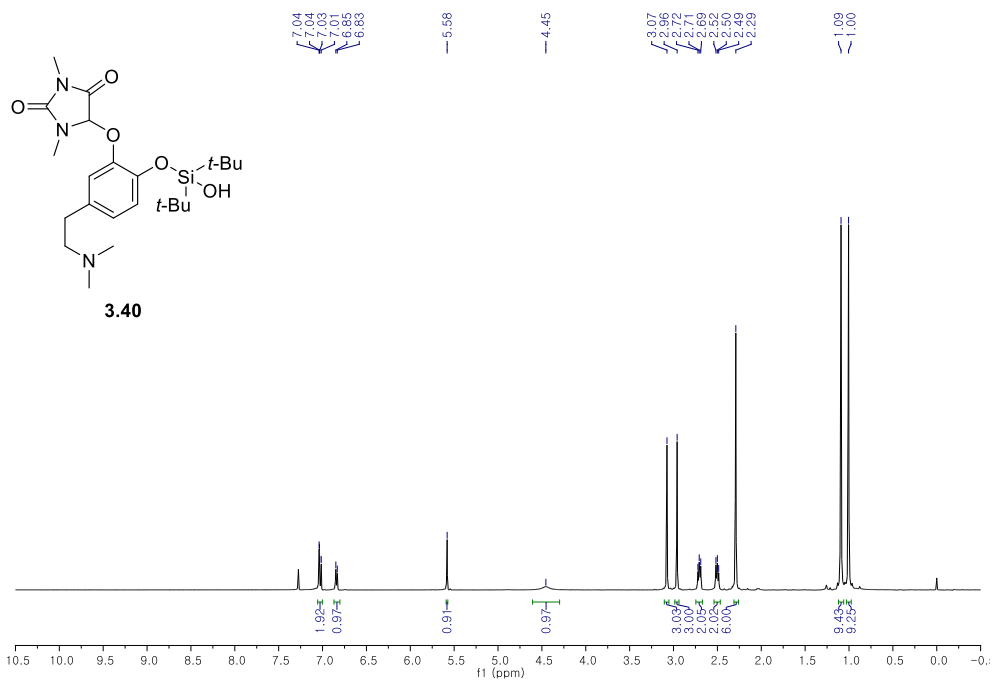


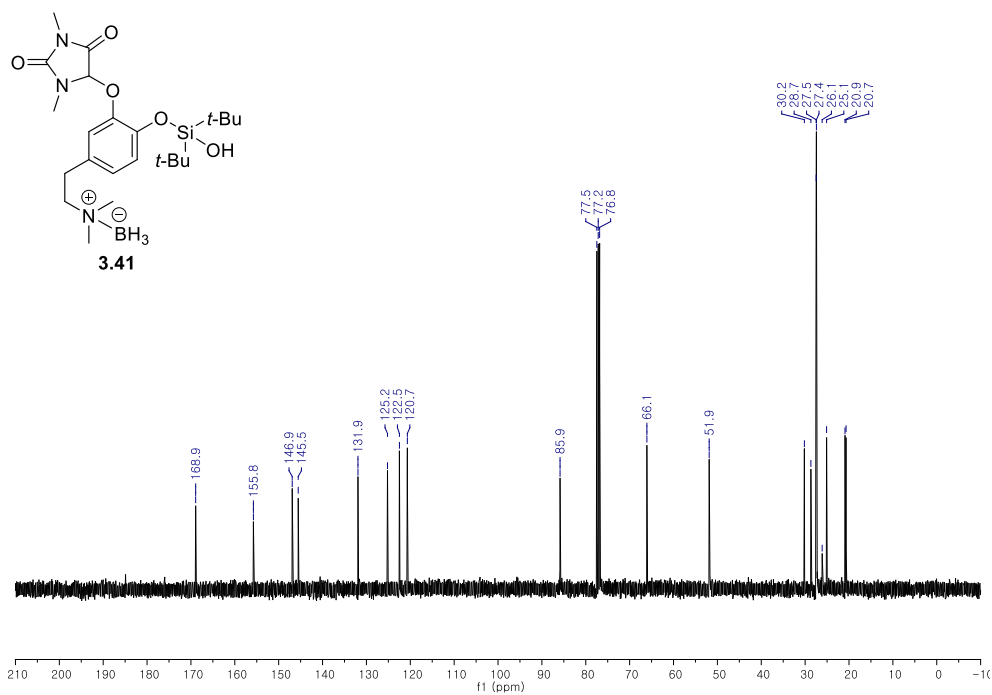
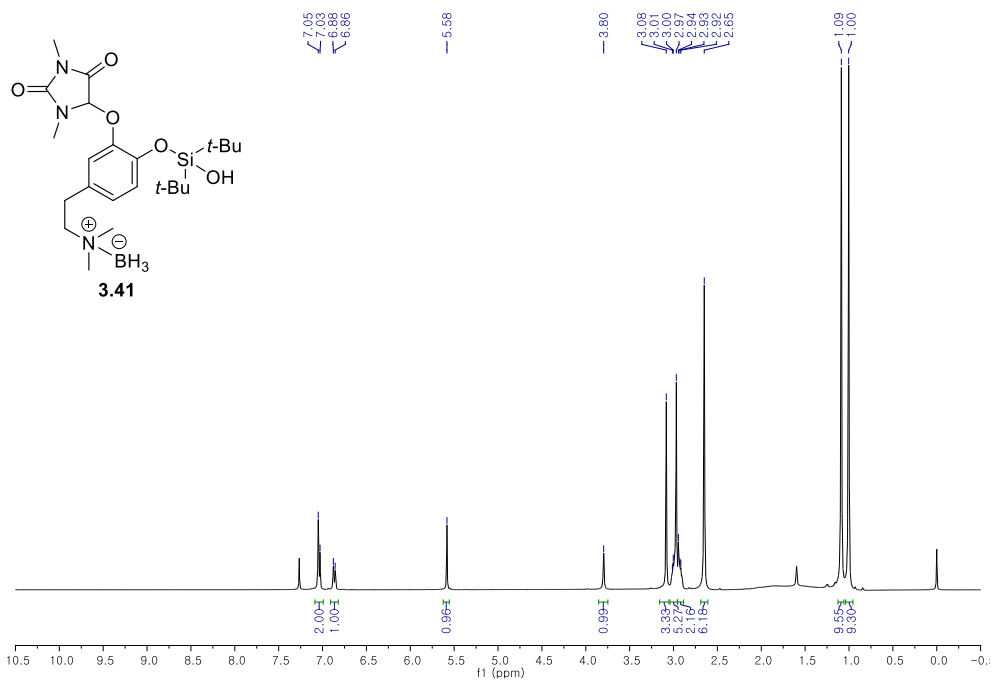


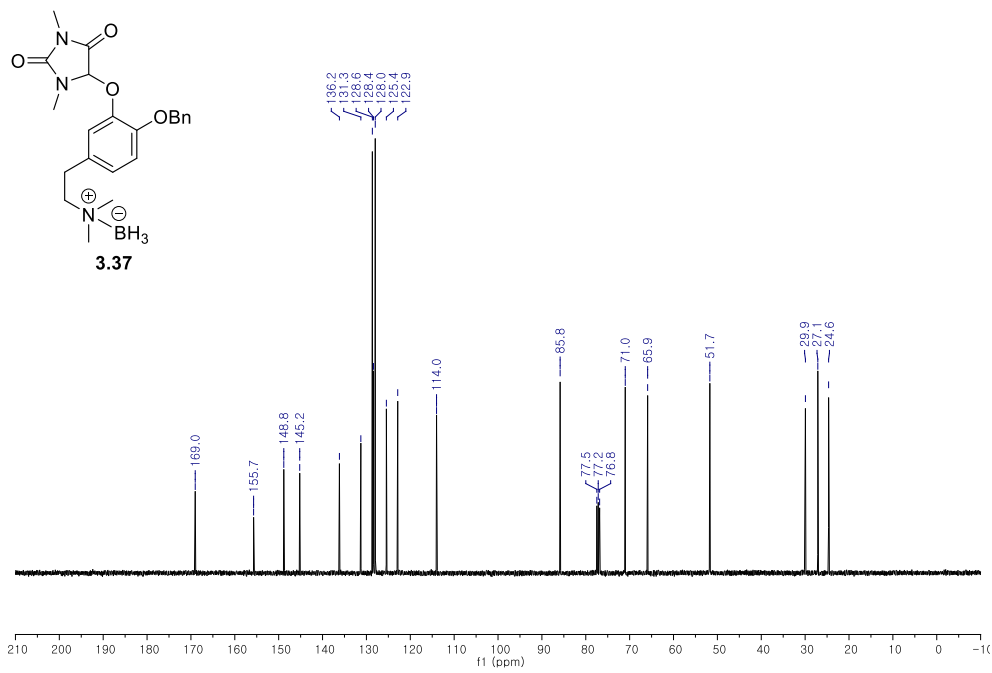
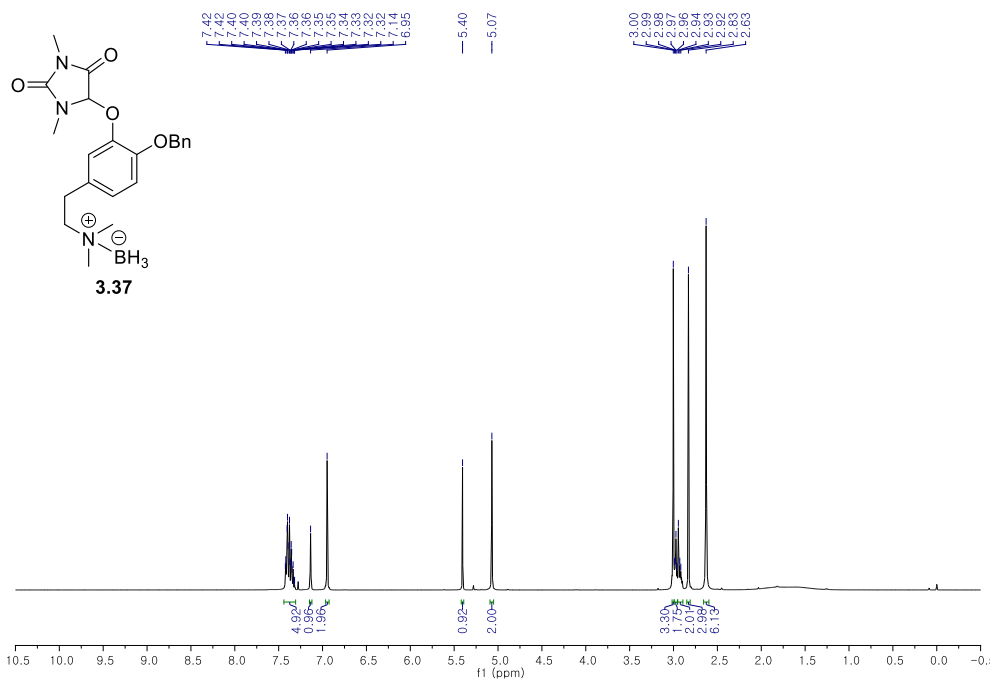


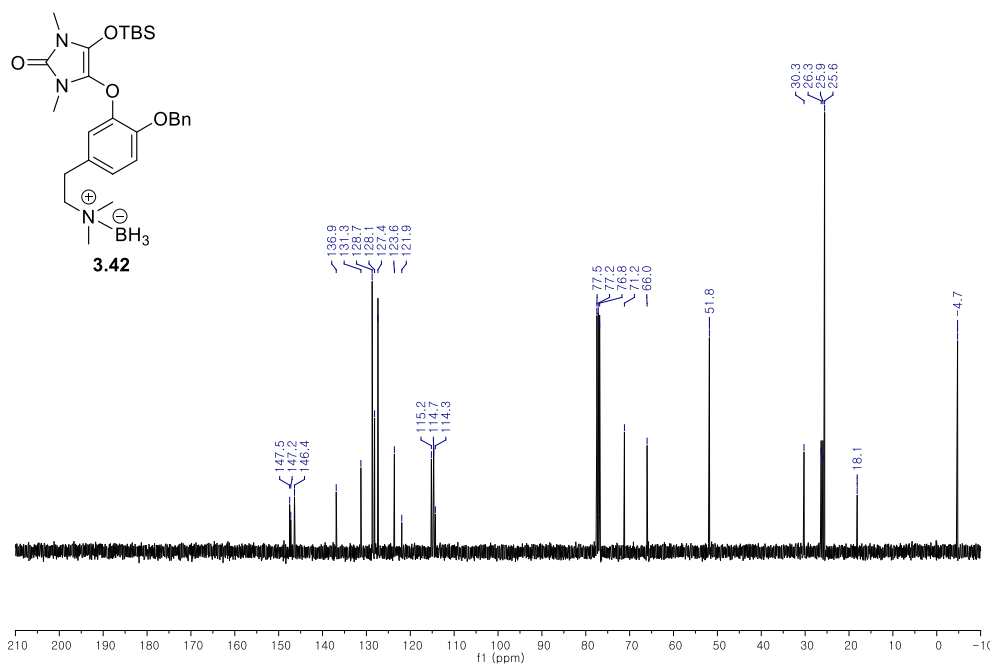
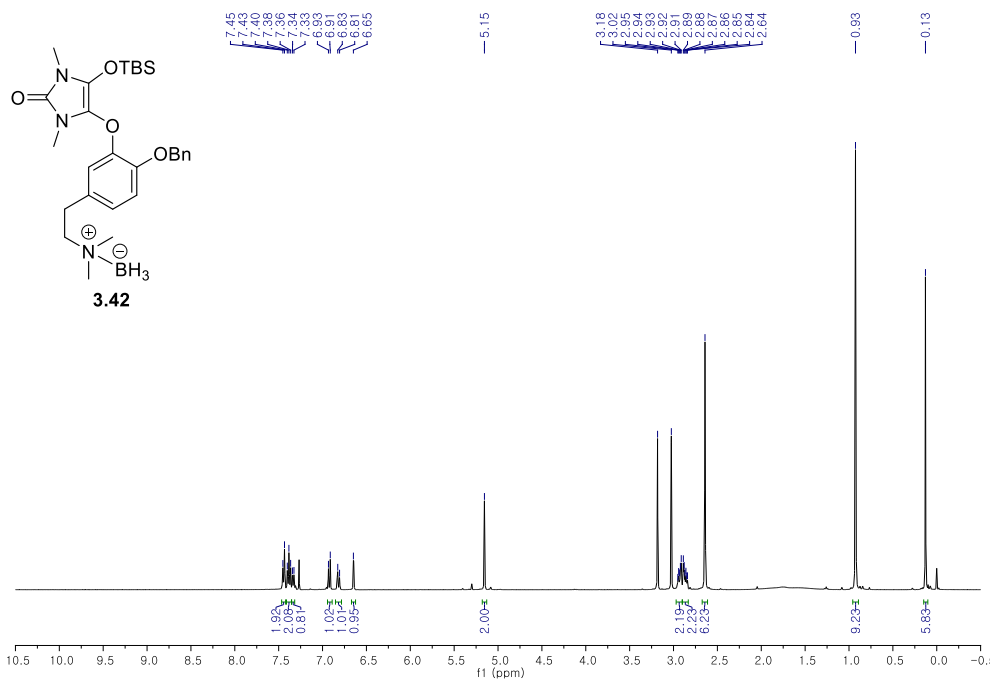


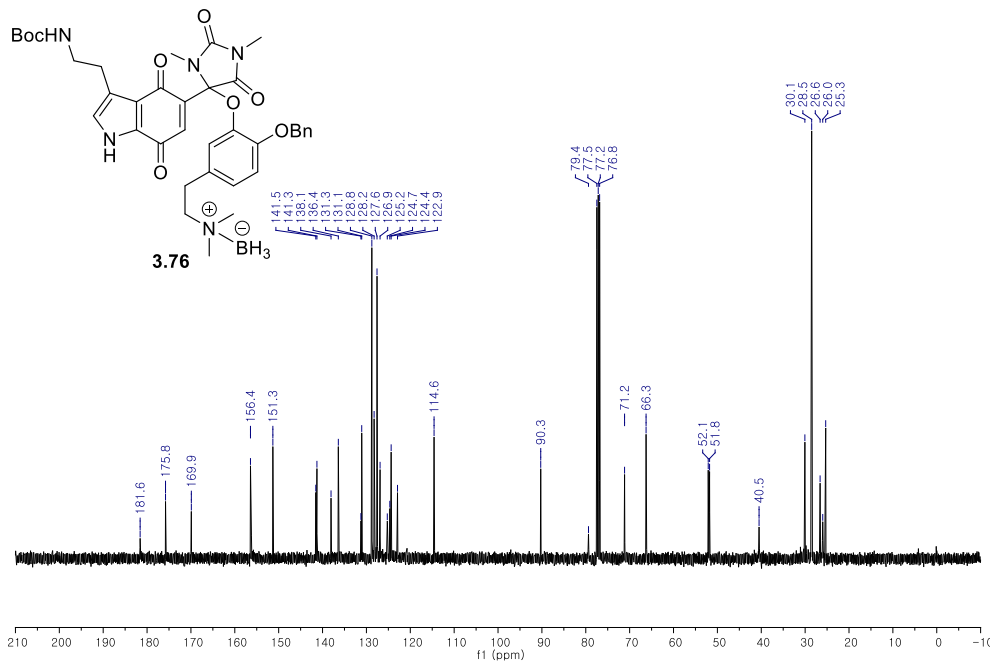
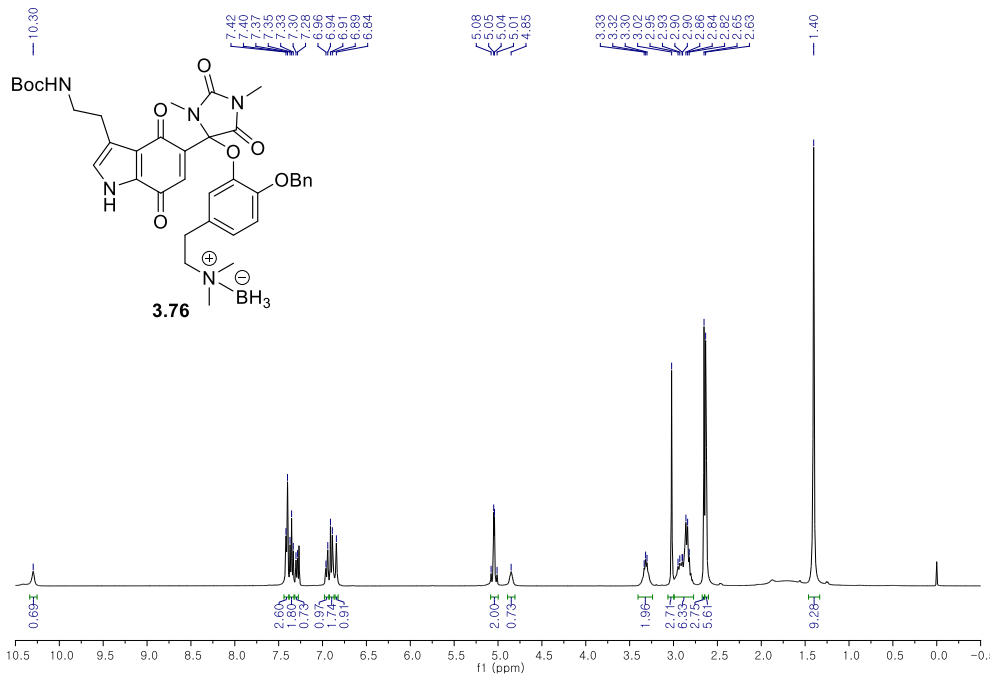


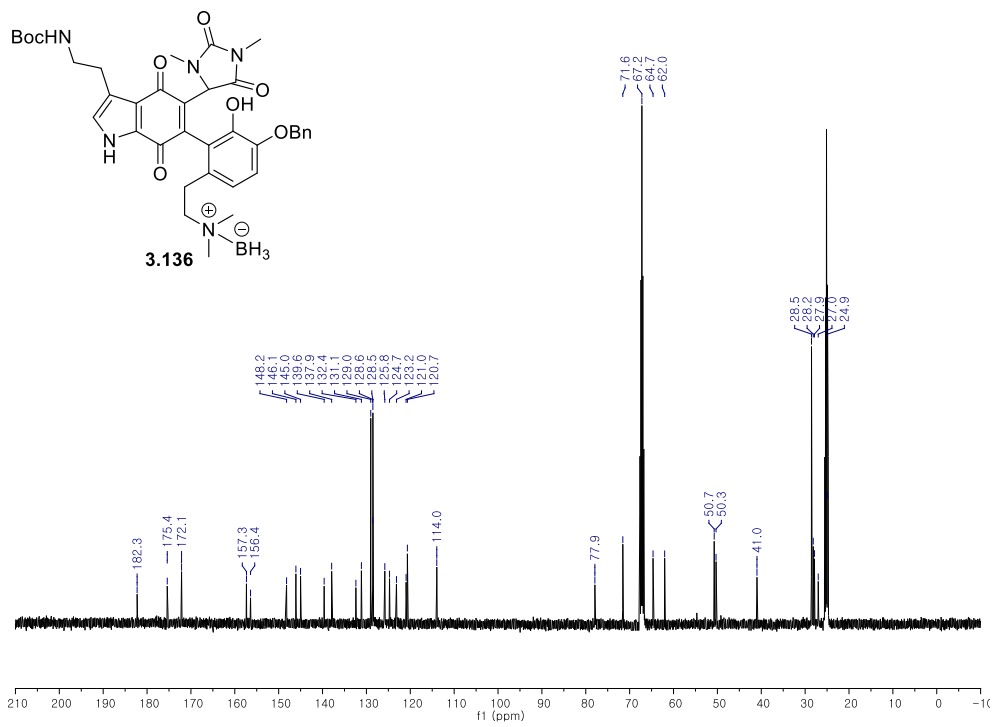
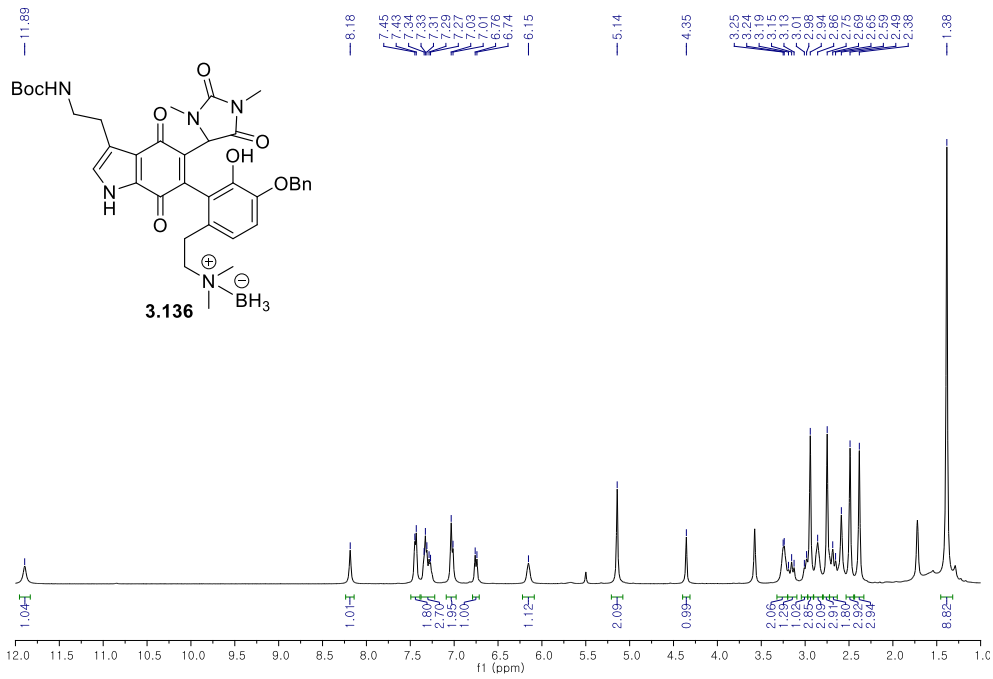


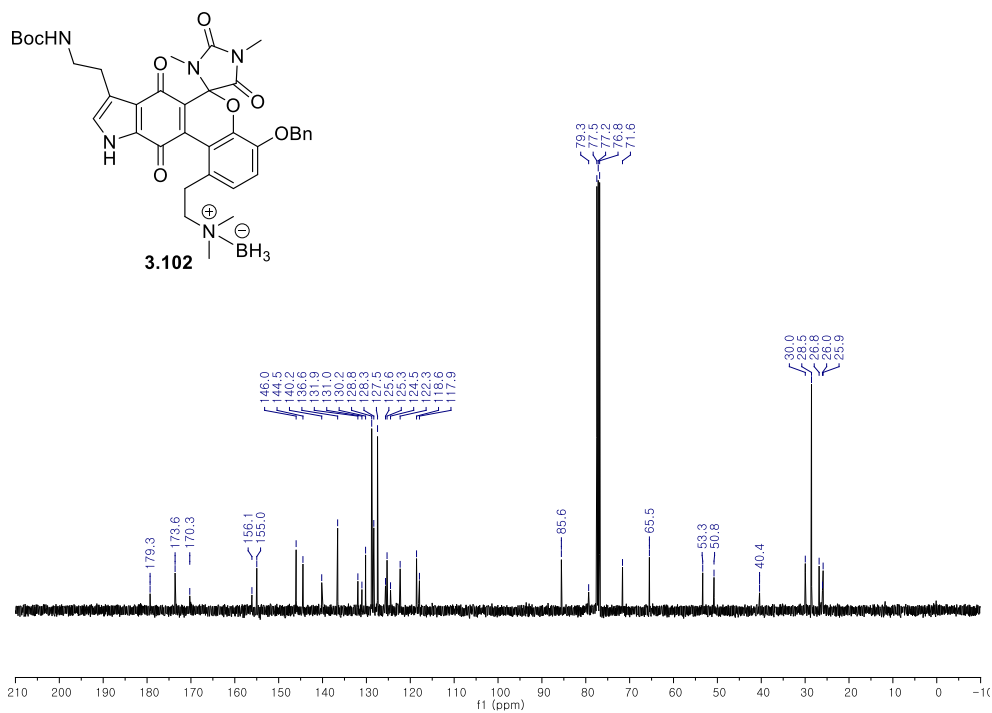
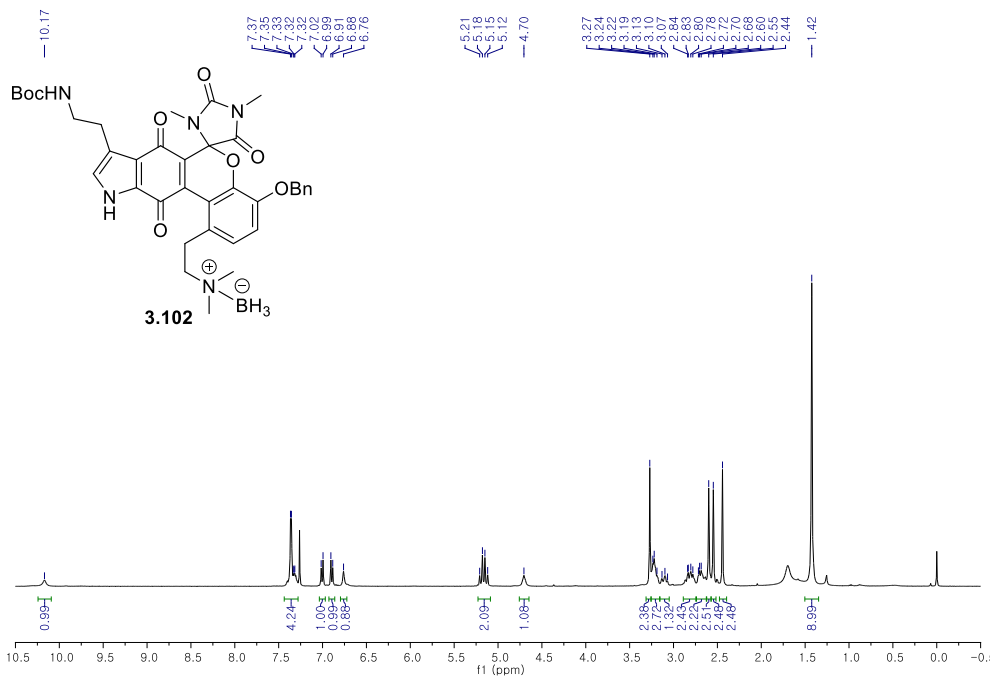


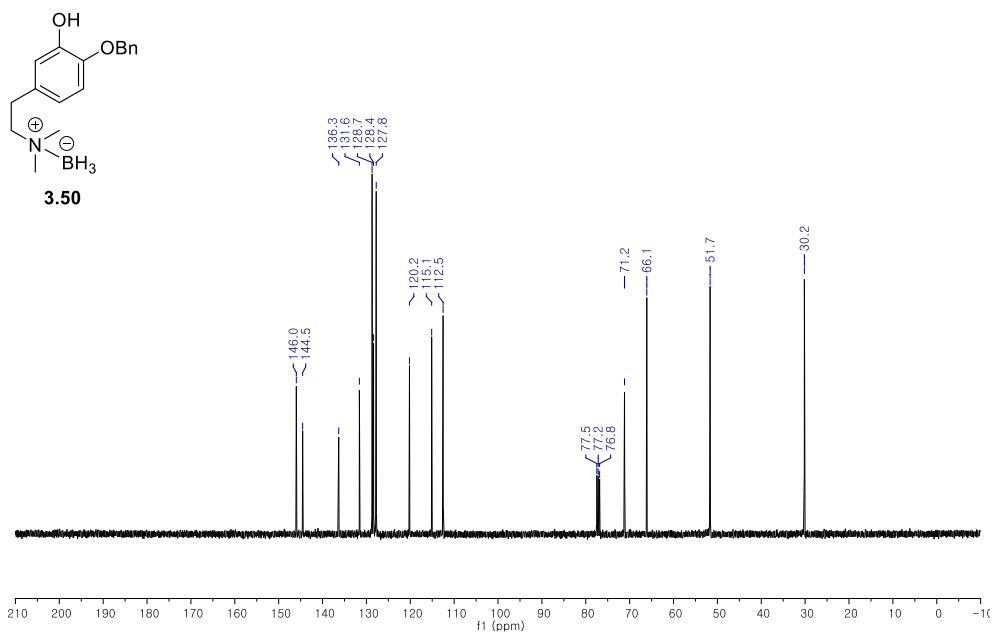
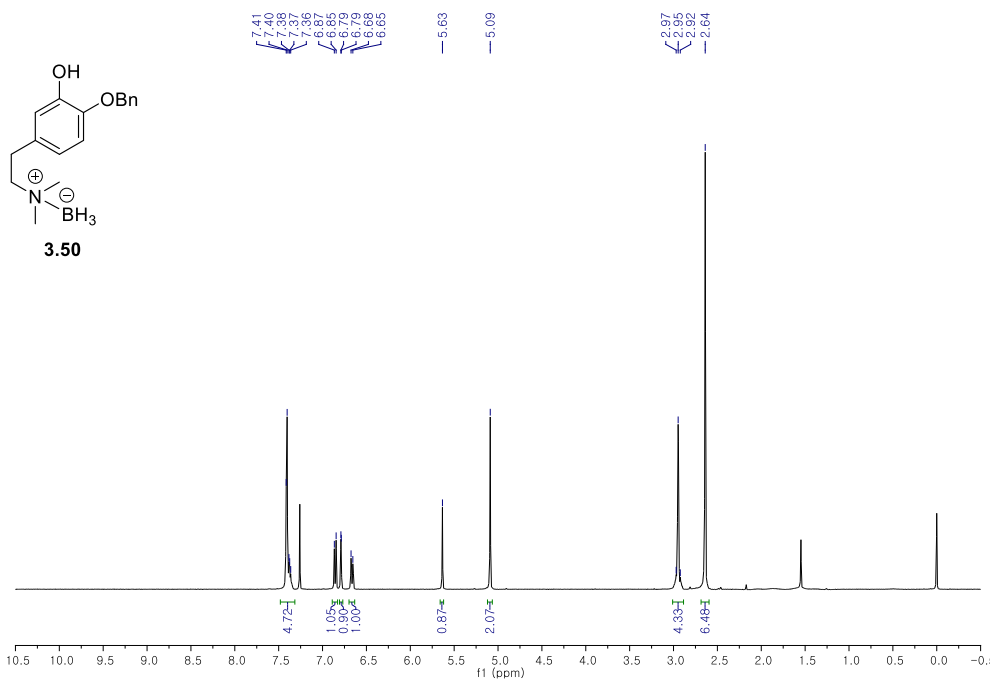


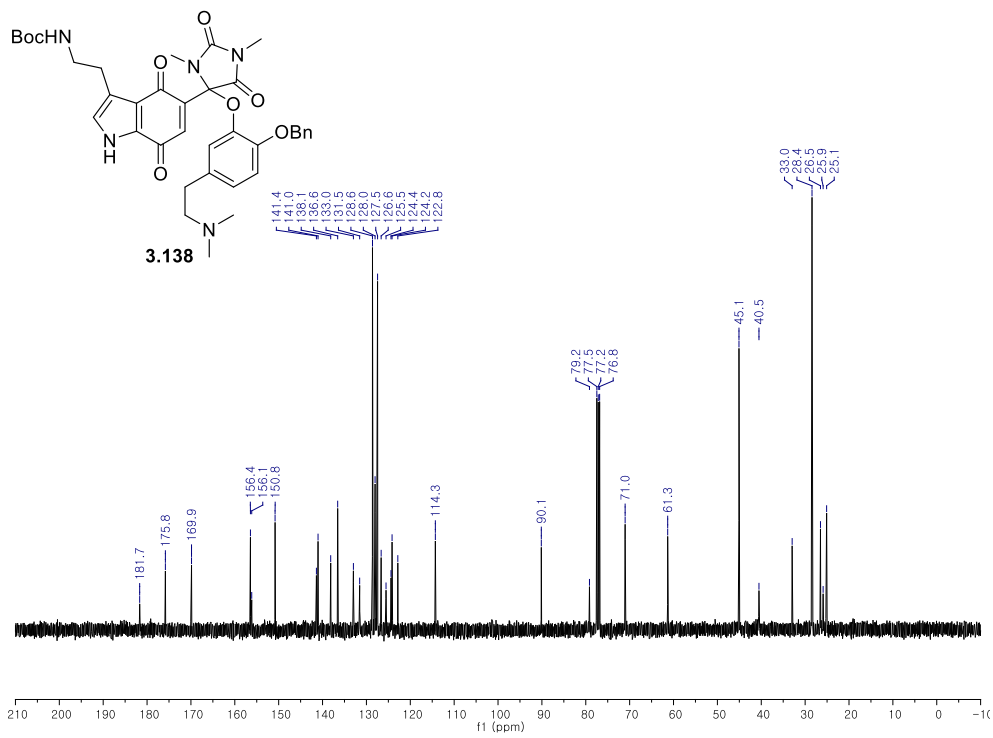
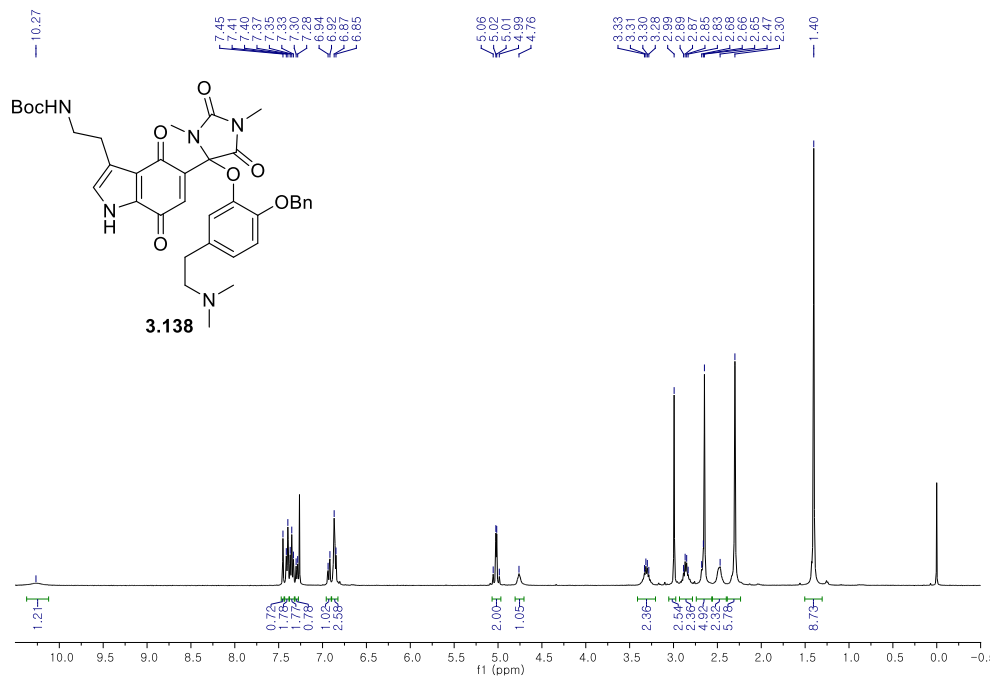


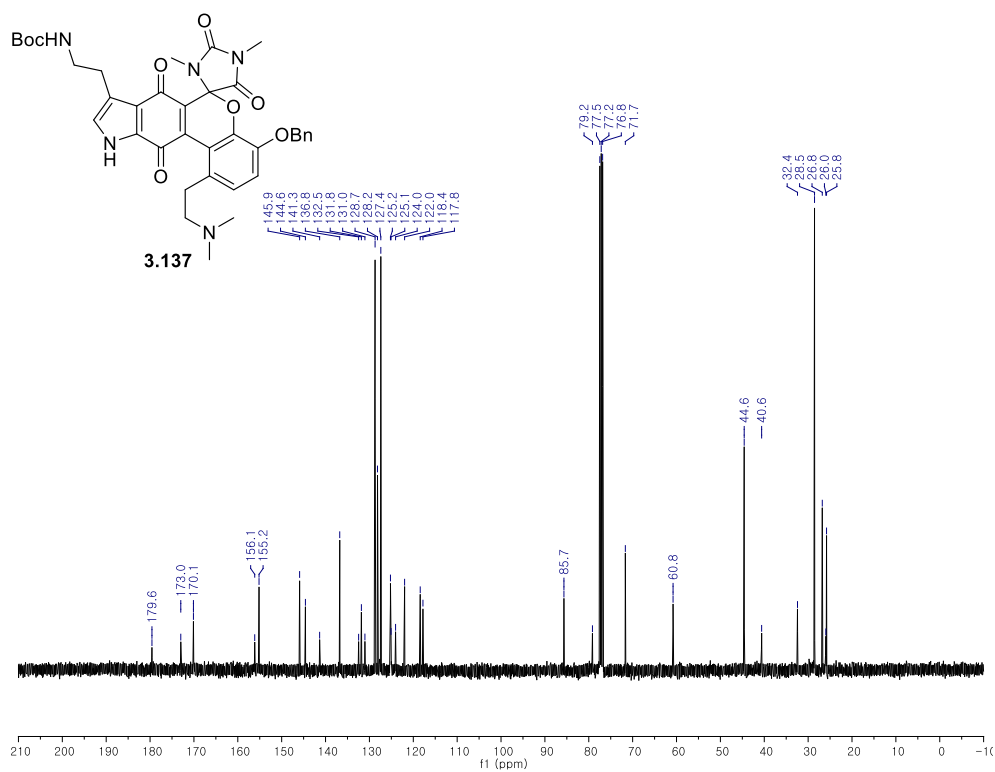
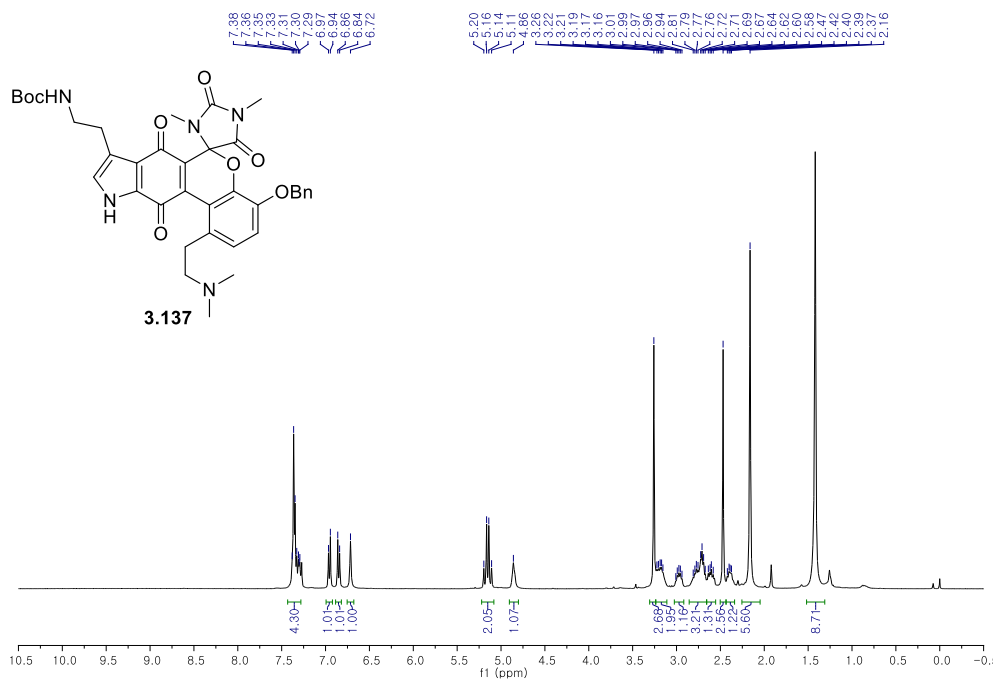


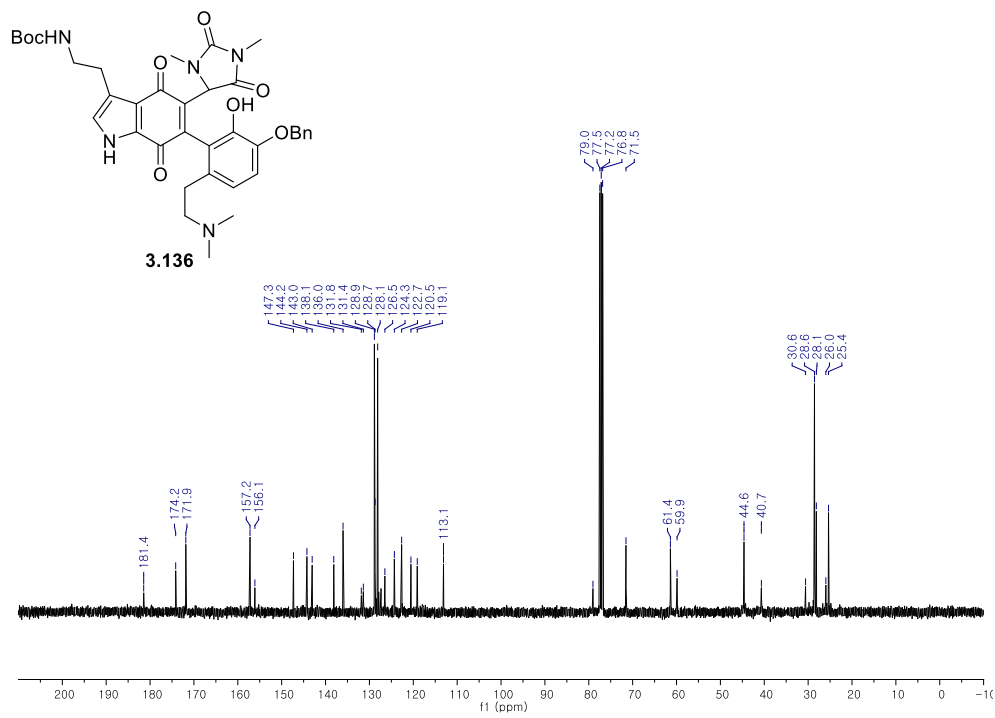
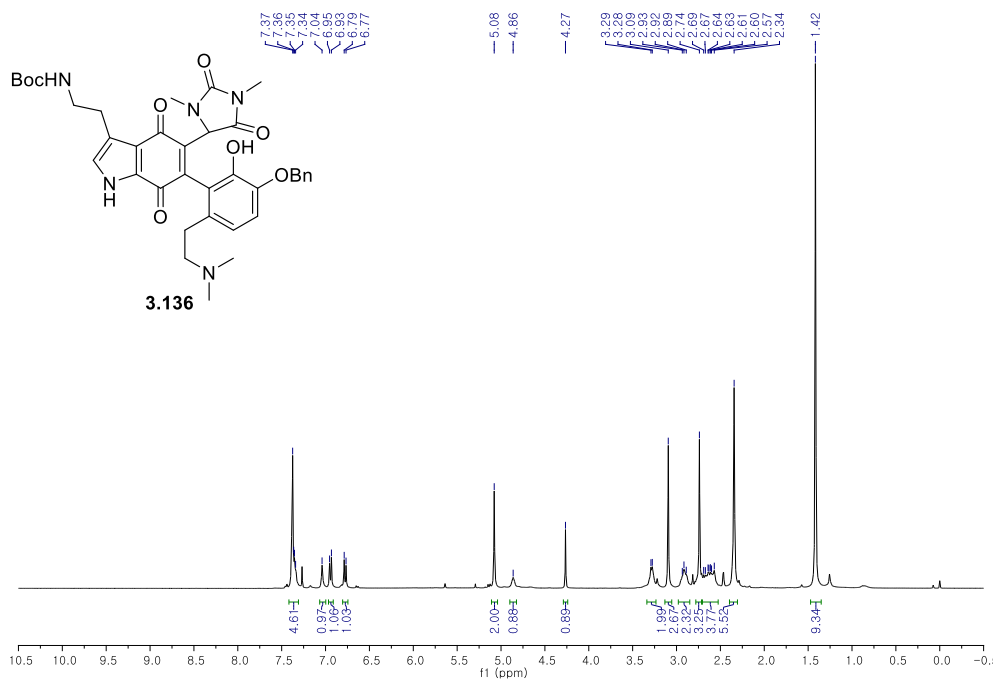


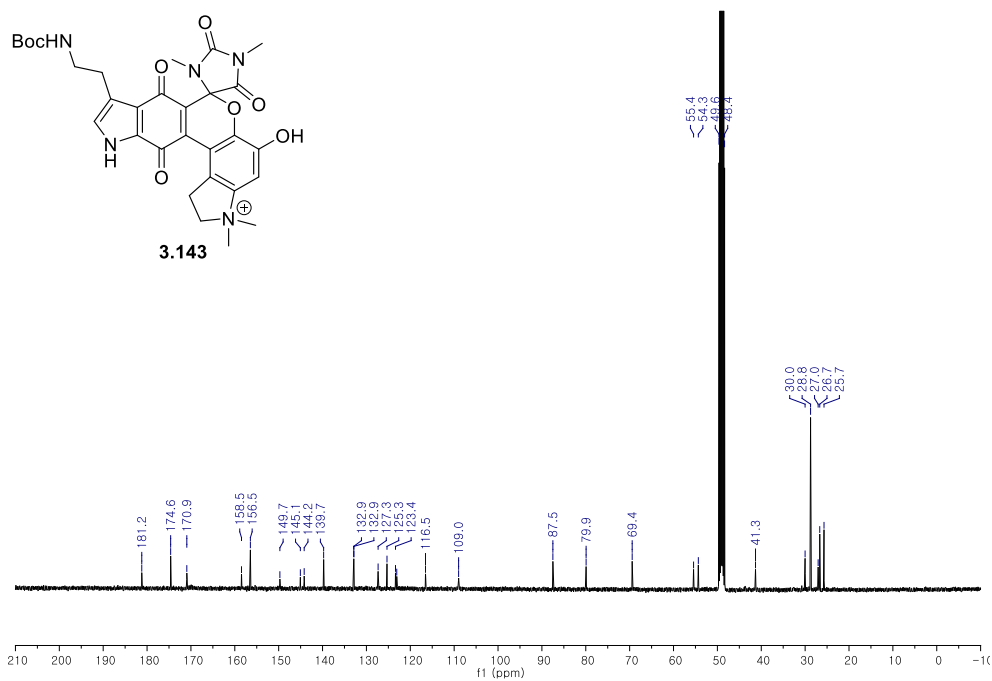
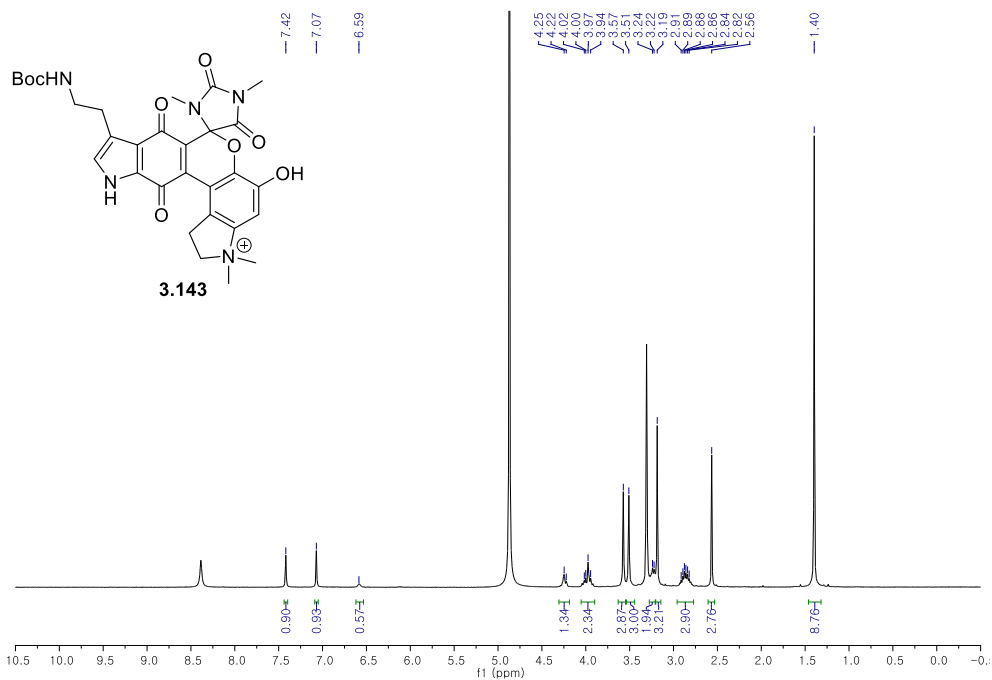


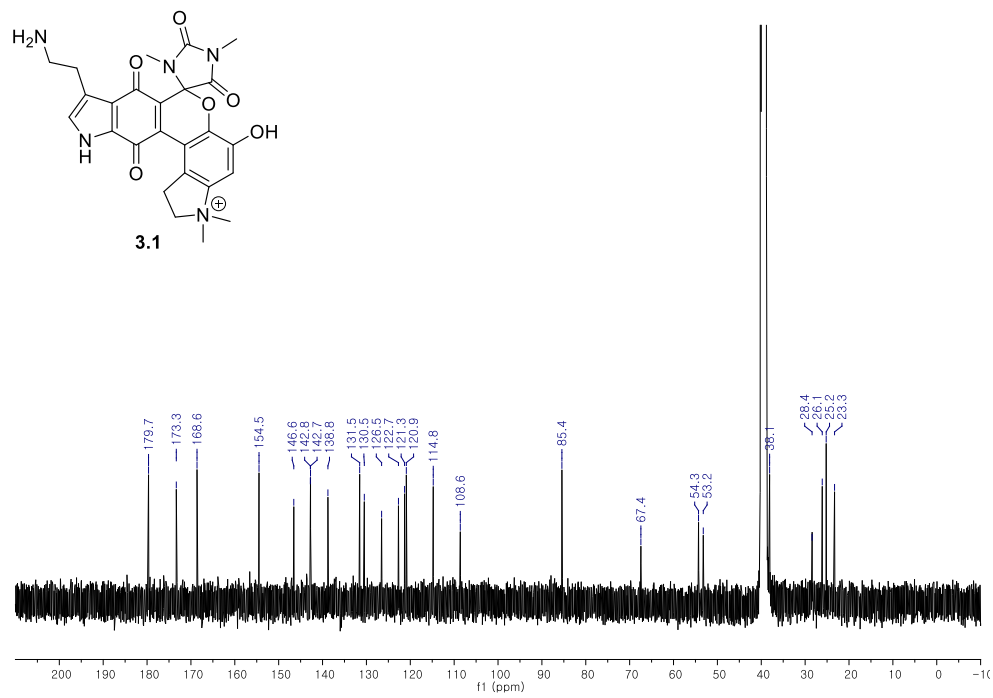
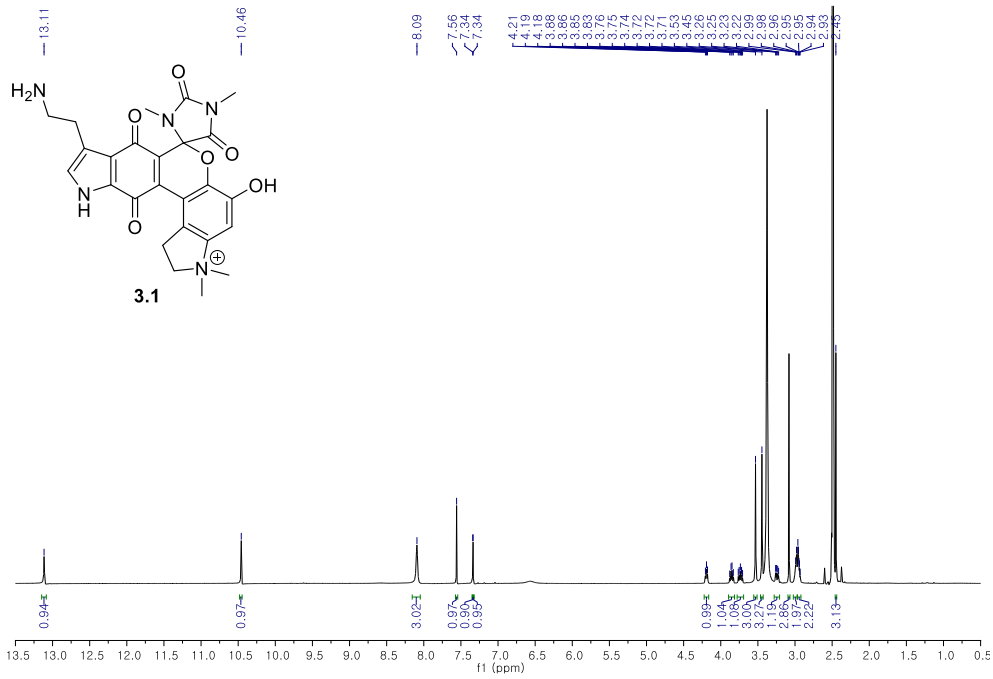


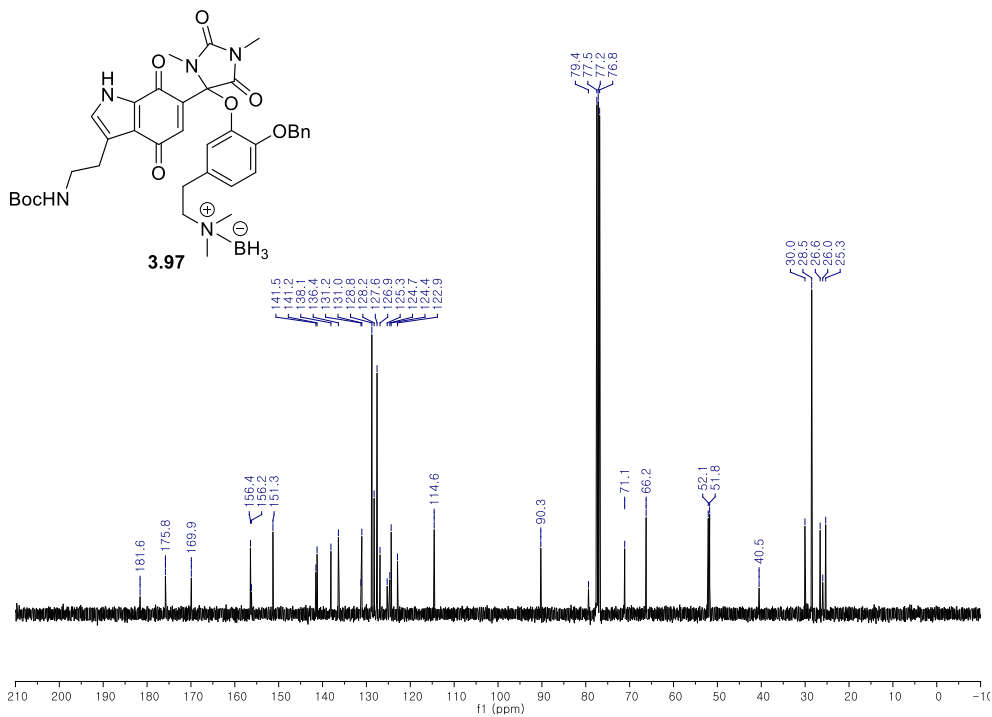
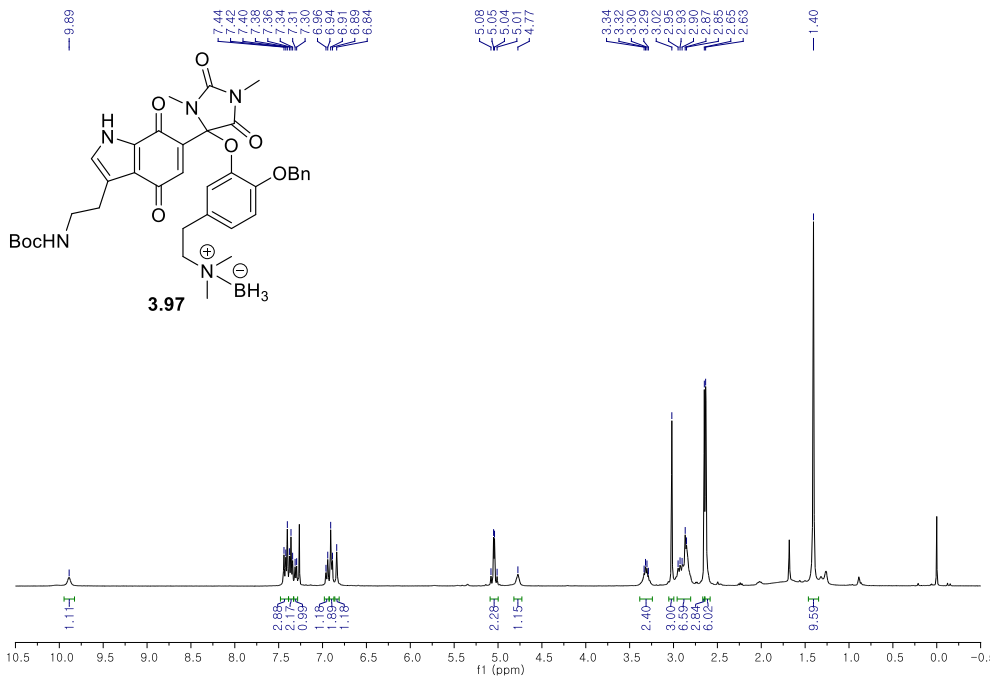


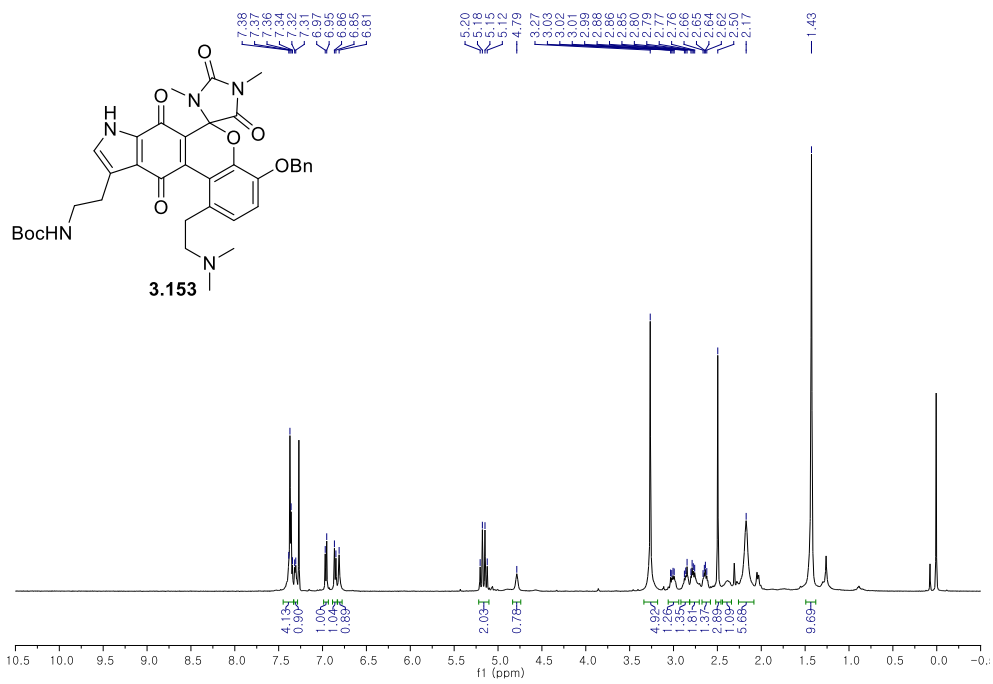
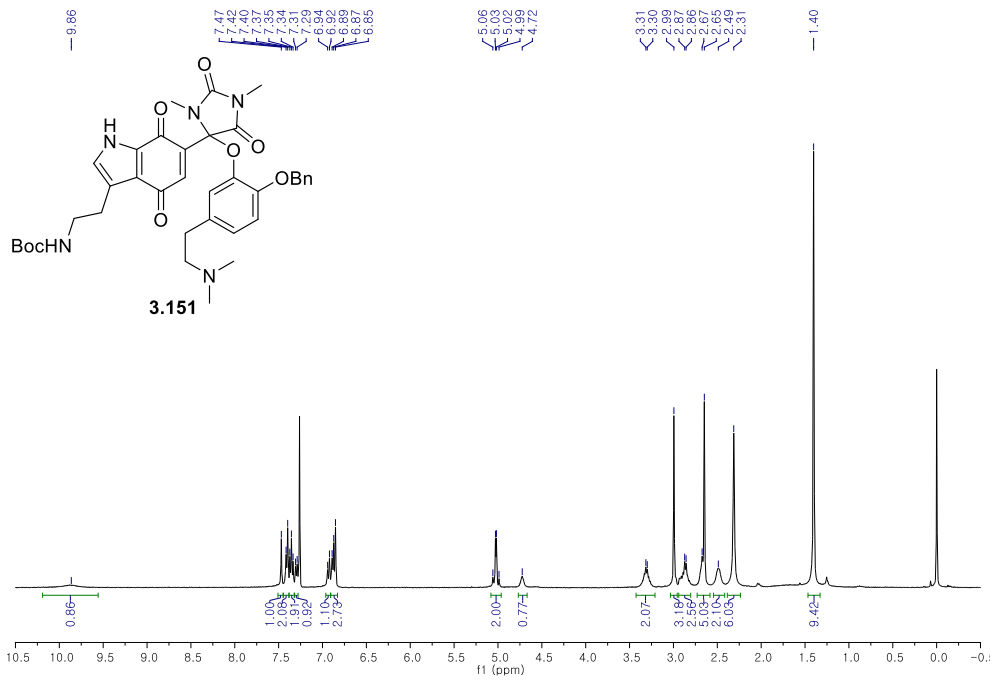


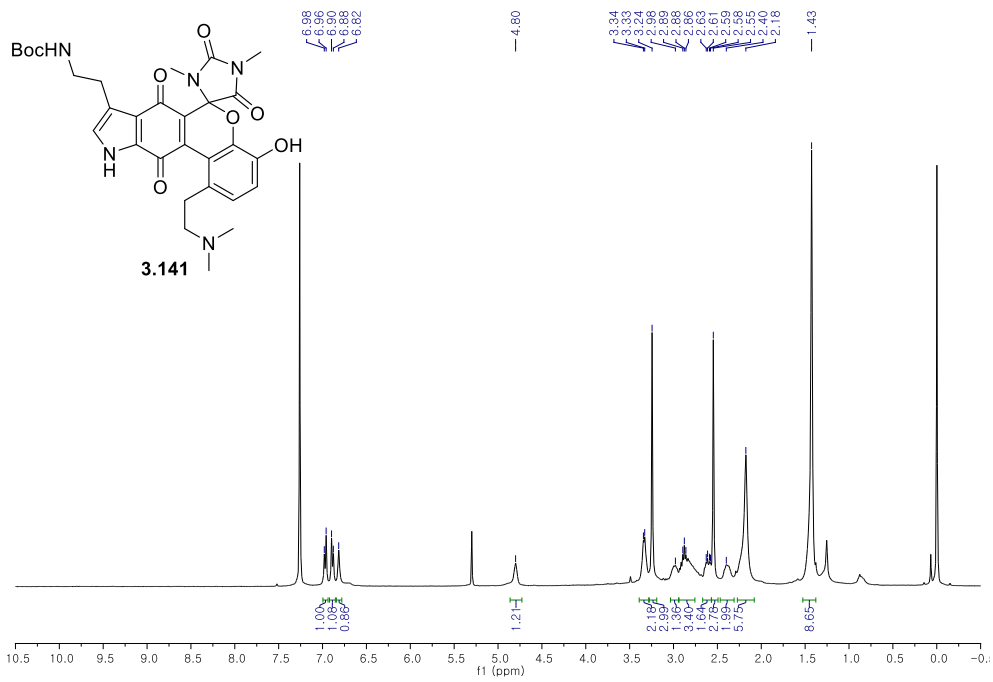
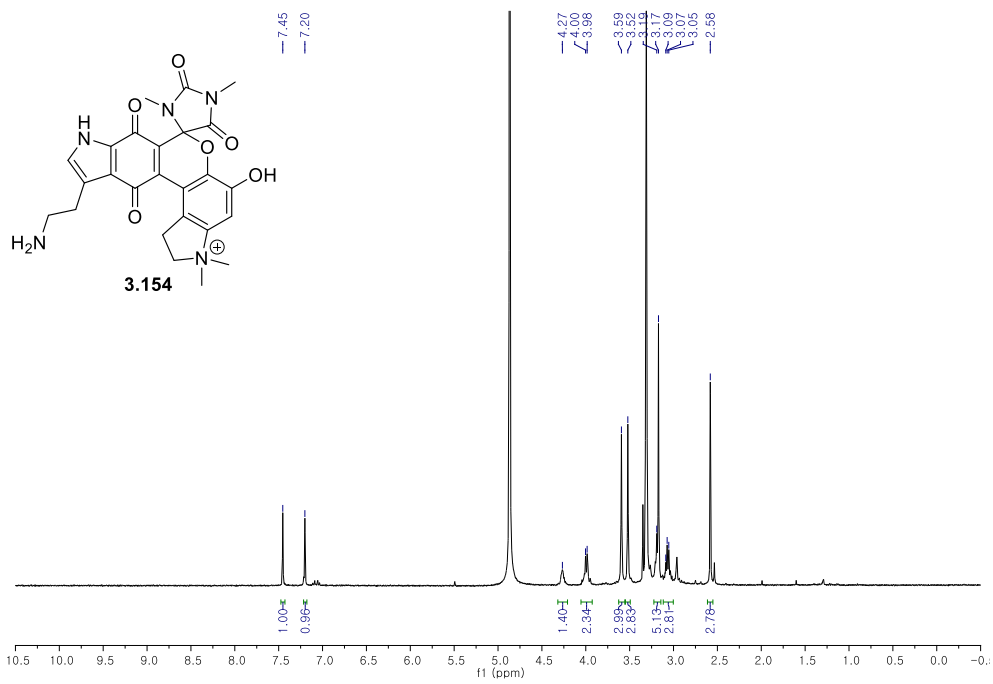


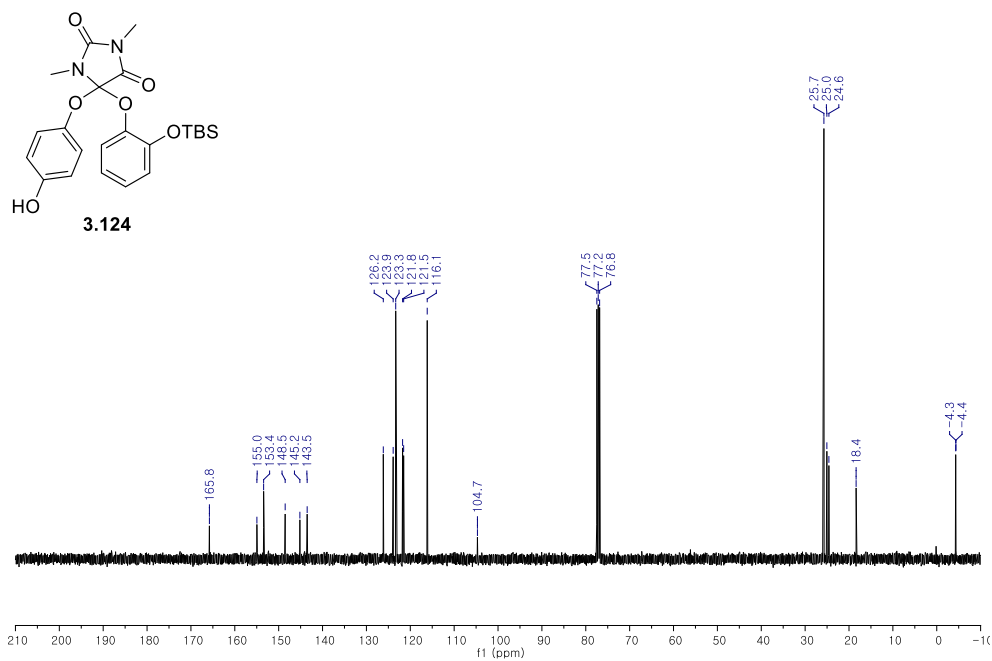
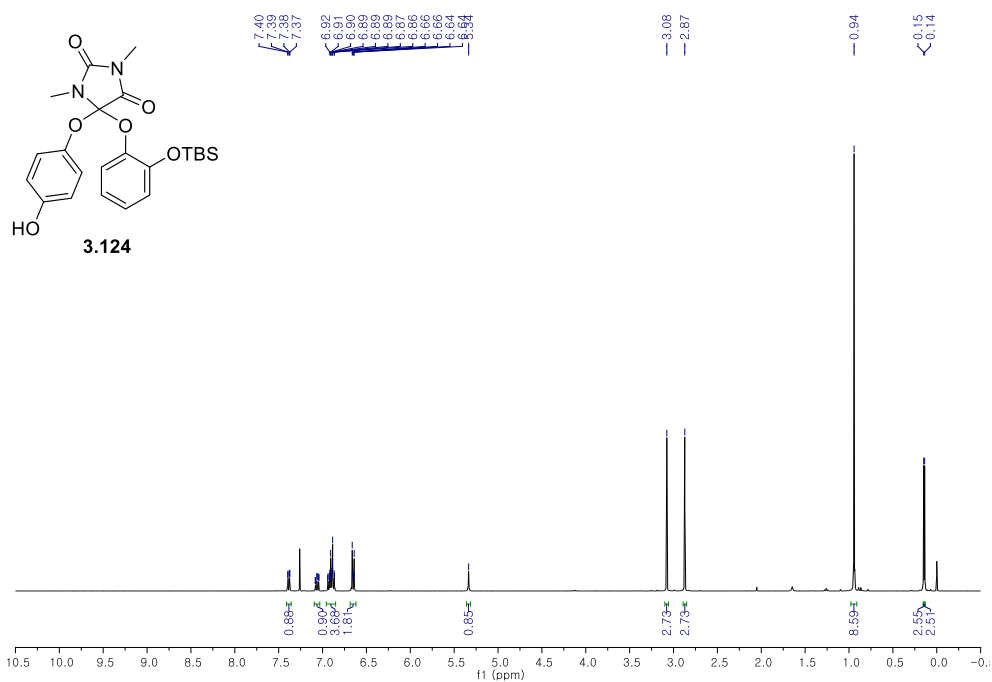


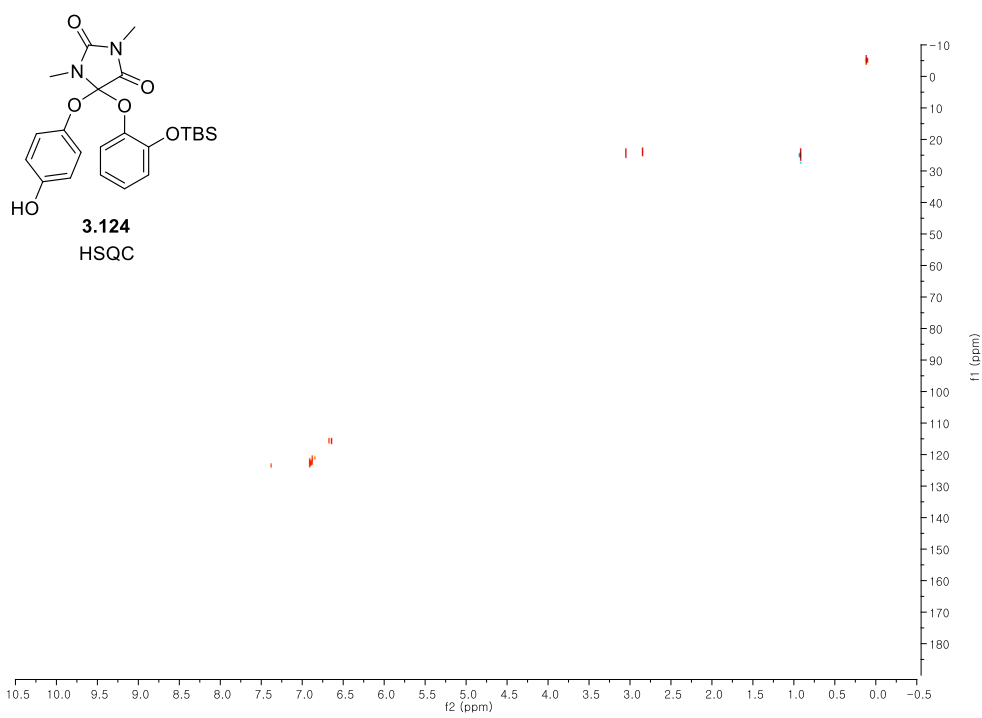
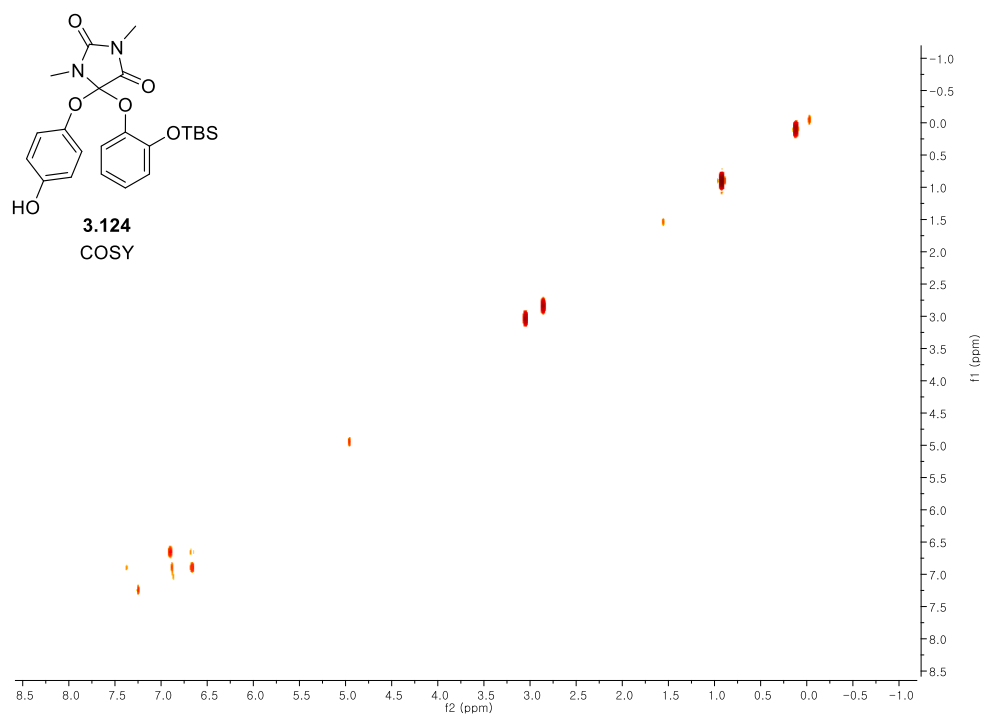


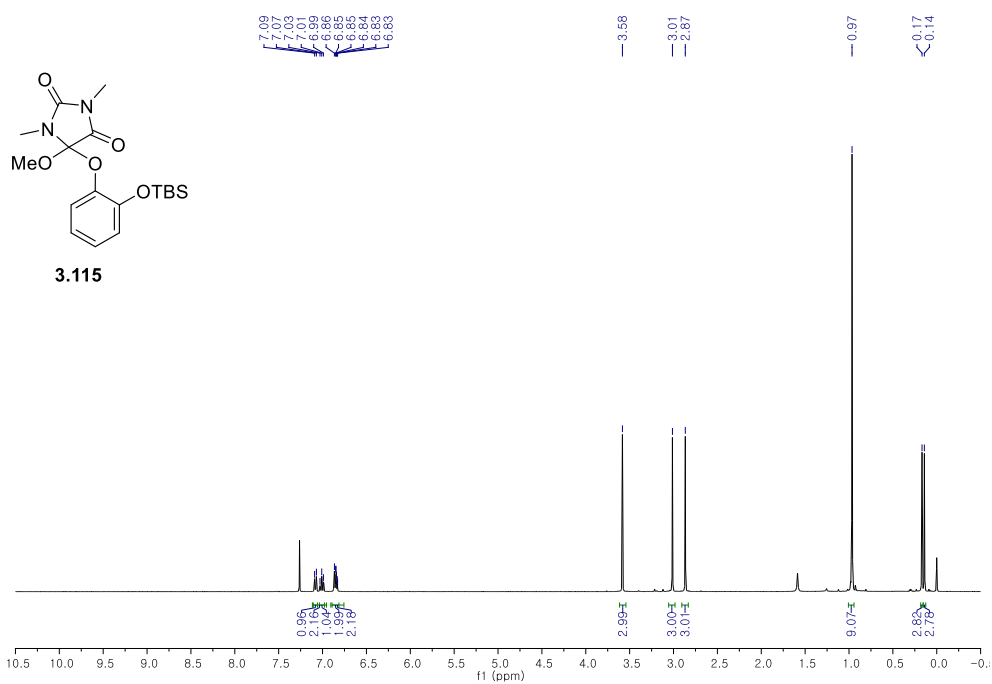
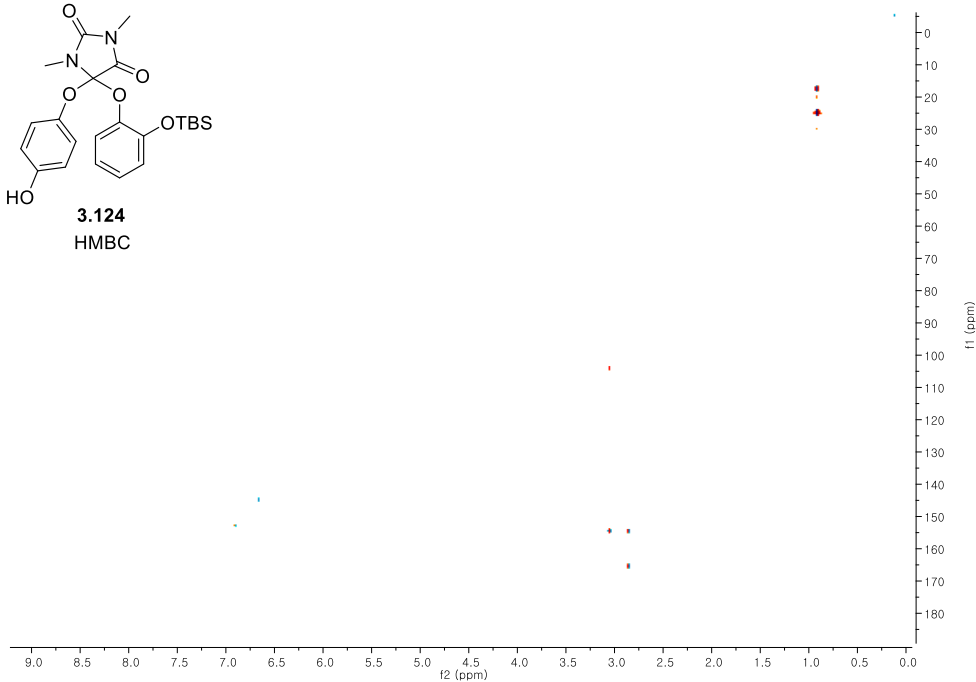
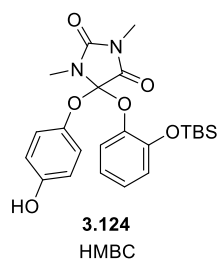


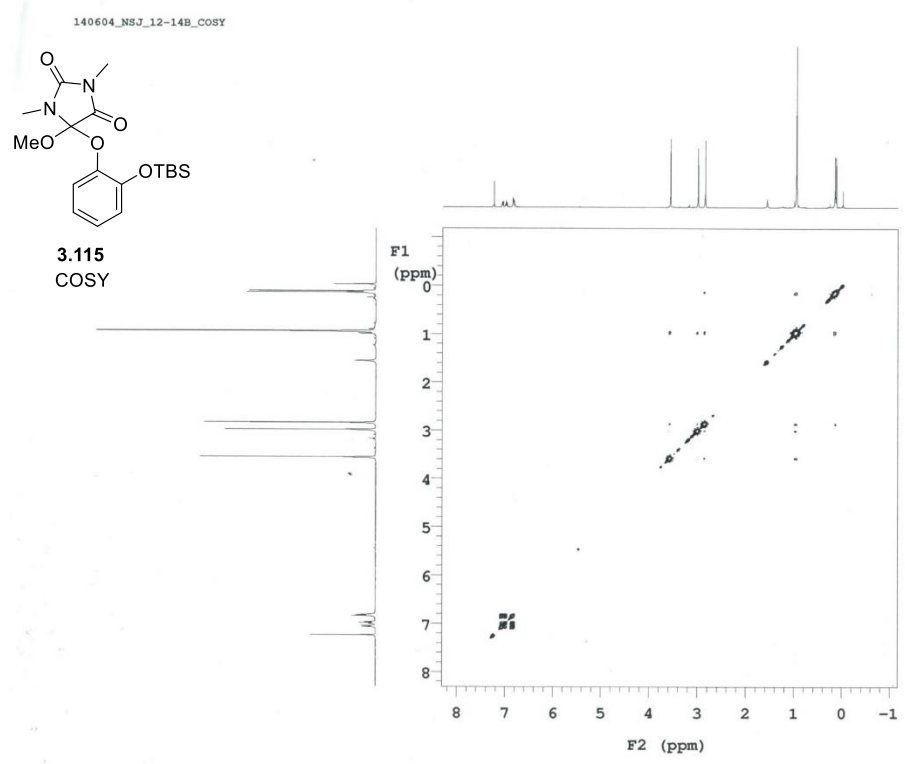
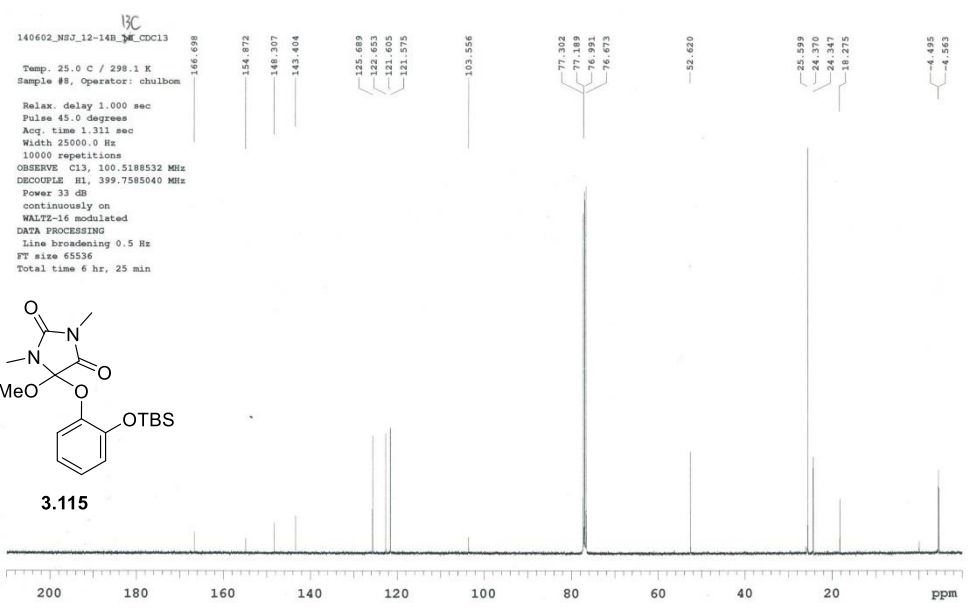




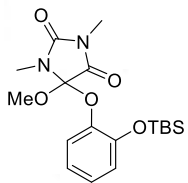




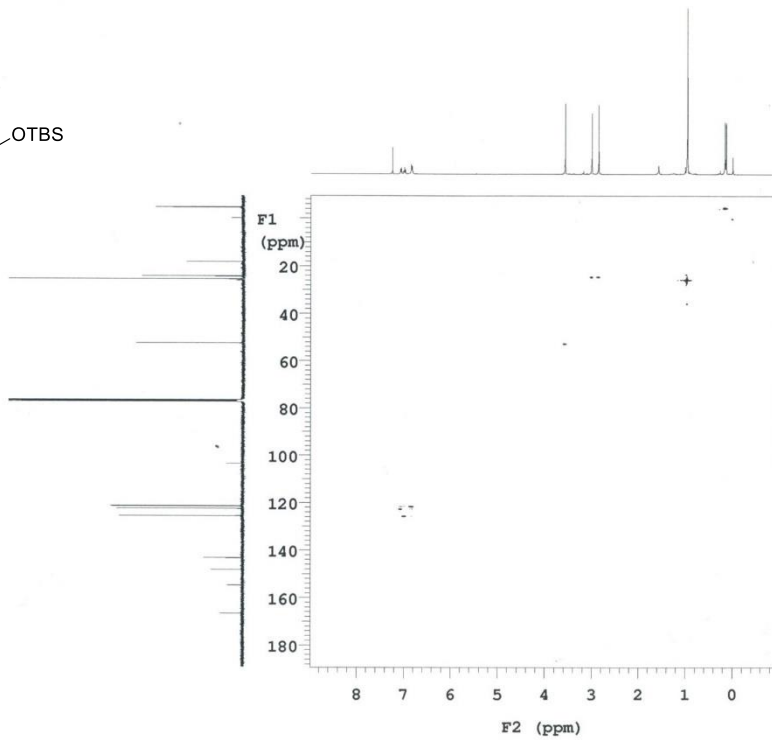




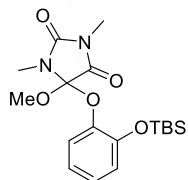
140604_NSJ_12-14B_HSQC



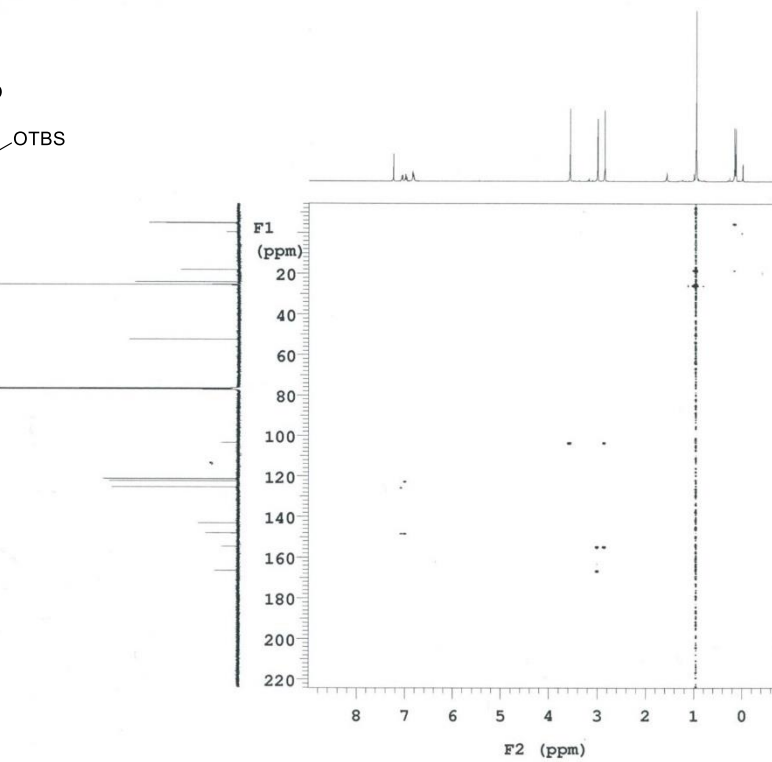
3.115
HSQC



140604_NSJ_12-14B_HMBC_CDCl3



3.115
HMBC



Appendix B

X-ray data of 3.76

Comments

X-ray crystallographic analysis was performed at the Western Seoul Center of Korea

Basic Science Institute by Dr. Ha Jin Lee.

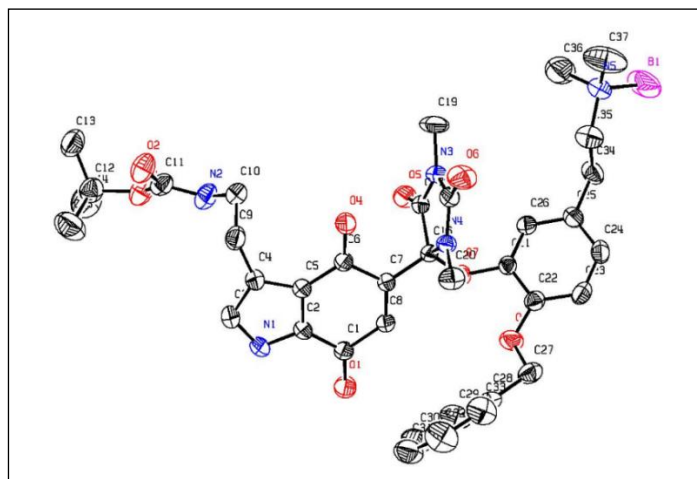


Figure 1. ORTEP Diagram of **3.76**

Table 1. Crystal data and structure refinement for **3.76**.

Empirical formula	$C_{37}H_{46}BN_5O_8, CH_3OH$
Formula weight	730.63
Temperature	223(2) K
Wavelength	1.54178 Å
Crystal system	Monoclinic
Space group	P2(1)/n
Unit cell dimensions	$a = 19.3940(9)$ Å $\alpha = 90^\circ$. $b = 9.8252(4)$ Å $\beta = 112.079(2)^\circ$. $c = 22.0809(9)$ Å $\gamma = 90^\circ$.
Volume	$3898.9(3)$ Å ³

Z	4
Density (calculated)	1.245 Mg/m ³
Absorption coefficient	0.727 mm ⁻¹
F(000)	1556
Crystal size	0.18 x 0.14 x 0.10 mm ³
Theta range for data collection	2.59 to 77.89°.
Index ranges	-24<=h<=24, -12<=k<=12, -27<=l<=26
Reflections collected	122935
Independent reflections	7620 [R(int) = 0.0679]
Completeness to theta = 77.89°	91.4 %
Absorption correction	Semi-empirical from equivalents
Max. and min. transmission	0.9308 and 0.8802
Refinement method	Full-matrix least-squares on F ²
Data / restraints / parameters	7620 / 0 / 487
Goodness-of-fit on F ²	1.105
Final R indices [I>2sigma(I)]	R1 = 0.0892, wR2 = 0.2792
R indices (all data)	R1 = 0.1070, wR2 = 0.2931
Largest diff. peak and hole	1.382 and -0.535 e.Å ⁻³

Table 2. Atomic coordinates (x 10⁴) and equivalent isotropic displacement parameters (Å²x 10³) for **3.76**. U(eq) is defined as one third of the trace of the orthogonalized U^{ij} tensor.

	x	y	z	U(eq)
C(1)	10114(2)	4167(4)	2886(2)	38(1)
C(2)	9399(2)	4764(4)	2788(2)	35(1)

N(1)	8936(2)	4429(4)	3095(2)	43(1)
C(3)	8327(2)	5263(4)	2870(2)	43(1)
C(4)	8391(2)	6149(4)	2411(2)	36(1)
C(5)	9078(2)	5820(4)	2354(2)	32(1)
C(6)	9441(2)	6360(4)	1944(2)	32(1)
C(7)	10170(2)	5720(4)	2015(2)	30(1)
C(8)	10474(2)	4730(4)	2451(2)	36(1)
O(1)	10415(2)	3278(4)	3281(2)	61(1)
C(9)	7842(2)	7216(4)	2044(2)	44(1)
C(10)	7427(2)	6874(5)	1322(2)	52(1)
N(2)	6928(2)	5730(4)	1218(2)	52(1)
C(11)	6233(2)	5892(4)	1190(2)	43(1)
O(2)	5952(2)	6988(3)	1214(2)	56(1)
O(3)	5886(2)	4690(3)	1120(2)	54(1)
C(12)	5173(3)	4548(5)	1208(2)	54(1)
C(13)	4566(3)	5384(6)	702(3)	65(1)
C(14)	5020(4)	3032(6)	1095(4)	88(2)
C(15)	5281(4)	4953(8)	1894(3)	85(2)
O(4)	9187(2)	7276(3)	1544(2)	49(1)
C(16)	10530(2)	6235(3)	1560(2)	29(1)
C(17)	9981(2)	6211(4)	841(2)	34(1)
N(3)	9994(2)	7467(3)	593(2)	38(1)
C(18)	10410(2)	8366(4)	1088(2)	38(1)
N(4)	10736(2)	7650(3)	1648(2)	31(1)
O(5)	9639(2)	5224(3)	558(1)	48(1)

C(19)	9550(3)	7874(6)	-71(2)	62(1)
O(6)	10463(2)	9581(3)	1021(2)	58(1)
C(20)	11124(2)	8303(4)	2268(2)	45(1)
O(7)	11138(1)	5345(2)	1629(1)	33(1)
C(21)	11704(2)	5867(3)	1456(2)	30(1)
C(22)	12383(2)	6141(4)	1968(2)	36(1)
C(23)	12976(2)	6579(4)	1809(2)	41(1)
C(24)	12892(2)	6735(4)	1165(2)	41(1)
C(25)	12221(2)	6463(4)	656(2)	37(1)
C(26)	11627(2)	6017(4)	817(2)	34(1)
O(8)	12393(2)	5900(3)	2578(1)	47(1)
C(27)	12920(2)	6596(5)	3129(2)	46(1)
C(28)	12593(2)	6603(4)	3645(2)	42(1)
C(29)	12255(3)	5452(5)	3772(2)	57(1)
C(30)	11920(3)	5484(5)	4220(3)	61(1)
C(31)	11930(3)	6646(6)	4568(3)	62(1)
C(32)	12262(3)	7786(6)	4451(3)	69(2)
C(33)	12582(3)	7769(5)	3985(3)	59(1)
C(34)	12115(3)	6641(5)	-54(2)	48(1)
C(35)	11789(3)	8012(5)	-292(2)	54(1)
N(5)	11523(2)	8274(4)	-1012(2)	45(1)
B(1)	12095(6)	7808(14)	-1332(5)	136(5)
C(36)	10798(4)	7644(8)	-1338(3)	88(2)
C(37)	11396(5)	9768(6)	-1108(3)	98(2)
C(38)	312(3)	4621(5)	4850(3)	68(2)

O(9)	999(3)	4078(6)	5278(2)	107(2)
------	--------	---------	---------	--------

Table 3. Bond lengths [Å] and angles [°] for **3.76**.

C(1)-O(1)	1.218(5)	C(1)-C(2)	1.445(5)
C(1)-C(8)	1.490(5)	C(2)-N(1)	1.353(5)
C(2)-C(5)	1.391(5)	N(1)-C(3)	1.369(5)
N(1)-H(1N)	0.8700	C(3)-C(4)	1.375(6)
C(3)-H(3)	0.9400	C(4)-C(5)	1.422(5)
C(4)-C(9)	1.497(5)	C(5)-C(6)	1.441(5)
C(6)-O(4)	1.228(4)	C(6)-C(7)	1.499(5)
C(7)-C(8)	1.340(5)	C(7)-C(16)	1.510(5)
C(8)-H(8)	0.9400	C(9)-C(10)	1.528(7)
C(9)-H(9A)	0.9800	C(9)-H(9B)	0.9800
C(10)-N(2)	1.444(6)	C(10)-H(10A)	0.9800
C(10)-H(10B)	0.9800	N(2)-C(11)	1.335(5)
N(2)-H(2N)	0.8700	C(11)-O(2)	1.217(5)
C(11)-O(3)	1.339(5)	O(3)-C(12)	1.473(6)
C(12)-C(15)	1.502(8)	C(12)-C(14)	1.521(8)
C(12)-C(13)	1.523(7)	C(13)-H(13A)	0.9700

C(13)-H(13B)	0.9700	C(13)-H(13C)	0.9700
C(14)-H(14A)	0.9700	C(14)-H(14B)	0.9700
C(14)-H(14C)	0.9700	C(15)-H(15A)	0.9700
C(15)-H(15B)	0.9700	C(15)-H(15C)	0.9700
C(16)-O(7)	1.428(4)	C(16)-N(4)	1.440(4)
C(16)-C(17)	1.546(5)	C(17)-O(5)	1.207(5)
C(17)-N(3)	1.353(5)	N(3)-C(18)	1.401(5)
N(3)-C(19)	1.450(5)	C(18)-O(6)	1.212(5)
C(18)-N(4)	1.356(5)	N(4)-C(20)	1.442(5)
C(19)-H(19A)	0.9700	C(19)-H(19B)	0.9700
C(19)-H(19C)	0.9700	C(20)-H(20A)	0.9700
C(20)-H(20B)	0.9700	C(20)-H(20C)	0.9700
O(7)-C(21)	1.390(4)	C(21)-C(26)	1.369(6)
C(21)-C(22)	1.403(5)	C(22)-O(8)	1.361(5)
C(22)-C(23)	1.389(5)	C(23)-C(24)	1.379(6)
C(23)-H(23)	0.9400	C(24)-C(25)	1.389(6)
C(24)-H(24)	0.9400	C(25)-C(26)	1.398(5)
C(25)-C(34)	1.514(6)	C(26)-H(26)	0.9400

O(8)-C(27)	1.434(5)	C(27)-C(28)	1.500(7)
C(27)-H(27A)	0.9800	C(27)-H(27B)	0.9800
C(28)-C(33)	1.374(6)	C(28)-C(29)	1.387(6)
C(29)-C(30)	1.373(7)	C(29)-H(29)	0.9400
C(30)-C(31)	1.371(7)	C(30)-H(30)	0.9400
C(31)-C(32)	1.364(8)	C(31)-H(31)	0.9400
C(32)-C(33)	1.387(8)	C(32)-H(32)	0.9400
C(33)-H(33)	0.9400	C(34)-C(35)	1.496(6)
C(34)-H(34A)	0.9800	C(34)-H(34B)	0.9800
C(35)-N(5)	1.499(6)	C(35)-H(35A)	0.9800
C(35)-H(35B)	0.9800	N(5)-C(36)	1.456(7)
N(5)-C(37)	1.490(7)	N(5)-B(1)	1.590(8)
B(1)-H(1A)	0.9700	B(1)-H(1B)	0.9700
B(1)-H(1C)	0.9700	C(36)-H(36A)	0.9700
C(36)-H(36B)	0.9700	C(36)-H(36C)	0.9700
C(37)-H(37A)	0.9700	C(37)-H(37B)	0.9700
C(37)-H(37C)	0.9700	C(38)-O(9)	1.416(7)
C(38)-C(38)#1	1.750(11)	C(38)-H(38A)	0.9800

C(38)-H(38B)	0.9800	O(9)-H(9)	0.8300
O(1)-C(1)-C(2)	125.0(4)	O(1)-C(1)-C(8)	120.9(3)
C(2)-C(1)-C(8)	114.1(3)	N(1)-C(2)-C(5)	108.5(3)
N(1)-C(2)-C(1)	127.3(3)	C(5)-C(2)-C(1)	124.2(3)
C(2)-N(1)-C(3)	108.5(3)	C(2)-N(1)-H(1N)	125.8
C(3)-N(1)-H(1N)	125.8	N(1)-C(3)-C(4)	110.0(3)
N(1)-C(3)-H(3)	125.0	C(4)-C(3)-H(3)	125.0
C(3)-C(4)-C(5)	105.6(3)	C(3)-C(4)-C(9)	126.9(3)
C(5)-C(4)-C(9)	127.6(3)	C(2)-C(5)-C(4)	107.5(3)
C(2)-C(5)-C(6)	120.6(3)	C(4)-C(5)-C(6)	131.9(3)
O(4)-C(6)-C(5)	124.3(3)	O(4)-C(6)-C(7)	119.3(3)
C(5)-C(6)-C(7)	116.4(3)	C(8)-C(7)-C(6)	121.5(3)
C(8)-C(7)-C(16)	122.1(3)	C(6)-C(7)-C(16)	116.4(3)
C(7)-C(8)-C(1)	123.1(3)	C(7)-C(8)-H(8)	118.5
C(1)-C(8)-H(8)	118.5	C(4)-C(9)-C(10)	113.6(4)
C(4)-C(9)-H(9A)	108.9	C(10)-C(9)-H(9A)	108.9
C(4)-C(9)-H(9B)	108.9	C(10)-C(9)-H(9B)	108.9

H(9A)-C(9)-H(9B)	107.7	N(2)-C(10)-C(9)	113.3(4)
N(2)-C(10)-H(10A)	108.9	C(9)-C(10)-H(10A)	108.9
N(2)-C(10)-H(10B)	108.9	C(9)-C(10)-H(10B)	108.9
H(10A)-C(10)-H(10B)	107.7	C(11)-N(2)-C(10)	121.3(4)
C(11)-N(2)-H(2N)	119.3	C(10)-N(2)-H(2N)	119.3
O(2)-C(11)-N(2)	124.3(4)	O(2)-C(11)-O(3)	124.9(4)
N(2)-C(11)-O(3)	110.8(4)	C(11)-O(3)-C(12)	121.6(3)
O(3)-C(12)-C(15)	109.0(4)	O(3)-C(12)-C(14)	101.8(4)
C(15)-C(12)-C(14)	111.7(5)	O(3)-C(12)-C(13)	110.9(4)
C(15)-C(12)-C(13)	111.9(5)	C(14)-C(12)-C(13)	110.9(5)
C(12)-C(13)-H(13A)	109.5	C(12)-C(13)-H(13B)	109.5
H(13A)-C(13)-H(13B)	109.5	C(12)-C(13)-H(13C)	109.5
H(13A)-C(13)-H(13C)	109.5	H(13B)-C(13)-H(13C)	109.5
C(12)-C(14)-H(14A)	109.5	C(12)-C(14)-H(14B)	109.5
H(14A)-C(14)-H(14B)	109.5	C(12)-C(14)-H(14C)	109.5
H(14A)-C(14)-H(14C)	109.5	H(14B)-C(14)-H(14C)	109.5
C(12)-C(15)-H(15A)	109.5	C(12)-C(15)-H(15B)	109.5
H(15A)-C(15)-H(15B)	109.5	C(12)-C(15)-H(15C)	109.5

H(15A)-C(15)-H(15C)	109.5	H(15B)-C(15)-H(15C)	109.5
O(7)-C(16)-N(4)	113.7(3)	O(7)-C(16)-C(7)	107.1(3)
N(4)-C(16)-C(7)	114.0(3)	O(7)-C(16)-C(17)	108.8(3)
N(4)-C(16)-C(17)	101.6(3)	C(7)-C(16)-C(17)	111.4(3)
O(5)-C(17)-N(3)	127.8(4)	O(5)-C(17)-C(16)	125.1(3)
N(3)-C(17)-C(16)	106.9(3)	C(17)-N(3)-C(18)	110.7(3)
C(17)-N(3)-C(19)	124.5(4)	C(18)-N(3)-C(19)	124.3(4)
O(6)-C(18)-N(4)	126.2(4)	O(6)-C(18)-N(3)	125.2(4)
N(4)-C(18)-N(3)	108.6(3)	C(18)-N(4)-C(16)	111.6(3)
C(18)-N(4)-C(20)	122.3(3)	C(16)-N(4)-C(20)	125.2(3)
N(3)-C(19)-H(19A)	109.5	N(3)-C(19)-H(19B)	109.5
H(19A)-C(19)-H(19B)	109.5	N(3)-C(19)-H(19C)	109.5
H(19A)-C(19)-H(19C)	109.5	H(19B)-C(19)-H(19C)	109.5
N(4)-C(20)-H(20A)	109.5	N(4)-C(20)-H(20B)	109.5
H(20A)-C(20)-H(20B)	109.5	N(4)-C(20)-H(20C)	109.5
H(20A)-C(20)-H(20C)	109.5	H(20B)-C(20)-H(20C)	109.5
C(21)-O(7)-C(16)	116.8(3)	C(26)-C(21)-O(7)	122.1(3)
C(26)-C(21)-C(22)	121.1(3)	O(7)-C(21)-C(22)	116.6(3)

O(8)-C(22)-C(23)	126.8(4)	O(8)-C(22)-C(21)	115.1(3)
C(23)-C(22)-C(21)	118.1(4)	C(24)-C(23)-C(22)	120.5(4)
C(24)-C(23)-H(23)	119.8	C(22)-C(23)-H(23)	119.8
C(23)-C(24)-C(25)	121.6(4)	C(23)-C(24)-H(24)	119.2
C(25)-C(24)-H(24)	119.2	C(24)-C(25)-C(26)	117.8(4)
C(24)-C(25)-C(34)	122.6(4)	C(26)-C(25)-C(34)	119.7(4)
C(21)-C(26)-C(25)	120.9(3)	C(21)-C(26)-H(26)	119.5
C(25)-C(26)-H(26)	119.5	C(22)-O(8)-C(27)	119.7(3)
O(8)-C(27)-C(28)	106.0(3)	O(8)-C(27)-H(27A)	110.5
C(28)-C(27)-H(27A)	110.5	O(8)-C(27)-H(27B)	110.5
C(28)-C(27)-H(27B)	110.5	H(27A)-C(27)-H(27B)	108.7
C(33)-C(28)-C(29)	117.7(5)	C(33)-C(28)-C(27)	121.1(4)
C(29)-C(28)-C(27)	121.1(4)	C(30)-C(29)-C(28)	120.9(5)
C(30)-C(29)-H(29)	119.5	C(28)-C(29)-H(29)	119.5
C(31)-C(30)-C(29)	120.7(5)	C(31)-C(30)-H(30)	119.6
C(29)-C(30)-H(30)	119.6	C(32)-C(31)-C(30)	119.1(5)
C(32)-C(31)-H(31)	120.5	C(30)-C(31)-H(31)	120.5
C(31)-C(32)-C(33)	120.4(5)	C(31)-C(32)-H(32)	119.8

C(33)-C(32)-H(32)	119.8	C(28)-C(33)-C(32)	121.2(5)
C(28)-C(33)-H(33)	119.4	C(32)-C(33)-H(33)	119.4
C(35)-C(34)-C(25)	110.0(4)	C(35)-C(34)-H(34A)	109.7
C(25)-C(34)-H(34A)	109.7	C(35)-C(34)-H(34B)	109.7
C(25)-C(34)-H(34B)	109.7	H(34A)-C(34)-H(34B)	108.2
C(34)-C(35)-N(5)	117.3(4)	C(34)-C(35)-H(35A)	108.0
N(5)-C(35)-H(35A)	108.0	C(34)-C(35)-H(35B)	108.0
N(5)-C(35)-H(35B)	108.0	H(35A)-C(35)-H(35B)	107.2
C(36)-N(5)-C(37)	105.7(5)	C(36)-N(5)-C(35)	109.6(4)
C(37)-N(5)-C(35)	107.1(4)	C(36)-N(5)-B(1)	111.3(7)
C(37)-N(5)-B(1)	109.0(6)	C(35)-N(5)-B(1)	113.8(5)
N(5)-B(1)-H(1A)	109.5	N(5)-B(1)-H(1B)	109.5
H(1A)-B(1)-H(1B)	109.5	N(5)-B(1)-H(1C)	109.5
H(1A)-B(1)-H(1C)	109.5	H(1B)-B(1)-H(1C)	109.5
N(5)-C(36)-H(36A)	109.5	N(5)-C(36)-H(36B)	109.5
H(36A)-C(36)-H(36B)	109.5	N(5)-C(36)-H(36C)	109.5
H(36A)-C(36)-H(36C)	109.5	H(36B)-C(36)-H(36C)	109.5
N(5)-C(37)-H(37A)	109.5	N(5)-C(37)-H(37B)	109.5

H(37A)-C(37)-H(37B)	109.5	N(5)-C(37)-H(37C)	109.5
H(37A)-C(37)-H(37C)	109.5	H(37B)-C(37)-H(37C)	109.5
O(9)-C(38)-C(38)#1	121.2(7)	O(9)-C(38)-H(38A)	107.0
C(38)#1-C(38)-H(38A)	107.0	O(9)-C(38)-H(38B)	107.0
C(38)#1-C(38)-H(38B)	107.0	H(38A)-C(38)-H(38B)	106.8
C(38)-O(9)-H(9)	109.5		

Symmetry transformations used to generate equivalent atoms:

#1 -x,-y+1,-z+1

Table 4. Anisotropic displacement parameters ($\text{\AA}^2 \times 10^3$) for **3.76**. The anisotropic displacement factor exponent takes the form: $-2 \pi^2 [h^2 a^{*2} U^{11} + \dots + 2 h k a^* b^* U^{12}]$

	U^{11}	U^{22}	U^{33}	U^{23}	U^{13}	U^{12}
C(1)	33(2)	42(2)	38(2)	13(2)	13(2)	2(2)
C(2)	35(2)	39(2)	33(2)	7(2)	15(2)	-2(2)
N(1)	41(2)	50(2)	40(2)	15(2)	19(1)	1(1)
C(3)	37(2)	53(2)	46(3)	6(2)	22(2)	0(2)
C(4)	34(2)	41(2)	36(2)	0(2)	16(2)	0(2)
C(5)	30(2)	35(2)	32(2)	3(2)	12(1)	-1(1)
C(6)	30(2)	33(2)	34(2)	5(2)	11(1)	0(1)
C(7)	28(2)	32(2)	30(2)	3(2)	11(1)	-2(1)
C(8)	30(2)	41(2)	37(2)	10(2)	13(1)	4(1)

O(1)	46(2)	69(2)	70(2)	43(2)	24(2)	14(2)
C(9)	36(2)	45(2)	55(3)	6(2)	22(2)	5(2)
C(10)	37(2)	70(3)	51(3)	17(2)	16(2)	9(2)
N(2)	37(2)	58(2)	60(3)	-6(2)	16(2)	9(2)
C(11)	39(2)	49(2)	37(2)	-8(2)	9(2)	5(2)
O(2)	44(2)	49(2)	72(2)	-15(2)	20(2)	4(1)
O(3)	42(2)	50(2)	66(2)	-15(2)	16(1)	2(1)
C(12)	47(2)	59(3)	53(3)	-7(2)	16(2)	-5(2)
C(13)	41(2)	83(4)	66(3)	-5(3)	15(2)	2(2)
C(14)	73(4)	67(4)	118(6)	-11(4)	27(4)	-17(3)
C(15)	100(5)	104(5)	56(4)	-2(4)	38(3)	-10(4)
O(4)	41(2)	52(2)	60(2)	28(2)	26(1)	14(1)
C(16)	26(2)	31(2)	29(2)	4(1)	9(1)	-2(1)
C(17)	28(2)	43(2)	30(2)	4(2)	10(1)	-4(1)
N(3)	34(2)	47(2)	30(2)	11(1)	8(1)	0(1)
C(18)	34(2)	38(2)	41(2)	10(2)	15(2)	1(2)
N(4)	32(1)	31(1)	27(2)	3(1)	9(1)	-2(1)
O(5)	45(2)	53(2)	37(2)	-6(1)	8(1)	-17(1)
C(19)	65(3)	75(3)	34(3)	22(2)	4(2)	2(2)
O(6)	68(2)	36(2)	63(2)	17(2)	18(2)	-1(1)
C(20)	50(2)	38(2)	41(2)	-3(2)	10(2)	-3(2)
O(7)	31(1)	32(1)	38(2)	5(1)	16(1)	0(1)
C(21)	29(2)	29(2)	35(2)	3(2)	14(1)	2(1)
C(22)	34(2)	34(2)	37(2)	2(2)	11(2)	1(1)
C(23)	27(2)	42(2)	50(3)	2(2)	9(2)	-1(2)

C(24)	35(2)	39(2)	55(3)	8(2)	24(2)	3(2)
C(25)	42(2)	35(2)	41(2)	7(2)	22(2)	8(2)
C(26)	33(2)	33(2)	35(2)	3(2)	12(1)	2(1)
O(8)	48(2)	57(2)	30(2)	0(1)	8(1)	-15(1)
C(27)	39(2)	52(2)	38(2)	-3(2)	3(2)	-4(2)
C(28)	41(2)	40(2)	35(2)	4(2)	1(2)	2(2)
C(29)	84(3)	40(2)	43(3)	0(2)	21(2)	-4(2)
C(30)	80(3)	54(3)	45(3)	5(2)	19(2)	-10(2)
C(31)	69(3)	72(3)	42(3)	2(3)	19(2)	2(3)
C(32)	90(4)	54(3)	63(4)	-16(3)	30(3)	-7(3)
C(33)	75(3)	43(2)	57(3)	-6(2)	22(2)	-15(2)
C(34)	57(2)	50(2)	50(3)	9(2)	34(2)	10(2)
C(35)	68(3)	50(2)	45(3)	2(2)	21(2)	6(2)
N(5)	54(2)	44(2)	39(2)	6(2)	20(2)	0(2)
B(1)	126(7)	227(13)	95(7)	84(8)	88(6)	91(8)
C(36)	79(4)	109(5)	62(4)	7(4)	11(3)	-30(4)
C(37)	164(7)	49(3)	70(5)	15(3)	31(4)	6(4)
C(38)	69(3)	53(3)	95(4)	38(3)	44(3)	15(2)
O(9)	99(3)	172(5)	50(3)	4(3)	29(2)	-72(3)

Table 5. Hydrogen coordinates ($\times 10^4$) and isotropic displacement parameters ($\text{\AA}^2 \times 10^3$) for **3.76**.

	x	y	z	U(eq)
H(1N)	9013	3791	3386	51
H(3)	7924	5235	3008	52

H(8)	10937	4374	2485	43
H(9A)	8105	8081	2076	53
H(9B)	7479	7339	2250	53
H(10A)	7141	7673	1099	63
H(10B)	7791	6672	1124	63
H(2N)	7082	4920	1172	63
H(13A)	4659	6345	800	97
H(13B)	4086	5141	714	97
H(13C)	4566	5198	271	97
H(14A)	4908	2823	638	133
H(14B)	4600	2785	1208	133
H(14C)	5456	2523	1365	133
H(15A)	5659	4379	2201	127
H(15B)	4816	4844	1958	127
H(15C)	5438	5896	1966	127
H(19A)	9539	7139	-369	93
H(19B)	9768	8676	-184	93
H(19C)	9047	8077	-106	93
H(20A)	11604	8626	2285	67
H(20B)	11197	7655	2619	67
H(20C)	10833	9067	2318	67
H(23)	13437	6770	2144	50
H(24)	13300	7033	1068	49
H(26)	11168	5816	482	41
H(27A)	12998	7528	3010	56

H(27B)	13399	6119	3285	56
H(29)	12256	4639	3548	68
H(30)	11681	4701	4290	73
H(31)	11711	6656	4882	74
H(32)	12274	8587	4687	82
H(33)	12795	8570	3900	71
H(34A)	12595	6550	-103	58
H(34B)	11782	5930	-318	58
H(35A)	12165	8699	-69	65
H(35B)	11369	8152	-155	65
H(1A)	12097	6822	-1358	204
H(1B)	12590	8127	-1066	204
H(1C)	11946	8190	-1768	204
H(36A)	10848	6662	-1298	132
H(36B)	10603	7895	-1796	132
H(36C)	10460	7955	-1136	132
H(37A)	11181	9969	-1572	148
H(37B)	11867	10243	-912	148
H(37C)	11059	10064	-903	148
H(38A)	44	3881	4558	82
H(38B)	427	5300	4577	82
H(9)	1210	4640	5570	160

Table 6. Torsion angles [°] for **3.76**.

O(1)-C(1)-C(2)-N(1)	-1.8(7)	O(1)-C(1)-C(2)-C(5)	177.1(4)
---------------------	---------	---------------------	----------

C(8)-C(1)-C(2)-C(5)	-3.2(6)	C(5)-C(2)-N(1)-C(3)	-0.6(5)
C(1)-C(2)-N(1)-C(3)	178.5(4)	C(2)-N(1)-C(3)-C(4)	0.1(5)
N(1)-C(3)-C(4)-C(5)	0.4(5)	N(1)-C(3)-C(4)-C(9)	179.5(4)
N(1)-C(2)-C(5)-C(4)	0.9(5)	C(1)-C(2)-C(5)-C(4)	-178.3(4)
N(1)-C(2)-C(5)-C(6)	-178.3(3)	C(1)-C(2)-C(5)-C(6)	2.6(6)
C(3)-C(4)-C(5)-C(2)	-0.8(4)	C(9)-C(4)-C(5)-C(2)	-179.8(4)
C(3)-C(4)-C(5)-C(6)	178.2(4)	C(9)-C(4)-C(5)-C(6)	-0.9(7)
C(2)-C(5)-C(6)-O(4)	178.9(4)	C(4)-C(5)-C(6)-O(4)	0.0(7)
C(2)-C(5)-C(6)-C(7)	0.1(5)	C(4)-C(5)-C(6)-C(7)	-178.8(4)
O(4)-C(6)-C(7)-C(8)	179.1(4)	C(5)-C(6)-C(7)-C(8)	-2.1(5)
O(4)-C(6)-C(7)-C(16)	-2.0(5)	C(5)-C(6)-C(7)-C(16)	176.8(3)
C(6)-C(7)-C(8)-C(1)	1.4(6)	C(16)-C(7)-C(8)-C(1)	-177.4(3)
O(1)-C(1)-C(8)-C(7)	-179.1(4)	C(2)-C(1)-C(8)-C(7)	1.2(6)
C(3)-C(4)-C(9)-C(10)	-108.4(5)	C(5)-C(4)-C(9)-C(10)	70.5(5)
C(4)-C(9)-C(10)-N(2)	67.7(4)	C(9)-C(10)-N(2)-C(11)	85.8(5)
C(10)-N(2)-C(11)-O(2)	4.0(7)	C(10)-N(2)-C(11)-O(3)	-177.2(4)
O(2)-C(11)-O(3)-C(12)	-13.6(7)	N(2)-C(11)-O(3)-C(12)	167.6(4)
C(11)-O(3)-C(12)-C(15)	-60.7(6)	C(11)-O(3)-C(12)-C(14)	-178.9(5)

C(11)-O(3)-C(12)-C(13)	63.0(5)	C(8)-C(7)-C(16)-O(7)	8.7(5)
C(6)-C(7)-C(16)-O(7)	-170.2(3)	C(8)-C(7)-C(16)-N(4)	-118.0(4)
C(6)-C(7)-C(16)-N(4)	63.1(4)	C(8)-C(7)-C(16)-C(17)	127.7(4)
C(6)-C(7)-C(16)-C(17)	-51.2(4)	O(7)-C(16)-C(17)-O(5)	63.0(4)
N(4)-C(16)-C(17)-O(5)	-176.8(4)	C(7)-C(16)-C(17)-O(5)	-55.0(5)
O(7)-C(16)-C(17)-N(3)	-113.9(3)	N(4)-C(16)-C(17)-N(3)	6.4(4)
C(7)-C(16)-C(17)-N(3)	128.2(3)	O(5)-C(17)-N(3)-C(18)	175.3(4)
C(16)-C(17)-N(3)-C(18)	-8.0(4)	O(5)-C(17)-N(3)-C(19)	3.7(7)
C(16)-C(17)-N(3)-C(19)	-179.6(4)	C(17)-N(3)-C(18)-O(6)	-173.0(4)
C(19)-N(3)-C(18)-O(6)	-1.3(7)	C(17)-N(3)-C(18)-N(4)	6.5(4)
C(19)-N(3)-C(18)-N(4)	178.2(4)	O(6)-C(18)-N(4)-C(16)	177.5(4)
N(3)-C(18)-N(4)-C(16)	-2.0(4)	O(6)-C(18)-N(4)-C(20)	7.7(6)
N(3)-C(18)-N(4)-C(20)	-171.8(3)	O(7)-C(16)-N(4)-C(18)	114.2(3)
C(7)-C(16)-N(4)-C(18)	-122.6(3)	C(17)-C(16)-N(4)-C(18)	-2.6(4)
O(7)-C(16)-N(4)-C(20)	-76.4(4)	C(7)-C(16)-N(4)-C(20)	46.8(4)
C(17)-C(16)-N(4)-C(20)	166.9(3)	N(4)-C(16)-O(7)-C(21)	-30.1(4)
C(7)-C(16)-O(7)-C(21)	-157.0(3)	C(17)-C(16)-O(7)-C(21)	82.4(3)
C(16)-O(7)-C(21)-C(26)	-76.2(4)	C(16)-O(7)-C(21)-C(22)	108.5(4)

C(26)-C(21)-C(22)-O(8)	-177.5(3)	O(7)-C(21)-C(22)-O(8)	-2.1(5)
C(26)-C(21)-C(22)-C(23)	0.5(5)	O(7)-C(21)-C(22)-C(23)	175.9(3)
O(8)-C(22)-C(23)-C(24)	177.7(4)	C(21)-C(22)-C(23)-C(24)	-0.1(6)
C(22)-C(23)-C(24)-C(25)	0.0(6)	C(23)-C(24)-C(25)-C(26)	-0.3(6)
C(23)-C(24)-C(25)-C(34)	179.4(4)	O(7)-C(21)-C(26)-C(25)	-175.9(3)
C(22)-C(21)-C(26)-C(25)	-0.8(5)	C(24)-C(25)-C(26)-C(21)	0.7(5)
C(34)-C(25)-C(26)-C(21)	-179.0(3)	C(23)-C(22)-O(8)-C(27)	26.0(6)
C(21)-C(22)-O(8)-C(27)	-156.2(3)	C(22)-O(8)-C(27)-C(28)	156.1(3)
O(8)-C(27)-C(28)-C(33)	-133.4(4)	O(8)-C(27)-C(28)-C(29)	43.2(5)
C(33)-C(28)-C(29)-C(30)	0.3(7)	C(27)-C(28)-C(29)-C(30)	-176.4(4)
C(28)-C(29)-C(30)-C(31)	-1.9(8)	C(29)-C(30)-C(31)-C(32)	1.7(8)
C(30)-C(31)-C(32)-C(33)	0.2(9)	C(29)-C(28)-C(33)-C(32)	1.6(7)
C(27)-C(28)-C(33)-C(32)	178.3(5)	C(31)-C(32)-C(33)-C(28)	-1.9(9)
C(24)-C(25)-C(34)-C(35)	-95.0(5)	C(26)-C(25)-C(34)-C(35)	84.6(5)
C(25)-C(34)-C(35)-N(5)	-169.7(4)	C(34)-C(35)-N(5)-C(36)	78.9(6)
C(34)-C(35)-N(5)-C(37)	-166.9(5)	C(34)-C(35)-N(5)-B(1)	-46.4(8)

Symmetry transformations used to generate equivalent atoms:

#1 -x,-y+1,-z+1

Table 7. Hydrogen bonds for **3.76** [\AA and $^\circ$].

D-H...A	d(D-H)	d(H...A)	d(D...A)	$\angle(\text{DHA})$
N(1)-H(1N)...O(2)#2	0.87	1.97	2.806(5)	161.3

Symmetry transformations used to generate equivalent atoms:

#1 $-x, -y+1, -z+1$ #2 $-x+3/2, y-1/2, -z+1/2$